

JPL Contract 953311

CAS

ψ
 \hbar
210

Outer Planets Entry Probe System Study

Final Report

**Volume III
Appendixes**

August 1972

MARTIN MARIETTA

OUTER PLANET
ENTRY PROBE SYSTEM
STUDY

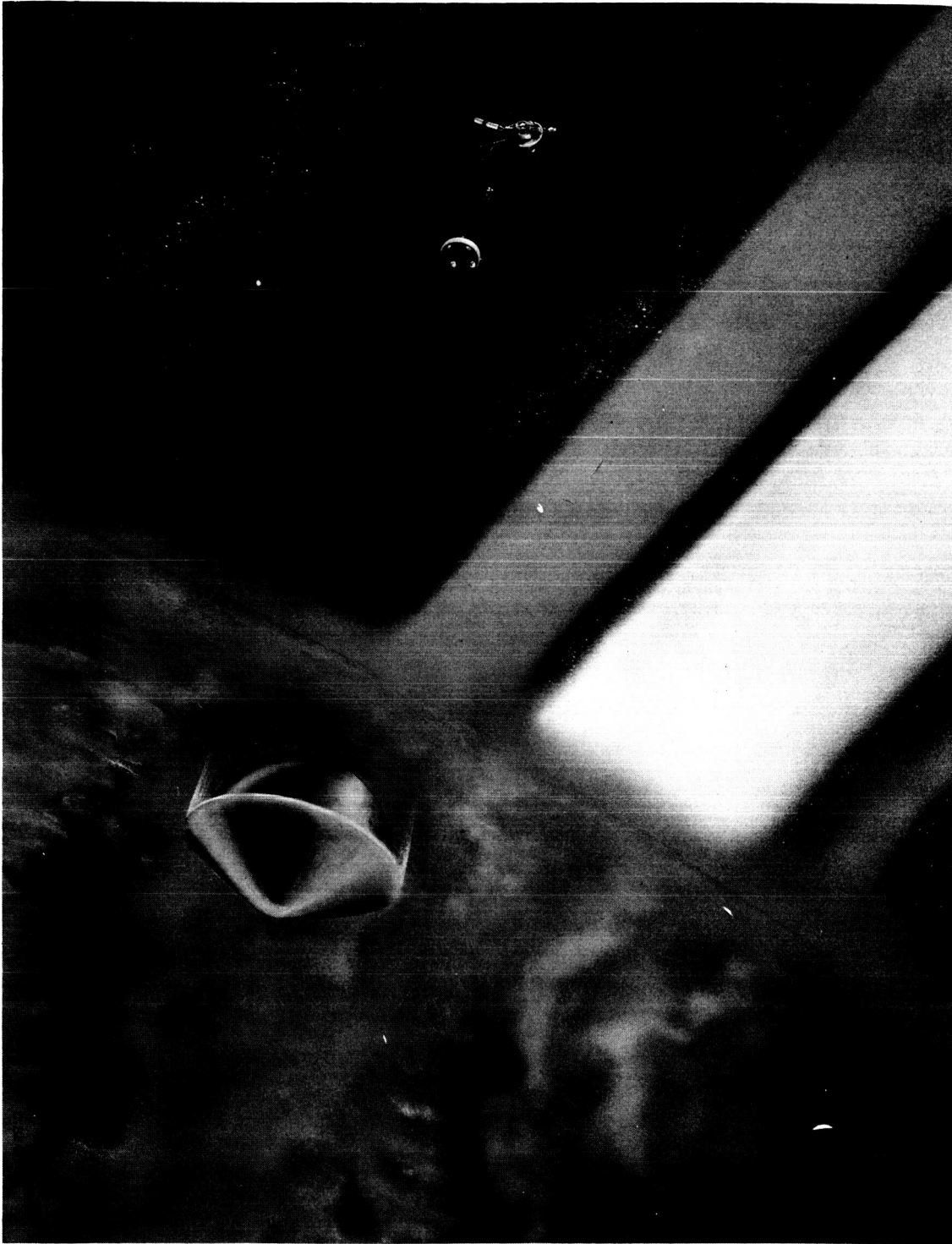
FINAL REPORT



R. S. Wiltshire
Program Manager

This work was performed for the Jet Propulsion Laboratory,
California Institute of Technology, sponsored by the
National Aeronautics and Space Administration under
Contract NAS7-100.

MARTIN MARIETTA CORPORATION
P. O. Box 179
Denver, Colorado 80201



Survivable Saturn Atmosphere Probe

FOREWORD

This final report has been prepared in accordance with requirements of Contract JPL-953311 to present data and conclusions from a six-month study for the Jet Propulsion Laboratory by Martin Marietta Aerospace, Denver Division. The report is divided into the following volumes:

Volume I - Summary

Volume II - Supporting Technical Studies

Volume III - Appendixes

ACKNOWLEDGEMENTS

The following Martin Marietta Corporation, Denver Division, personnel participated in this study, and their efforts are greatly appreciated:

Raymond S. Wiltshire	Study Leader, Program Manager
Allen R. Barger	Science Integration
Eugene A. Berkery	Telecommunications, Data Handling, Power, and ACS, Lead
Dennis V. Byrnes	Navigation
Philip C. Carney	Mission Analysis
Patrick C. Carroll	Systems
Revis E. Compton, Jr.	Telecommunications
Robert G. Cook	Mechanical Design
Douglas B. Cross	Mission Analysis
Ralph F. Fearn	Propulsion
Robert B. Fischer	Mission Analysis
Thomas C. Hendricks	Mission Analysis
John W. Hungate	Systems, Lead
Carl L. Jensen	Thermal Analysis
Melvin W. Kuethe/ Rufus O. Moses	Mechanical/Structural/Probe Integration, Lead
Kenneth W. Ledbetter	Science, Lead
Paula S. Lewis	Mission Analysis
John R. Mellin	Structures
Jack D. Pettus	Data Link Analysis
Robert J. Richardson	Receiver Systems
Arlen I. Reichert	Propulsion
E. Doyle Vogt	Mission Analysis, Lead
Donald E. Wainwright	Systems
Clifford M. Webb	Thermal Analysis
Charles E. Wilkerson	Data Handling

CONTENTS

APPENDIXES

	<u>Page</u>
A. Microwave Losses in the Atmospheres of Jupiter, Saturn, and Uranus	A-1 thru A-23
B. Microwave Frequency Selection	B-1 thru B-19
C. Spacecraft Receiver	C-1 thru C-13
D. Mission Antenna Analysis and Design	D-1 thru D-12
E. Summary of Planetary Atmospheres and Related Constraints	E-1 thru E-25
F. Attitude Control Subsystem Analysis	F-1 thru F-17
G. Electrical Power and Pyrotechnic Subsystems . . .	G-1 thru G-19
H. Data Handling Subsystem Analysis and Definition	H-1 thru H-10
I. Monte Carlo Deflection Dispersion Analysis . . .	I-1 thru I-15
J. Multilayer Insulation Conductivity Evaluation . .	J-1 thru J-3
K. NH ₃ and H ₂ O Cloud Models for the Outer Planets	K-1 thru K-28
L. Vertical Descent Program for Science Instrument Simulation (DATAT), Descent Runs for Jupiter and Saturn	L-1 thru L-48

M.	Propulsion Subsystem Analysis and Definition	M-1 thru M-33
N.	Response Time for a Ballast Volume Type Mass Spectrometer Inlet System	N-1 thru N-3
O.	Aeroshell Structure Parametric Weight Study . . .	O-1 thru O-26
P.	Lightweight Jupiter Probe Definition	P-1 thru P-5
Q.	Separation Spring Analysis	Q-1 and Q-2

APPENDIX A

MICROWAVE LOSSES IN THE ATMOSPHERES
OF JUPITER, SATURN, AND URANUS

R. J. Richardson
and
R. E. Compton, Jr.

June 6, 1972

MICROWAVE LOSSES IN THE ATMOSPHERE OF JUPITER, SATURN, AND URANUS

The techniques used to calculate microwave losses in the planet atmospheres are essentially those used on the original Jupiter atmospheric study as described in the final report of that contract (Ref 1). A long list of references given in this report will not be repeated here (Ref 1, p IV-136). Some changes have been made in the methods of calculating cloud absorption, which are outlined in this appendix.

The atmospheres of the three planets are all quite similar, being composed primarily of hydrogen (H_2) and helium (He) with trace amounts of other gasses. The principal sources of absorption in the atmospheres are (1) pressure broadening of absorption lines in the polarizable gasses, ammonia (NH_3) and water (H_2O) and (2) absorption in the clouds. Total attenuation increases as the aspect angle is moved away from zenith. Absorption is computed as a function of elevation, z , measured from an altitude where the pressure is one bar; the look vector aspect angle measured from zenith, ψ ; and the transmission frequency, f . A second source of signal loss is defocusing loss caused by ray-bending in the dense atmosphere. This loss is computed as a function of z and ψ and is independent of frequency. The atmosphere models are derived from the contractual documents supplied by JPL. Both the "nominal" and the "cool/dense" atmospheres were worked for Jupiter, while only the "nominal" atmospheres were analyzed for the other two planets.

A. ABSORPTION LOSSES

Ammonia (NH_3) has a large group of absorption lines (the inversion spectrum) centered around 25 GHz. These lines are very narrow at low pressure and are broadened by increasing pressure, merging into a single line for pressures greater than one atm. Although 25 GHz is remote from the frequency band of interest for telecommunications (around 1 to 2 GHz), line broadening caused by the very high pressures encountered in the mission is sufficient to cause substantial attenuation even at these relatively low frequencies. It was found that even the rotational spectrum of NH_3 , extending upward from 600 GHz, results in an absorption at these pressures that is not completely negligible. Similarly, water (H_2O) has a spectrum of absorption lines extending upward from 22 GHz with pressure broadening causing the effects to be perceptible at the much lower frequencies of interest for this mission.

1. Ammonia Absorption

The Ben-Reuven (Ref 2) line shape was used for absorption caused by gaseous NH_3 . The Ben-Reuven shape factor is given by

$$\text{SF} = \frac{2(\gamma - \beta)f^2 + 2(\gamma + \beta)(\nu_0^2 + \gamma^2 - \beta^2)}{(f^2 - \nu_0^2 - \gamma^2 + \beta^2)^2 + (2f\gamma)^2} \quad [\text{A-1}]$$

ν_0 is the line resonant frequency, 25 GHz. For this application, $f \ll \nu_0$. β and γ are proportional to density. This gives

$$\text{SF} \cong \frac{2(\gamma + \beta)}{\nu_0^2 + \gamma^2 - \beta^2} \quad [\text{A-2}]$$

$$\cong \frac{2(\gamma + \beta)}{\nu_0^2} \text{ (low pressures)} \quad [\text{A-3}]$$

$$\cong \frac{2}{\gamma - \beta} \text{ (high pressures)} \quad [\text{A-4}]$$

and β , γ , ν_0 , and f are in GHz.

Computation of the absorption coefficient, $\alpha(z)$, was done using Equation [A-5]. This was then integrated over the atmosphere

profile to give the total zenith absorption. $\alpha(z)$ and $\int_{z_0}^{\infty} \alpha(z) dz$

are converted to dB per km and dB by the factor $10 \log_{10}(e) = 4.35$. The absorption coefficient is computed from

$$\alpha(z) = k_1 f^2 A_N \text{SF}(z) \left[\frac{P(z)}{T(z)^2} \right] \text{ km}^{-1} \quad [\text{A-5}]$$

where A_N is the abundance of ammonia, P is the pressure in atm,

T is the temperature in $^{\circ}\text{K}$, $\text{SF}(z)$ is defined by Equations [A-2] through [A-4], f is the applied frequency in GHz, and k_1 is matched to experimental data. Since γ and β are proportional to density, which increases with depth in the atmosphere, we can write

$$\gamma(z) = k_2 \frac{P(z)}{T(z)} \quad [\text{A-6}]$$

$$\beta(z) = k_3 \frac{P(z)}{T(z)} \quad [A-7]$$

where k_2 and k_3 are matched to experimental data and are a function of the foreign gasses, H_2 and He , as well as the absorbing gas, ammonia.

Values used for k_1 , k_2 , and k_3 are

$$k_1 = 2.028 \times 10^6 \quad [A-8]$$

$$k_2 = 462.8 (A_{H_2} + 0.24 A_{He}) \quad [A-9]$$

$$k_3 = 231.4 (A_{H_2} + 0.24 A_{He}) \quad [A-10]$$

where A_{H_2} and A_{He} are abundances of H_2 and He , respectively.

The contribution caused by the rotational spectrum of ammonia is quite small, less than 5% of the inversion spectrum contribution at high pressures in a nominal atmosphere and less at low pressures. However, it was included in the computation. It follows the relationship

$$\alpha_{rot} = 71.1 A_N f^2 (A_{H_2} + 0.267 A_{He}) \frac{P(z)^2}{T(z)^{2.5}} \quad km^{-1} \quad [A-11]$$

2. Water Vapor

Based on measured data, it was decided that the approach used by Ho (Ref 3), modified to match the $H_2 - He$ foreign gasses on the outer planets, will give more accurate results at high pressure than the line-broadening approach. This gives the relationship

$$\alpha_{H_2O} = 7.35 \times 10^6 (1023 A_{H_2} + 870 A_{He}) A_{H_2O} f^2 \frac{P(z)^2}{T(z)^5} \quad [A-12]$$

where A_{H_2O} is the water vapor abundance. Water contribution to the absorption is less than 10% of the total in all of the model atmospheres for which absorption was computed.

3. Clouds

The only clouds that give significant absorption are the liquid droplet water-ammonia ($H_2O - NH_3$) solution clouds. Calculation of these losses is complicated by the electrical conductivity of the solution, which is a function of solution strength, and varies with elevation within the cloud. In order to determine the effect of these clouds, it is necessary to determine the dielectric constant and electrical conductivity as a function of temperature and solution strength. Conductivity, σ ($ohm^{-1} m^{-1}$), as a function of solution strength, at 291°K is shown in Figure A-1 (Ref 4). Conductivity varies with temperature in °K, with respect to the conductivity at 291°K as shown in Figure A-1, approximately as

$$\sigma(T) \cong \sigma(291) \left(\frac{T}{291} \right)^{6.2} \quad [A-13]$$

The NH_3 and H_2O solution is characterized as weak electrolytes with low conductivity. The complex dielectric constant, ϵ_j , is taken from Reference 5 and defined by

$$\epsilon_j = \epsilon_r + j\epsilon_i \quad [A-14]$$

where

$$\epsilon_r = \frac{\epsilon_\infty + \epsilon_o \left(\frac{\lambda_c}{\lambda} \right)^2}{1 + \left(\frac{\lambda_c}{\lambda} \right)^2} \quad [A-15]$$

$$\epsilon_\infty \cong 81.1 \left(\frac{291}{T} \right)^{1.4}, \text{ and } \epsilon_o \cong 5 \quad [A-16]$$

over the temperature range of interest for water. The RF wavelength, λ , is given by

$$\lambda = \frac{30}{f} \text{ cm} \quad [A-17]$$

for the frequency, f , in GHz.

The critical wavelength, λ_c , is approximated by

$$\lambda_c \cong 3.34 \left(\frac{273}{T} \right)^{7.2} \text{ cm} \quad [A-18]$$

with T in °K.

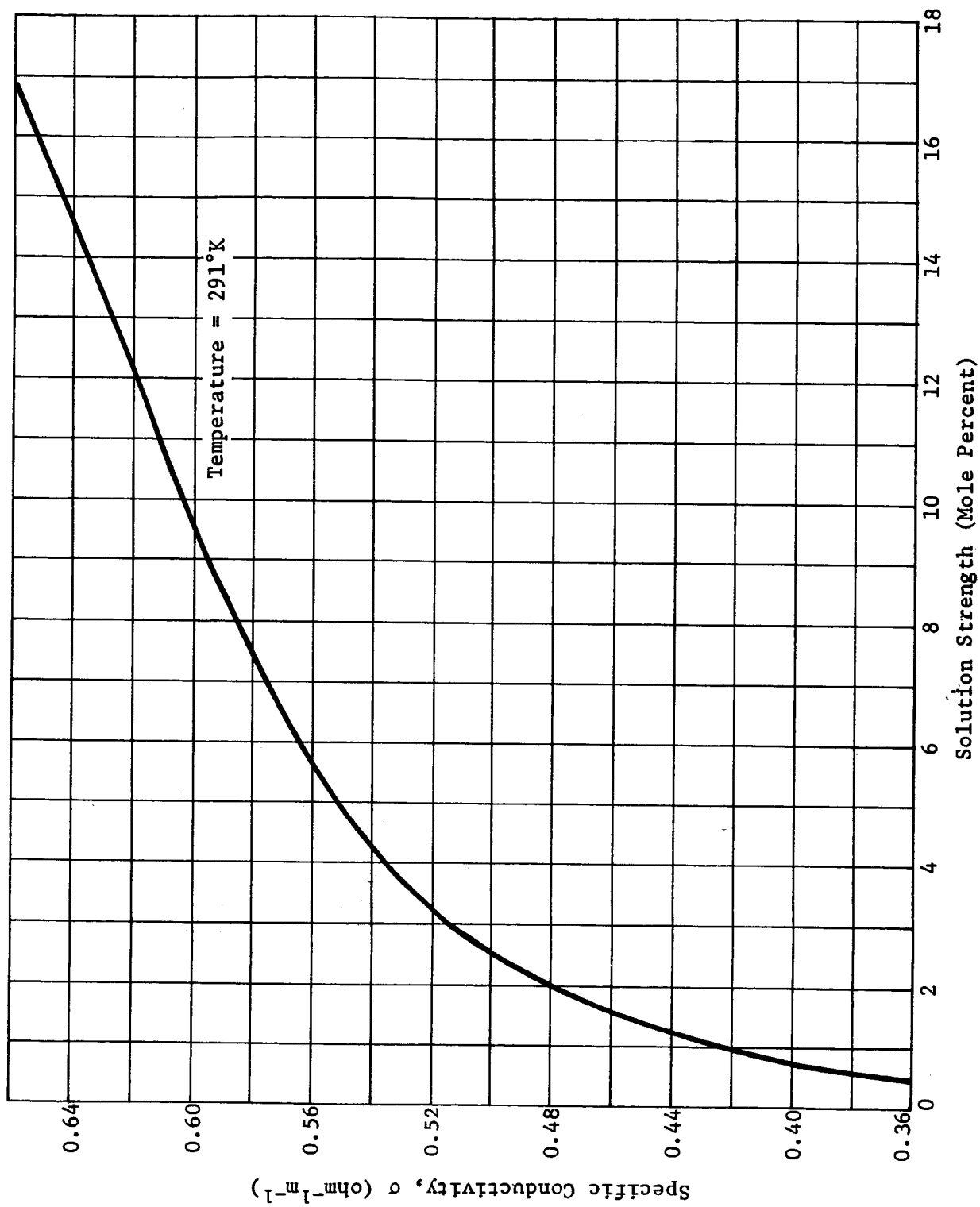


Figure A-1 Specific Conductivity of $\text{NH}_3 - \text{H}_2\text{O}$ Solution Clouds

The imaginary portion of the dielectric constant is given by

$$\epsilon_i = \frac{(\epsilon_\infty - \epsilon_o) (\lambda_c / \lambda)}{1 + (\lambda_c / \lambda)^2} + 60 \lambda \sigma. \quad [A-19]$$

The cloud absorption coefficient α_c is given by

$$\alpha_c = BM \text{ dB/km} \quad [A-20]$$

where M is the cloud density in g/m³ and B is ideally given by

$$B = 0.4343 \frac{6\pi}{\lambda} \text{Im} \left(-\frac{\epsilon_j - 1}{\epsilon_j + 2} \right). \quad [A-21]$$

Over the frequency range of interest, this simplifies to

$$B \cong \frac{24.53 \epsilon_i}{\left[(\epsilon_r + 2)^2 + \epsilon_i^2 \right] \lambda} \quad [A-22]$$

4. Absorption Results

The equations cited above were programmed to compute gaseous absorption and the integral of absorption versus depth of penetration into the atmosphere. The model atmosphere data were placed into the computation using a data deck of P, T, and z with 5-km intervals on z. Abundances used deep in the atmosphere were taken from the contract model atmospheres. Variations in NH₃ and H₂O abundances in and above the clouds were computed for one case. It was found that these abundances dropped so rapidly in and above the clouds that adequate accuracy for absorption computations is given by

$$A'_{\text{NH}_3} = \begin{cases} A_{\text{NH}_3} & \text{when } T(z) \geq T_{\text{sat}} \\ 0 & \text{when } T(z) < T_{\text{sat}} \end{cases} \quad [A-23]$$

where

A'_{NH_3} = ammonia abundance

z = elevation from pressure of one bar, km

T = temperature, °K

T_{sat} = saturation temperature in the given model, °K

A similar expression was used for water.

A program was developed to compute cloud mass, cloud state (liquid or solid), and cloud composition (solution strength for the H₂O and NH₃ solution cloud) as a function of elevation in these atmospheres. The results were used in a separate program to compute cloud absorption as a function of frequency using the formulas given previously. The results, gaseous absorption plus cloud absorption, were then combined. Figures A-2 through A-5 give the results for Jupiter cool/dense, Jupiter nominal, Saturn nominal, and Uranus nominal. Jupiter nominal and Saturn nominal do not have solution clouds, so absorption scales as f^2 in these models. Jupiter cool and Uranus nominal do have solution clouds, so scaling is not exactly as f^2 , though it is very nearly so.

B. REFRACTION EFFECTS

1. Defocusing Loss

The technique used to compute defocusing loss has been described in detail in Reference 6 and is summarized here.

First, the refractivity profile was computed, using the equation

$$N'(z) = \frac{P(z)}{T(z)} (37180 A_{H_2} + 9550 A_{He}) \quad [A-24]$$

where the coefficients of A_{H_2} and A_{He} are matched to measured values at $P = 1$ atm and $T = 273^\circ K$. These are $N'_{H_2} = 136.1$ and $N'_{He} = 35.0$ from the International Critical Tables.

$N'(z)$ is defined by $n = 1.0 + 10^{-6} N'(z)$, where n is the index of refraction. In subsequent formulas, we use $N(z) = 10^{-6} N'(z)$.

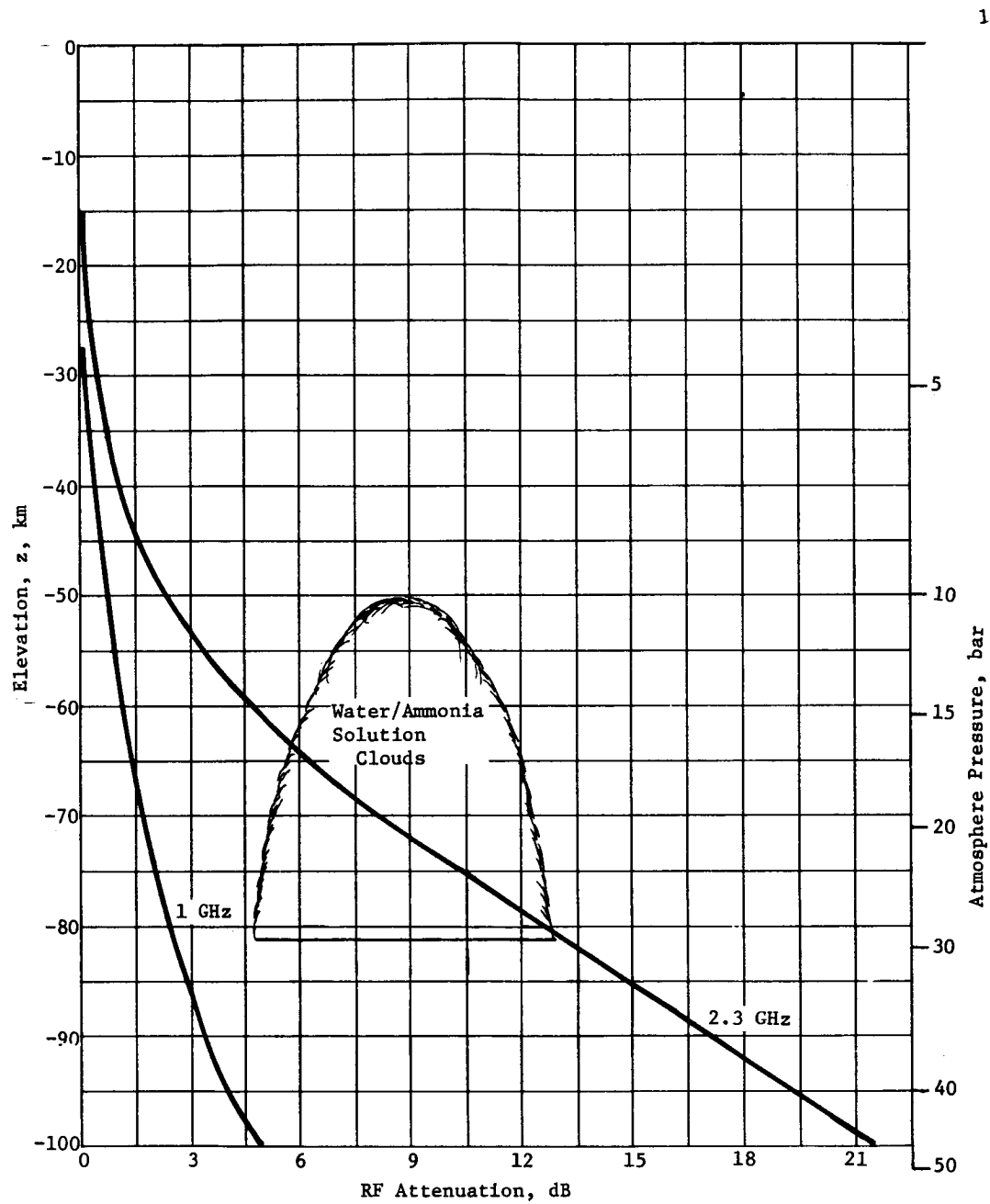


Figure A-2 Zenith Absorption for the Jupiter Cool/Dense Atmosphere

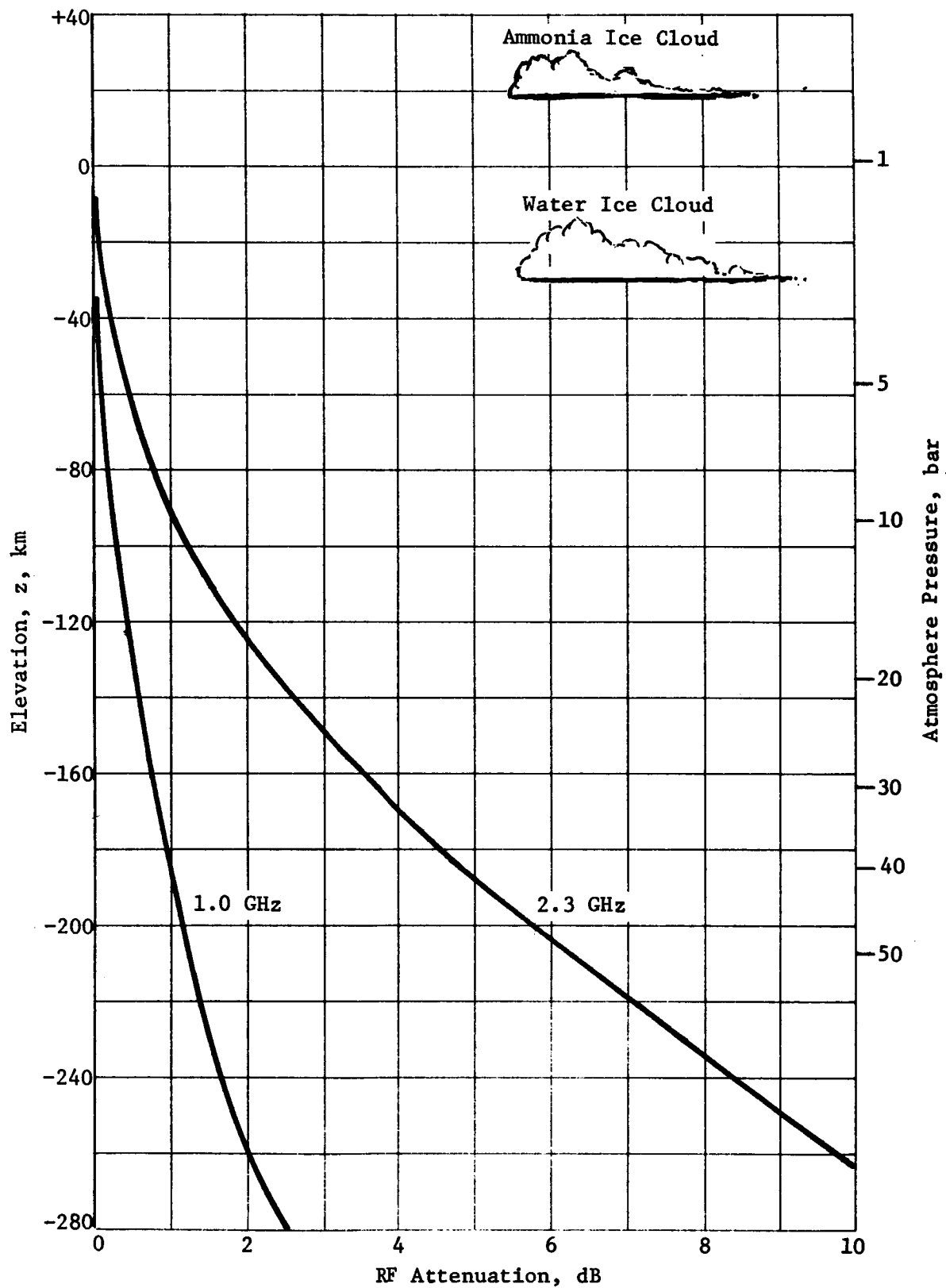


Figure A-3 Zenith Absorption for the Jupiter Nominal Atmosphere

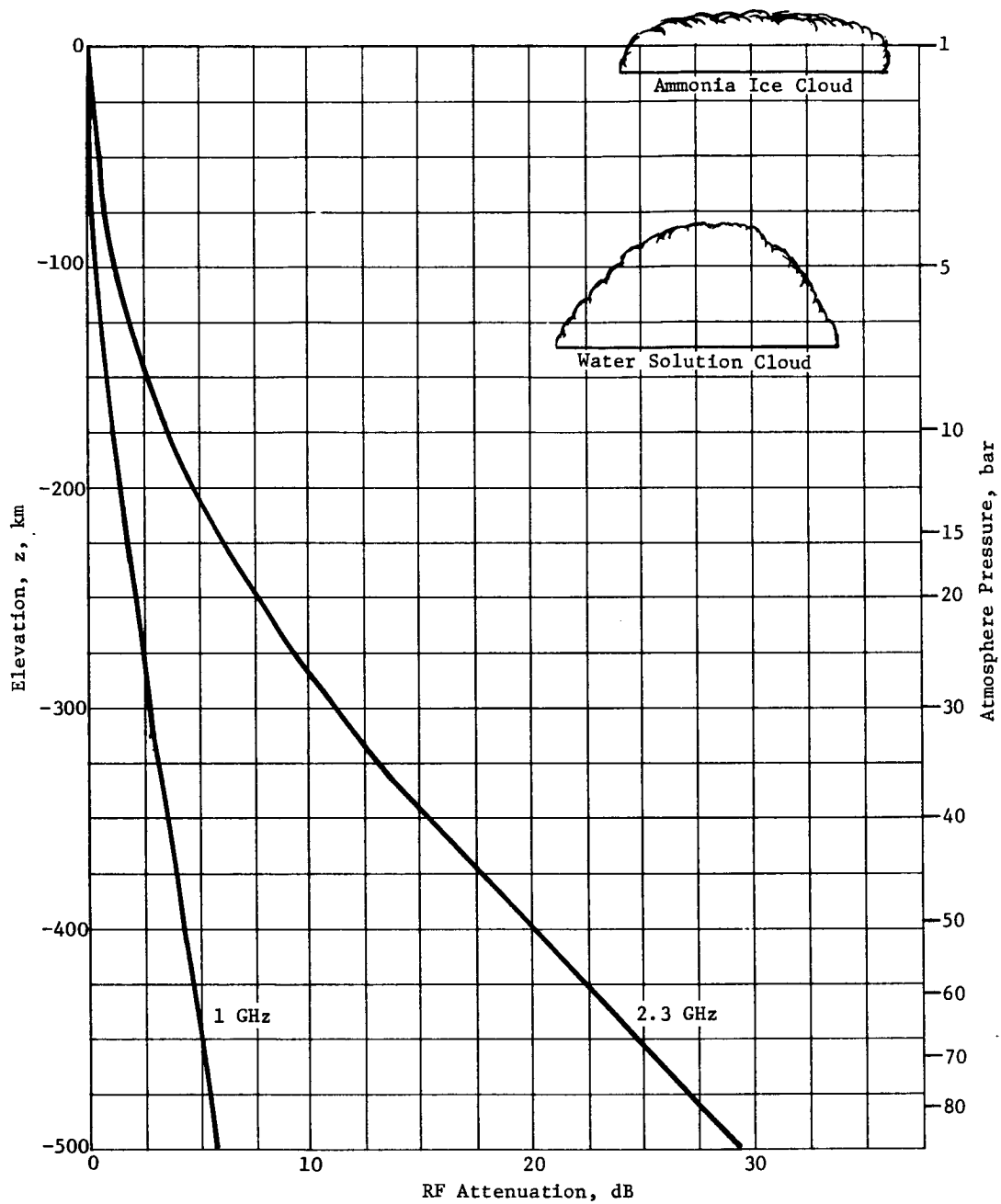


Figure A-4 Zenith Absorption for the Saturn Nominal Atmosphere

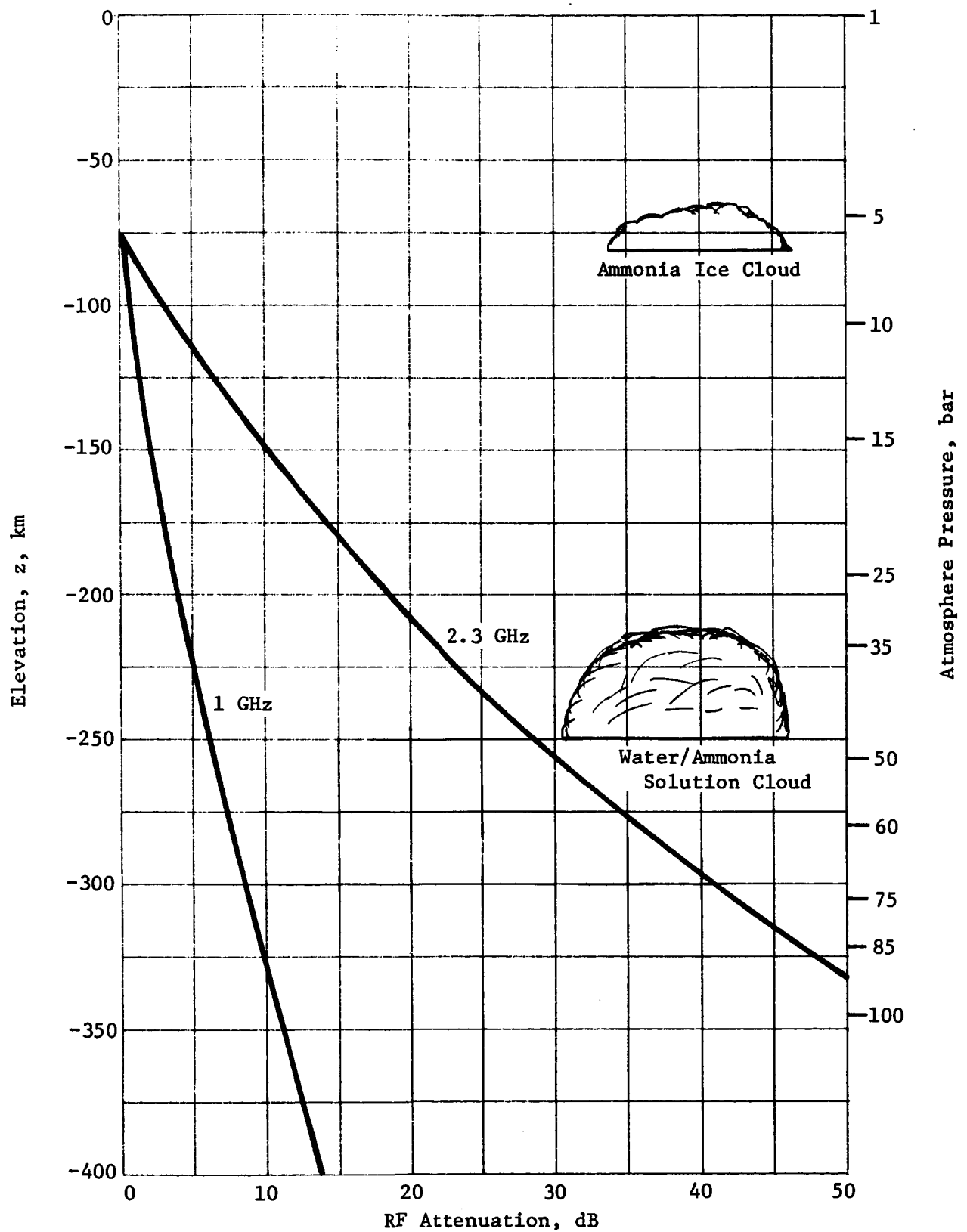


Figure A-5 Zenith Attenuation for the Uranus Nominal Atmosphere

The N-profile is then approximated by an exponential

$$N(z) = N(z_0) \exp \left[-\beta (z - z_0) \right] \quad [A-25]$$

by selecting β that best matches the profile starting from the selected z_0 . β^{-1} is the scale height.

Ray bending (or pointing error, E) for an exponential atmosphere can be computed from the refraction integral. The ray launch angle, θ , is measured from zenith.

The pointing error as a function of the ray angle is given by

$$E(\theta) = N_0 n_0 \sin \theta \int_0^\infty \frac{e^{-x} dx}{\left(1 + N_0 e^{-x}\right) \sqrt{\left(1 + \frac{x}{\beta r_s}\right)^2 \left(1 + N_0 e^{-x}\right)^2 - n_0^2 \sin^2 \theta}}. \quad [A-26]$$

The defocusing loss is calculated from

$$L_d(\theta) = \frac{1}{1 + \frac{dE}{d\theta}}. \quad [A-27]$$

It is independent of frequency, but is a function of z_0 and θ . It is more convenient to plot L_d vs $\psi = \theta + E(\theta)$, the angle at which the ray emerges from the atmosphere. Results for the four atmospheres are shown in Figure A-6 through A-9 with the ray angles defined in Figure A-6.

2. Absorption Loss

For small departures from zenith, attenuation due to atmospheric absorption, $L_a(\theta)$, increases as $\sec \theta \cong \sec \psi$. For larger ψ , ray-bending effects must be considered. $L_a(\theta)$ is bounded by

$$\begin{aligned} L_a(0) \sec \theta & \text{ (lower bound)} \\ L_a(0) \sec \psi & \text{ (upper bound).} \end{aligned} \quad [A-28]$$

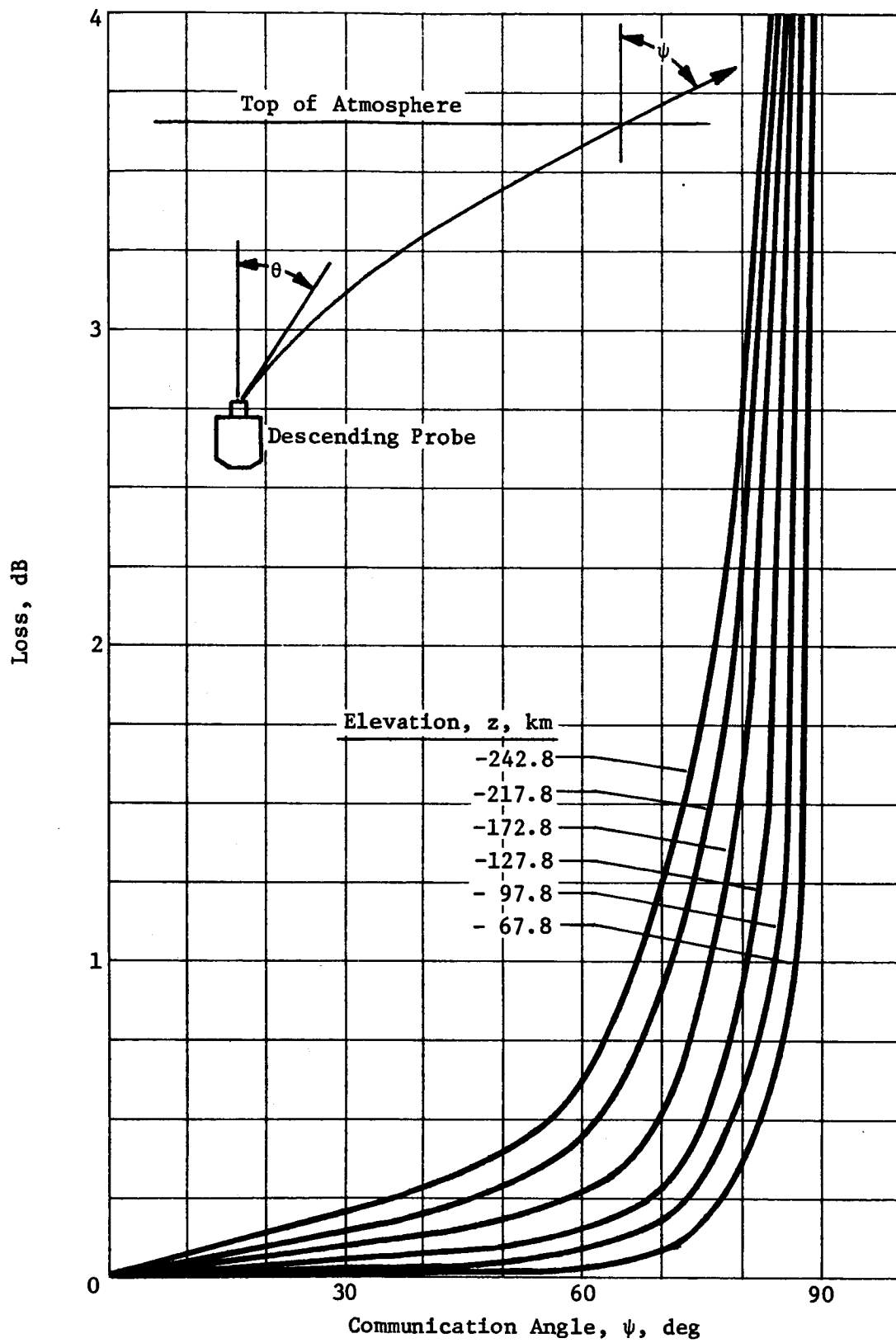


Figure A-6 Defocusing Loss for the Jupiter Cool/Dense Atmosphere

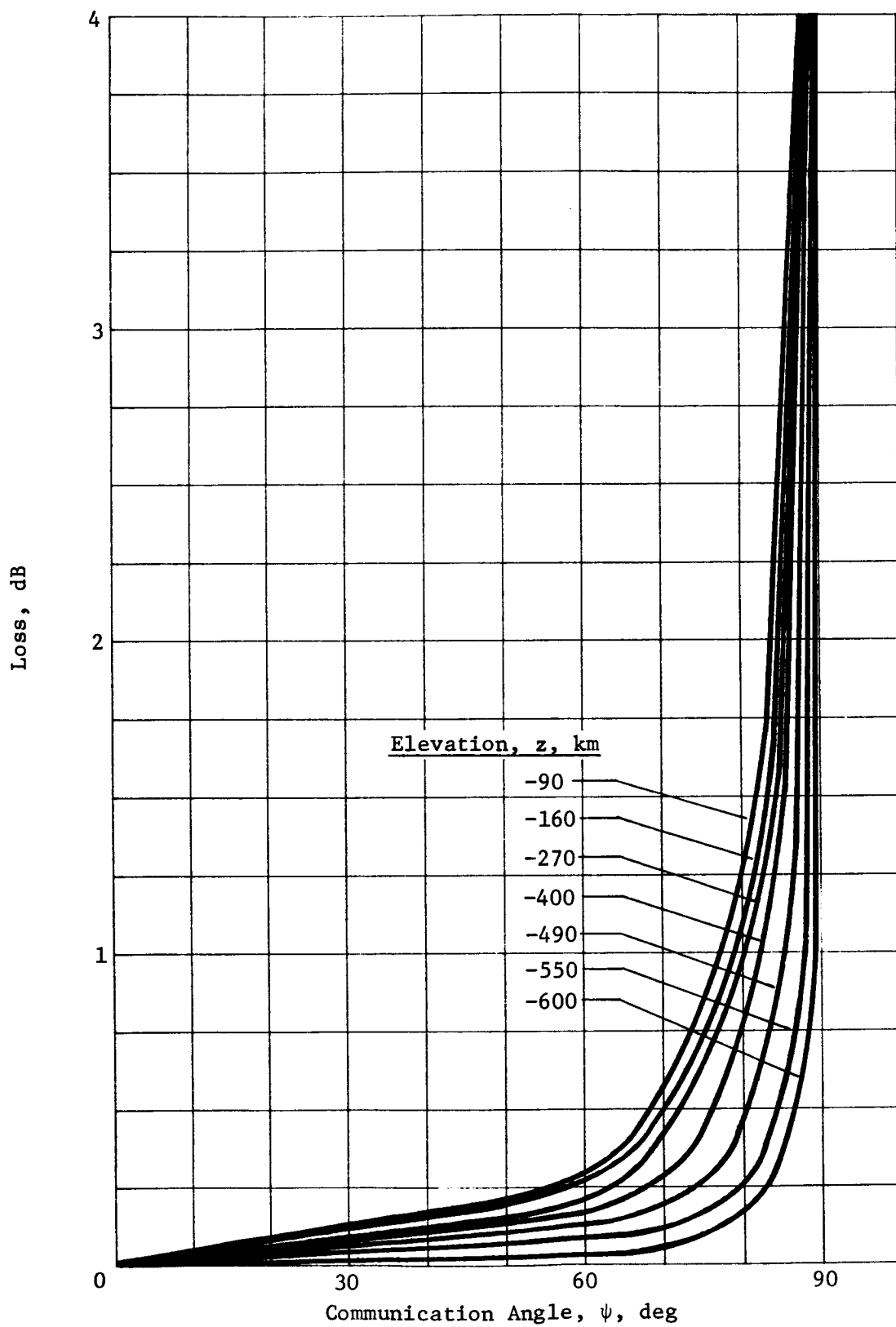


Figure A-7 Defocusing Loss for the Jupiter Nominal Atmosphere

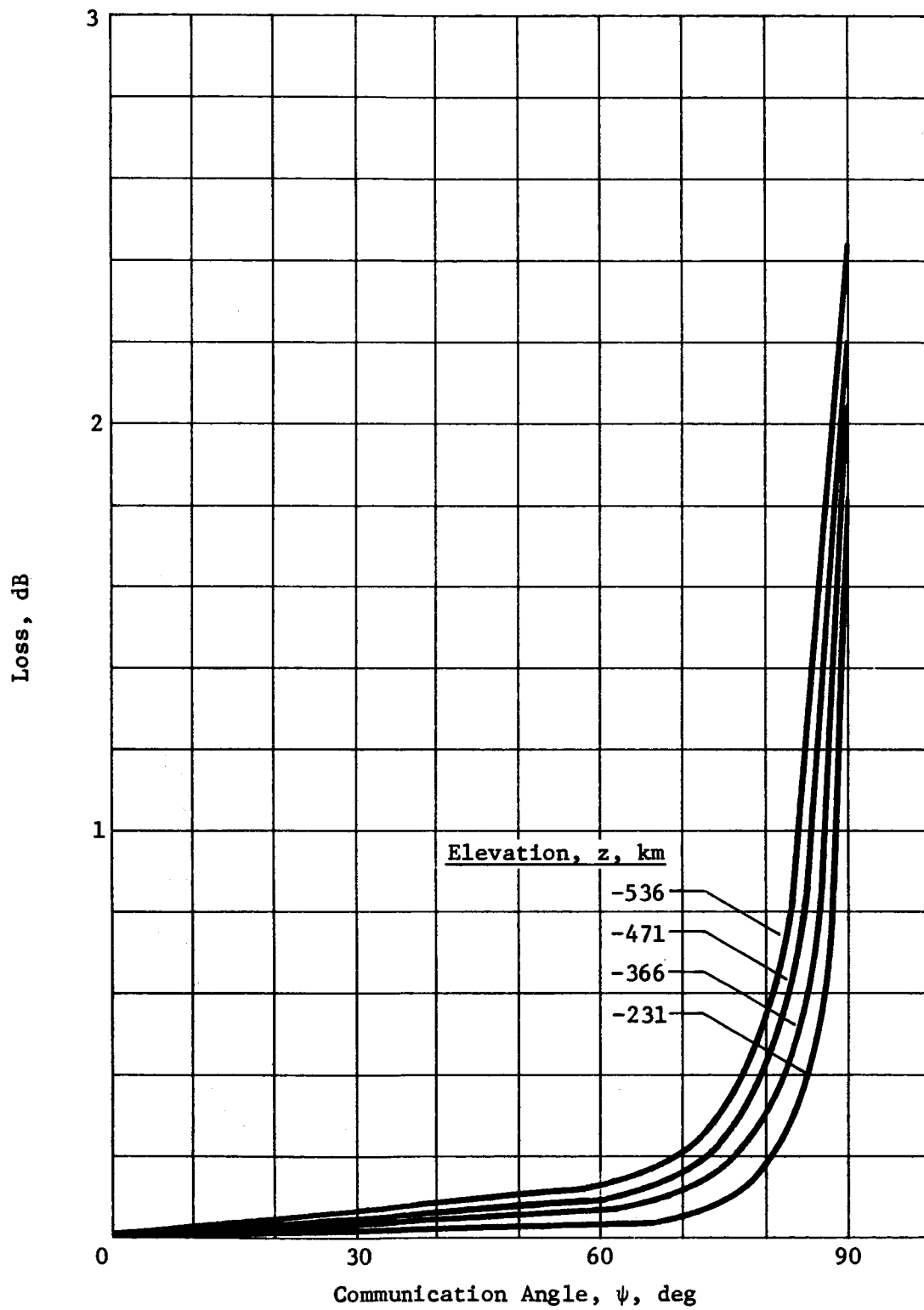


Figure A-8 Defocusing Loss for the Saturn Nominal Atmosphere

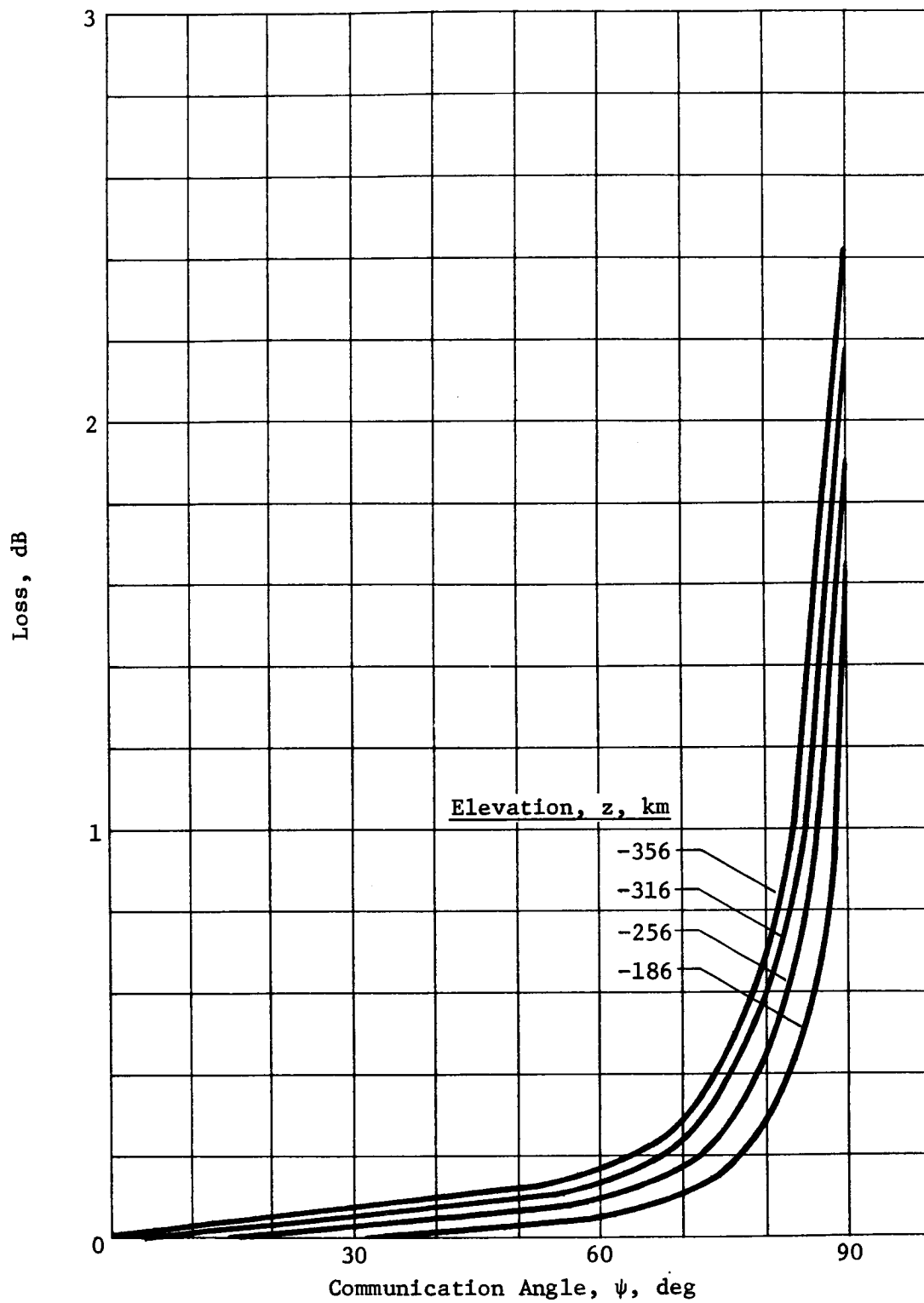


Figure A-9 Defocusing Loss for the Uranus Nominal Atmosphere

A value midway between these bounds gives adequate accuracy for $L_a(\theta)$. As with L_d , it is more useful to plot L_a as a function of ψ . A normalized absorption loss, L_{an} , is plotted for various depths, z , in all four model atmospheres in Figures A-10 through A-13. The plots are normalized to a zenith absorption of 1 dB. To use them, the appropriate value of $L_{an}(\psi, z)$, taken from these curves, must be multiplied by the actual value of zenith absorption, $L_a(0, z, f)$, taken or scaled from Figures A-2 through A-5. It is clear from these curves that the sec ψ approximation is quite good out to 60 deg off zenith.

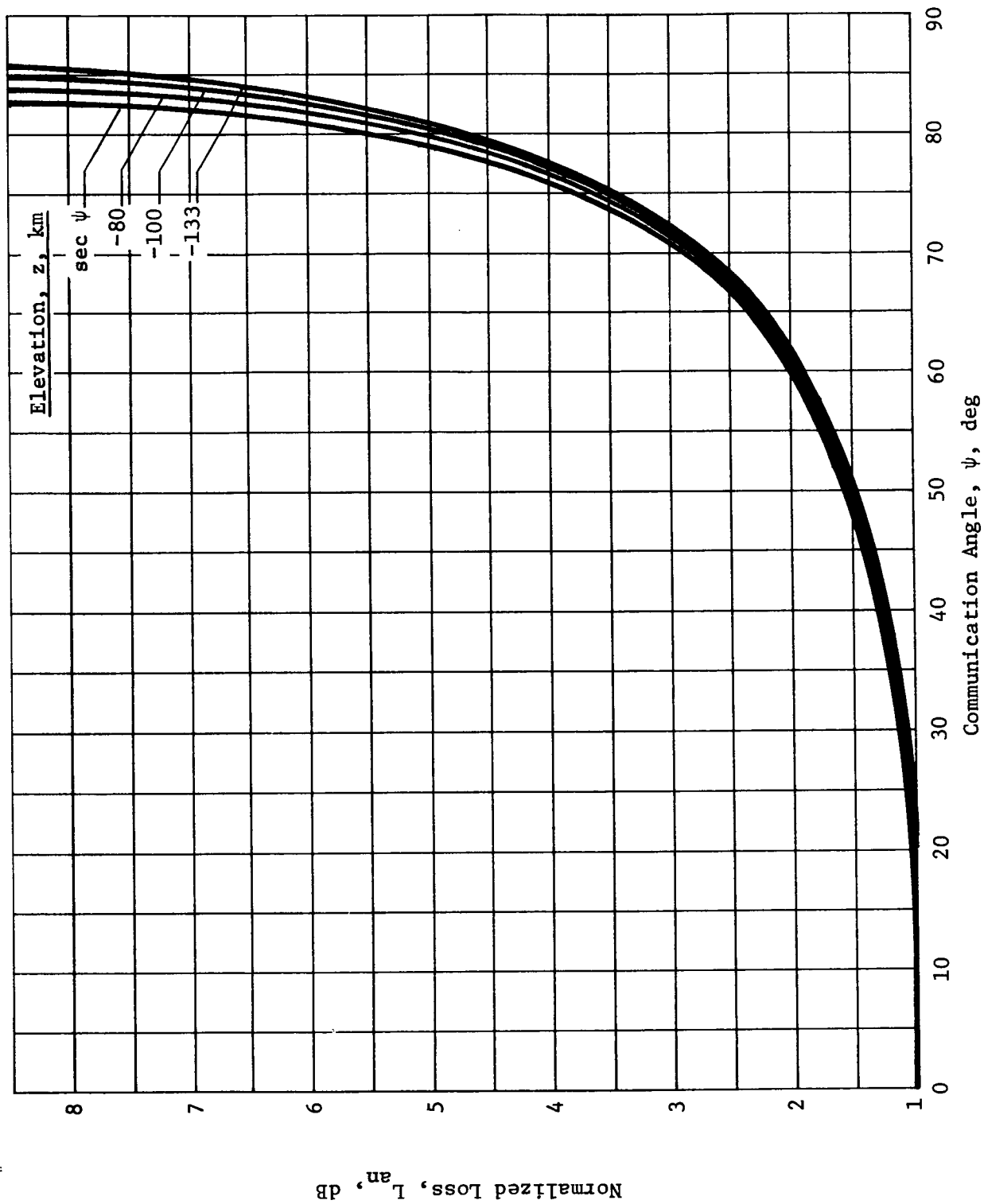


Figure A-10 Normalized Absorption Loss for the Jupiter Cool/Dense Atmosphere

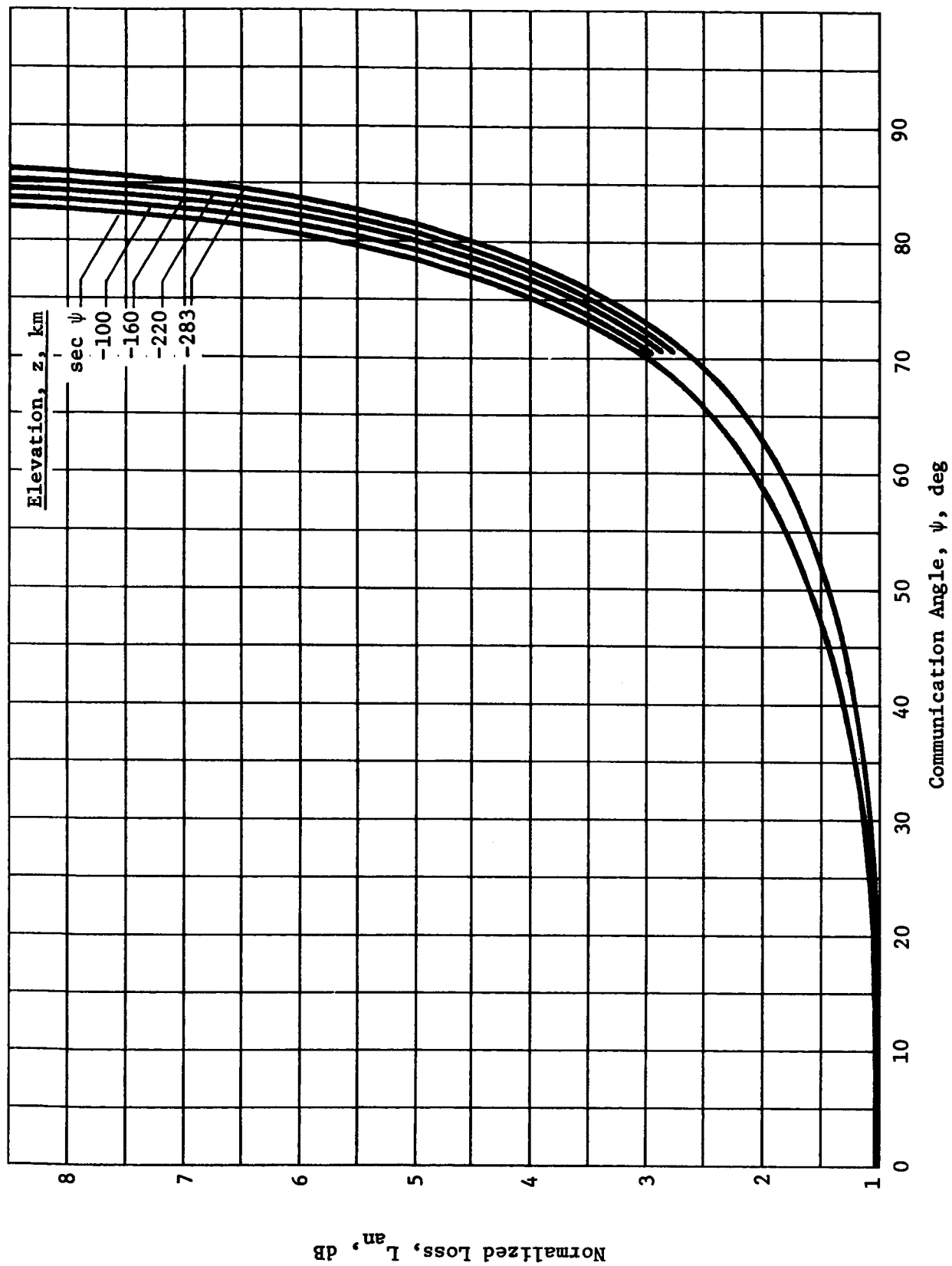


Figure A-11 Normalized Absorption Loss for the Jupiter Nominal Atmosphere

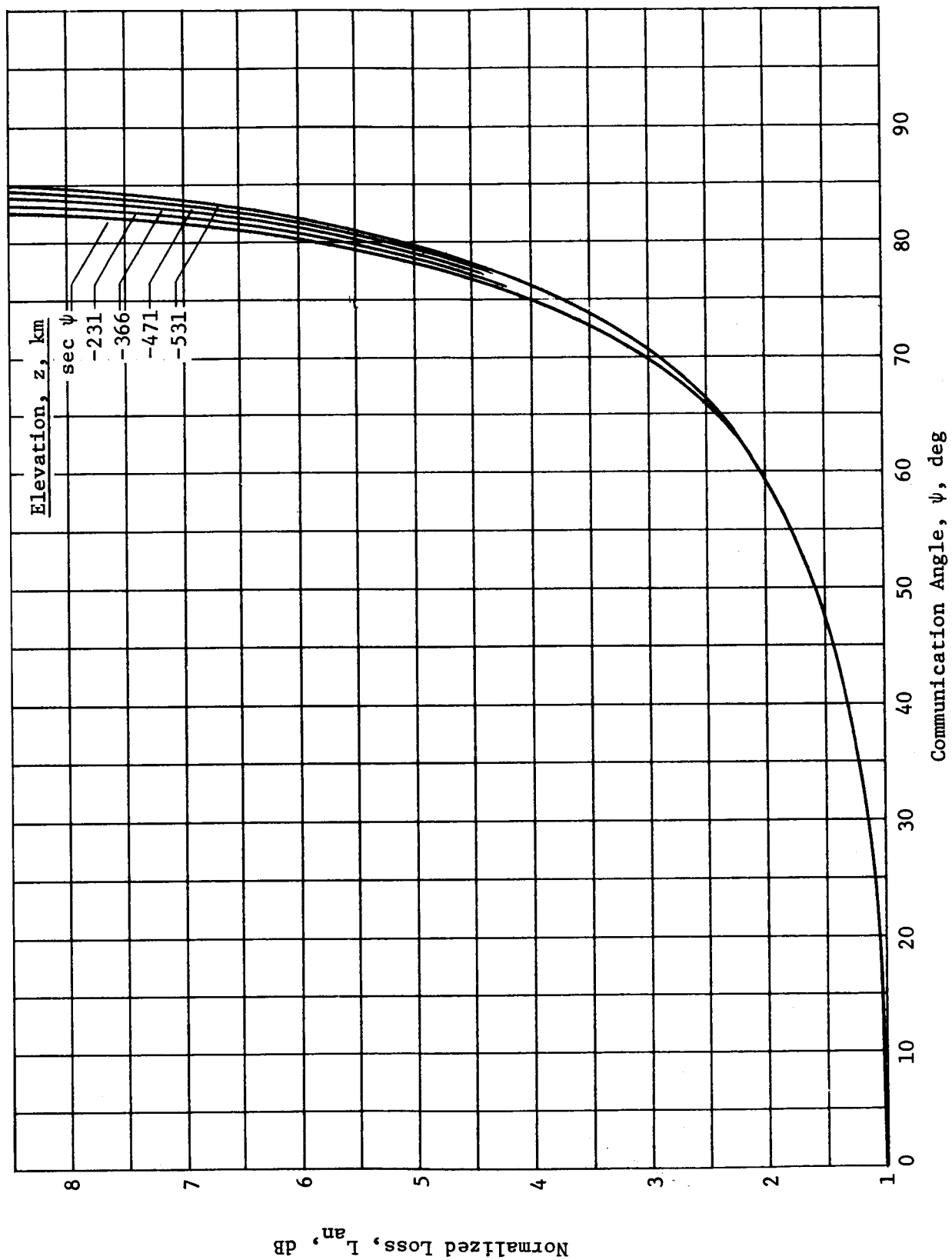


Figure A-12 Normalized Absorption Loss for the Saturn Nominal Atmosphere

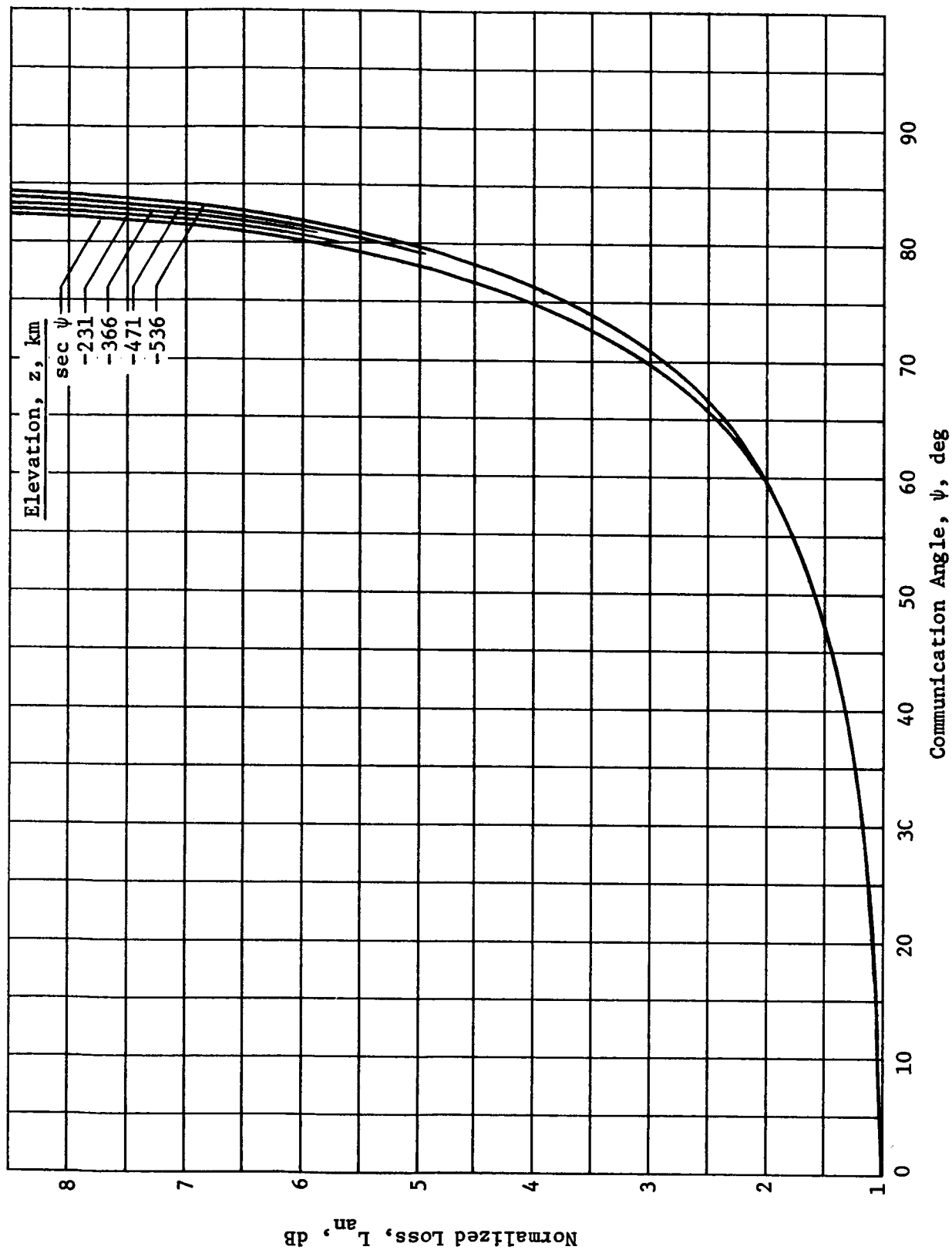


Figure A-13 Normalized Absorption Loss for the Uranus Nominal Atmosphere

TRAJECTORY PROGRAM INPUTS

The curves of Figures A-2 through A-13 were not generally used directly in the link calculations. These calculations have been programmed and incorporated as a subroutine (RATMA) into the trajectory program. Empirical curves were matched to these data, giving combined absorption and defocusing loss in a readily computable form as a function of ψ , z , and f . Atmosphere absorption is calculated for zenith as a function of frequency and elevation. Next, absorption is calculated at the probe aspect angle, ψ . Defocusing loss is also calculated at ψ and the total atmosphere attenuation is the sum of absorption and defocusing losses at ψ . Typical missions are designed with small probe aspect angles ($<20^\circ$) at atmosphere entry and decreasing angle with descent. Therefore, the zenith attenuation is approximately the total attenuation because $L_d(\psi)$ is quite small and $L_a(\psi)$ differs little from $L_a(0)$. In general,

$$L_A(\psi, z, f) = L_a(\psi, z, f) + L_d(\psi, z) \quad [A-29]$$

where

L_A = total atmosphere attenuation including absorption and defocusing loss, dB

L_a = atmosphere absorption, dB

L_d = defocusing loss, dB.

D. REFERENCES

1. S. J. Ducsai: *Jupiter Atmospheric Entry Mission Study, Final Report*, Martin Marietta Corporation, Denver, Colorado, MCR-71-1 (Vol III), Contract JPL 952811, April 1971, pp IV-82 through IV-158.
2. A. Ben-Reuven: "Impact Broadening of Microwave Spectra." *Physical Review*, Vol 145, No. 1, May 1966, p 7.
3. W. Ho, *et al*: "Laboratory Measurements of Microwave Absorption in Models of the Atmosphere of Venus." *Journal of Geophysical Research*, Vol 71, No. 21, November 1, 1966, pp 5091 through 5107.
4. Condon and Odeshaw: *Handbook of Physics*. McGraw-Hill, 1959, Ch 9.
5. W. J. Welch and D. G. Rea: "Upper Limits of Liquid Water in the Venus Atmosphere" *Astrophysical Journal*, Vol 148, No. 6, June 1967, p L151 through L154.
6. S. J. Ducsai: *1975 Venus Multiprobe Mission Study, Final Study Report*. Martin Marietta Corporation, Denver, Colorado, MCR-70-89 (Vol II), Contract JPL 952534, April 1970, pp VII-1 through VII-18.

APPENDIX B

MICROWAVE FREQUENCY SELECTION

R. E. Compton, Jr.

June 7, 1972

MICROWAVE FREQUENCY SELECTION

There are three factors that contribute heavily to the selection of an optimum RF frequency for the probe-to-spacecraft link. These are the system noise temperature, the atmospheric attenuation, and the space loss which is a function of range and frequency. Lower limit bounds are determined by the physical size of the probe antenna for a given wavelength. In general, the receiver system noise temperature increases, the atmospheric attenuation decreases, and the space loss decreases as the frequency is decreased. In addition, for a mission designed with decreasing range and probe aspect angle versus descent, the space loss will also decrease versus time. The probe antenna gain also increases during descent because of a decrease in the probe aspect angle towards the maximum antenna beam gain point.

A. SPACECRAFT ANTENNA TEMPERATURE FOR A JOVIAN MISSION

The noise temperature of the probe relay antenna on the spacecraft is determined by investigating the sources and magnitudes of decimetric (UHF) radiation from Jupiter. There are two sources of RF noise: thermal radiation from the disk and nonthermal UHF radiation from the Jovian magnetosphere. The spacecraft antenna is directed towards the planet disk while the probe is transmitting descent data and encounters the greatest amount of UHF radiation. The antenna temperature used in the previous Jupiter study (Ref 1) was taken from the microwave brightness temperature curve (Ref 2, Fig. 2-2). This curve is depicted in Figure B-1 for reference. The curve attributed all the measured temperature to the planet disk, which results in a higher radiative flux than if the magnetosphere volume had also been considered. At about 3 cm, the equivalent blackbody disk temperature begins to increase rapidly because of contributions from nonthermal sources, as seen in the 1967 curve of Figure B-1. This effect is also evident in the flux density versus wavelength curve which indicates a slowly decreasing trend departing from that expected for blackbody emissions at a fixed temperature.

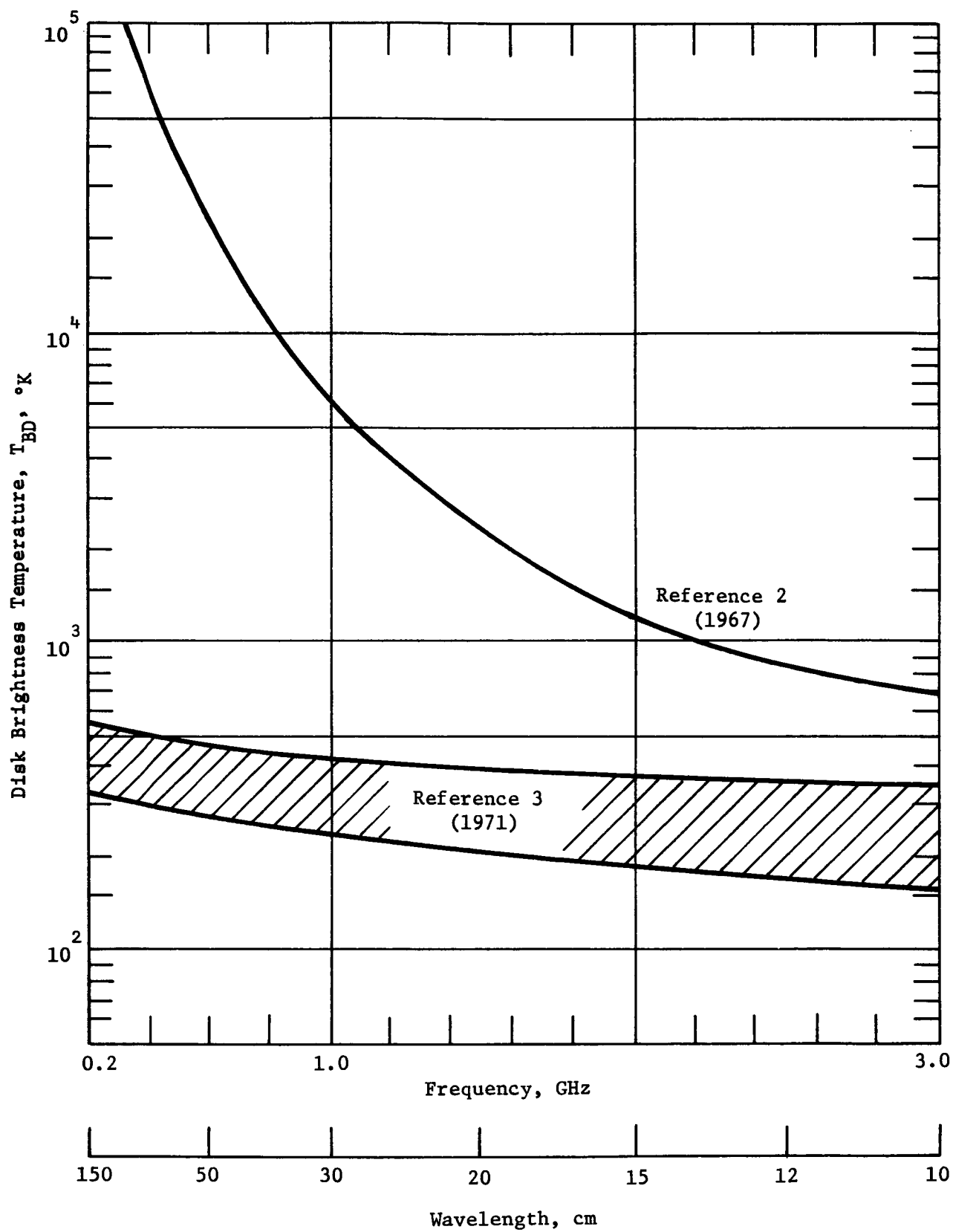


Figure B-1 Jovian Disk Brightness Temperature

It was suggested in 1967 (Ref 2, pp 56, 60-62) that the irregular (decimetric) emission apparently originates in the Jovian radiation belts. Various investigations have shown that the intensity of decimetric radiation appears to be constant over long periods of time and has a strong linearly polarized component with a source dimension several times the size of the visible planet disk. It is generally accepted that the radiation is caused by electrons trapped in the magnetic field of Jupiter, forming a Van Allen belt similar to that about Earth. Synchrotron (relativistic) radiation is the mechanism that explains these observed radiation characteristics. Cyclotron radiation is rejected since it requires the presence of an abnormally strong magnetic field.

The latest available information (Ref 3) provides additional knowledge on the radio radiation environment, particularly the Jovian magnetosphere. The environmental design criteria separate the brightness temperature into the two aforementioned sources and provide a model for synchrotron radiation and a disk brightness temperature curve that is lower than the 1967 data.

Kellermann (Ref 4) summarizes the data of many observers in terms of the brightness temperature, T_{BD} , of Jupiter's thermal disk radiation in the lower curves of Figure B-1. The band indicates, with ample uncertainty limits, the range of values reported by several observers. This curve is also used in the design criteria monograph (Ref 3) for the disk brightness temperature. As seen in Figure B-1, the nonthermal radiation contribution has been removed from the earlier curve (1967) resulting in a lower temperature that is in agreement with the latest observations. Thermal radiation from Jupiter's disk is randomly polarized and its brightness temperature is constant in time and uniform over the Jovian disk surface. The slight increase of T_{BD} with wavelength in the centimeter region implies that the radiation emerges from lower, warmer atmospheric levels at longer wavelengths. Thermal radiation is a significant contributor to the UHF radiation environment near Jupiter.

The 1971 monograph (Ref 3) also provides information for determining the noise temperature caused by the Jovian magnetosphere. Non-thermal radiation is observed from a region several Jupiter radii in extent, elongated parallel to the magnetic equator. The axis of the magnetic field is at an angle to the rotational axis and the center of the field is displaced to the south by $0.75 R_J$ (Ref 2, p 47). Close to Jupiter spatial distribution of the synchrotron radiation requires the use of data reported by Berge (Ref 5) and Branson (Ref 6).

The monograph (Ref 3, p 47) provides a model and equations that yield approximately correct brightness temperatures for the synchrotron source. The model is shown in Figure B-2. A volume is illustrated enclosed by a sphere of radius $3 R_J$ centered on the magnetic dipole and truncated by two planes parallel to and $1 R_J$ away from the magnetic equator. The magnetic axis is tilted from the rotational axis by 8 deg. Displacement of the magnetosphere from the planet disk center was not considered in the model. If D is the path length within the described volume in the direction of observation, the synchrotron brightness temperature, T_{BS} , is given by:

$$T_{BS} = \frac{D\lambda^2}{R_J} (0.3 \pm 0.15) \quad [B-1]$$

with

T_{BS} = synchrotron brightness temperature, °K

D = path length, km

λ = wavelength, cm

= $30/f$

f = frequency, GHz

R_J = Jupiter radius, 71,422 km.

The noise temperature of the spacecraft relay antenna is the sum of the thermal disk noise and synchrotron noise since they are considered to be two separate sources and the fluxes add directly. Initial analysis indicated that the worst-case temperature existed when both sources are within the beam of the antenna. For the nominal Jupiter probe mission (Vol. II, Section VB), this geometry exists from near entry to the end of the mission as seen in Figure B-3. The probe-to-spacecraft range decreases with range from E - 1.2 hr and then increases to entry. During descent, the range again begins to decrease as seen in Figure B-3. The maximum range during probe transmission occurs at entry and is 9.7×10^4 km or $1.36 R_J$. Periapsis ($2 R_J$) is not reached until after mission completion. The maximum synchrotron temperature from Equation [B-1] is:

$$T_{BS} = 1.36 \times 0.45 \lambda^2 = 0.61 \lambda^2 \quad [B-2]$$

and

$$T_A = T_{BD} + T_{BS} \quad [B-3]$$

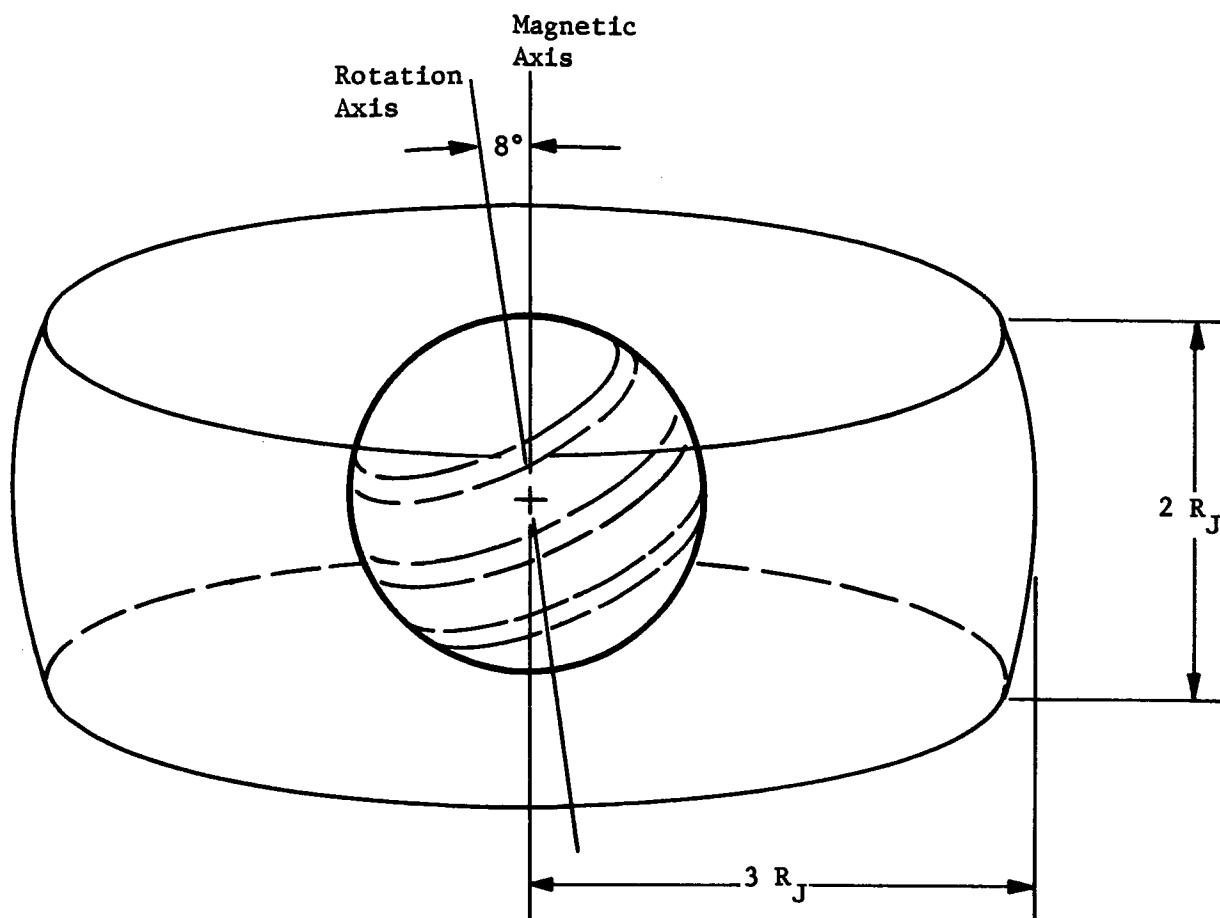


Figure B-2 Jovian Magnetosphere Model

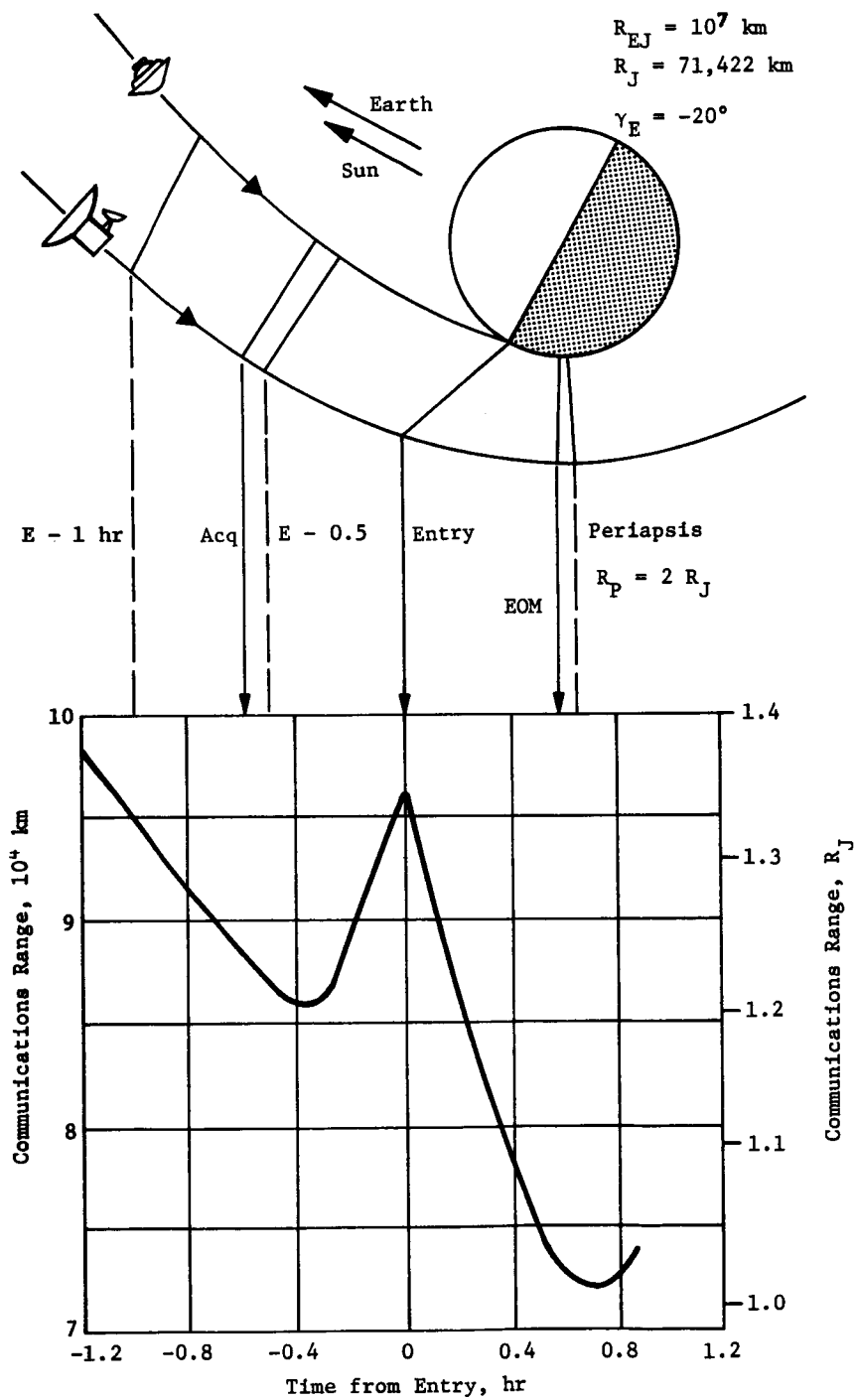


Figure B-3 Probe-to-Spacecraft Communications Range for the Nominal Jupiter Probe

The worst-case antenna noise temperature is shown in Figure B-4 and is the sum of radiation fluxes from the two sources (Equation [B-3]). The thermal disk brightness temperature is the upper limit curve of Figure B-1 from the new (1971) monograph. Results of the original study are also shown for comparison. The new curve is reduced by a factor of 6 at 1 GHz. The noise temperature contribution from the magnetosphere is a function of the spacecraft trajectory and the extent that the line-of-sight vector from the antenna to the probe intersects the magnetosphere model (Ref 7). Any periapsis radius greater than $3 R_J$ will penetrate the total magnetosphere model boundary and the maximum path length in the volume without intersecting the planet disk is $5.7 R_J$ as seen in Figure B-5. The maximum synchrotron temperature for trajectories that do not intersect the magnetosphere is given from Equation [B-1] for $5.7 R_J$ by :

$$T_{BS} = 5.7 \times 0.45 \lambda^2 = 2.57 \lambda^2 \quad [B-4]$$

with the wavelength in cm and the temperature in °K. Equation [B-4] is equal to the antenna temperature if the planet disk is not within the field of view of the antenna. The thermal disk temperature must be added to Equation [B-4] if the planet disk falls within the 3-dB beamwidth of the antenna.

The curve shown in Figure B-4 was used for the spacecraft antenna noise temperature and is the worst-case condition for a mission with the spacecraft in the magnetosphere such as for the nominal Jupiter probe (Vol II, Section VB) and for the probe-dedicated Jupiter mission (Vol II, Section VC).

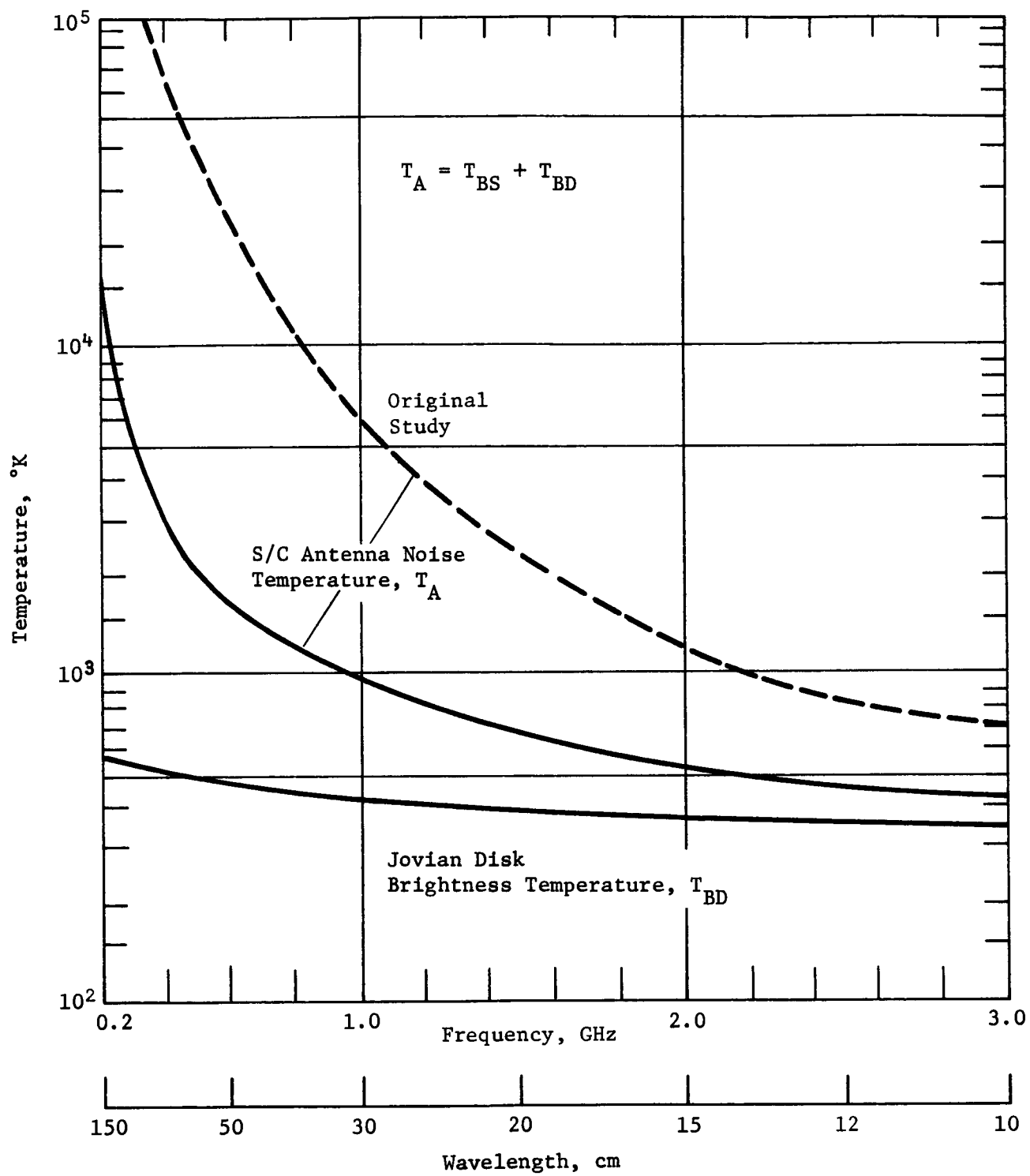
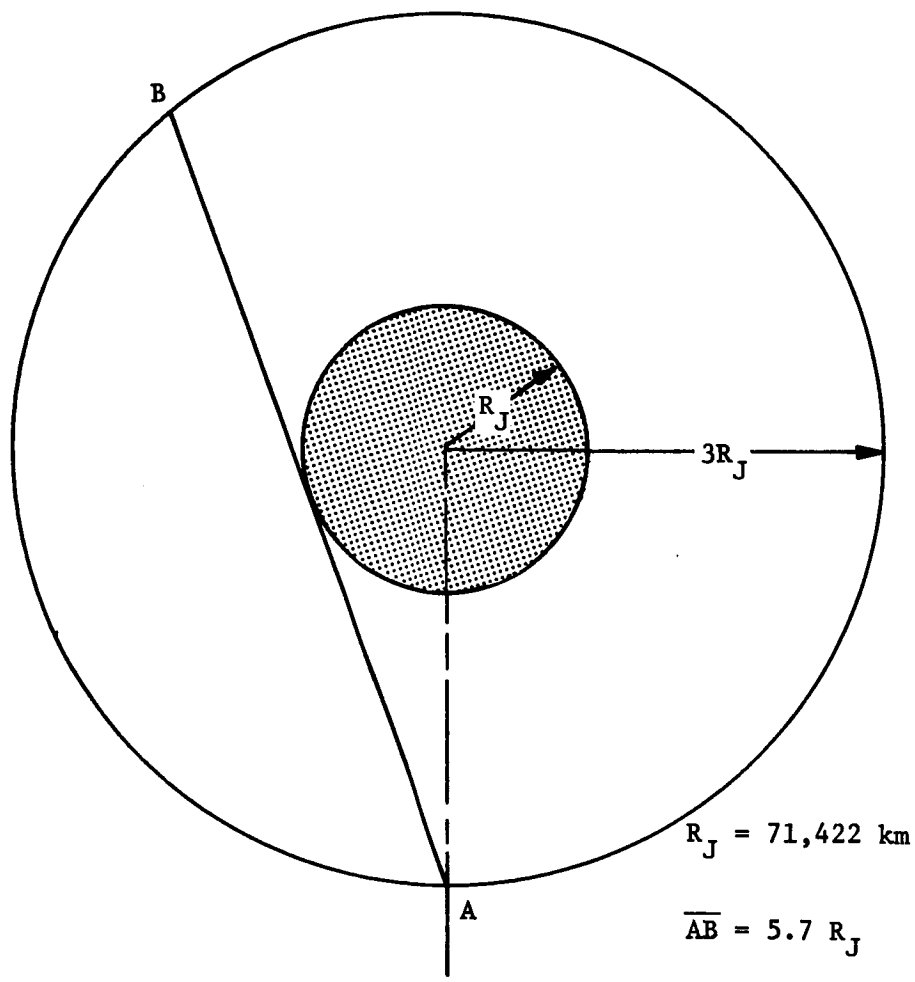


Figure B-4 Spacecraft Antenna Noise Temperature



Top View of Magnetosphere Model

Figure B-5 Jovian Magnetosphere Penetration Distance

B. SPACECRAFT RECEIVING SYSTEM TEMPERATURE

The noise temperature of the receiving system at the receiver output is determined by the sum of the spacecraft antenna noise temperature, T_A and receiver effective noise temperature (ENT),

T_R , as follows:

$$T_S = T_A + T_R. \quad [B-5]$$

As discussed in the previous section, the antenna noise temperature, as shown in Figure B-4, is the sum of thermal disk and synchrotron noise (Equation [B-3]). The two sources of radiation, the thermal disk brightness temperature and synchrotron radiation from the Jovian magnetosphere, are added directly to determine the total spacecraft antenna temperature. Synchrotron radiation is dependent upon the relative geometry of the magnetosphere and line-of-sight vector as seen in Figure B-5.

The ENT of solid-state receivers for the frequency range of interest is shown in Figure B-6. The curves depict the temperature and noise figure (with 290°K reference) for tunnel diode and transistor receivers based upon the 1972 state of the art. An average value, one decibel above the minimum curves shown, was used in the study. As seen in the figure, the average value falls along the germanium transistor values. Using the average curve, results in the receiver ENT increasing with increasing frequency, and is 4 dB at S-band. Receiver ENT and noise figure (NF) are related by

$$NF = 10 \log_{10} \left(1 + \frac{ENT}{T_R} \right) \quad [B-6]$$

where

NF = receiver noise figure, dB

ENT = receiver effective noise temperature, T_R , °K

T_r = ambient reference temperature, 290°K.

The spacecraft antenna noise temperature of Figure B-4 is added to the average ENT from Figure B-6 to obtain the spacecraft receiving system temperature, as shown in Figure B-7. The decrease in antenna temperature with increasing frequency is compensated by the corresponding increase in receiver ENT resulting in a nearly constant system temperature of 1000°K from 1.5 GHz through S-band.

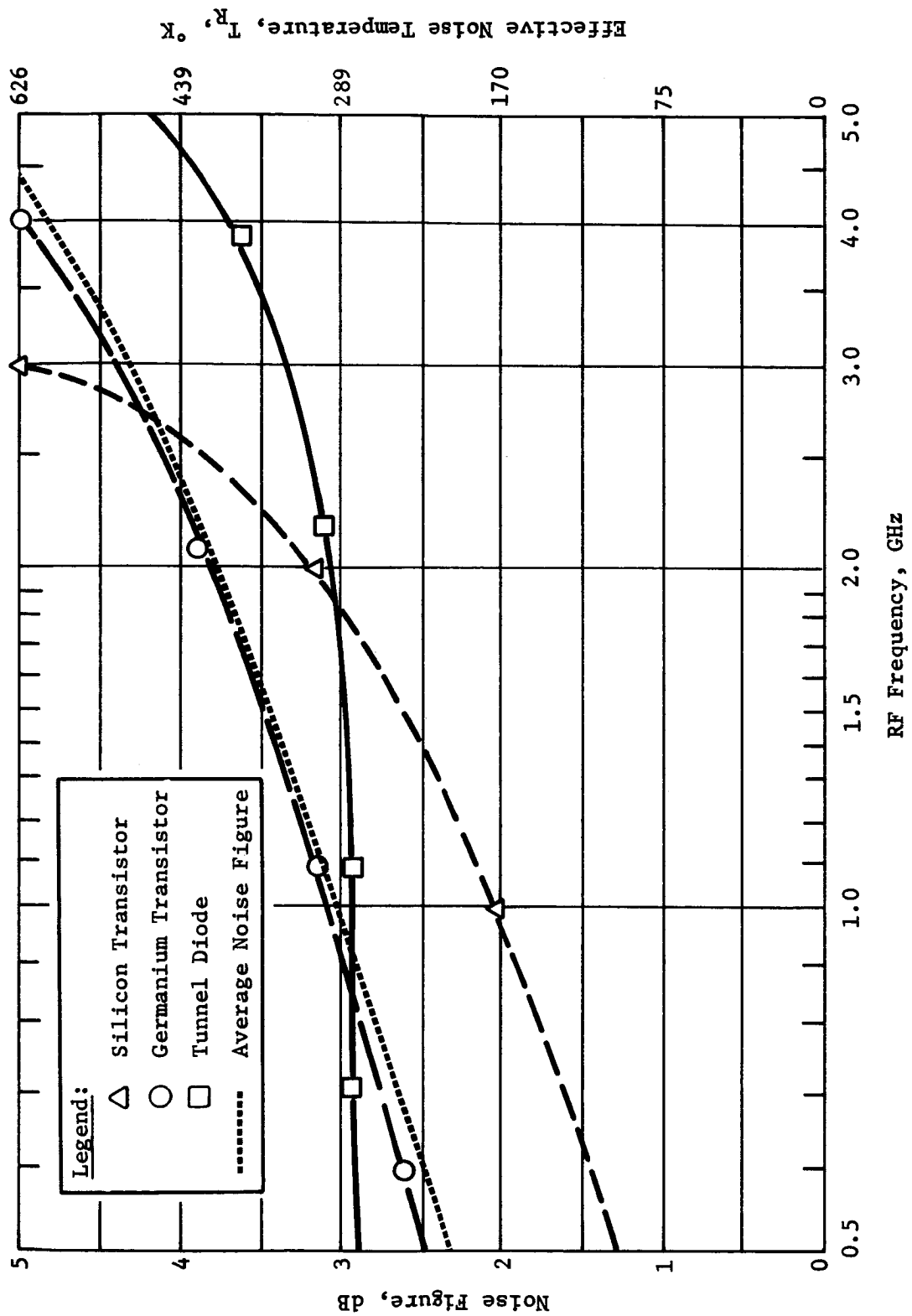


Figure B-6 1972 Noise Figure State of the Art for Tunnel Diodes and Transistor Amplifiers

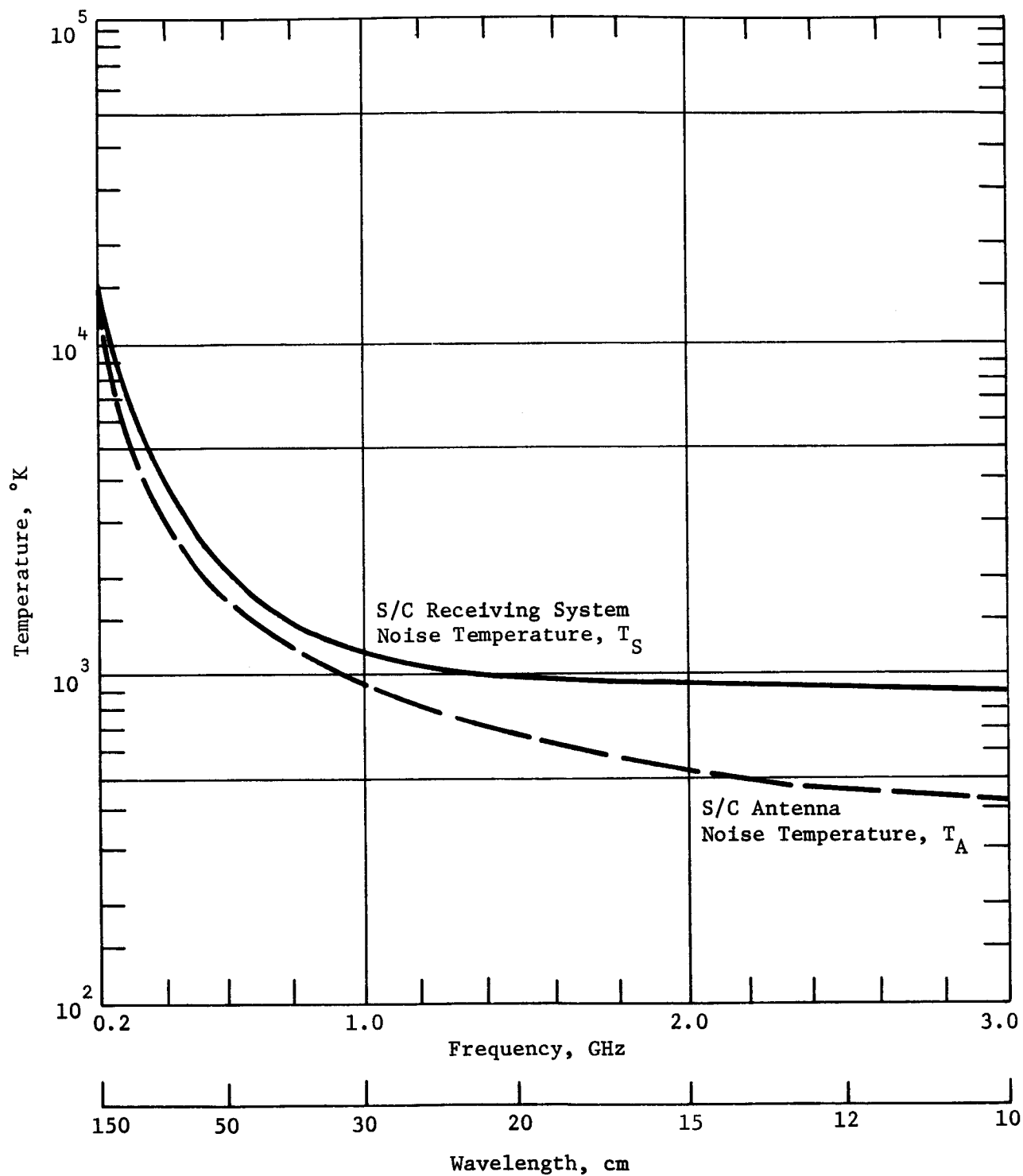


Figure B-7 Spacecraft Receiving System Temperature

C. ATMOSPHERIC ATTENUATION

The second dominant factor to be considered along with receiving system temperature is atmospheric losses. As described in detail in Appendix A, these include atmospheric attenuation due to the atmospheric constituents including clouds, as well as defocusing losses resulting from ray bending and diffraction. Figure B-8 shows the Jovian atmosphere attenuation versus frequency for the cool/dense atmosphere. The curves are for different depths into the cool/dense atmosphere at mission completion. The nominal Jupiter probe trajectory is adjusted in lead time to give decreasing probe aspect angle (ψ) versus descent time. Atmosphere absorption increases from the zenith value according to the relation

$$A_T = \frac{A_z}{\cos \psi} = A_z \sec \psi \quad [B-7]$$

where

A_z = zenith attenuation, dB

A_T = atmosphere attenuation at path angle ψ , dB

ψ = probe aspect angle, deg.

The aspect angle for the depths shown is approximately 5 deg. The results are less than 1% greater than the zenith value ($\sec 5^\circ$).

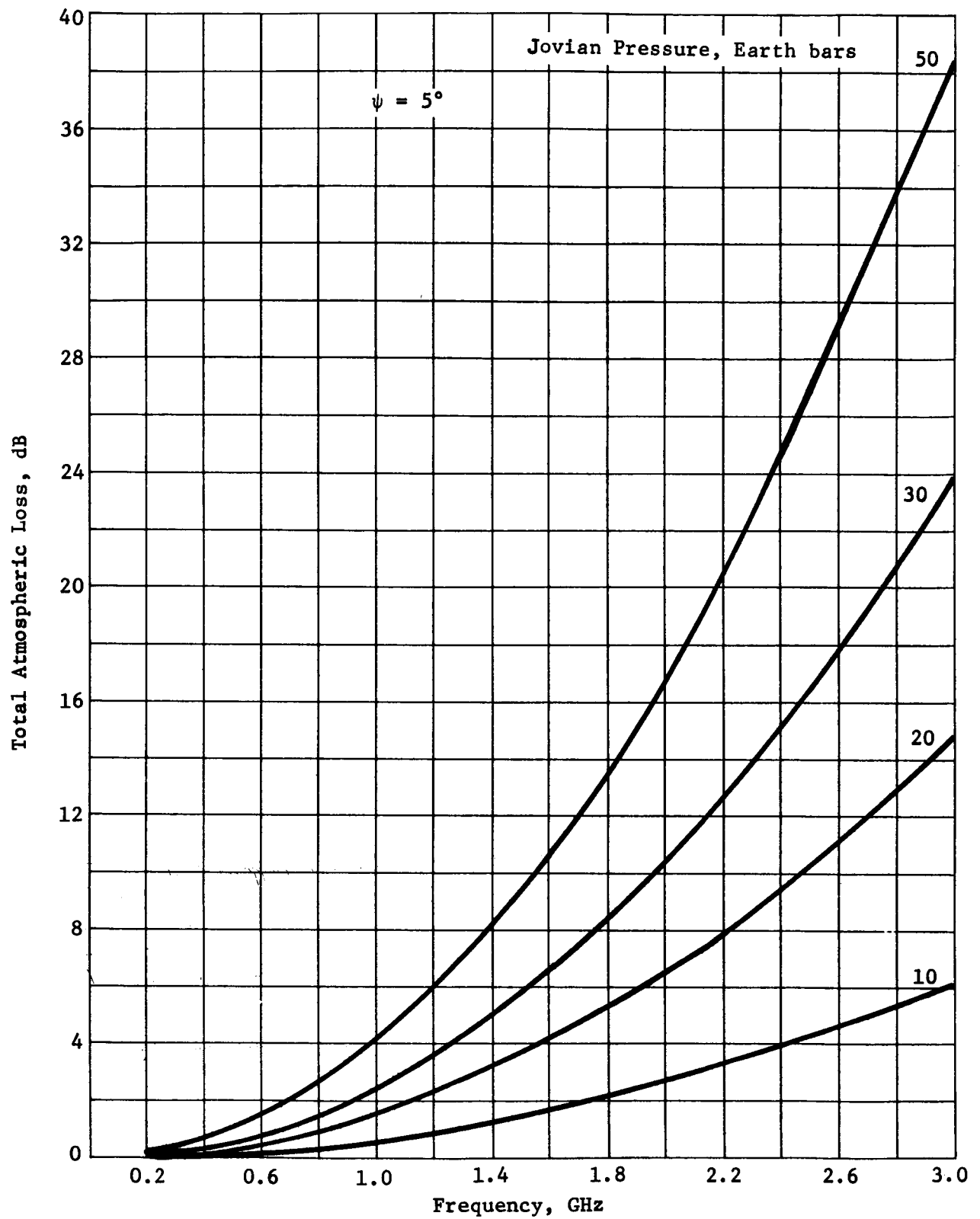


Figure B-8 End-of-Mission Attenuation for Jupiter Cool/Dense Atmosphere

D. FREQUENCY-DEPENDENT POWER REQUIREMENTS

Figure B-9 shows the relative effects on a communication link of the spacecraft receiving system temperature and atmospheric losses at a probe aspect angle of 5 deg for various descent depths as a function of frequency. The curves were obtained from the algebraic sum of Figures B-7 and B-8, with Figure B-7 converted to decibels with a reference frequency of 1 GHz. The relative power gain represents the additional link power gain required to overcome the combined effects of system temperature and atmospheric attenuation for other frequencies and penetration into the atmosphere. It is further assumed that the probe antenna gain is constant for all frequencies (constant beamwidth, variable size) and the spacecraft antenna diameter is constant (variable gain and beamwidth with frequency) such that the product of space loss and space antenna gain at any frequency of interest is constant.

The RF link computer program used in the study maintains constant probe and spacecraft antenna beamwidth and maximum gain (variable aperture size) as a function of frequency, so decreasing range will affect the relative power required. The relative power required for the nominal Jupiter probe is shown in Figure B-10 for the conditions noted on the figure. Space loss reduction and higher probe antenna gain resulting from decreasing aspect angle during descent, as seen in Figure B-11, considerably alters the shape of the curves from these shown in Figure B-9. As seen in Figure B-10, increasing frequencies above 400 MHz results in increasing relative power required to achieve a particular depth. Stated in another way, the lower frequencies are affected less by the variables in the RF link such as atmosphere loss, noise temperature, space loss, and probe antenna gain. The curves of Figure B-10 are for a trajectory optimized to 30 bars. Below 900 MHz, more power is required at entry than at a depth of 30 bars which result from trajectory optimization of range and probe aspect angle. Above 900 MHz, atmospheric loss, which is proportional to frequency, dominates and the worst-case power requirement occurs at the end of the mission (30 bars). Other various combinations can be determined from the curves in Figure B-10, keeping in mind that the probe antenna is size-limited for effective apertures equal to 22.85 cm (9 in.).

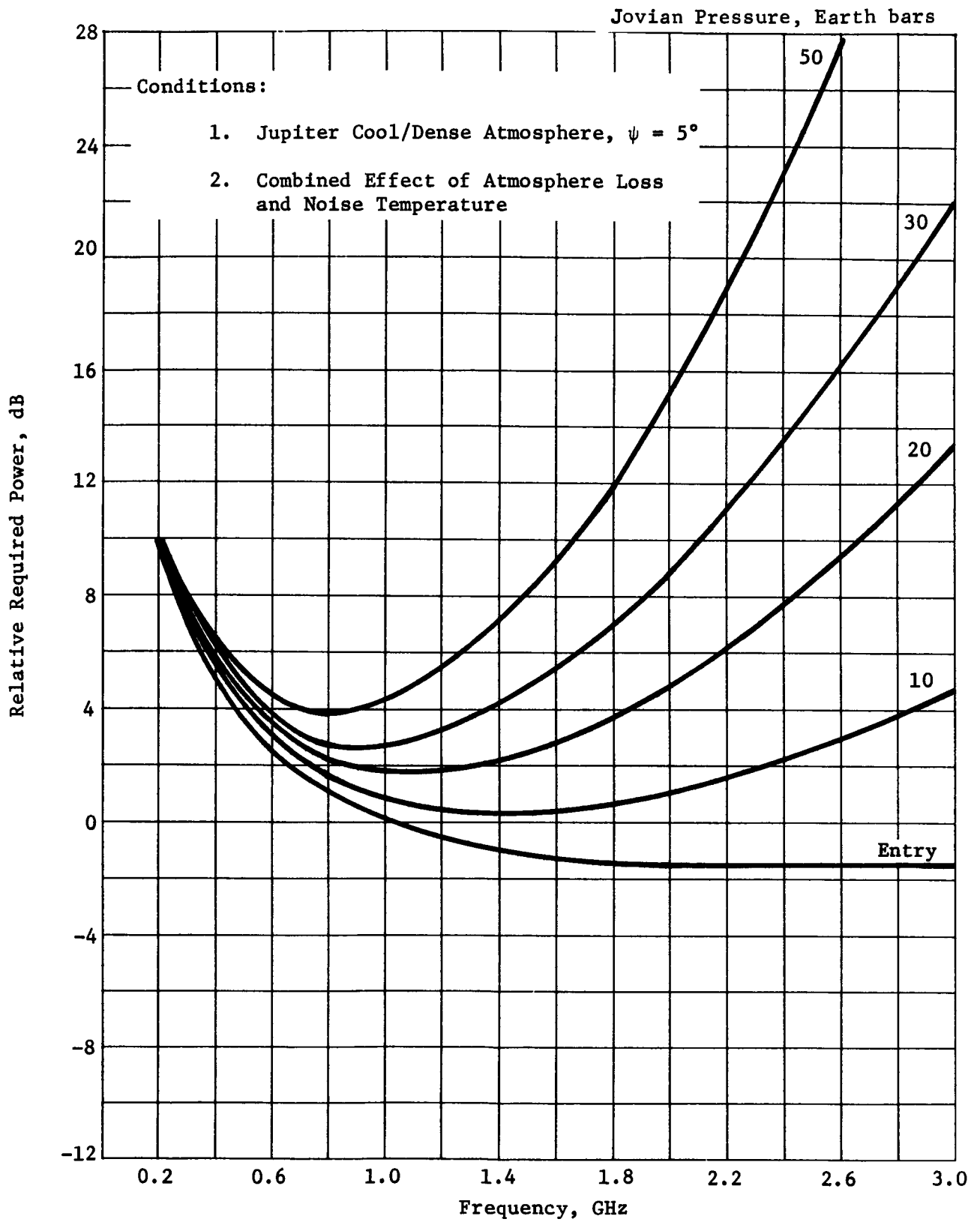


Figure B-9 Relative Required Power for the Nominal Jupiter Probe Descent with Constant S/C Antenna Diameter and Fixed Probe Antenna Gain

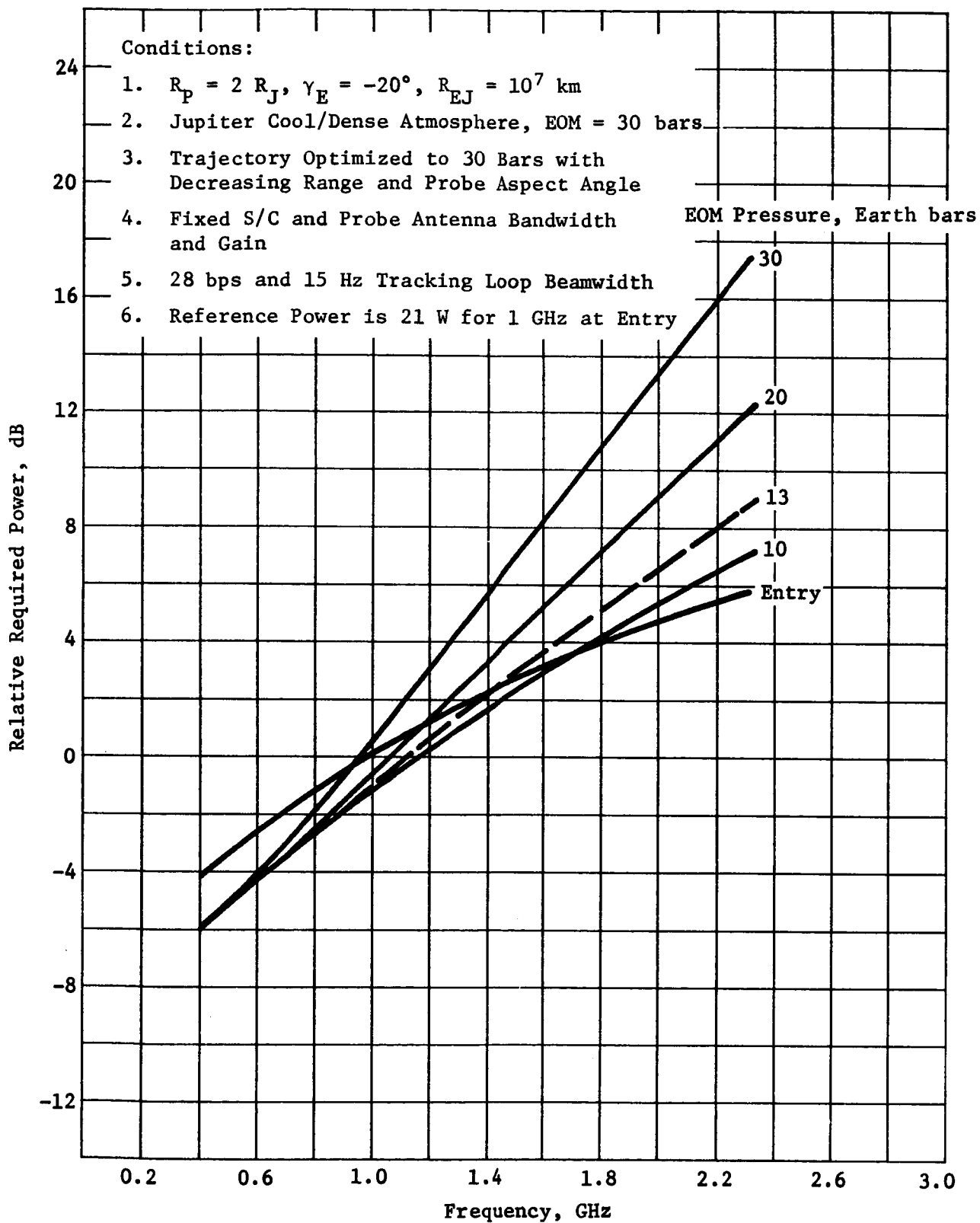
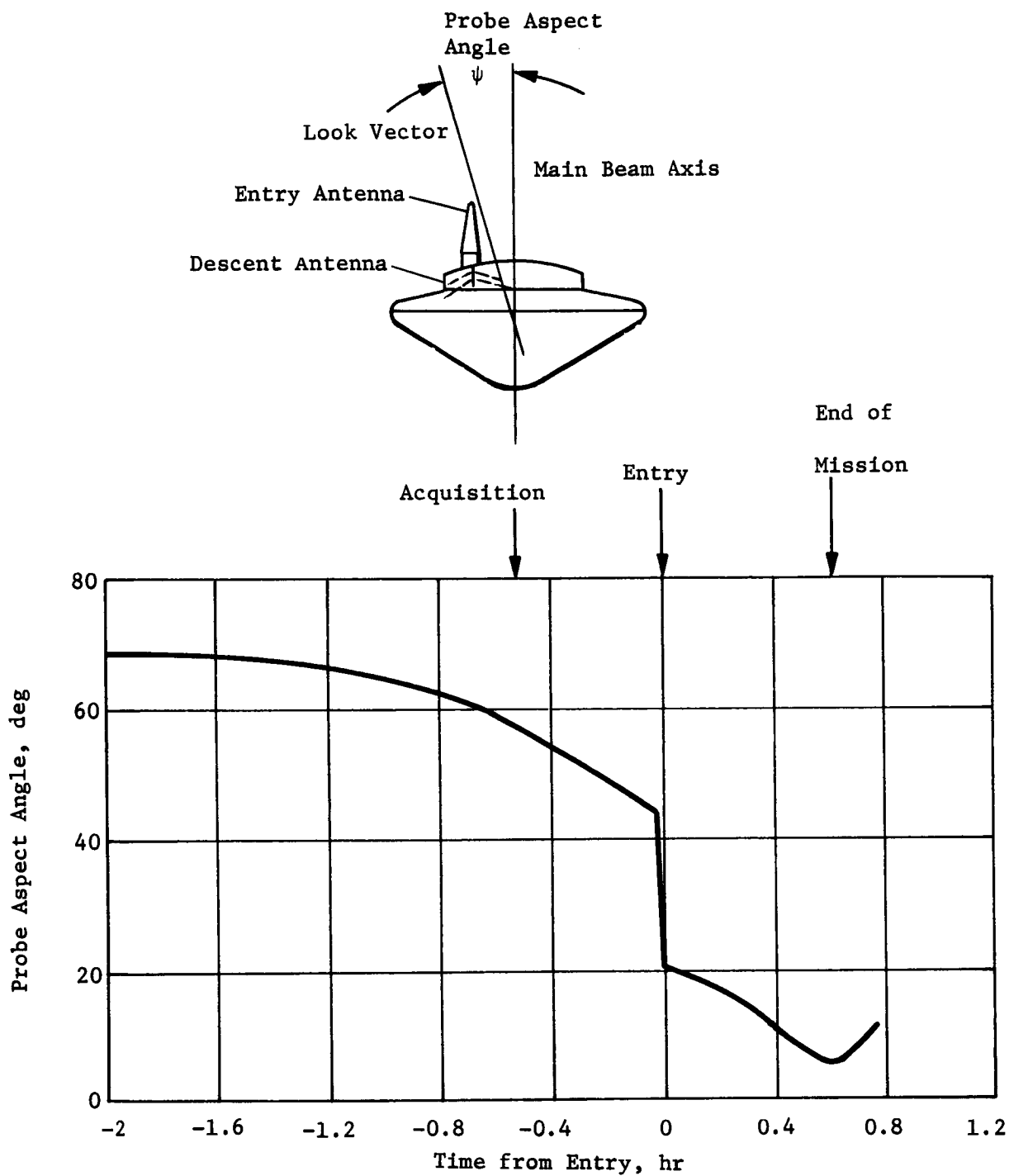


Figure B-10 Relative Power Required for Jovian Descent,
Nominal Jupiter Probe



Conditions: $R_P = 2 R_J$

$T_L = 46 \text{ min}$

$R_{RJ} = 10^7 \text{ km}$

EOM = 30 bars

$\gamma_E = -20^\circ$

Cool/Dense Atmosphere

Figure B-11 Nominal Jupiter Probe Aspect Angle

For simple dipole structures, we set

$$\frac{\lambda}{2} = 22.85$$

and

$$\lambda = 45.7 \text{ cm};$$

therefore

$$f = \frac{30}{\lambda} = 650 \text{ MHz.}$$

[B-8]

Therefore, the minimum operating frequency is 650 MHz because of probe antenna size limits, unless a complex phased array is considered. This is not practical because of the additional costs associated with array development.

E. REFERENCES

1. *Jupiter Atmospheric Entry Mission Study Final Report*, Vol III. Contract JPL 952811, Martin Marietta Corporation, Denver, Colorado, MCR-71-1 (III), April 1971, pp IV-106 through 112
2. C. M. Michaux, et al: *Handbook of the Physical Properties of the Planet Jupiter*. NASA SP-3031, 1967, pp 47-56, 60-62
3. *The Planet Jupiter (1970)*. NASA Space Vehicle Design Criteria (Environment), NASA SP-8069, December 1971, pp 13-15
4. K. I. Kellermann: "Thermal Radio Emission from the Major Planets." *Radio Science*, Vol 5, No. 2, 1970, p 487
5. G. L. Berge: "An Interferometric Study of Jupiter's Decimeter Radio Emission." *Astrophysics Journal*, Vol 146, No. 3, 1966, p 767
6. N. J. Branson: "High Resolution Radio Observations of the Planet Jupiter." *Royal Astronomical Society Monthly Notices*, Vol 139, 1968, p 155
7. J. W. Davenport and D. A. DeWolf: *Investigation of Line-of-Sight Propagation in Dense Atmosphere, Phase II*. RCA Labs, Princeton, N. J. NASA CR-114288, July 1971, pp 24-34.

APPENDIX C

SPACECRAFT RECEIVER

E. A. Berkery

June 7, 1972

SPACECRAFT RECEIVER

The design of the spacecraft receiver is a function of the modulation technique, coding, Doppler uncertainty and Doppler rate. The modulation technique was selected for the purpose of evaluation rather than optimization. PSK modulation has been well studied for many applications and evaluated in the Jupiter atmospheric study.* Although PSK would provide the lowest power link, it is subject to phase disturbances in the planetary atmospheres which are largely unknown. Binary FSK modulation was therefore chosen as a less susceptible approach. This type of modulation has problem areas associated with acquisition and tracking. The possibility of receiving and recording a broadband corresponding to the frequency uncertainty was considered and discarded because of the large storage requirements on the spacecraft and the ultimate difficulty of demodulating and decoding the signal at the ground terminal. As a result, the principle efforts in the development of the spacecraft receiver configuration were directed at specifying and defining the method of tracking and acquisition. The final approach by which the data is relayed to the ground terminal may select one of several alternatives, recording a narrow pre-demodulation bandwidth or demodulation with or without decoding. A full evaluation of these alternatives involves basic communication research, is also influenced by spacecraft capability, and is considered beyond the scope of this contract.

A. ACQUISITION

The problem of acquisition was initially studied with the intent to acquire and track the data tones. First approaches considered methods for combining the two data signals, both before and after demodulation. The former was considered in systems that used a beat oscillator frequency midway between the two data tones, and two beat oscillator frequencies located at equal frequency distances from the two tones. These predetection combination methods would make maximum use of the received signal but had been discarded because of difficulty in establishing that phase coherency of the summed output signals could be achieved. Tracking and

*Jupiter Atmospheric Entry Mission Study Final Report, Vol III. Contract JPL 952811, Martin Marietta Aerospace, Denver, Colorado, MCR-71-1 (III), April 1971. pp IV-27 through IV-34.

acquisition of combined post detection signals had to be discarded because of insufficient signal-to-noise ratio. This approach is further compromised by the use of coding, which decreases signal power and increases bandwidth. There is an obvious tradeoff for this approach as the data rate decreases, uncoded data would provide sufficient power density in a narrow band to allow acquisition and tracking of the data signal. Also, since many of the probe missions require RF power outputs that are well below the present state-of-the-art capability, increasing the power could decrease the complexity of the spacecraft receiver as compared with the approach selected in this study. It is reasonable to consider that a flight design will provide excess margin wherever possible rather than the minimum power required by the analysis of the mission. In view of the above considerations, a link that provided a constant tone signal in addition to the binary FSK tones was finally selected as a realizable system.

The basis of the evaluation is given here and is derived directly from NASA CR-73005, Appendix G. This paper considers the acquisition of a signal, with frequency changing linearly with time, and having 99% probability of acquisition and 1% probability of false alarm. Although the reference considers a data signal, the analysis is based on a tone and is therefore appropriate to the analysis of a binary FSK system with a tracking and acquisition tone. The results of the analysis are summarized in the following equations.

$$\left(\frac{S}{N_o}\right)_a \geq 4.66 \sqrt{R} + 10.86 \frac{R}{B}$$

$$\left(\frac{S}{N}\right)_a \geq 1$$

$$\left(\frac{S}{N}\right)_T \geq 10$$

R = frequency rate of change, Hertz/sec

B = filter bandwidth

N_o = noise power spectral density

N = noise in bandwidth = BN_o

*S. Georgiev: *A Feasibility Study of an Experiment for Determining the Properties of the Mars Atmosphere*. Final Report, Vol III, *Subsystem and Technical Analysis*. Contract NAS2-2970, Avco Corporation, Lowell, Mass. NASA CR-73005, Appendix G, September 1966.

Subscripts

a = acquisition

T = tracking

The first equation has been somewhat modified from the original (Eq [G-72] in Appendix G) for application to the probe acquisition problem. These equations are plotted in Figure C-1. A 20-dB signal-to-noise ratio line, which is pertinent to the receiver configuration and the data power for a nominal Jupiter probe design (Vol II Section V.B) is also plotted for completeness. The original goal in this design was to achieve acquisition in 100 seconds with the probabilities previously stated, and minimum acquisition and tracking tone power. The acquisition technique used here is to sweep the local oscillator with a sawtooth waveform so that the combination of sweep rate and maximum Doppler rate provides a rate of change equal to selected rate R. Initial acquisition takes place in a wide band filter/detector $[(S/N)_a \geq 0 \text{ dB}]$. The sweep rate is then decreased and final acquisition takes place in a narrow band filter $[(S/N)_a \geq 13 \text{ dB}]$. The frequency tracking loop $[(S/N) \geq 10 \text{ dB}]$ is then activated and tracking ensues. Since the center frequency of the narrow band filter will be the same as that of the tracking filter, acquisition and lock by the tracking loop is assured. As an example,

$\Delta f = 40 \text{ kHz}$ (frequency uncertainty)

$T_a = 100 \text{ sec}$ (acquisition time)

Then $R = \Delta f / T_a = 400 \text{ Hz/sec}$

$B_a = 120 \text{ Hz}$, $P/N_o = 130$ ($R = 400 \text{ Hz/sec}$, $S/N = 0 \text{ dB}$).

Subsequent to initial acquisition, the sweep rate is reduced to a lower value (i.e., 100 Hz/sec) and acquisition may take place in the narrow band filter ($S/N = 13 \text{ dB}$) in $t \leq 1.2$ seconds. The configuration of the resulting receiver is illustrated in Figure C-2. It should be noted that the P/N_o value plotted in Figure C-1 will be that appearing on the RF bus at the input to all the BPFs in Figure C-2. Since the P_D/N_o value is that required by the data receiver and is determined by the E_b/N_o figure of merit

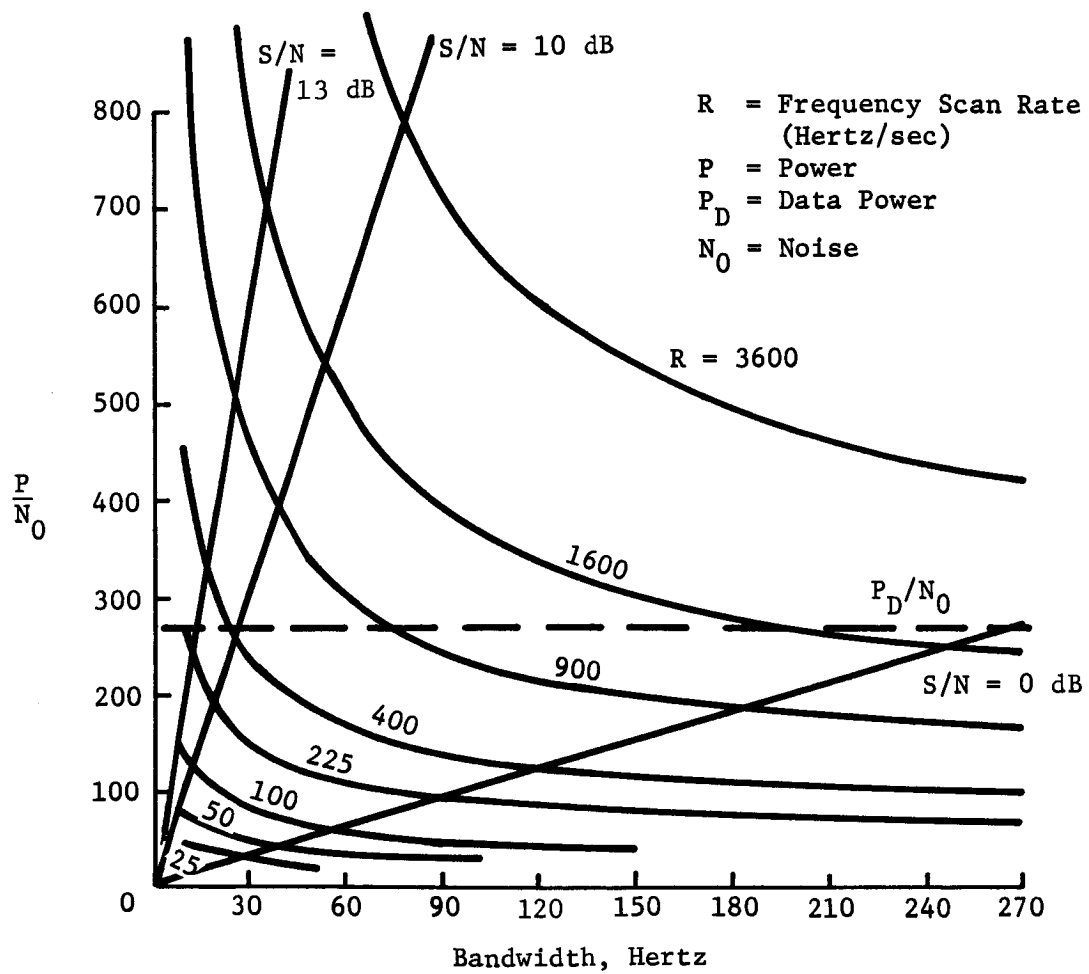


Figure C-1 Acquisition Bandwidth and Power

and fixed adverse tolerances, P_D/N_0 is a function of the data rate which remains relatively constant for the Jupiter, Saturn, and Uranus missions. Consequently, for equal uncertainty bandwidth sweep rates, acquisition and tracking tone power is equal to approximately 50% of the data power (i.e., 1.75 dB increase in transmitter power). The tracking loop frequency uncertainty has some influence on the power in the tracking tone, since this establishes the predetection bandwidth in the tracking loop. The worst case considered was a Jupiter mission with a data link RF frequency of 2.3 GHz. The effect of the Doppler rate was to produce a maximum frequency deviation of -7.5 Hz as is demonstrated here. Although this loop stress will be relieved somewhat by a preprogrammed frequency shift in the tracking loop, a 15 Hz bandwidth was selected for the tracking loop BPF for all mission. This has the effect of fixing the received tone power at $P/N_0 = 150$ and $R(\text{Max}) = 400$ for all missions. The effect of differing uncertainty bandwidth/frequency is to change the acquisition time. Some transmission power reduction can, in general, be achieved by decreasing the tracking BPF bandwidth and increasing acquisition time; however, approximately 1.0 dB is the maximum improvement that should be expected.

The characteristics of the BPFs of Figure C-2 in the frequency domain are shown in Figure C-3. The figure is not to scale for purposes of illustration. The IF frequency bandwidth is approximately equal to the total possible variation from nominal of the received probe frequency. The data BPFs bandwidth are of the order of the bit rate plus frequency tracking deviation. The high rate acquisition filters (A/U, A/L) may overlap slightly to provide logic signals during tracking. The narrow band acquisition filter (A/A) is located at the junction of the two wide-band filters. The tracking filter is located symmetrically with respect to the narrow-band acquisition filter. The local oscillator frequency will be swept from low to high frequency so that the difference (IF) frequency will sweep from high to low frequency. Under these circumstances, the upper acquisition BPF will detect the probe signal first and will not be perturbed by data signals. When the search logic registers a wide-band, (A_U) acquisition, it will decrease the sweep rate to enable acquisition in the narrow band (A_A) . Once acquisition is achieved in narrow band, the sweep is discontinued and the tracking loop is enabled.

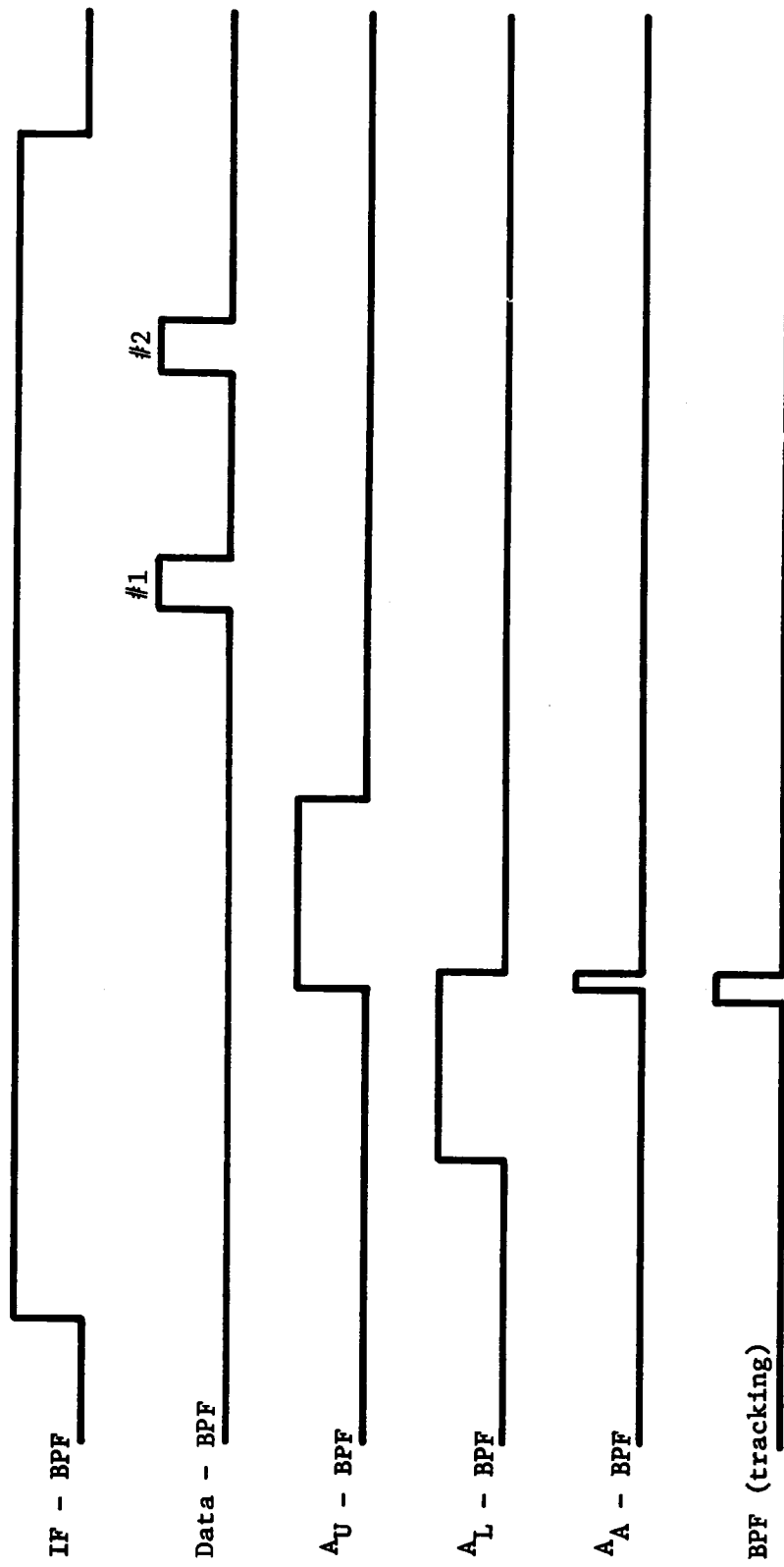


Figure C-3 Receiver Bandpass Characteristics

In the event that the narrow band does not acquire, the lower wide band (A_L) will register acquisition within a fraction of a second (i.e., broad-band acquisition response time is approximately 0.3 sec) after the signal moves into the lower bandpass. The search logic will respond to acquisition of the signal in A_L and loss of acquisition in A_U by reversing the slow sweep rate and driving the signal higher in frequency and back into the narrow bandpass, A_A . This logic is illustrated in Table C-1. The first six lines have been discussed. The last two lines could conceivably occur because of variations in signal strength and degrees of overlap of the BPFs. Loss of signal could occur due to a noise burst or a system transient. It may be desirable to include some time delay between logic transitions for this type of disturbance. The analysis of the detection probabilities uses integrate and dump configurations. The acquisition circuitry should therefore continuously sample (time = t), store, sum, and dump samples acquired at previous times which are in excess of the design hold period (τ). The output of the circuitry would then be

$$E_o = \int_{t-\tau}^t e dt$$

Since the analysis is also based on threshold levels, the gain of the wide band IF amplifier may be controlled by its own noise output which should predominate. No problem is anticipated if the probe signal is strong enough to affect the gain control. The condition to be achieved is to maintain the noise level in the absence of signal below the desired threshold. In the presence of a strong signal, it is advantageous to depress the gain further and avoid excessive clipping with resultant signal-to-noise ratio loss.

Table C-1 Search and Acquisition Logic

A_L	A_A	A_U	Logic State
0	0	0	Sweep Down/High Rate
1	0	0	Sweep Up/Low Rate
1	1	0	Frequency Hold/Enable Track
1	1	1	Frequency Hold/Enable Track
0	1	1	Frequency Hold/Enable Track
0	0	1	Sweep Down/Low Rate
0	1	0	Maintain Previous State
1	0	1	Maintain Previous State

B. TRACKING

The tracking loop and its equivalent servo loop are shown in Figure C-4. The evaluation of this loop follows.

Open loop gain

$$\left. \frac{W_o(S)}{W_i(S)} \right|_{OL} = K_D K_V B_n(S) B_t(S) \quad [C-1]$$

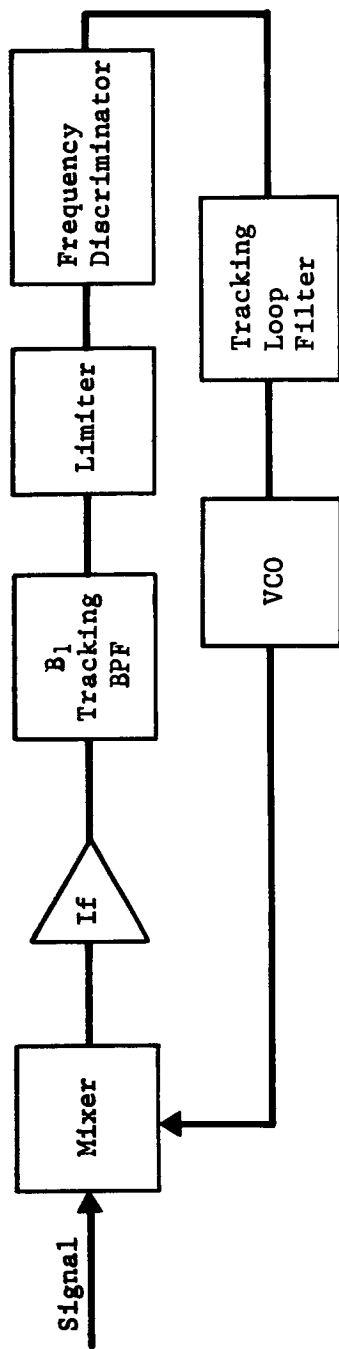
Let

$$K = K_D K_V \quad [C-2]$$

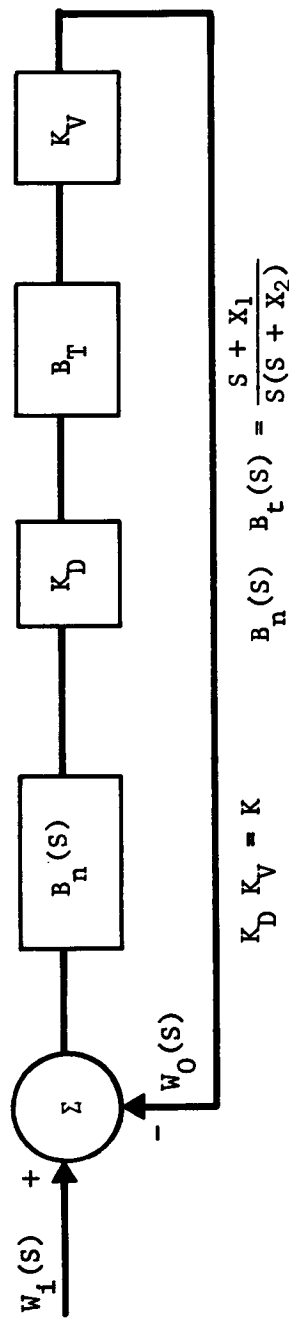
$$B_n(S) B_t(S) = \frac{S + X_1}{S(S + X_2)} \quad [C-3]$$

where Equation [C-3] assumes a second order loop and implies

$$(\text{Bandwidth})_n \gg (\text{Bandwidth})_t. \quad [C-4]$$



A. a. AFL Loop Configuration



b. Equivalent Servo of AFC Loop

Figure: C-4 AFC Loop

The problem consists of selecting loop parameters such that the tracking error due to Doppler rate is acceptable. It is assumed that acquisition has already been achieved. The input is assumed to be a ramp in frequency with slope equivalent to the maximum Doppler rate.

$$W_i(S) = \frac{\dot{W}_d}{S^2} \quad [C-5]$$

$$\dot{W}_d = \text{maximum Doppler rate} \quad [C-6]$$

The closed loop gain is

$$\frac{W_o(S)}{W_i(S)} = \frac{K(S + X_1)}{S(S + X_2) + K(S + X_1)}$$

$$\frac{W_o(S)}{W_i(S)} = \frac{\frac{1}{X_1}(S + X_1)}{\frac{S^2}{KX_1} + \left(\frac{K + X_2}{K X_1}\right)S + 1}$$

Denominator analysis

$$\frac{S^2}{X_\eta^2} + \frac{2\zeta}{X_\eta}S + 1 = \frac{S^2}{K X_1} + \left(\frac{K + X_2}{K X_1}\right)S + 1$$

$$X_\eta^2 = KX_1 = \text{Closed loop bandwidth}$$

$$= \frac{X_\eta}{2} \left(\frac{K + X_2}{K X_1} \right) = \text{Damping Coefficient}$$

Steady-State error

$$\Delta W_{SS} = \lim_{S \rightarrow 0} S [\Delta W(S)]$$

$$S \rightarrow 0$$

$$\Delta W(S) = W_i(S) - W_o(S)$$

and

$$\Delta W_{SS} = \lim_{s \rightarrow 0} s \left[\frac{\dot{W}_D s(s + X_2)}{s^2 s(s + X_2) + K(s + X_1)} \right]$$

$$\Delta W_{SS} = \frac{\dot{W}_D X_2}{K X_1}$$

The selection of K , X_1 , X_2 , determines the dynamic transient characteristics and steady-state error. These factors in an optimum design would determine tracking filter bandwidth and tone power. It is sufficient here to select values that define a realizable system.

Hence, set $K = 4$ $X_1 = 2.25 \text{ Hz}$ $X_2 = 0.25 \text{ Hz}$

Closed loop bandwidth = $KX_1 = 3 \text{ Hz}$

$\dot{W}_D = 70 \text{ Hz}$ (Alternate Jupiter Probe: $6 R_J$, 0.86 GHz $t = E-0$:
see Vol II, Section V.D)

$$\Delta W_{SS} = 1.95 \text{ Hz}$$

Assuming a tone line bandwidth of 2 Hz , the expected frequency deviation subsequent to lock is,

$$W = \pm 3.95 \text{ Hz}$$

The plus/minus sign tends to be conservative since the Doppler rate is always negative. From the above, if a factor of 1.9 is allowed for acquisition and noise transients, the tracking filter bandwidth becomes

$$(BPF)_t = 15 \text{ Hz}$$

Although this mission is essentially a worst case, the same tracking bandwidth is used on all missions. It should be noted that the acquisition transient has not been evaluated. The factor of 1.9 is conservative and this initial transient can essentially be reduced by various acquisition logic approaches. With the design constants given above,

Damping coefficient $\zeta = 0.707$

Loop phase margin $\theta_m = 43^\circ$

The effect of noise on the system has not been evaluated. However, the link analysis allows

$(S/N)_T = 10 \text{ dB}$

The noise will cause some additional deviation of the frequency which is considered to be well within the conservatism of the above design. A more rigorous evaluation of the effects of narrow band noise in the presence of signal, acquisition transient and transmitter frequency perturbations (line width) is indicated, but it is not expected that the results would change the above feasibility evaluation. For the purpose of evaluating the effects of frequency deviation on various missions:

Nominal Jupiter Probe	1.0 GHz _z	$\dot{W}_D = 65 \text{ Hz}$	$\Delta W = 3.8 \text{ Hz}$	(See Vol II, Section V.B)
Spacecraft Radiation Compatible Alternate Probe	0.86 GHz	$\dot{W}_D = 70 \text{ Hz}$	$\Delta W = 3.95 \text{ Hz}$	(See Vol II, Section V.D)
Saturn Probe	0.86 GHz	$\dot{W}_D = 26 \text{ Hz}$	$\Delta W = 2.72 \text{ Hz}$	(See Vol II, Section VI.B)
Uranus Probe	0.86 GHz	$\dot{W}_D = 21 \text{ Hz}$	$\Delta W = 2.58 \text{ Hz}$	(See Vol II, Section VII.B)

APPENDIX D

MISSION ANTENNA ANALYSIS AND DESIGNS

R. E. Compton, Jr.

June 23, 1972

MISSION ANTENNA ANALYSIS AND DESIGN

Several types of antennas are required on the spacecraft and probe with axial and butterfly patterns to satisfy trajectory requirements. The contract did not specifically require detailed hardware designs but greater detail was required in order to perform mechanical design and configuration integration. Antenna sizes and weights were necessary in order to calculate mass properties and probe weights. The payload fairing also limits the size of a probe tracking dish to 1.5 m (60 in.) in order to fit within the payload envelope.

The probe spins about its longitudinal axis to maintain attitude stability. Therefore, circular polarization will allow the probe to rotate without the received energy being affected significantly by cross-polarization. A small loss does exist from pattern ellipticity and ripple. If linear polarization were used for the probe antenna, loss of 3 dB or more would be encountered depending upon the look vectors at the transmitting and receiving antennas and the extent of the respective aspect angle off boresight of the main beam patterns.

Several types of antennas were chosen for each application and a final type was based upon size, weight, polarization, side lobe level, maximum gain, and pattern shape. The designs described herein and used on the various missions are preliminary and subject to design refinements. The primary objective was to determine envelope size and weight. Such design details as feed techniques and the possibility of RF breakdown were not investigated in depth.

A. SPACECRAFT ANTENNAS

The antennas selected for the spacecraft are of two designs depending upon the required beamwidth. For a mission, such as shown in Figure D-1, the beamwidth requirements are small and a dish antenna provides an efficient design. For large beamwidths, such as shown in Figure D-2, a dish antenna becomes too inefficient at UHF and a low gain antenna such as a helix was selected. A conventional parabolic dish antenna, fed by a pair of crossed dipoles in a cup, and a helix antenna both provide the required circular polarization. The sense of polarization is not important as long as both transmitting and receiving antennas have the same sense; i.e., right-hand or left-hand circular patterns.

The spacecraft antenna platform must be despun on spacecraft such as Pioneer which is spin stabilized. Spacecraft such as TOPS, MOPS, or Mariner that are three-axis stabilized, do not require a despun platform. Despinning is required in order to maintain a fixed pointing direction of the antenna in space. As seen in Figures D-1 and D-2, relative probe motion is greater in cone angle than in clock or elevation (cross cone) angle. Elliptical patterns were not required to increase the gain. A circular pattern provides a more conservative design from the standpoint of compensating for position errors in the probe.

Parabolic dish antenna gain is based on an efficiency of 55% with a focal length (f/d) of 0.3 and uniform aperture illumination. The sidelobe level has maximum suppression under these conditions (>20 dB) and the subtended angle of the reflector is 159°. The maximum gain is calculated from

$$G_m = 10 \log_{10} \left[0.55 \pi^2 \left(\frac{d}{\lambda} \right)^2 \right] \quad [D-1]$$

where

G_m = maximum dish gain, dB

d = dish diameter, cm

λ = wavelength, 30/f, cm

f = operating frequency, GHz.

The half-power (-3 dB) beamwidth in degrees is symmetrical in both the E and H planes and equal to

$$\theta_{hp} = 70 \frac{\lambda}{d} \quad [D-2]$$

Probe position dispersions, such as shown in Figure D-1, were used for each mission to determine minimum spacecraft antenna beamwidth. The launch vehicle payload fairing envelope restricts the stowed spacecraft antenna dish size to 1.5 m (60 in.) in order to clear the fairing. As seen from Equation [D-2], the dish diameter, d , is inversely proportional to the 3-dB beamwidth. A dish with this diameter at 0.86 GHz has a beamwidth of 17°. At 1 GHz the minimum beamwidth is 14°. Therefore, a size limitation was not necessary on the spacecraft dish antenna.

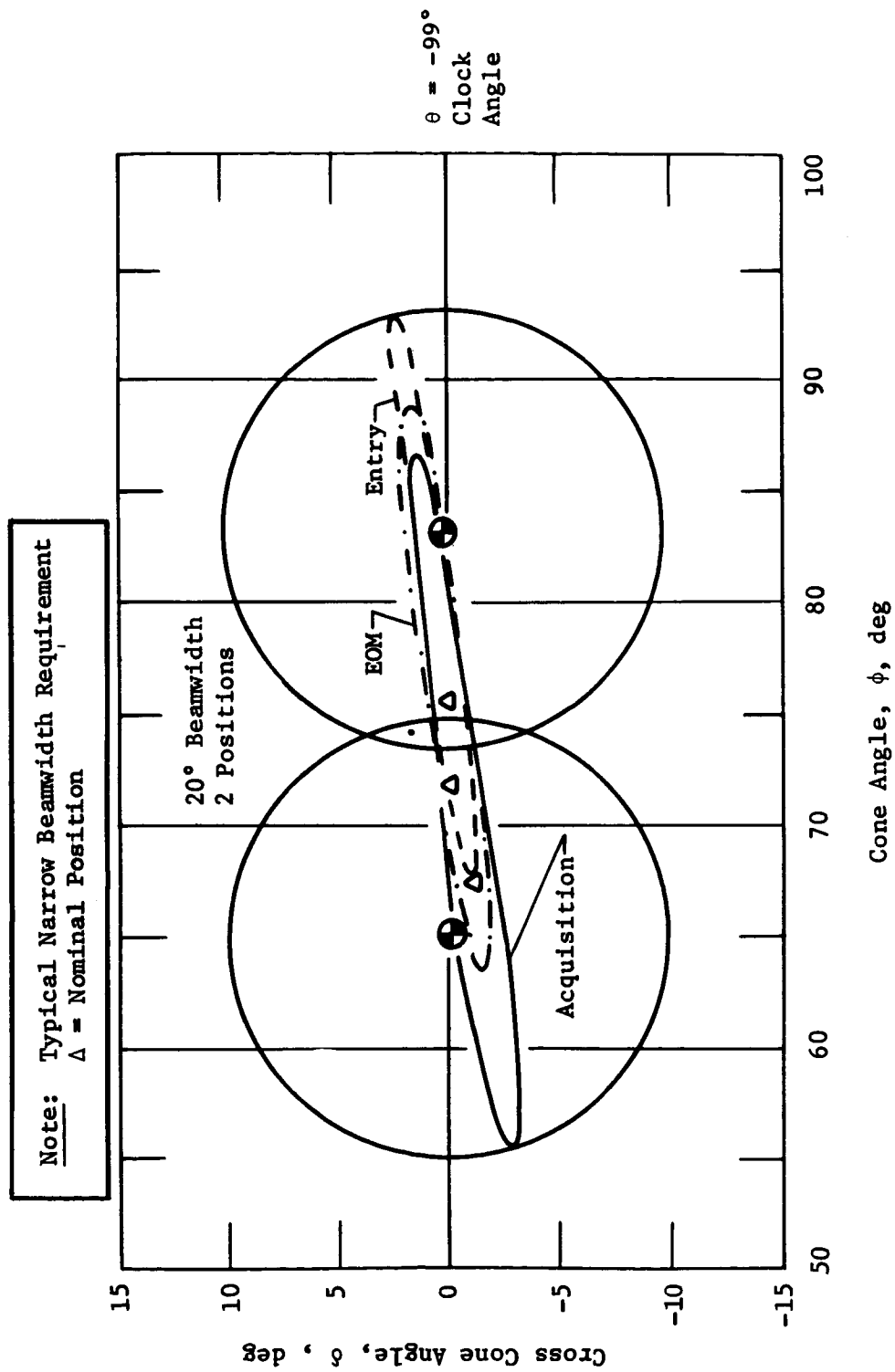


Figure D-1 Spacecraft Antenna Requirements for Jupiter Mission Point Design 8

Note: Typical Broadbeam Antenna Requirement
 Δ = Nominal Position

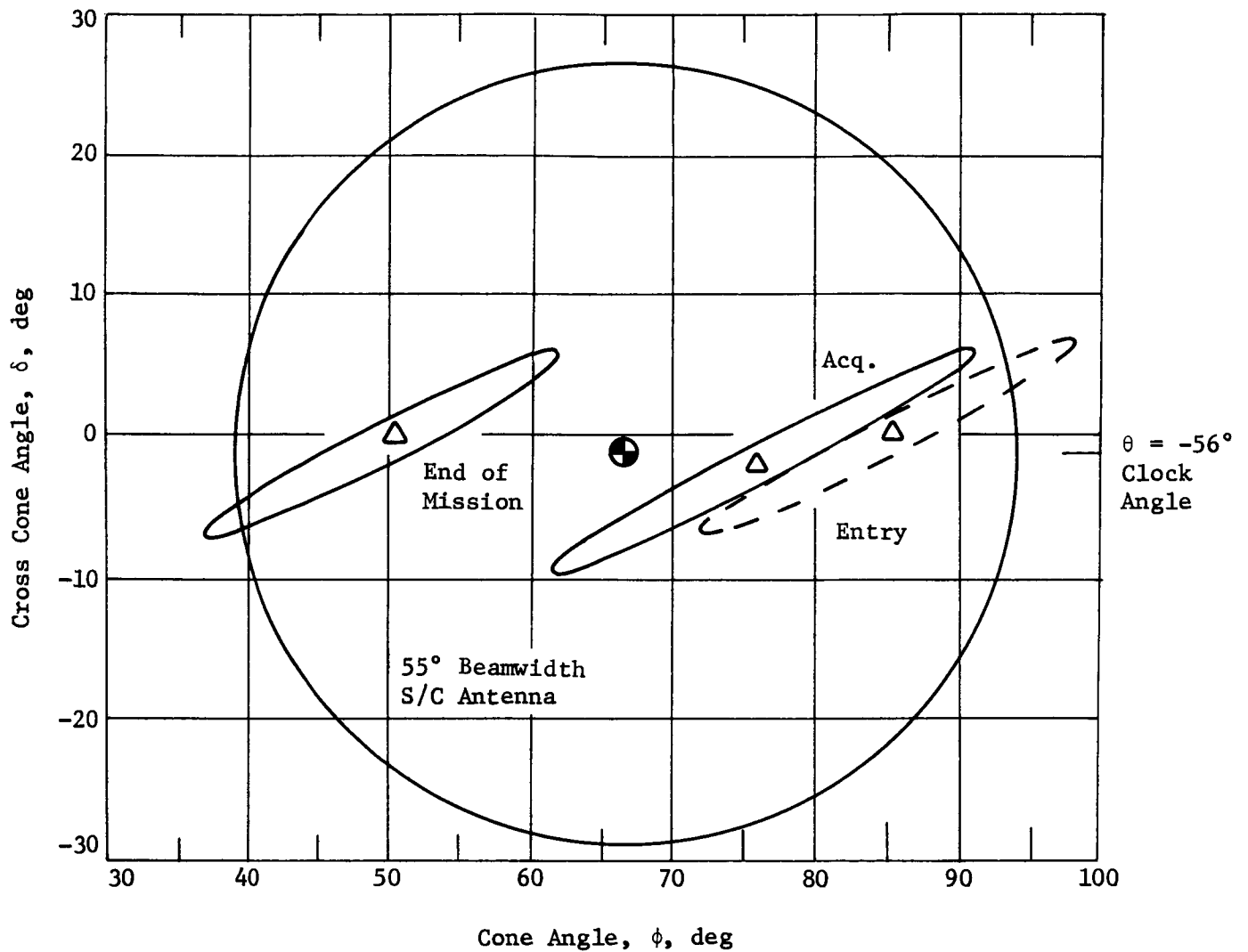


Figure D-2 Spacecraft Antenna Requirements for the Jupiter Probe Dedicated Mission

A parabolic dish provides a compact design with circular polarization up to approximately 30° at 1 GHz, and for larger beamwidths the dish diameter is less than 0.75m (2.5 ft) and the feed mechanism becomes a problem in size (aperture blockage) and efficiency. For this reason, a helix was selected for large beamwidths. Helical antennas are commonly used on spacecraft for low gain applications requiring circular polarization. For a beamwidth of 30° at 1 GHz, a 13-turn helix is required that is 3λ (0.9 m) long. Larger beamwidths are smaller in length for a fixed frequency so the payload fairing size limitation is not a problem because of excessive length.

An optimum design for an axial mode helix has a circumference equal to the wavelength and a slant angle on the loops of 12.5°. Under these conditions, the maximum gain is equal to

$$G_m = 12 L_\lambda C_\lambda^2 = 12 L_\lambda \quad [D-3]$$

where:

G_m = maximum gain ratio

$C_\lambda = 1$, circumference in wavelengths

$\alpha = 12.5^\circ$, loop slant angle

L_λ = axial length in wavelengths = $n S_\lambda$

n = number of turns

S_λ = loop spacing in wavelengths.

The half-power beamwidth, in degrees, is symmetrical in both planes and, for $C_\lambda = 1$, equal to

$$\theta_{hp} = \frac{52}{C_\lambda \sqrt{L_\lambda}} = \frac{52}{\sqrt{L_\lambda}} \quad [D-4]$$

These relationships are depicted in graphical form in Figure D-3. The circumference may be varied between 0.8 and 1.2 λ . For larger diameters with a given beamwidth, the length and number of turns are reduced, as seen in Figure D-3. A value of one C_λ results in an optimum ratio of diameter to length, D/L .

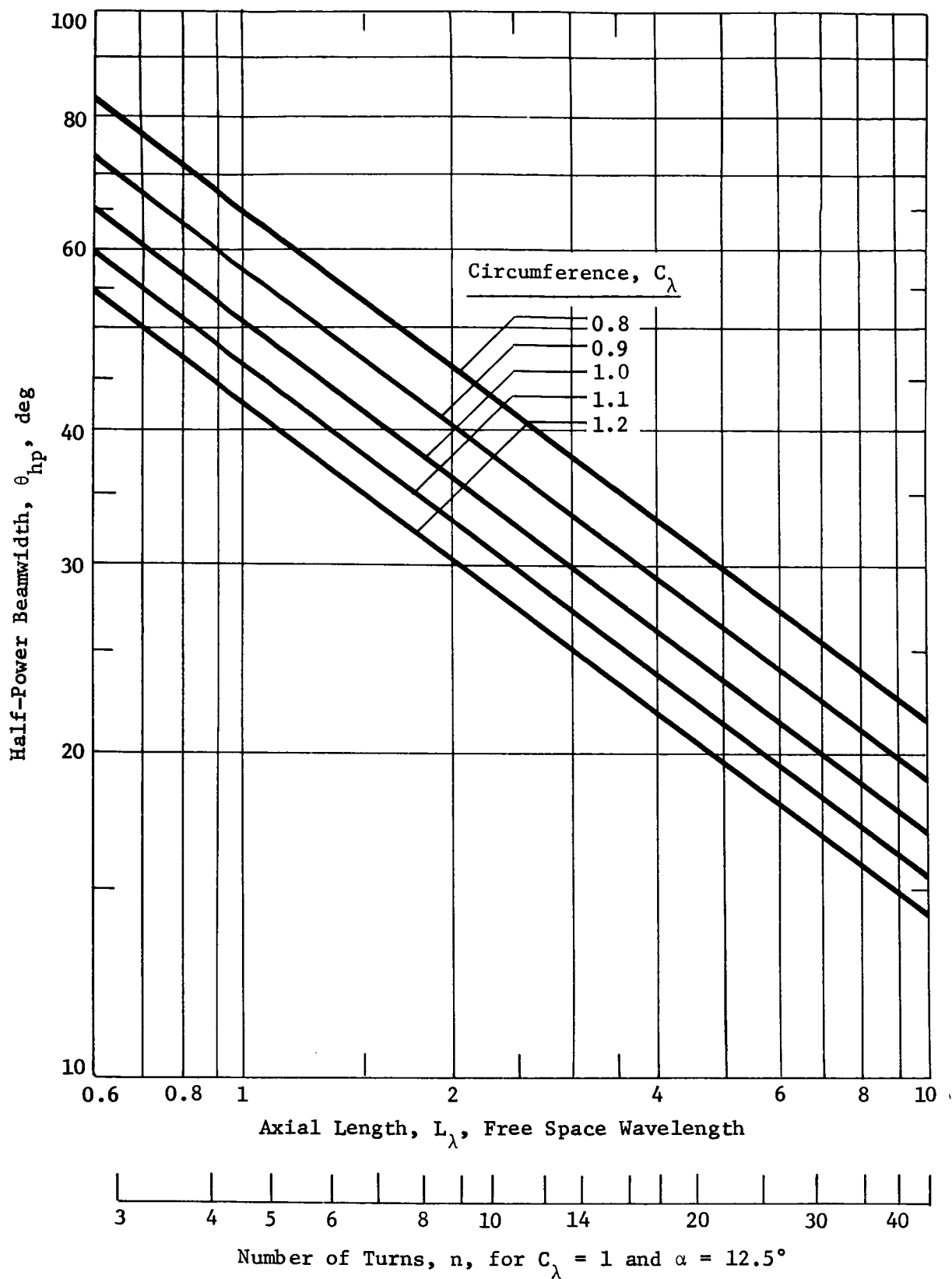


Figure D-3 Axial Mode Helical Antenna Parameters

Beamwidths on the order of 50° to 60° result in 5 turns or less, and an axial length less than λ (30 cm for 1 GHz). As seen, the helical antenna provides a compact design for low-gain applications (Ref D-1).

2. Probe Entry Antenna

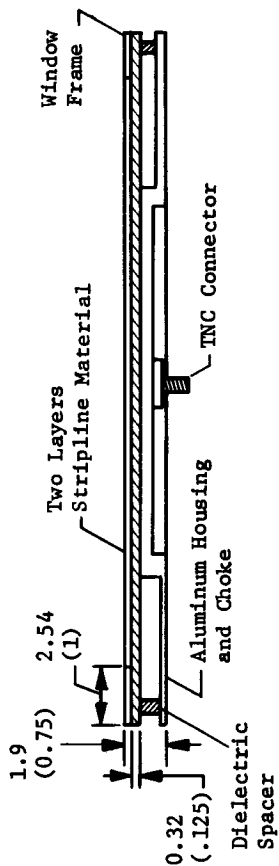
Probe aspect angle during acquisition and initial descent is typically on the order of 50° to 60° . Dispersions in the angle are usually small, which result in small beamwidths requirements.

Since the probe is spin stabilized, a butterfly antenna pattern is required. For the original higher frequencies anticipated, a four-arm equiangular spiral on a cone was selected. The truncated cone length is 0.9λ and base diameter is 0.75λ . For 0.86 GHz, the cone dimensions become excessive and another design was considered. An annular slot antenna was selected to be used at this frequency. It is 43 cm (17 in.) in diameter and only 1.9 cm (0.75 in.) thick, and is placed under the deflection motor. The main drawback to this design is that the antenna is linearly polarized and cross-polarization loss is 3 dB with a circularly polarized spacecraft antenna. Annular slot antennas are very popular for airborne use in communications, and provide a butterfly pattern that is adjustable to a small degree by variations in design parameters. Printed circuit feed techniques are common. The annular slot entry antenna for 0.86 GHz is shown in Figure D-4 (Ref D-2).

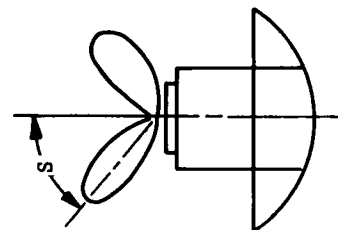
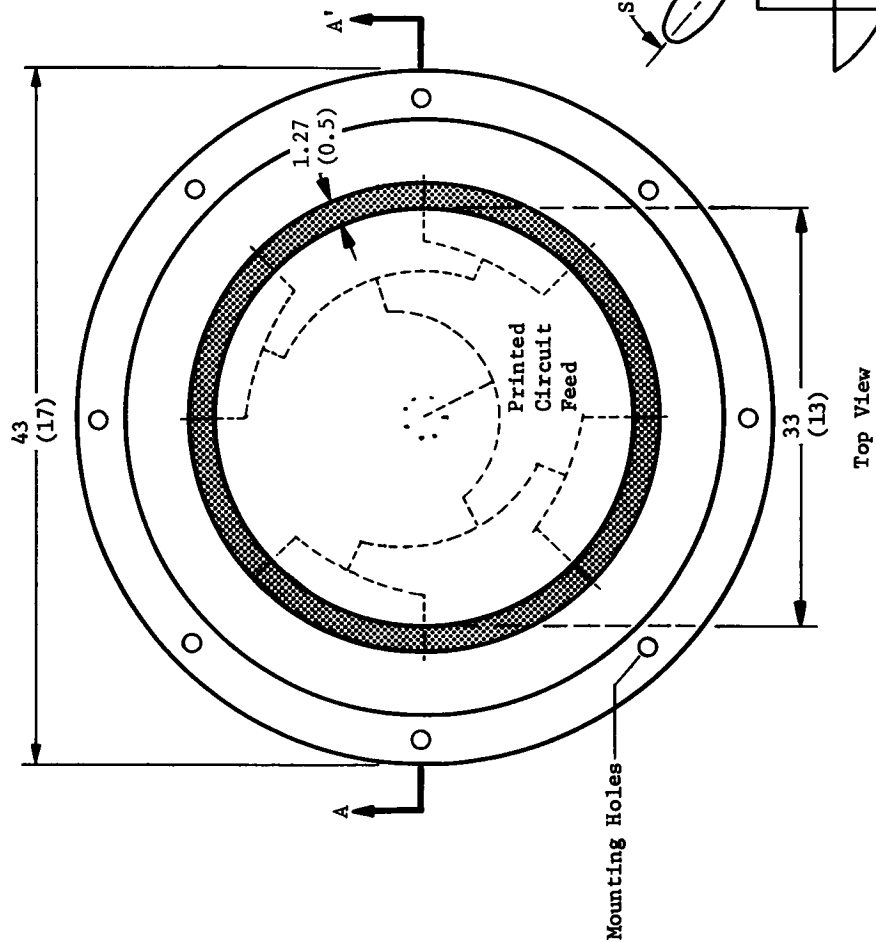
3. Probe Descent Antenna

The descent antenna on the probe is also of two designs depending on the mission and frequency. For 1 GHz, a crossed dipole in a cup was chosen. For circular polarization, the dipoles are unequal in length. The longest dipole is 18.75 cm (7.4 in.) long. The antenna is 7.6 cm (3 in.) deep. This configuration fits into the probe baseplate.

For the Jupiter parametric studies, the frequency was lowered to 0.86 GHz and the antenna increased in size to 21.8 by 8.84 cm (8.6 by 3.5 in.) and could not be placed on the probe because of structural interference. Another design was selected that is more compact and provides circular polarization with the required pattern.



Sectional Side View A-A'



Note: Linearly Polarized

$f = 860 \text{ MHz}$
 $\lambda = 34.9 \text{ cm (13.75 in.)}$
 $S = 55^\circ$
 $\theta_{hp} = 45^\circ$
 $G_m = 5 \text{ dB}$
 $Wt = 0.2 \text{ kg (4.7 lb)}$
 Dimension in cm with (in.)

Figure D-4 Annular Slot Entry Antenna

The crossed dipole in a cup was replaced with a modification developed by Martin Marietta for the Viking Program. It is a turnstile design over a flared cone. The Viking model is shown in Figure D-5. The large baseplate seen in the figure is required on the Viking Lander to reduce backlobes and is not needed for the probe mission. For circular polarization, the turnstile arms are unequal by $\lambda/4$. The antenna shown in the figure has linear polarization and operates at 1 GHz. For the probe descent antenna at 0.86 GHz, the same design techniques would be employed as are being used by Martin Marietta to develop this antenna for the Viking Program.

The antenna generates an axial beam pattern with a broad beamwidth and good circularity. A typical pattern is shown in Figure D-6 for linear polarization at 1.75 GHz. The gain/beamwidth relationship is varied by adjusting the dipole flare angle and height above the cone. Design details of the antenna are shown in Figure D-7 for 0.86 GHz and circular polarization. The height and 30° flare angle are preliminary values and are typical for a beamwidth of 100° with a maximum on-axis gain of 5.5 dB.

4.

References

- D-1 J. D. Kramers: *Antennas*. McGraw-Hill, 1950, pp 173 through 216.
- D-2 H. Jasik: *Antenna Engineering Handbook*. McGraw-Hill, 1961, pp 8-8 and 27-34 through 27-36.

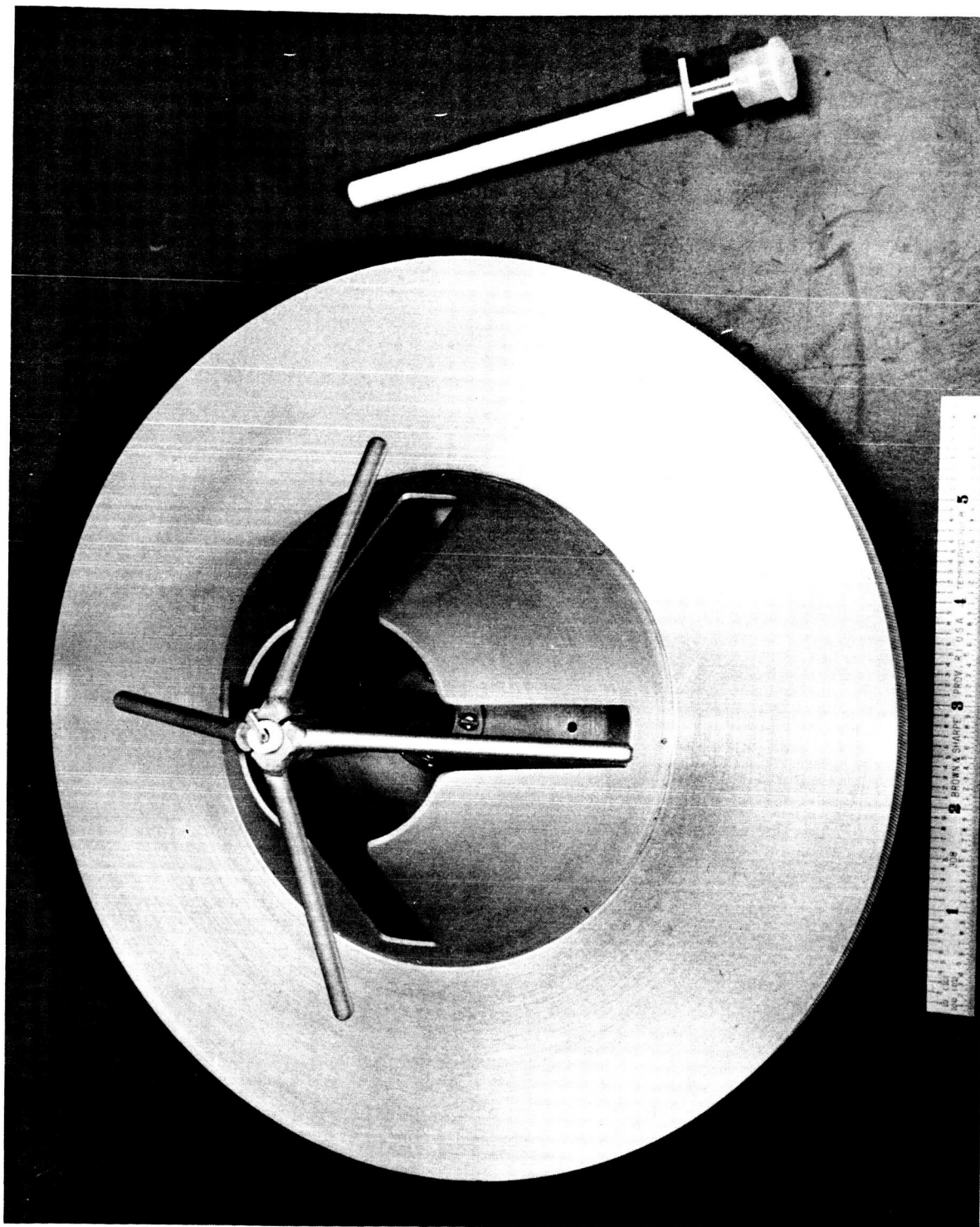


Figure D-5 Turnstile/Cone Descent Antenna

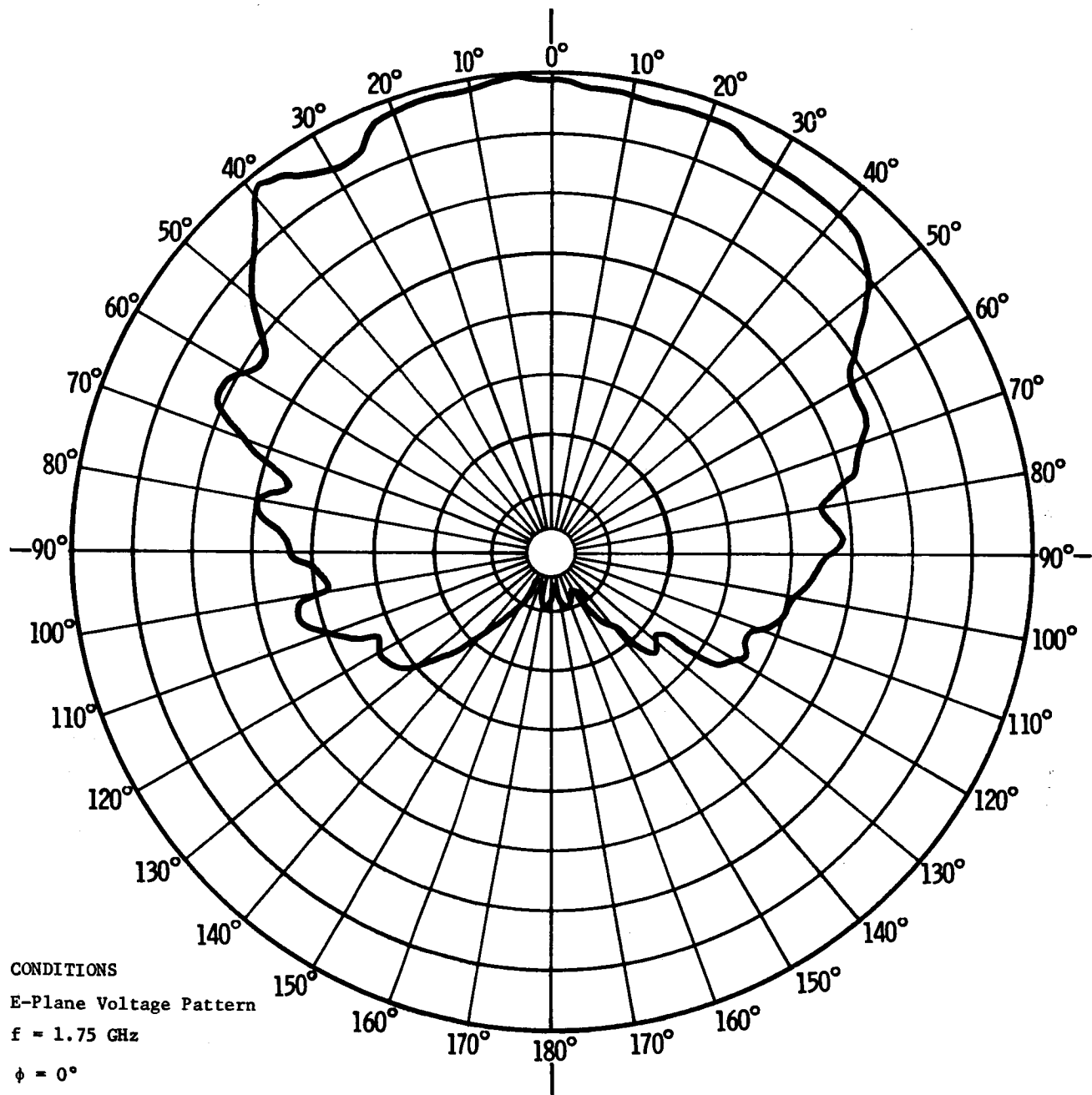


Figure D-6 Turnstile/Cone Antenna Pattern

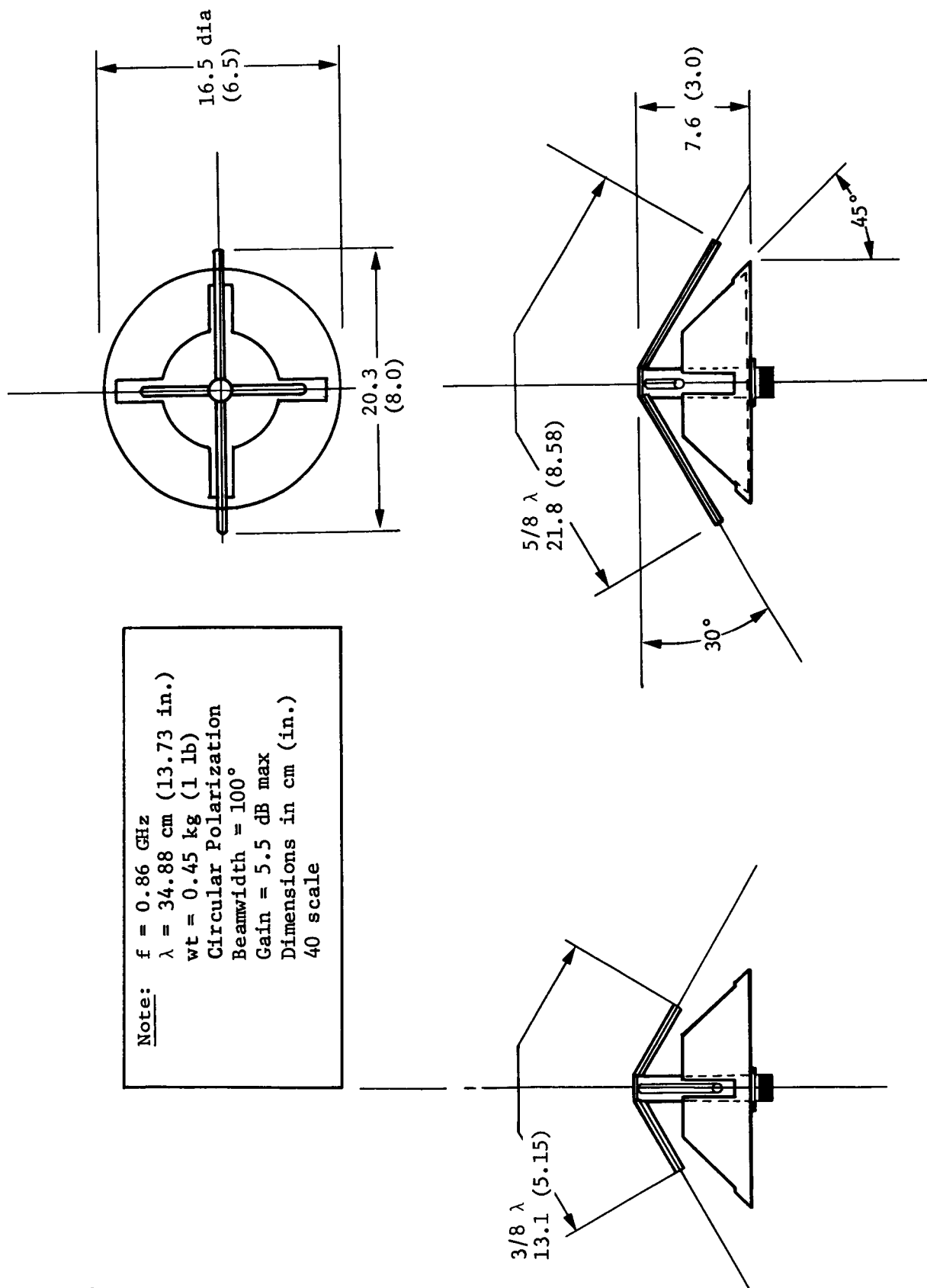


Figure D-7 Survivable Probe Turnstile/Cone Descent Antenna

APPENDIX E

SUMMARY OF PLANETARY ATMOSPHERES
AND RELATED CONSTRAINTS

D. Cross
and
R. Fischer

June 8, 1972

SUMMARY OF PLANETARY ATMOSPHERES AND RELATED CONSTRAINTS

The data compiled in this appendix summarizes the pertinent information to be used in modeling the atmospheres of Jupiter, Saturn, Uranus, and Neptune. As far as possible, these data are a duplication of the information provided by References 1, 2, and 3 and were calculated in order to provide a more extensive table (5 km print interval) for use in various analyses. These tables of the atmospheres are presented in Sections B through G. Slight differences arise between the references and the atmospheric tables because of slight variations in the equations which are used to extend the atmosphere from a pressure of one atmosphere at zero altitude. The data presented in the tables given represent the best compromise that yields a good planet atmosphere description. Section G is a summary of these differences.

Section A presents parameters and constants related to the planets and their atmospheres.

A tabular description of the cool-dense Jupiter atmosphere is given in Section B.

Section C presents a tabular description of the nominal Jupiter atmosphere.

The nominal Saturn atmosphere description is tabulated in Section D.

Section E presents a tabular description of the nominal Uranus atmosphere.

A tabular description of the nominal Neptune atmosphere is given in Section F.

Section G presents a comparison of models described in Sections B through F with the models described in the references.

It should be noted that probe entries into the various planetary atmospheres may be at high latitudes, possibly even polar entries. Significant differences in entry radius and entry velocity occur between a polar and an equatorial entry for each of the planets considered, since each planet is oblate. These parameters are defined in Section A.

Two gravitational constants will be used to simulate the probe trajectory. Before entry, an "ephemeris" (μ) will be used to compute the position and velocity as a function of time. After the entry point is reached, a slightly different constant, the "atmospheric" μ will be used to simulate the trajectory within the atmosphere of the planet. The atmospheric μ to be used will be consistent with the specified values for gravitational acceleration (g_0) at the reference radius (r_0). The result of changing the value of μ at entry does not materially affect the descent trajectory of the probe. The two values of μ are given in Section A for each planetary atmosphere.

The molecular weight, grams/mole of the atmospheres of Jupiter and Saturn are a constant value (independent of altitude), and are given in Section A, Table E-2. The molecular weight of the nominal atmospheric models of Uranus and Saturn are variable with a altitude, and are listed in Sections E and F, respectively.

PLANETARY CONSTANTS AND ATMOSPHERIC COMPOSITION PARAMETERS FOR JUPITER, SATURN, URANUS, AND NEPTUNE

This section lists a large number of parameters which are required to define each of the planets physical characteristics and their atmospheres. They are summarized here for reference:

Table E-1 lists the planetary constants of each of the planets (Jupiter, Saturn, Uranus, and Neptune)

Table E-2 lists the compositions and other parameters for model atmospheres of Jupiter, Saturn, Uranus, and Neptune.

Table E-3 summarizes the constants and conversion factors which are related to the study of the planets and their atmospheres.

Entry trajectory studies have indicated that differences between gravitational constant (μ) for planet ephemeris (Table E-1) and (μ) for atmospheres (consistent with given reference radius (r_0) and given reference acceleration of gravity (g_0) makes no significant difference in max g or dynamic pressure values, or altitude of occurrence for $\gamma = -20^\circ$ and greater. Also, at an altitude where Mach = 1.0 occurs, no difference is noted. However, the altitude of Mach = 0.5 shows a noticeable difference of 1.5 km, or 4%.

Table E-1 Planetary Constants

	JUPITER	SATURN	URANUS	NEPTUNE	SYMBOL
Equatorial Radius, km (P = 1 atm)	71422 ± 200	59800 ± 350	26468 ± 1000	24857 ± 200	R _o
Polar Radius, km (P = 1 atm)	66815 ± 200	53500 ± 350	25674 ± 1000	24360 ± 200	R _{polar}
Flattening (e) (Optical)	0.0645	0.10535	0.03 ± 0.03	0.02 ± 0.02	ε
Entry Radius, km (equatorial entry)	71726.9	60291.4	27000 ± 1000	25200 ± 200	Re
Entry Altitude, km	304.9	491.4	532	343	he
($\mu_{\text{sun}} = 1.32712499 \times 10^{11} \text{ km}^3/\text{sec}^2$)					
Reciprocal Mass	1047.391	3498.70	22930.0	19260.0	μ
Gravitational Constant (km ³ /sec ²) (used with flyby trajectory calculation)	126707718.8	37932000.	5787723.5	6890576.3	
Acceleration of Gravity (g _o) at R _o (cm/sec ²)	2500 (Nominal) 2700 (Cool) 2300 (Warm)	1050 (Nom)	810 (Nom)	1100 (Nom.)	g _o
Gravitational Constant (Consistent with reference g _o and R _o)	127,527,552.1 (N) 137,729,756. (C) 117,325,348. (W)	37,548,420. (N) (Ro = 59800)	5,674,449.57 (N) (Ro = 26468)	6796574.94 (N) (Ro = 24857)	μ _a
Period of Rotation	9 ^h 55 ^m 29 ^s .73	10 ^h 26 ^m ±14 ^m	10.816667 ^h 10 ^h 49 ^m	12 ^h 43 ^m	τ
Angular Rotation Rate (Rad/Sec)	1.75853x10 ⁻⁴	1.67 x 10 ⁻⁴	1.613 x 10 ⁻⁴	1.372 x 10 ⁻⁴	ω
Inclination of Orbit Plane to Ecliptic Plane	1.30631°	2.49°	0.77255°	1.77327°	
Inclination of Equatorial Plane to Orbit Plane	3.102°	26.7°	97.884°	29°	
Mean Distance From Sun (AU)	5.202803	9.5388	19.181951	30.057779	
Period of Revolution about Sun (Years)	11.862	29.45772	84.01331	164.79342	
Orbital Velocity (km/s)	13.1	9.7	6.8	5.4	
Orbit Eccentricity	0.048435	0.055682	0.047209	0.008575	
Escape Velocity (km/sec)	59.6 ± 0.6	37	22	25	
Mean Density (g/cm ³)	1.32 ± 0.01	0.69	1.56	2.27	ρ

Table E-2 Compositions and Other Parameters for Model Atmospheres of Jupiter, Saturn, Uranus, and Neptune

PARAMETER		JUPITER COOL MODEL	JUPITER NOMINAL MODEL	JUPITER WARM MODEL	SATURN NOMINAL	URANUS NOMINAL	NEPTUNE NOMINAL
Fractions by mass (or weight)	H ₂	0.50696	0.76348	0.87674	0.78514		
	He	0.46000	0.23000	0.11500	0.19373		
	CH ₄	0.00857	0.00429	0.00214	0.00444		
	NH ₃	0.00219	0.00109	0.00055	0.00113		
	H ₂ O	0.01601	0.00800	0.00400	0.00828		
	Ne	0.00229	0.00115	0.00057	0.00120		
	Others	0.00398	0.00199	0.00100	0.00244		
Fractions by number (or volume)	H ₂	0.68454	0.86578	0.93754	0.88572	0.88572	0.85853
	He	0.31057	0.13214	0.06149	0.11213	0.11000	0.11000
	CH ₄	0.00145	0.00062	0.00028	0.00063	0.03000	0.03000
	NH ₃	0.00035	0.00015	0.00007	0.00015	0.00015	0.00015
	H ₂ O	0.00240	0.00102	0.00048	0.00105	0.00100	0.00100
	Ne	0.00031	0.00013	0.00006	0.00013	0.00013	0.00013
	Others	0.00038	0.00016	0.00008	0.00019	0.00019	0.00019
Mean molecular weight, u, grams/mole	MWT	2.70	2.30	2.14	2.27	2.68 to -2.23	2.68 -2.25
Acceleration of Grav- ity, g, cm/sec ²		2700	2500	2300	1050	810	1100
Effective Temperature, t _o , °K		128	134	140	97	---	---
Troposphere lapse	β ₀	0.222	0.236	0.259	0.234	0.230	0.23
Rate Parameters	K ₁ (°K)	500	500	500	484	484	484
	K ₂ (°K)	500	295	324	282	282	282
Correspondence level Temperature, °K		125	125	125	95	84	57
Correspondence level Pressure, atm		0.50	0.30	0.20	0.30	1.0	1.0
Stratosphere temperature, °K		108	113	118			
Stratosphere vertical extent (scale heights)			1.0	1.0	2.0		
Inversion level Temperature, °K	(none)	(none)	145	500			
Inversion level pressure, atm	(none)	(none)	0.0065	2 x 10 ⁻⁷			
Ratio of Specific Heats, γ		1.467 (1.45±.15)	1.431 (1.45±.15)	1.418 1.45±.15	1.428	1.447	1.447
Tropopause Temperature, °K		108	113	118	77	54	42
C _{p1} , Cal/mol C°		6.24632	6.60464	6.74651	6.64218	6.4448	6.4448

Table E-3 Constants and Conversion Factors

Heliocentric Gravitational Constant	$2,959122083 \times 10^{-44} \text{ AU/day}^2$
Heliocentric Gravitational Constant	$1.32712499 \times 10^{11} \text{ km}^3/\text{s}^2$
Measure of 1 AU in km	149597893,0 km
Velocity of Light, C	299792,5 km/s
Universal Gravitational Constant, G	$6.673 \times 10^{-23} \text{ km}^3 \text{sec}^{-2} \text{g}^{-1}$
Feet to Meter	0.3048 (exactly)
Reciprocal Mass (Jupiter)	1047.3908 ± 0.0074
Reciprocal Mass (Saturn)	3499.2 ± 0.4
Reciprocal Mass (Uranus)	22930 ± 6
Reciprocal Mass (Neptune)	$19260. \pm 100$
Universal Gas Constant, R	8.3143 Joules/mole C°
Universal Gas Constant, R	$8.3143 \times 10^7 \text{ ERGS/mole K}^\circ$
Universal Gas Constant, R	1.9868 Cal(15°)mole C°
1 Atmosphere of Pressure	$1.01325 \times 10^6 \text{ dynes/cm}^2$
1 Atmosphere of Pressure	$1.01325 \times 10^5 \text{ Newtons/m}^2$
1 Bar of Pressure	$10^6 \text{ dynes/cm}^2 = 10^5 \text{ Newtons/m}^2$
Ballistic Coefficient of 1 slug/ft ²	157.09 kg/m ²

Section B

Table 1-R356397

DATE 01/13/72.

JUPIT

COOL DENSE JUPITER ATMOSPHERE,

MEAN MOLECULAR MASS = 2.700 GRAMS/MOLE

INITIAL PRESSURE = 1.013250E+06 DYNES/SQCM AT 71422.00 KM RADIUS

PRINT INTERVAL = 5 KM, GAS CONSTANT = 8.31430000E+07 JOULES/(MOLE.DEG KELVIN

ONE ATMOSPHERE = 1.01325000E+06 DYNES/CM2, MU= 1.37729756E+08 KM3/SEC2

GREF = 2.69999999E-02 KM/SEC2

ALTITUDE IS ABOVE 71422.0 KM RADIUS

RADIUS KM	ALTITUDE KM	TEMPERATURE		PRESSURE		DENSITY GM/CM3
		KELVIN	FAHREN	DYNE/CM2	ATMOSPHERES	
71288.70	-133.300	405.300	269.870	1.021039E+08	1.007637E+02	8.180948E-03
71293.70	-128.300	395.549	252.319	9.147804E+07	9.028181E+01	7.510246E-03
71298.70	-123.300	385.799	234.768	8.173483E+07	8.066600E+01	6.879933E-03
71303.70	-118.300	376.048	217.217	7.282029E+07	7.186804E+01	6.288495E-03
71308.70	-113.300	366.293	199.666	6.468255E+07	6.383672E+01	5.734438E-03
71313.70	-108.300	356.547	182.115	5.727179E+07	5.552296E+01	5.216289E-03
71318.70	-103.300	346.797	164.564	5.054015E+07	4.987925E+01	4.732597E-03
71323.70	-98.300	337.046	147.013	4.444177E+07	4.386051E+01	4.281934E-03
71328.70	-93.300	327.296	129.462	3.893271E+07	3.842360E+01	3.862891E-03
71333.70	-88.300	317.545	111.911	3.397096E+07	3.352674E+01	3.474086E-03
71334.80	-87.200	315.400	108.050	3.294881E+07	3.251794E+01	3.392470E-03
71337.50	-84.500	310.200	98.690	3.054155E+07	3.014216E+01	3.197329E-03
71338.70	-83.300	307.869	94.495	2.951684E+07	2.913085E+01	3.113448E-03
71343.70	-78.300	298.158	77.014	2.553219E+07	2.519831E+01	2.780867E-03
71347.90	-74.100	290.000	62.330	2.252083E+07	2.222633E+01	2.521880E-03
71348.70	-73.300	288.447	59.534	2.198010E+07	2.169268E+01	2.474585E-03
71353.70	-68.300	278.733	42.058	1.882578E+07	1.857960E+01	2.193285E-03
71358.20	-63.800	270.000	26.330	1.629962E+07	1.608647E+01	1.960432E-03
71358.70	-63.300	269.025	24.576	1.603616E+07	1.582646E+01	1.935732E-03
71363.70	-58.300	259.279	7.032	1.357974E+07	1.340216E+01	1.700835E-03
71368.70	-53.300	249.533	-10.511	1.142684E+07	1.127741E+01	1.487089E-03
71372.00	-50.000	243.100	-22.090	1.015859E+07	1.002575E+01	1.357021E-03
71373.70	-48.300	239.793	-28.043	9.549593E+06	9.424716E+00	1.293263E-03
71378.70	-43.300	230.056	-45.551	7.921832E+06	7.818241E+00	1.118180E-03
71383.70	-38.300	220.339	-63.060	6.518862E+06	6.433617E+00	9.607683E-04
71388.70	-33.300	210.612	-80.568	5.317501E+06	5.247956E+00	8.199034E-04
71393.70	-28.300	200.885	-98.077	4.296083E+06	4.239904E+00	6.944856E-04
71398.70	-23.300	191.158	-115.586	3.434415E+06	3.389504E+00	5.834428E-04
71401.30	-20.700	186.100	-124.690	3.043199E+06	3.003404E+00	5.310337E-04
71403.70	-18.300	181.415	-133.123	2.713730E+06	2.678243E+00	4.857707E-04
71408.70	-13.300	171.655	-150.691	2.116507E+06	2.088928E+00	4.004250E-04
71413.70	-8.300	161.895	-168.260	1.627084E+06	1.605807E+00	3.263742E-04
71415.90	-6.100	157.600	-175.990	1.441965E+06	1.423109E+00	2.971232E-04
71418.70	-3.300	152.144	-185.812	1.230534E+06	1.214442E+00	2.626503E-04
71419.80	-2.200	150.000	-189.670	1.154422E+06	1.139325E+00	2.499259E-04
71422.00	0.	145.800	-197.230	1.013250E+06	1.000000E+00	2.256821E-04
71423.70	1.700	142.513	-203.146	9.137137E+05	9.017654E-01	2.082058E-04
71425.00	3.000	140.000	-207.670	8.428824E+05	8.318603E-01	1.955136E-04
71428.70	6.700	132.792	-220.644	6.644472E+05	6.557584E-01	1.624897E-04
71432.70	10.700	125.000	-234.670	5.061550E+05	4.995362E-01	1.314957E-04
71433.70	11.700	123.053	-238.166	4.716185E+05	4.654512E-01	1.244569E-04
71438.70	16.700	113.348	-255.644	3.254538E+05	3.211198E-01	9.324258E-05
71439.60	17.600	111.600	-258.790	3.034122E+05	2.994446E-01	8.828908E-05
71441.40	19.400	108.000	-265.270	2.628059E+05	2.593693E-01	7.902227E-05
71443.70	21.700	108.000	-265.270	2.180658E+05	2.152142E-01	6.556950E-05
71448.70	26.700	108.000	-265.270	1.453500E+05	1.434493E-01	4.370482E-05
71453.10	31.100	108.000	-265.270	1.017194E+05	1.003892E-01	3.058566E-05

TABLE 1-R356397

DATE 01/13/72.

JUPIT

COOL DENSE JUPITER ATMOSPHERE,

MEAN MOLECULAR MASS = 2.700 GRAMS/MOLE

INITIAL PRESSURE = 1.013250E+06 DYNES/SQCM AT 71422.00 KM RADIUS

PRINT INTERVAL = 5 KM, GAS CONSTANT = 8.31430000E+07 JOULES/(MOLE.DEG KELVIN;

ONE ATMOSPHERE = 1.01325000E+06 DYNES/CM2, MU= 1.37729756E+08 KM3/SEC2

GREF = 2.69999999E-02 KM/SEC2

ALTITUDE IS ABOVE 71422.0 KM RADIUS

RADIUS KM	ALTITUDE KM	TEMPERATURE		PRESSURE		DENSITY GM/CM3
		KELVIN	FAHREN	DYNE/CM2	ATMOSPHERES	
71453.70	31.700	108.000	-265.270	9.688737E+04	9.562040E-02	2.913275E-05
71458.70	36.700	108.000	-265.270	6.458683E+04	6.374224E-02	1.942040E-05
71463.70	41.700	108.000	-265.270	4.305716E+04	4.249411E-02	1.294672E-05
71468.00	46.000	108.000	-265.270	3.038228E+04	2.998498E-02	9.135549E-06
71468.70	46.700	108.000	-265.270	2.870592E+04	2.833054E-02	8.631490E-06
71473.70	51.700	108.000	-265.270	1.913913E+04	1.888885E-02	5.754883E-06
71478.70	56.700	108.000	-265.270	1.276138E+04	1.259450E-02	3.837177E-06
71481.50	59.500	108.000	-265.270	1.017032E+04	1.003732E-02	3.058080E-06
71483.70	61.700	108.000	-265.270	8.509372E+03	8.398097E-03	2.558656E-06
71488.70	66.700	108.000	-265.270	5.674428E+03	5.500225E-03	1.706225E-06
71493.70	71.700	108.000	-265.270	3.784176E+03	3.734691E-03	1.137852E-06
71496.30	74.300	108.000	-265.270	3.065396E+03	3.025311E-03	9.217241E-07
71498.70	76.700	108.000	-265.270	2.523743E+03	2.490741E-03	7.588561E-07
71503.70	81.700	108.000	-265.270	1.683230E+03	1.661219E-03	5.061251E-07
71508.70	86.700	108.000	-265.270	1.122707E+03	1.108026E-03	3.375832E-07
71509.90	87.900	108.000	-265.270	1.018731E+03	1.005410E-03	3.063191E-07
71513.70	91.700	108.000	-265.270	7.488833E+02	7.390904E-04	2.251793E-07
71518.70	96.700	108.000	-265.270	4.995585E+02	4.930259E-04	1.502106E-07
71523.70	101.700	108.000	-265.270	3.332500E+02	3.289020E-04	1.002069E-07
71524.70	102.700	108.000	-265.270	3.073445E+02	3.033254E-04	9.241442E-08
71528.70	106.700	108.000	-265.270	2.223333E+02	2.194259E-04	6.685268E-08
71533.70	111.700	108.000	-265.270	1.483373E+02	1.463975E-04	4.460307E-08
71538.30	116.300	108.000	-265.270	1.022300E+02	1.008932E-04	3.073921E-08
71538.70	116.700	108.000	-265.270	9.897395E+01	9.767970E-05	2.976016E-08
71543.70	121.700	108.000	-265.270	6.604135E+01	6.517775E-05	1.985776E-08
71548.70	126.700	108.000	-265.270	4.406924E+01	4.349296E-05	1.325104E-08
71553.10	131.100	108.000	-265.270	3.087146E+01	3.046776E-05	9.282639E-09
71553.70	131.700	108.000	-265.270	2.940897E+01	2.902439E-05	8.842887E-09
71558.70	136.700	108.000	-265.270	1.962675E+01	1.937010E-05	5.901505E-09
71563.70	141.700	108.000	-265.270	1.309311E+01	1.292781E-05	3.938729E-09
71566.60	144.600	108.000	-265.270	1.036099E+01	1.022550E-05	3.115411E-09
71568.70	146.700	108.000	-265.270	8.742981E+00	8.628651E-06	2.628899E-09
71573.70	151.700	108.000	-265.270	5.835820E+00	5.759506E-06	1.754754E-09
71578.70	156.700	108.000	-265.270	3.895549E+00	3.844608E-06	1.171340E-09
71581.50	159.500	108.000	-265.270	3.106568E+00	3.065944E-06	9.341039E-10
71583.70	161.700	108.000	-265.270	2.600519E+00	2.566513E-06	7.819418E-10
71588.70	166.700	108.000	-265.270	1.736105E+00	1.713402E-06	5.220238E-10
71593.70	171.700	108.000	-265.270	1.159088E+00	1.143931E-06	3.485224E-10
71595.00	173.000	108.000	-265.270	1.043520E+00	1.029874E-06	3.137727E-10
71598.70	176.700	108.000	-265.270	7.738937E-01	7.637737E-07	2.326996E-10
71603.70	181.700	108.000	-265.270	5.167384E-01	5.099811E-07	1.553764E-10
71608.70	186.700	108.000	-265.270	3.450520E-01	3.405399E-07	1.037526E-10
71609.80	187.800	108.000	-265.270	3.157206E-01	3.115920E-07	9.493301E-11
71613.70	191.700	108.000	-265.270	2.304215E-01	2.274083E-07	6.928470E-11
71614.80	192.800	108.000	-265.270	2.108370E-01	2.080799E-07	6.339588E-11

Section C

TABLE 2-R356397

DATE 01/13/72.

JUPIT
 NOMINAL JUPITER ATMOSPHERE;
 MEAN MOLECULAR MASS = 2.300 GRAMS/MOLE
 INITIAL PRESSURE = 1.013250E+06 DYNES/SQCM AT 71422.00 KM RADIUS
 PRINT INTERVAL = 5 KM, GAS CONSTANT = 8.31430000E+07 JOULES/(MOLE.DEG KELVIN)
 ONE ATMOSPHERE = 1.01325000E+06 DYNES/CM2, MU= 1.27527552E+08 KM3/SEC2
 GREF = 2.50000000E-02 KM/SEC2

ALTITUDE IS ABOVE 71422.0 KM RADIUS

RADIUS KM	ALTITUDE KM	TEMPERATURE		PRESSURE		DENSITY GM/CM3
		KELVIN	FAHREN	DYNE/CM2	ATMOSPHERES	
71139.20	-282.800	777.000	938.930	1.052698E+08	1.038932E+02	3.747874E-03
71144.20	-277.800	767.087	921.087	1.006233E+08	9.930745E+01	3.628739E-03
71149.20	-272.800	757.175	903.244	9.612599E+07	9.486898E+01	3.511938E-03
71154.20	-267.800	747.262	885.402	9.177499E+07	9.057487E+01	3.397454E-03
71159.20	-262.800	737.349	867.559	8.756732E+07	8.542223E+01	3.285269E-03
71164.20	-257.800	727.437	849.716	8.350007E+07	8.240816E+01	3.175366E-03
71169.20	-252.800	717.524	831.873	7.957032E+07	7.852930E+01	3.067728E-03
71174.20	-247.800	707.611	814.030	7.577521E+07	7.478432E+01	2.962337E-03
71179.20	-242.800	697.699	796.188	7.211187E+07	7.116889E+01	2.859177E-03
71184.20	-237.800	687.786	778.345	6.857748E+07	6.768071E+01	2.758229E-03
71189.20	-232.800	677.873	760.502	6.516922E+07	6.431702E+01	2.659476E-03
71194.20	-227.800	667.961	742.659	6.188431E+07	6.107507E+01	2.562901E-03
71199.20	-222.800	658.048	724.816	5.871998E+07	5.795212E+01	2.468485E-03
71204.20	-217.800	648.135	706.974	5.567351E+07	5.494548E+01	2.376211E-03
71209.20	-212.800	638.223	689.131	5.274216E+07	5.205246E+01	2.286061E-03
71214.20	-207.800	628.310	671.288	4.992325E+07	4.927042E+01	2.198017E-03
71219.20	-202.800	618.397	653.445	4.721412E+07	4.659671E+01	2.112061E-03
71224.20	-197.800	608.485	635.602	4.461211E+07	4.402873E+01	2.028174E-03
71229.20	-192.800	598.572	617.760	4.211461E+07	4.156389E+01	1.946339E-03
71234.20	-187.800	588.659	599.917	3.971902E+07	3.919963E+01	1.866537E-03
71239.20	-182.800	578.747	582.074	3.742278E+07	3.593341E+01	1.788750E-03
71244.20	-177.800	568.834	564.231	3.522332E+07	3.476272E+01	1.712959E-03
71249.20	-172.800	558.921	546.389	3.311814E+07	3.268506E+01	1.639145E-03
71253.70	-168.300	550.000	530.330	3.130201E+07	3.089269E+01	1.574388E-03
71254.20	-167.800	548.923	528.392	3.110472E+07	3.069797E+01	1.567533E-03
71259.20	-162.800	538.155	509.009	2.917884E+07	2.879727E+01	1.499901E-03
71264.20	-157.800	527.387	489.626	2.733711E+07	2.697963E+01	1.433922E-03
71269.20	-152.800	515.619	470.244	2.557744E+07	2.524297E+01	1.369586E-03
71274.20	-147.800	505.851	450.861	2.389776E+07	2.358525E+01	1.306884E-03
71279.20	-142.800	495.082	431.478	2.229598E+07	2.200442E+01	1.245808E-03
71284.20	-137.800	484.314	412.096	2.077006E+07	2.049846E+01	1.186350E-03
71289.20	-132.800	473.546	392.713	1.931795E+07	1.906534E+01	1.128498E-03
71294.20	-127.800	462.778	373.330	1.793762E+07	1.770305E+01	1.072246E-03
71299.20	-122.800	452.010	353.948	1.662705E+07	1.640962E+01	1.017582E-03
71304.20	-117.800	441.242	334.565	1.538423E+07	1.518305E+01	9.644980E-04
71309.20	-112.800	430.473	315.182	1.420717E+07	1.402138E+01	9.129841E-04
71314.20	-107.800	419.705	295.800	1.309388E+07	1.292266E+01	8.630304E-04
71319.20	-102.800	408.937	276.417	1.204241E+07	1.188493E+01	8.146272E-04
71324.20	-97.800	398.169	257.034	1.105079E+07	1.090628E+01	7.677645E-04
71325.30	-96.700	395.800	252.770	1.084047E+07	1.069871E+01	7.576604E-04
71329.20	-92.800	387.774	238.324	1.011742E+07	9.985117E+00	7.217600E-04
71334.20	-87.800	377.485	219.803	9.241021E+06	9.120179E+00	6.772083E-04
71339.20	-82.800	367.196	201.283	8.419539E+06	8.309439E+00	6.342970E-04
71344.20	-77.800	356.907	182.762	7.650913E+06	7.550864E+00	5.930084E-04
71349.20	-72.800	346.617	164.241	6.933108E+06	6.842445E+00	5.533244E-04
71354.20	-67.800	336.328	145.721	6.264111E+06	6.182197E+00	5.152268E-04

TABLE 2-R356397

DATE 01/13/72.

JUPIT
 NOMINAL JUPITER ATMOSPHERE,
 MEAN MOLECULAR MASS = 2.300 GRAMS/MOLE
 INITIAL PRESSURE = 1.013250E+06 DYNES/SQCM AT 71422.00 KM RADIUS
 PRINT INTERVAL = 5 KM, GAS CONSTANT = 8.31430000E+07 JOULES/(MOLE.DEG KELVIN)
 ONE ATMOSPHERE = 1.01325000E+06 DYNES/CM2, MU= 1.27527552E+08 KM3/SEC2
 GREF = 2.50000000E-02 KM/SEC2

ALTITUDE IS ABOVE 71422.0 KM RADIUS

RADIUS KM	ALTITUDE KM	TEMPERATURE		PRESSURE		DENSITY GM/CM3
		KELVIN	FAHREN	DYNE/CM2	ATMOSPHERES	
71359.20	-62.800	326.039	127.200	5.641933E+06	5.568155E+00	4.786970E-04
71364.20	-57.800	315.750	108.679	5.064610E+06	4.998382E+00	4.437163E-04
71369.20	-52.800	305.460	90.159	4.530202E+06	4.470962E+00	4.102654E-04
71374.20	-47.800	295.171	71.638	4.036794E+06	3.984006E+00	3.783249E-04
71379.20	-42.800	284.882	53.117	3.582497E+06	3.535650E+00	3.478750E-04
71384.20	-37.800	274.593	34.597	3.165447E+06	3.124053E+00	3.188955E-04
71385.80	-36.200	271.300	28.670	3.039556E+06	2.999809E+00	3.099292E-04
71389.00	-33.000	264.200	15.890	2.798190E+06	2.761599E+00	2.929858E-04
71389.20	-32.800	263.752	15.084	2.783553E+06	2.747153E+00	2.919483E-04
71394.00	-28.000	253.000	-4.270	2.447633E+06	2.415626E+00	2.676258E-04
71394.20	-27.800	252.545	-5.088	2.434266E+06	2.402434E+00	2.666433E-04
71398.40	-23.600	243.000	-22.270	2.164776E+06	2.136467E+00	2.464386E-04
71399.20	-22.800	241.207	-25.498	2.115835E+06	2.088166E+00	2.426577E-04
71404.20	-17.800	230.000	-45.670	1.826809E+06	1.802920E+00	2.197189E-04
71404.20	-17.800	230.000	-45.670	1.826809E+06	1.802920E+00	2.197189E-04
71409.20	-12.800	218.532	-66.312	1.565623E+06	1.545149E+00	1.981865E-04
71414.20	-7.800	207.064	-86.954	1.330694E+06	1.313293E+00	1.777769E-04
71415.10	-6.900	205.000	-90.670	1.291087E+06	1.274204E+00	1.742223E-04
71419.20	-2.800	195.552	-107.676	1.120596E+06	1.105942E+00	1.585216E-04
71422.00	0.	189.100	-119.290	1.013250E+06	1.000000E+00	1.482270E-04
71424.20	2.200	183.919	-128.617	9.338718E+05	9.216598E-01	1.404636E-04
71429.20	7.200	172.143	-149.813	7.689789E+05	7.589231E-01	1.235743E-04
71434.20	12.200	160.367	-171.010	6.245586E+05	6.163914E-01	1.077361E-04
71439.20	17.200	148.591	-192.207	4.992894E+05	4.927604E-01	9.295288E-05
71440.30	18.300	146.000	-196.870	4.741687E+05	4.679681E-01	8.984257E-05
71443.20	21.200	139.000	-209.470	4.119369E+05	4.065501E-01	8.198192E-05
71444.20	22.200	136.586	-213.815	3.917836E+05	3.866604E-01	7.934902E-05
71446.10	24.100	132.000	-222.070	3.552841E+05	3.506382E-01	7.445674E-05
71449.00	27.000	125.000	-234.670	3.039656E+05	2.999908E-01	6.726925E-05
71449.20	27.200	124.524	-235.527	3.006169E+05	2.966858E-01	6.678257E-05
71451.10	29.100	120.000	-243.670	2.700035E+05	2.564727E-01	6.224296E-05
71453.90	31.900	113.000	-256.270	2.286769E+05	2.256866E-01	5.598169E-05
71454.20	32.200	113.000	-256.270	2.245203E+05	2.215843E-01	5.496412E-05
71459.20	37.200	113.000	-256.270	1.653814E+05	1.632188E-01	4.048652E-05
71464.20	42.200	113.000	-256.270	1.218250E+05	1.202320E-01	2.982361E-05
71467.20	45.200	113.000	-256.270	1.014134E+05	1.000872E-01	2.482670E-05
71469.20	47.200	113.000	-256.270	8.974388E+04	8.857033E-02	2.196992E-05
71470.30	48.300	113.000	-256.270	8.390858E+04	8.281133E-02	2.054140E-05
71474.20	52.200	115.645	-251.509	6.629558E+04	6.542865E-02	1.585844E-05
71479.20	57.200	119.036	-245.406	4.939571E+04	4.874978E-02	1.147927E-05
71484.20	62.200	122.426	-239.302	3.711086E+04	3.662557E-02	8.385480E-06
71487.70	65.700	124.800	-235.030	3.052173E+04	3.012261E-02	6.765451E-06
71489.20	67.200	125.814	-233.204	2.810103E+04	2.773356E-02	6.178662E-06
71494.20	72.200	129.195	-227.119	2.143706E+04	2.115674E-02	4.590087E-06
71499.20	77.200	132.576	-221.033	1.646878E+04	1.625342E-02	3.436354E-06
71504.20	82.200	135.957	-214.947	1.273669E+04	1.257014E-02	2.591533E-06
71508.70	86.700	139.000	-209.470	1.016186E+04	1.002898E-02	2.022370E-06

TABLE 2-R356397

DATE 01/13/72.

JUPIT

NOMINAL JUPITER ATMOSPHERE,

MEAN MOLECULAR MASS = 2.300 GRAMS/MOLE

INITIAL PRESSURE = 1.013250E+06 DYNES/SQCM AT 71422.00 KM RADIUS

PRINT INTERVAL = 5 KM, GAS CONSTANT = 8.31430000E+07 JOULES/(MOLE.DEG KELVIN)

ONE ATMOSPHERE = 1.01325000E+06 DYNES/CM2, MU= 1.27527552E+08 KM3/SEC2

GREF = 2.50000000E-02 KM/SEC2

ALTITUDE IS ABOVE 71422.0 KM RADIUS

RADIUS KM	ALTITUDE KM	TEMPERATURE		PRESSURE		DENSITY
		KELVIN	FAHREN	DYNE/CM2	ATMOSPHERES	GM/CM3
71509.20	87.200	139.341	-208.856	9.913083E+03	9.783452E-03	1.968032E-06
71514.20	92.200	142.750	-202.720	7.762435E+03	7.560928E-03	1.504264E-06
71517.50	95.500	145.000	-198.670	6.626550E+03	6.539896E-03	1.264217E-06
71519.20	97.200	145.000	-198.670	6.111797E+03	6.031875E-03	1.166012E-06
71524.20	102.200	145.000	-198.670	4.818244E+03	4.755237E-03	9.192273E-07
71529.20	107.200	145.000	-198.670	3.798596E+03	3.748922E-03	7.246982E-07
71533.70	111.700	145.000	-198.670	3.066876E+03	3.026772E-03	5.851004E-07
71534.20	112.200	145.000	-198.670	2.994827E+03	2.955665E-03	5.713549E-07
71539.20	117.200	145.000	-198.670	2.361212E+03	2.330335E-03	4.504734E-07
71544.20	122.200	145.000	-198.670	1.861712E+03	1.837367E-03	3.551785E-07
71549.20	127.200	145.000	-198.670	1.467927E+03	1.448732E-03	2.800520E-07
71554.20	132.200	145.000	-198.670	1.157473E+03	1.142337E-03	2.208234E-07
71556.80	134.800	145.000	-198.670	1.022954E+03	1.009577E-03	1.951597E-07
71559.20	137.200	145.000	-198.670	9.127081E+02	9.007728E-04	1.741270E-07
71564.20	142.200	145.000	-198.670	7.197260E+02	7.103143E-04	1.373097E-07
71569.20	147.200	145.000	-198.670	5.675667E+02	5.501447E-04	1.082807E-07
71574.20	152.200	145.000	-198.670	4.475906E+02	4.417376E-04	8.539160E-08
71579.20	157.200	145.000	-198.670	3.529877E+02	3.483717E-04	6.734319E-08
71582.00	160.000	145.000	-198.670	3.090422E+02	3.050009E-04	5.895925E-08
71584.20	162.200	145.000	-198.670	2.783892E+02	2.747488E-04	5.311126E-08
71589.20	167.200	145.000	-198.670	2.195633E+02	2.166921E-04	4.188941E-08
71594.20	172.200	145.000	-198.670	1.731735E+02	1.709090E-04	3.303814E-08
71599.20	177.200	145.000	-198.670	1.365896E+02	1.348034E-04	2.605864E-08
71604.20	182.200	145.000	-198.670	1.077378E+02	1.063289E-04	2.055428E-08
71605.10	183.100	145.000	-198.670	1.032335E+02	1.018836E-04	1.959495E-08
71609.20	187.200	145.000	-198.670	8.498319E+01	8.387189E-05	1.621314E-08
71614.20	192.200	145.000	-198.670	6.703666E+01	6.516003E-05	1.278929E-08
71619.20	197.200	145.000	-198.670	5.288177E+01	5.219025E-05	1.008882E-08
71624.20	202.200	145.000	-198.670	4.171710E+01	4.117157E-05	7.958812E-09
71629.20	207.200	145.000	-198.670	3.291065E+01	3.248029E-05	6.278713E-09
71630.30	208.300	145.000	-198.670	3.123801E+01	3.082952E-05	5.959606E-09
71634.20	212.200	145.000	-198.670	2.596410E+01	2.562458E-05	4.953447E-09
71639.20	217.200	145.000	-198.670	2.048446E+01	2.021659E-05	3.908037E-09
71644.20	222.200	145.000	-198.670	1.616181E+01	1.595047E-05	3.083360E-09
71649.20	227.200	145.000	-198.670	1.275176E+01	1.258500E-05	2.432787E-09
71653.40	231.400	145.000	-198.670	1.045029E+01	1.031363E-05	1.993712E-09
71654.20	232.200	145.000	-198.670	1.006154E+01	9.929964E-06	1.919546E-09
71659.20	237.200	145.000	-198.670	7.939130E+00	7.835313E-06	1.514632E-09
71664.20	242.200	145.000	-198.670	6.264637E+00	6.182716E-06	1.195171E-09
71669.20	247.200	145.000	-198.670	4.943486E+00	4.878841E-06	9.431211E-10
71674.20	252.200	145.000	-198.670	3.901081E+00	3.850068E-06	7.442505E-10
71678.60	256.600	145.000	-198.670	3.167309E+00	3.125891E-06	6.042610E-10
71679.20	257.200	145.000	-198.670	3.078584E+00	3.038327E-06	5.873341E-10
71684.20	262.200	145.000	-198.670	2.429582E+00	2.397811E-06	4.635170E-10
71689.20	267.200	145.000	-198.670	1.917460E+00	1.892386E-06	3.658140E-10
71694.20	272.200	145.000	-198.670	1.513336E+00	1.493546E-06	2.887151E-10

TABLE 2-R356397

DATE 01/13/72.

JUPIT
 NOMINAL JUPITER ATMOSPHERE,
 MEAN MOLECULAR MASS = 2.300 GRAMS/MOLE
 INITIAL PRESSURE = 1.013250E+06 DYNES/SQCM AT 71422.00 KM RADIUS
 PRINT INTERVAL = 5 KM, GAS CONSTANT = 8.31430000E+07 JOULES/(MOLE.DEG KELVIN)
 ONE ATMOSPHERE = 1.01325000E+06 DYNES/CM2, MU= 1.27527552E+08 KM3/SEC2
 GREF = 2.50000000E-02 KM/SEC2

ALTITUDE IS ABOVE 71422.0 KM RADIUS

RADIUS KM	ALTITUDE KM	TEMPERATURE		PRESSURE		DENSITY GM/CM3
		KELVIN	FAHREN	DYNE/CM2	ATMOSPHERES	
71699.20	277.200	145.000	-198.570	1.194425E+00	1.178805E-06	2.278730E-10
71701.70	279.700	145.000	-198.670	1.061148E+00	1.047271E-06	2.024464E-10
71704.20	282.200	145.000	-198.670	9.427499E-01	9.304218E-07	1.798584E-10
71709.20	287.200	145.000	-198.670	7.441296E-01	7.343988E-07	1.419655E-10
71714.20	292.200	145.000	-198.670	5.873744E-01	5.796934E-07	1.120596E-10
71719.20	297.200	145.000	-198.670	4.636558E-01	4.575927E-07	8.845653E-11
71724.20	302.200	145.000	-198.670	3.660082E-01	3.612220E-07	6.982725E-11
71726.90	304.900	145.000	-198.670	3.221336E-01	3.179212E-07	6.145684E-11
71729.20	307.200	145.000	-198.670	2.889350E-01	2.851567E-07	5.512319E-11
71734.20	312.200	145.000	-198.670	2.280993E-01	2.251165E-07	4.351691E-11
71735.40	313.400	145.000	-198.670	2.155181E-01	2.126998E-07	4.111666E-11

Section D

TABLE 4-R356397

DATE 01/13/72.

SATURN

NOMINAL SATURN ATMOSPHERE,

MEAN MOLECULAR MASS = 2.270 GRAMS/MOLE

INITIAL PRESSURE = 1.013250E+06 DYNES/SQCM AT 59800.00 KM RADIUS

PRINT INTERVAL = 10 KM, GAS CONSTANT = 8.31430000E+07 JOULES/(MOLE.DEG KELVIN

ONE ATMOSPHERE = 1.01325000E+06 DYNES/CM2, MU= 3.75484200E+07 KM3/SEC2

GREF = 1.05000000E-02 KM/SEC2

ALTITUDE IS ABOVE 59800.0 KM RADIUS

RADIUS KM	ALTITUDE KM	TEMPERATURE		PRESSURE		DENSITY GM/CM3
		KELVIN	FAHREN	DYNE/CM2	ATMOSPHERES	
59264.00	-536.000	617.300	652.370	1.053257E+08	1.039484E+02	4.654647E-03
59274.00	-526.000	609.412	637.271	1.004336E+08	9.912022E+01	4.499540E-03
59284.00	-516.000	601.024	622.173	9.570707E+07	9.445554E+01	4.347630E-03
59294.00	-506.000	592.636	607.074	9.114275E+07	8.995090E+01	4.198890E-03
59304.00	-496.000	584.247	591.975	8.673711E+07	8.560287E+01	4.053295E-03
59314.00	-486.000	575.859	576.877	8.248671E+07	8.140805E+01	3.910819E-03
59324.00	-476.000	567.471	561.778	7.838812E+07	7.736306E+01	3.771435E-03
59334.00	-466.000	559.083	546.680	7.443797E+07	7.346456E+01	3.635116E-03
59344.00	-456.000	550.695	531.581	7.063288E+07	6.970924E+01	3.501838E-03
59354.00	-446.000	542.307	516.482	6.696956E+07	6.609381E+01	3.371572E-03
59364.00	-436.000	533.919	501.384	6.344468E+07	6.261504E+01	3.244294E-03
59374.00	-426.000	525.531	486.285	6.005501E+07	5.926969E+01	3.119977E-03
59384.00	-416.000	517.142	471.186	5.679731E+07	5.605458E+01	2.998594E-03
59394.00	-406.000	508.754	456.088	5.366837E+07	5.296656E+01	2.880119E-03
59404.00	-396.000	500.366	440.989	5.066503E+07	5.000250E+01	2.764525E-03
59414.00	-386.000	491.978	425.891	4.778417E+07	4.715931E+01	2.651786E-03
59424.00	-376.000	483.590	410.792	4.502266E+07	4.443391E+01	2.541874E-03
59434.00	-366.000	475.202	395.693	4.237745E+07	4.182329E+01	2.434764E-03
59444.00	-356.000	466.814	380.595	3.984548E+07	3.932443E+01	2.330428E-03
59454.00	-346.000	458.426	365.496	3.742376E+07	3.593438E+01	2.228839E-03
59464.00	-336.000	450.037	350.397	3.510930E+07	3.465018E+01	2.129971E-03
59474.00	-326.000	441.649	335.299	3.289915E+07	3.246894E+01	2.033796E-03
59483.00	-317.000	434.100	321.710	3.099680E+07	3.059147E+01	1.949518E-03
59484.00	-316.000	433.222	320.130	3.079040E+07	3.038776E+01	1.940460E-03
59494.00	-306.000	424.445	304.331	2.877912E+07	2.840278E+01	1.851213E-03
59504.00	-296.000	415.667	288.531	2.686189E+07	2.651062E+01	1.764374E-03
59514.00	-286.000	406.890	272.732	2.503611E+07	2.470872E+01	1.679925E-03
59524.00	-276.000	398.113	256.933	2.329920E+07	2.299452E+01	1.597847E-03
59534.00	-266.000	389.335	241.134	2.164859E+07	2.136550E+01	1.518120E-03
59544.00	-256.000	380.558	225.334	2.008175E+07	1.981915E+01	1.440725E-03
59554.00	-246.000	371.781	209.535	1.859617E+07	1.835299E+01	1.365642E-03
59564.00	-236.000	363.003	193.736	1.718934E+07	1.696456E+01	1.292852E-03
59574.00	-226.000	354.226	177.936	1.585880E+07	1.565142E+01	1.222335E-03
59584.00	-216.000	345.448	162.137	1.460211E+07	1.441116E+01	1.154071E-03
59594.00	-206.000	336.671	146.338	1.341684E+07	1.324140E+01	1.088040E-03
59604.00	-196.000	327.894	130.539	1.230061E+07	1.213976E+01	1.024221E-03
59614.00	-186.000	319.116	114.739	1.125102E+07	1.110390E+01	9.625943E-04
59624.00	-176.000	310.339	98.940	1.026575E+07	1.013150E+01	9.031388E-04
59624.50	-175.500	309.900	98.150	1.021813E+07	1.008451E+01	9.002227E-04
59634.00	-166.000	301.264	82.605	9.342036E+06	9.219873E+00	8.466326E-04
59644.00	-156.000	292.173	66.241	8.477192E+06	8.366338E+00	7.921593E-04
59654.00	-146.000	283.082	49.877	7.669082E+06	7.568795E+00	7.396590E-04
59661.90	-138.100	275.900	36.950	7.069400E+06	6.976955E+00	6.995697E-04
59664.00	-136.000	273.971	33.478	6.915589E+06	6.825155E+00	6.891667E-04
59674.00	-126.000	264.787	16.946	6.214464E+06	6.133199E+00	6.407777E-04
59684.00	-116.000	255.602	.414	5.563591E+06	5.490838E+00	5.942789E-04
59690.10	-109.900	250.000	-9.670	5.190372E+06	5.122499E+00	5.668376E-04

TABLE 4-R356397

DATE 01/13/72.

SATURN

NOMINAL SATURN ATMOSPHERE,

MEAN MOLECULAR MASS = 2.270 GRAMS/MOLE

INITIAL PRESSURE = 1.013250E+06 DYNES/SQCM AT 59800.00 KM RADIUS

PRINT INTERVAL = 10 KM, GAS CONSTANT = 8.31430000E+07 JOULES/(MOLE.DEG KELVIN)

ONE ATMOSPHERE = 1.01325000E+06 DYNES/CM2, MU= 3.75484200E+07 KM3/SEC2

GREF = 1.05000000E-02 KM/SEC2

ALTITUDE IS ABOVE 59800.0 KM RADIUS

RADIUS KM	ALTITUDE KM	TEMPERATURE		PRESSURE		DENSITY GM/CM3
		KELVIN	FAHREN	DYNE/CM2	ATMOSPHERES	
59694.00	-106.000	246.372	-16.200	4.960931E+06	4.396058E+00	5.497584E-04
59704.00	-96.000	237.070	-32.944	4.404293E+06	4.346699E+00	5.072245E-04
59711.60	-88.400	230.000	-45.670	4.010801E+06	3.358353E+00	4.761057E-04
59714.00	-86.000	227.703	-49.804	3.891672E+06	3.340781E+00	4.666238E-04
59724.00	-76.000	219.134	-67.029	3.420783E+06	3.376050E+00	4.281563E-04
59732.50	-67.500	210.000	-81.670	3.051861E+06	3.011953E+00	3.967762E-04
59734.00	-66.000	208.563	-84.256	2.989657E+06	2.350562E+00	3.913664E-04
59744.00	-56.000	198.985	-101.496	2.596496E+06	2.562542E+00	3.562597E-04
59754.00	-46.000	189.407	-118.737	2.239516E+06	2.210231E+00	3.228177E-04
59764.00	-36.000	179.830	-135.977	1.916945E+06	1.891877E+00	2.910373E-04
59774.00	-26.000	170.252	-153.217	1.627013E+06	1.605737E+00	2.609155E-04
59784.00	-16.000	160.674	-170.457	1.367958E+06	1.350070E+00	2.324493E-04
59794.00	-6.000	151.096	-187.698	1.138023E+06	1.123141E+00	2.056358E-04
59794.10	-5.900	151.000	-187.870	1.135865E+06	1.121011E+00	2.053760E-04
59800.00	0.	145.200	-198.310	1.013250E+06	1.000000E+00	1.905242E-04
59804.00	4.000	141.226	-205.463	9.352829E+05	9.230525E-01	1.808123E-04
59814.00	14.000	131.292	-223.345	7.578077E+05	7.478981E-01	1.575878E-04
59815.30	15.300	130.000	-225.670	7.365062E+05	7.268751E-01	1.546797E-04
59824.00	24.000	121.174	-241.557	6.038788E+05	5.359821E-01	1.360633E-04
59834.00	34.000	111.029	-259.818	4.717923E+05	4.656228E-01	1.160151E-04
59844.00	44.000	100.884	-278.079	3.600081E+05	3.353004E-01	9.742938E-05
59849.80	49.800	95.000	-288.670	3.038629E+05	2.998894E-01	8.732815E-05
59854.00	54.000	90.630	-296.536	2.669479E+05	2.534571E-01	8.041822E-05
59864.00	64.000	80.225	-315.264	1.908953E+05	1.883991E-01	6.496559E-05
59867.10	67.100	77.000	-321.070	1.705298E+05	1.682998E-01	6.046579E-05
59874.00	74.000	77.000	-321.070	1.319766E+05	1.302508E-01	4.679575E-05
59881.10	81.100	77.000	-321.070	1.013898E+05	1.000640E-01	3.595040E-05
59884.00	84.000	77.000	-321.070	9.104025E+04	8.984974E-02	3.228069E-05
59894.00	94.000	77.000	-321.070	6.280926E+04	6.198792E-02	2.227066E-05
59904.00	104.000	77.000	-321.070	4.333789E+04	4.277117E-02	1.536658E-05
59913.40	113.400	77.000	-321.070	3.057949E+04	3.017961E-02	1.084276E-05
59914.00	114.000	77.000	-321.070	2.990650E+04	2.951542E-02	1.060413E-05
59920.80	120.800	77.000	-321.070	2.324058E+04	2.293666E-02	8.240552E-06
59924.00	124.000	77.329	-320.479	2.064557E+04	2.037559E-02	7.289321E-06
59934.00	134.000	78.355	-318.630	1.430775E+04	1.412065E-02	4.985431E-06
59943.20	143.200	79.300	-316.930	1.025498E+04	1.012088E-02	3.530709E-06
59944.00	144.000	79.380	-316.786	9.964174E+03	9.833875E-03	3.427139E-06
59954.00	154.000	80.377	-314.992	6.971871E+03	6.880702E-03	2.368201E-06
59964.00	164.000	81.374	-313.197	4.900277E+03	4.836197E-03	1.644128E-06
59974.00	174.000	82.371	-311.402	3.459451E+03	3.414213E-03	1.146656E-06
59977.30	177.300	82.700	-310.810	3.086876E+03	3.046510E-03	1.019093E-06
59984.00	184.000	83.385	-309.578	2.452861E+03	2.420785E-03	8.031332E-07
59994.00	194.000	84.406	-307.739	1.746642E+03	1.723802E-03	5.649757E-07
60004.00	204.000	85.428	-305.900	1.248987E+03	1.232654E-03	3.991706E-07
60009.60	209.600	86.000	-304.870	1.036994E+03	1.023433E-03	3.292136E-07
60014.00	214.000	86.441	-304.076	8.967849E+02	8.950579E-04	2.832486E-07

TABLE 4-R356397

DATE 01/13/72.

SATURN

NOMINAL SATURN ATMOSPHERE,

MEAN MOLECULAR MASS = 2.270 GRAMS/MOLE

INITIAL PRESSURE = 1.013250E+06 DYNES/SQCM AT 59800.00 KM RADIUS

PRINT INTERVAL = 10 KM, GAS CONSTANT = 8.31430000E+07 JOULES/(MOLE.DEG KELVIN

ONE ATMOSPHERE = 1.01325000E+06 DYNES/CM2, MU= 3.75484200E+07 KM3/SEC2

GREF = 1.05000000E-02 KM/SEC2

ALTITUDE IS ABOVE 59800.0 KM RADIUS

RADIUS KM	ALTITUDE KM	TEMPERATURE		PRESSURE		DENSITY GM/CM3
		KELVIN	FAHREN	DYNE/CM2	ATMOSPHERES	
60024.00	224.000	87.444	-302.271	6.464431E+02	6.379897E-04	2.018371E-07
60034.00	234.000	88.447	-300.466	4.677782E+02	4.616612E-04	1.443973E-07
60044.00	244.000	89.449	-298.661	3.397659E+02	3.353228E-04	1.037058E-07
60046.50	246.500	89.700	-298.210	3.138449E+02	3.097408E-04	9.552627E-08
60054.00	254.000	90.469	-296.825	2.476983E+02	2.444592E-04	7.475190E-08
60064.00	264.000	91.495	-294.979	1.812415E+02	1.788714E-04	5.408303E-08
60074.00	274.000	92.521	-293.133	1.330912E+02	1.313508E-04	3.927457E-08
60081.60	281.600	93.300	-291.730	1.054987E+02	1.041191E-04	3.087206E-08
60084.00	284.000	93.540	-291.298	9.807594E+01	9.579343E-05	2.862631E-08
60094.00	294.000	94.540	-289.498	7.251700E+01	7.156871E-05	2.094230E-08
60104.00	304.000	95.540	-287.698	5.379476E+01	5.309130E-05	1.537287E-08
60114.00	314.000	96.540	-285.898	4.003441E+01	3.951089E-05	1.132208E-08
60121.60	321.600	97.300	-284.530	3.205047E+01	3.163136E-05	8.993355E-09
60124.00	324.000	97.540	-284.098	2.988761E+01	2.949678E-05	8.365823E-09
60134.00	334.000	98.540	-282.298	2.238132E+01	2.208865E-05	6.201166E-09
60144.00	344.000	99.540	-280.498	1.681085E+01	1.659102E-05	4.610970E-09
60154.00	354.000	100.540	-278.698	1.266419E+01	1.249858E-05	3.439050E-09
60159.60	359.600	101.100	-277.690	1.082035E+01	1.067886E-05	2.922068E-09
60164.00	364.000	101.546	-276.887	9.568069E+00	9.442950E-06	2.572535E-09
60174.00	374.000	102.560	-275.062	7.249672E+00	7.154870E-06	1.929927E-09
60184.00	384.000	103.574	-273.237	5.508552E+00	5.436518E-06	1.452071E-09
60194.00	394.000	104.588	-271.412	4.197181E+00	4.142295E-06	1.095665E-09
60203.00	403.000	105.500	-269.770	3.293773E+00	3.250701E-06	8.523960E-10
60204.00	404.000	105.602	-269.587	3.206682E+00	3.164749E-06	8.290584E-10
60214.00	414.000	106.619	-267.756	2.456470E+00	2.424348E-06	6.290404E-10
60224.00	424.000	107.636	-265.926	1.886705E+00	1.862033E-06	4.785731E-10
60234.00	434.000	108.653	-264.095	1.452821E+00	1.433822E-06	3.650667E-10
60244.00	444.000	109.669	-262.265	1.121539E+00	1.106873E-06	2.792087E-10
60244.30	444.300	109.700	-262.210	1.112908E+00	1.098355E-06	2.769829E-10
60254.00	454.000	110.689	-260.431	8.679458E-01	8.565959E-07	2.140869E-10
60264.00	464.000	111.708	-258.596	6.733292E-01	6.645243E-07	1.645678E-10
60274.00	474.000	112.727	-256.762	5.236005E-01	5.167535E-07	1.268157E-10
60284.00	484.000	113.746	-254.927	4.081234E-01	4.027865E-07	9.796165E-11
60291.40	491.400	114.500	-253.570	3.399089E-01	3.354640E-07	8.105077E-11
60294.00	494.000	114.762	-253.099	3.188478E-01	3.146783E-07	7.585538E-11
60304.00	504.000	115.768	-251.287	2.496606E-01	2.463958E-07	5.887893E-11
60314.00	514.000	116.775	-249.475	1.959167E-01	1.933547E-07	4.580586E-11
60324.00	524.000	117.782	-247.663	1.540746E-01	1.520598E-07	3.571517E-11
60334.00	534.000	118.789	-245.851	1.214264E-01	1.198385E-07	2.790863E-11
60336.10	536.100	119.000	-245.470	1.155343E-01	1.140235E-07	2.650722E-11

Section E

TABLE 5-R356397

DATE 01/13/72.

URANUS

NOMINAL URANUS ATMOSPHERE,

MEAN MOLECULAR MASS = 2.680 GRAMS/MOLE

INITIAL PRESSURE = 1.013250E+06 DYNES/SQCM AT 26468.00 KM RADIUS

PRINT INTERVAL = 5 KM, GAS CONSTANT = 8.31430000E+07 JOULES/(MOLE.DEG KELVIN)

ONE ATMOSPHERE = 1.01325000E+06 DYNES/CM2, MU = 5.67444957E+06 KM3/SEC2

GREF = 8.09993416E-03 KM/SEC2

ALTITUDE IS ABOVE 26468.0 KM RADIUS

RADIUS KM	ALTITUDE KM	TEMPERATURE		PRESSURE		DENSITY GM/CM3
		KELVIN	FAHREN	DYNE/CM2	ATMOSPHERES	
26112.10	-355.900	382.300	228.470	1.115883E+08	1.101291E+02	9.404984E-03
26117.10	-350.900	376.033	217.190	1.077119E+08	1.063033E+02	9.230296E-03
26122.10	-345.900	369.767	205.910	1.039095E+08	1.025507E+02	9.056109E-03
26127.10	-340.900	363.500	194.631	1.001808E+08	9.887079E+01	8.882425E-03
26132.10	-335.900	357.234	183.351	9.652569E+07	9.526345E+01	8.709249E-03
26137.10	-330.900	350.967	172.071	9.294379E+07	9.172839E+01	8.536581E-03
26142.10	-325.900	344.701	160.791	8.943484E+07	8.826533E+01	8.364426E-03
26147.10	-320.900	338.434	149.511	8.599859E+07	8.487401E+01	8.192786E-03
26152.10	-315.900	332.168	138.232	8.263476E+07	8.155417E+01	8.021665E-03
26157.10	-310.900	325.901	126.952	7.934308E+07	7.830554E+01	7.851065E-03
26162.10	-305.900	319.634	115.672	7.612329E+07	7.512784E+01	7.680990E-03
26167.10	-300.900	313.368	104.392	7.297510E+07	7.202082E+01	7.511444E-03
26172.10	-295.900	307.101	93.112	6.989825E+07	6.898420E+01	7.342430E-03
26177.10	-290.900	300.834	81.832	6.695517E+07	6.674431E+01	7.172832E-03
26182.10	-285.900	294.567	70.552	6.406688E+07	6.403851E+01	7.004732E-03
26187.10	-280.900	288.300	59.272	6.129357E+07	6.120915E+01	6.837482E-03
26192.10	-275.900	282.033	48.000	5.865005E+07	5.832091E+01	6.670239E-03
26197.10	-270.900	275.767	36.728	5.611210E+07	5.537834E+01	6.502202E-03
26202.10	-265.900	269.500	25.456	5.367583E+07	5.297393E+01	6.334660E-03
26207.10	-260.900	263.234	14.184	5.133750E+07	5.066617E+01	6.167529E-03
26212.10	-255.900	256.967	2.912	4.909347E+07	4.845148E+01	6.000889E-03
26217.10	-250.900	250.701	-8.360	4.694024E+07	4.632641E+01	5.834660E-03
26222.10	-245.900	244.434	-19.632	4.487443E+07	4.428762E+01	5.668431E-03
26222.80	-245.200	244.000	-20.360	4.459201E+07	4.400889E+01	5.644871E-03
26227.10	-240.900	238.168	-31.304	4.288581E+07	4.232500E+01	5.480990E-03
26232.10	-235.900	232.334	-42.552	4.096061E+07	4.042498E+01	5.31887E-03
26237.10	-230.900	226.500	-53.800	3.909743E+07	3.858616E+01	5.157565E-03
26242.10	-225.900	220.667	-65.048	3.729505E+07	3.680735E+01	4.996321E-03
26247.10	-220.900	214.833	-76.296	3.555228E+07	3.508737E+01	4.835187E-03
26252.10	-215.900	209.000	-87.544	3.386792E+07	3.342504E+01	4.674045E-03
26253.50	-214.500	208.000	-89.400	3.340561E+07	3.296976E+01	4.621377E-03
26257.10	-210.900	202.168	-99.304	3.224026E+07	3.181866E+01	4.569356E-03
26260.70	-207.300	196.334	-109.208	3.110193E+07	3.069522E+01	4.517565E-03
26262.10	-205.900	194.500	-111.300	3.066677E+07	3.026575E+01	4.466321E-03
26267.10	-200.900	188.667	-122.548	2.914698E+07	2.876583E+01	4.415187E-03
26272.10	-195.900	182.833	-133.796	2.768007E+07	2.731811E+01	4.364045E-03
26277.10	-190.900	177.000	-145.044	2.626499E+07	2.592153E+01	4.312902E-03
26282.10	-185.900	171.168	-156.292	2.490069E+07	2.457507E+01	4.261760E-03
26287.10	-180.900	165.334	-167.540	2.358613E+07	2.327770E+01	4.210618E-03
26292.10	-175.900	159.500	-178.788	2.232028E+07	2.202841E+01	4.159476E-03
26297.10	-170.900	153.667	-189.936	2.110211E+07	2.082617E+01	4.108334E-03
26302.10	-165.900	147.833	-201.184	1.993060E+07	1.966998E+01	4.057192E-03
26307.10	-160.900	142.000	-212.432	1.880473E+07	1.855883E+01	4.006050E-03
26312.10	-155.900	136.168	-223.680	1.772350E+07	1.749173E+01	3.954908E-03
26317.10	-150.900	130.334	-234.928	1.668588E+07	1.646769E+01	3.903766E-03

TABLE 5-R356397

DATE 01/13/72.

URANUS

NOMINAL URANUS ATMOSPHERE,

MEAN MOLECULAR MASS = 2.680 GRAMS/MOLE

INITIAL PRESSURE = 1.013250E+06 DYNES/SQCM AT 26468.00 KM RADIUS

PRINT INTERVAL = 5 KM, GAS CONSTANT = 8.31430000E+07 JOULES/(MOLE.DEG KELVIN)

ONE ATMOSPHERE = 1.01325000E+06 DYNES/CM2, MU= 5.67444957E+06 KM3/SEC2

GREF = 8.09993416E-03 KM/SEC2

ALTITUDE IS ABOVE 26468.0 KM RADIUS

RADIUS KM	ALTITUDE KM	TEMPERATURE		PRESSURE		DENSITY GM/CM3
		KELVIN	FAHREN	DYNE/CM2	ATMOSPHERES	
26322.10	-145.900	212.464	-77.235	1.569090E+07	1.548572E+01	2.378515E-03
26327.10	-140.900	208.259	-84.804	1.473756E+07	1.454484E+01	2.278912E-03
26332.10	-135.900	204.054	-92.373	1.382486E+07	1.364408E+01	2.181636E-03
26337.10	-130.900	199.849	-99.942	1.295183E+07	1.278246E+01	2.086677E-03
26342.10	-125.900	195.644	-107.511	1.211750E+07	1.195904E+01	1.994023E-03
26347.10	-120.900	191.439	-115.079	1.132089E+07	1.117285E+01	1.903660E-03
26352.10	-115.900	187.234	-122.648	1.056104E+07	1.042294E+01	1.815579E-03
26354.40	-113.600	185.300	-126.130	1.022359E+07	1.008990E+01	1.775824E-03
26357.10	-110.900	182.964	-130.335	9.836986E+06	9.708351E+00	1.729892E-03
26362.10	-105.900	178.638	-138.121	9.147702E+06	9.028080E+00	1.646547E-03
26367.10	-100.900	174.312	-145.908	8.492247E+06	8.381196E+00	1.565419E-03
26372.10	-95.900	169.987	-153.694	7.869692E+06	7.766782E+00	1.486497E-03
26377.10	-90.900	165.661	-161.481	7.279114E+06	7.183927E+00	1.409771E-03
26381.10	-86.900	162.200	-167.710	6.829060E+06	6.739758E+00	1.349963E-03
26382.10	-85.900	161.333	-169.271	6.719569E+06	6.631699E+00	1.335941E-03
26387.10	-80.900	155.995	-177.079	6.189227E+06	6.108292E+00	1.266852E-03
26389.40	-78.600	155.000	-180.670	5.954716E+06	5.876848E+00	1.235642E-03
26392.10	-75.900	152.611	-184.971	5.686955E+06	5.612589E+00	1.198851E-03
26397.10	-70.900	148.186	-192.935	5.212364E+06	5.144204E+00	1.132152E-03
26400.70	-67.300	145.000	-198.670	4.887394E+06	4.823483E+00	1.085283E-03
26402.10	-65.900	143.751	-200.918	4.764730E+06	4.702423E+00	1.067270E-03
26407.10	-60.900	139.290	-208.947	4.343318E+06	4.286521E+00	1.004146E-03
26412.10	-55.900	134.830	-216.976	3.947360E+06	3.895741E+00	9.429103E-04
26417.10	-50.900	130.369	-225.005	3.576068E+06	3.529305E+00	8.835620E-04
26422.10	-45.900	125.909	-233.034	3.228658E+06	3.186437E+00	8.261017E-04
26424.80	-43.200	123.500	-237.370	3.050709E+06	3.010816E+00	7.958584E-04
26427.10	-40.900	121.397	-241.155	2.904315E+06	2.866336E+00	7.708198E-04
26432.10	-35.900	115.825	-249.385	2.602078E+06	2.568051E+00	7.176875E-04
26437.10	-30.900	112.253	-257.614	2.321166E+06	2.290813E+00	6.663396E-04
26442.10	-25.900	107.682	-265.843	2.060838E+06	2.033889E+00	6.167820E-04
26447.10	-20.900	103.110	-274.072	1.820350E+06	1.796545E+00	5.690211E-04
26452.10	-15.900	98.538	-282.301	1.598957E+06	1.578048E+00	5.230639E-04
26457.10	-10.900	93.966	-290.530	1.395912E+06	1.377658E+00	4.789179E-04
26462.10	-5.900	89.395	-298.760	1.210466E+06	1.194638E+00	4.365916E-04
26467.10	-.900	84.823	-306.989	1.041867E+06	1.028243E+00	3.960940E-04
26468.00	0.	84.000	-308.470	1.013250E+06	1.000000E+00	3.889994E-04
26470.30	2.300	81.900	-312.250	9.424638E+05	9.301394E-01	3.710553E-04
26472.10	4.100	80.199	-315.312	8.893812E+05	8.777510E-01	3.573229E-04
26477.10	9.100	75.473	-323.819	7.522641E+05	7.424269E-01	3.204526E-04
26477.60	9.600	75.000	-324.670	7.393676E+05	7.296991E-01	3.168690E-04
26482.10	14.100	71.218	-331.477	6.319937E+05	6.237292E-01	2.737923E-04
26487.10	19.100	67.017	-339.040	5.298433E+05	5.229147E-01	2.323411E-04
26489.50	21.500	65.000	-342.670	4.864899E+05	4.801282E-01	2.145877E-04
26492.10	21.100	62.942	-346.374	4.430145E+05	4.372213E-01	1.991421E-04
26497.10	29.100	58.986	-353.496	3.681521E+05	3.633379E-01	1.717982E-04
26502.10	34.100	55.029	-360.618	3.037691E+05	2.997968E-01	1.473713E-04
26503.40	35.400	54.000	-362.470	2.886031E+05	2.848291E-01	1.414712E-04

TABLE 5-R356397

URANUS

DATE 01/13/72.

NOMINAL URANUS ATMOSPHERE,

MEAN MOLECULAR MASS = 2.680 GRAMS/MOLE

INITIAL PRESSURE = 1.013250E+06 DYNES/SQCM AT 26468.00 KM RADIUS

PRINT INTERVAL = 5 KM, GAS CONSTANT = 8.3143000E+07 JOULES/(MOLE.DEG KELVIN)

ONE ATMOSPHERE = 1.01325000E+06 DYNES/CM2, MU= 5.67444957E+06 KM3/SEC2

GREF = 8.09993416E-03 KM/SEC2

ALTITUDE IS ABOVE 26468.0 KM RADIUS

RADIUS KM	ALTITUDE KM	TEMPERATURE		PRESSURE		DENSITY GM/CM3
		KELVIN	FAHREN	DYNE/CM2	ATMOSPHERES	
26507.10	39.100	54.296	-361.937	2.493441E+05	2.460835E-01	1.217624E-04
26512.10	44.100	54.696	-361.217	2.048311E+05	2.021526E-01	9.951456E-05
26517.10	49.100	55.096	-360.497	1.684457E+05	1.662430E-01	8.142135E-05
26522.10	54.100	55.496	-359.777	1.386712E+05	1.368578E-01	6.669043E-05
26527.10	59.100	55.896	-359.057	1.142800E+05	1.127856E-01	5.468365E-05
26530.90	62.900	56.200	-358.510	9.872365E+04	9.743266E-02	4.705996E-05
26532.10	64.100	56.302	-358.327	9.427877E+04	9.304591E-02	4.485678E-05
26537.10	69.100	56.725	-357.565	7.788826E+04	7.686974E-02	3.677071E-05
26542.10	74.100	57.148	-356.804	6.444696E+04	6.360420E-02	3.019078E-05
26547.10	79.100	57.571	-356.042	5.340659E+04	5.270820E-02	2.482759E-05
26552.10	84.100	57.994	-355.280	4.432402E+04	4.374441E-02	2.044899E-05
26557.10	89.100	58.418	-354.518	3.684050E+04	3.635874E-02	1.686850E-05
26562.10	94.100	58.841	-353.757	3.066509E+04	3.026409E-02	1.393599E-05
26562.80	94.800	58.900	-353.650	2.989088E+04	2.950001E-02	1.356995E-05
26567.10	99.100	59.256	-353.009	2.555957E+04	2.522533E-02	1.154055E-05
26572.10	104.100	59.670	-352.264	2.133003E+04	2.105110E-02	9.570380E-06
26577.10	109.100	60.084	-351.519	1.782176E+04	1.758871E-02	7.946391E-06
26582.10	114.100	60.498	-350.774	1.490817E+04	1.471322E-02	6.606055E-06
26587.10	119.100	60.912	-350.029	1.248550E+04	1.232223E-02	5.498438E-06
26592.10	124.100	61.325	-349.284	1.046863E+04	1.033174E-02	4.581999E-06
26593.00	125.000	61.400	-349.150	1.014308E+04	1.001044E-02	4.434620E-06
26597.10	129.100	61.732	-348.553	8.787887E+03	8.672970E-03	3.821124E-06
26602.10	134.100	62.136	-347.825	7.386038E+03	7.289452E-03	3.190313E-06
26607.10	139.100	62.540	-347.097	6.215338E+03	6.134062E-03	2.666987E-06
26612.10	144.100	62.945	-346.369	5.236454E+03	5.167978E-03	2.232268E-06
26617.10	149.100	63.349	-345.641	4.416948E+03	4.359189E-03	1.870695E-06
26622.10	154.100	63.754	-344.913	3.730038E+03	3.581261E-03	1.569581E-06
26627.10	159.100	64.158	-344.185	3.153577E+03	3.112338E-03	1.318506E-06
26632.10	164.100	64.562	-343.458	2.669234E+03	2.634329E-03	1.108896E-06
26637.10	169.100	64.967	-342.730	2.261812E+03	2.232234E-03	9.336931E-07
26642.10	174.100	65.371	-342.002	1.918699E+03	1.893608E-03	7.870735E-07
26647.10	179.100	65.776	-341.274	1.629414E+03	1.608107E-03	6.642293E-07
26652.10	184.100	66.180	-340.546	1.385240E+03	1.367125E-03	5.611853E-07
26657.10	189.100	66.585	-339.818	1.178911E+03	1.163495E-03	4.746506E-07
26661.00	193.000	66.900	-339.250	1.040314E+03	1.026710E-03	4.168425E-07
26662.10	194.100	66.991	-339.087	1.004371E+03	9.912372E-04	4.018946E-07
26667.10	199.100	67.403	-338.345	8.565653E+02	8.453642E-04	3.406500E-07
26672.10	204.100	67.815	-337.603	7.312652E+02	7.217026E-04	2.890474E-07
26677.10	209.100	68.227	-336.861	6.249310E+02	6.167590E-04	2.455209E-07
26682.10	214.100	68.639	-336.119	5.345972E+02	5.276064E-04	2.087668E-07
26687.10	219.100	69.051	-335.377	4.577764E+02	4.517901E-04	1.776978E-07
26692.10	224.100	69.464	-334.635	3.923801E+02	3.872491E-04	1.514068E-07
26697.10	229.100	69.876	-333.894	3.366531E+02	3.322507E-04	1.291355E-07
26702.10	234.100	70.288	-333.152	2.891179E+02	2.853372E-04	1.102499E-07
26707.10	239.100	70.700	-332.410	2.485303E+02	2.452804E-04	9.421883E-08
26712.10	244.100	71.112	-331.668	2.138410E+02	2.110447E-04	8.059767E-08

TABLE 5-R356397

DATE 01/13/72.

URANUS

NOMINAL URANUS ATMOSPHERE,

MEAN MOLECULAR MASS = 2.680 GRAMS/MOLE

INITIAL PRESSURE = 1.013250E+06 DYNES/SQCM AT 26468.00 KM RADIUS

PRINT INTERVAL = 5 KM, GAS CONSTANT = 8.31430000E+07 JOULES/(MOLE.DEG KELVIN)

ONE ATMOSPHERE = 1.01325000E+06 DYNES/CM2, MU= 5.67444957E+06 KM3/SEC2

GREF = 8.09993416E-03 KM/SEC2

ALTITUDE IS ABOVE 26468.0 KM RADIUS

RADIUS KM	ALTITUDE KM	TEMPERATURE		PRESSURE		DENSITY GM/CM3
		KELVIN	FAHREN	DYNE/CM2	ATMOSPHERES	
26717.10	249.100	71.524	-330.926	1.841641E+02	1.817559E-04	6.901092E-08
26722.10	254.100	71.937	-330.184	1.587512E+02	1.566752E-04	5.914646E-08
26727.10	259.100	72.349	-329.442	1.369689E+02	1.351778E-04	5.073962E-08
26732.10	264.100	72.761	-328.700	1.182812E+02	1.167345E-04	4.356809E-08
26735.00	267.000	73.000	-328.270	1.086782E+02	1.072571E-04	3.989952E-08
26737.10	269.100	73.175	-327.954	1.022338E+02	1.008969E-04	3.744306E-08
26742.10	274.100	73.593	-327.202	8.844191E+01	8.728537E-05	3.220692E-08
26747.10	279.100	74.011	-326.450	7.657787E+01	7.557648E-05	2.772828E-08
26752.10	284.100	74.429	-325.699	6.636295E+01	6.549514E-05	2.389394E-08
26757.10	289.100	74.846	-324.947	5.756004E+01	5.580734E-05	2.060817E-08
26762.10	294.100	75.264	-324.195	4.996723E+01	4.933138E-05	1.778990E-08
26767.10	299.100	75.682	-323.443	4.341244E+01	4.284474E-05	1.537042E-08
26772.10	304.100	76.099	-322.691	3.774884E+01	3.725521E-05	1.329144E-08
26777.10	309.100	76.517	-321.939	3.285109E+01	3.242150E-05	1.150346E-08
26782.10	314.100	76.935	-321.187	2.861203E+01	2.923787E-05	9.964381E-09
26787.10	319.100	77.353	-320.435	2.493999E+01	2.461386E-05	8.638416E-09
26792.10	324.100	77.770	-319.683	2.175651E+01	2.147200E-05	7.495072E-09
26797.10	329.100	78.188	-318.931	1.899430E+01	1.874592E-05	6.508359E-09
26802.10	334.100	78.606	-318.180	1.659568E+01	1.637867E-05	5.656104E-09
26807.10	339.100	79.024	-317.428	1.451113E+01	1.432137E-05	4.919373E-09
26812.10	344.100	79.441	-316.676	1.269807E+01	1.253202E-05	4.281983E-09
26814.00	346.000	79.600	-316.390	1.207250E+01	1.191463E-05	4.062874E-09
26817.10	349.100	79.848	-315.944	1.111982E+01	1.097441E-05	3.730763E-09
26822.10	354.100	80.248	-315.224	9.744629E+00	9.617201E-06	3.253261E-09
26827.10	359.100	80.648	-314.504	8.545474E+00	8.433727E-06	2.838925E-09
26832.10	364.100	81.048	-313.784	7.499067E+00	7.401004E-06	2.479132E-09
26837.10	369.100	81.448	-313.064	6.585301E+00	6.499187E-06	2.166472E-09
26842.10	374.100	81.848	-312.344	5.786800E+00	5.711127E-06	1.894572E-09
26847.10	379.100	82.248	-311.624	5.088536E+00	5.021994E-06	1.657948E-09
26852.10	384.100	82.648	-310.904	4.477504E+00	4.418952E-06	1.451876E-09
26857.10	389.100	83.048	-310.184	3.942440E+00	3.890885E-06	1.272284E-09
26862.10	394.100	83.448	-309.464	3.473581E+00	3.428158E-06	1.115659E-09
26867.10	399.100	83.848	-308.744	3.062459E+00	3.022412E-06	9.789703E-10
26872.10	404.100	84.248	-308.024	2.701725E+00	2.666395E-06	8.595973E-10
26877.10	409.100	84.648	-307.304	2.384993E+00	2.353806E-06	7.552756E-10
26882.10	414.100	85.048	-306.584	2.106716E+00	2.079167E-06	6.640458E-10
26887.10	419.100	85.448	-305.864	1.862066E+00	1.837716E-06	5.842116E-10
26892.10	424.100	85.848	-305.144	1.646841E+00	1.625305E-06	5.143033E-10
26897.10	429.100	86.248	-304.424	1.457382E+00	1.438324E-06	4.530466E-10
26902.10	434.100	86.648	-303.704	1.290500E+00	1.273624E-06	3.993359E-10
26904.00	436.000	86.800	-303.430	1.232413E+00	1.216297E-06	3.807005E-10
26907.10	439.100	87.055	-302.971	1.143416E+00	1.128464E-06	3.521784E-10
26912.10	444.100	87.467	-302.230	1.013716E+00	1.000460E-06	3.107680E-10
26917.10	449.100	87.878	-301.490	8.992737E-01	8.875141E-07	2.743993E-10
26922.10	454.100	88.289	-300.749	7.982310E-01	7.877927E-07	2.424377E-10
26927.10	459.100	88.701	-300.008	7.089637E-01	6.996928E-07	2.143313E-10

TABLE 5-R356397

DATE 01/13/72.

URANUS

NOMINAL URANUS ATMOSPHERE,

MEAN MOLECULAR MASS = 2.680 GRAMS/MOLE

INITIAL PRESSURE = 1.013250E+06 DYNES/SQCM AT 26468.00 KM RADIUS

PRINT INTERVAL = 5 KM, GAS CONSTANT = 8.31430000E+07 JOULES/(MOLE.DEG KELVIN)

ONE ATMOSPHERE = 1.01325000E+06 DYNES/CM2, MU= 5.67444957E+06 KM3/SEC2

GREF = 8.09993416E-03 KM/SEC2

ALTITUDE IS ABOVE 26468.0 KM RADIUS

RADIUS KM	ALTITUDE KM	TEMPERATURE		PRESSURE		DENSITY GM/CM3
		KELVIN	FAHREN	DYNE/CM2	ATMOSPHERES	
26932.10	464.100	89.112	-299.268	6.300511E-01	6.218121E-07	1.895992E-10
26937.10	469.100	89.524	-298.527	5.602495E-01	5.529233E-07	1.678226E-10
26942.10	474.100	89.935	-297.786	4.984697E-01	4.919514E-07	1.486364E-10
26947.10	479.100	90.347	-297.046	4.437573E-01	4.379544E-07	1.317220E-10
26952.10	484.100	90.758	-296.305	3.952749E-01	3.901060E-07	1.168013E-10
26957.10	489.100	91.170	-295.565	3.522880E-01	3.476812E-07	1.036311E-10
26962.10	494.100	91.581	-294.824	3.141514E-01	3.100433E-07	9.199929E-11
26967.10	499.100	91.993	-294.083	2.802984E-01	2.766330E-07	8.171990E-11
26972.10	504.100	92.404	-293.343	2.502307E-01	2.469585E-07	7.263034E-11
26977.10	509.100	92.816	-292.602	2.235099E-01	2.205871E-07	6.458818E-11
26982.10	514.100	93.227	-291.861	1.997501E-01	1.971380E-07	5.746859E-11
26987.10	519.100	93.638	-291.121	1.786115E-01	1.762758E-07	5.116212E-11
26992.10	524.100	94.050	-290.380	1.597944E-01	1.577048E-07	4.557270E-11
26997.10	529.100	94.461	-289.640	1.430348E-01	1.411644E-07	4.061601E-11
27000.00	532.000	94.700	-289.210	1.341640E-01	1.324096E-07	3.800146E-11

TABLE 5-R356397

DATE 01/13/72.

URANUS

NOMINAL URANUS ATMOSPHERE,

MEAN MOLECULAR MASS = 2.680 GRAMS/MOLE

INITIAL PRESSURE = 1.013250E+06 DYNES/SQCM AT 26468.00 KM RADIUS

PRINT INTERVAL = 5 KM, GAS CONSTANT = 8.31430000E+07 JOULES/(MOLE.DEG KELVIN)

ONE ATMOSPHERE = 1.01325000E+06 DYNES/CM², MU = 5.67444957E+06 KM³/SEC²GREF = 8.09993416E-03 KM/SEC²

TEMPERATURE PROFILE INPUTS

BASE ALTITUDE		KINETIC TEMPERATURE		MOLEC SCALE TEMP		MOLEC WT G/GMOLE
KM	KFT	KELVIN	RANKINE	KELVIN	RANKINE	
-355.900	*167.651	382.300	688.140	382.446	688.402	2.679
-295.500	-969.488	306.600	551.880	306.353	551.435	2.682
-245.200	-804.462	295.000	531.000	294.845	530.721	2.681
-214.500	-703.740	270.000	486.000	270.354	486.637	2.676
-207.300	-680.118	264.100	475.380	264.103	475.385	2.680
-113.600	-372.703	185.300	333.540	185.572	334.030	2.676
-86.900	-285.105	162.200	291.960	163.060	293.509	2.666
-78.600	-257.874	155.000	279.000	155.338	279.608	2.674
-67.300	-220.801	145.000	261.000	145.159	261.286	2.677
-43.200	-141.732	123.500	222.300	123.559	222.406	2.679
0.	0.	84.000	151.200	83.961	151.130	2.681
2.300	7.546	81.900	147.420	81.872	147.370	2.681
9.600	31.495	75.000	135.000	75.212	135.382	2.672
21.500	70.538	65.000	117.000	73.077	131.538	2.384
35.400	116.142	54.000	97.200	65.757	118.363	2.201
62.900	206.365	56.200	101.160	67.621	121.717	2.227
94.800	311.024	58.900	106.020	71.002	127.803	2.223
125.000	410.105	61.400	110.520	73.726	132.707	2.232
193.000	533.202	66.900	120.420	80.445	144.802	2.229
267.000	875.984	73.000	131.400	87.798	158.036	2.228
346.000	1135.171	79.600	143.280	95.780	172.403	2.227
436.000	1430.446	85.800	156.240	104.348	187.826	2.229
532.000	1745.407	94.700	170.460	113.801	204.941	2.230

Section F

TABLE 6-R356397

DATE 01/13/72.

NEPTUN

NOMINAL NEPTUNE ATMOSPHERE,

MEAN MOLECULAR MASS = 2.680 GRAMS/MOLE

INITIAL PRESSURE = 1.013250E+06 DYNES/SQCM AT 24857.00 KM RADIUS

PRINT INTERVAL = 5 KM, GAS CONSTANT = 8.31430000E+07 JOULES/(MOLE.DEG KELVIN)

ONE ATMOSPHERE = 1.01325000E+06 DYNES/CM2, MU= 6.79657494E+06 KM3/SEC2

GREF = 1.10000000E-02 KM/SEC2

ALTITUDE IS ABOVE 24857.0 KM RADIUS

RADIUS KM	ALTITUDE KM	TEMPERATURE		PRESSURE		DENSITY GM/CM3
		KELVIN	FAHREN	DYNE/CM2	ATMOSPHERES	
24675.00	-182.000	270.000	26.330	9.584474E+07	9.459140E+01	1.148394E-02
24680.00	-177.000	264.315	16.097	8.958245E+07	8.841100E+01	1.096256E-02
24685.00	-172.000	258.630	5.864	8.360975E+07	8.251641E+01	1.045467E-02
24690.00	-167.000	252.945	-4.369	7.791893E+07	7.690000E+01	9.960170E-03
24695.00	-162.000	247.260	-14.602	7.250230E+07	7.155421E+01	9.478385E-03
24700.00	-157.000	241.575	-24.834	6.735227E+07	6.647152E+01	9.011023E-03
24705.00	-152.000	235.890	-35.067	6.246126E+07	6.164447E+01	8.556196E-03
24710.00	-147.000	230.205	-45.300	5.782179E+07	5.706567E+01	8.114417E-03
24715.00	-142.000	224.521	-55.533	5.342642E+07	5.272777E+01	7.685596E-03
24720.00	-137.000	218.836	-65.766	4.926776E+07	4.862350E+01	7.269646E-03
24725.00	-132.000	213.151	-75.999	4.533850E+07	4.474562E+01	6.866475E-03
24730.00	-127.000	207.466	-86.232	4.163136E+07	4.108696E+01	6.475994E-03
24735.00	-122.000	201.781	-96.465	3.813916E+07	3.764042E+01	6.098112E-03
24740.00	-117.000	196.096	-106.697	3.485473E+07	3.439895E+01	5.732737E-03
24745.00	-112.000	190.411	-116.930	3.177101E+07	3.135555E+01	5.379778E-03
24748.00	-109.000	187.000	-123.070	3.001418E+07	2.962170E+01	5.173923E-03
24750.00	-107.000	184.597	-127.395	2.888045E+07	2.850279E+01	5.043681E-03
24755.00	-102.000	178.590	-138.209	2.617171E+07	2.582947E+01	4.725326E-03
24760.00	-97.000	172.582	-149.022	2.363771E+07	2.332860E+01	4.417318E-03
24761.40	-95.600	170.900	-152.050	2.295870E+07	2.265847E+01	4.332929E-03
24765.00	-92.000	166.652	-159.696	2.127170E+07	2.099354E+01	4.123846E-03
24766.40	-90.600	165.000	-162.670	2.063816E+07	2.036828E+01	4.043838E-03
24770.00	-87.000	160.714	-170.384	1.906908E+07	1.881971E+01	3.825459E-03
24774.80	-82.200	155.000	-180.670	1.711045E+07	1.688670E+01	3.545217E-03
24775.00	-82.000	154.760	-181.102	1.703205E+07	1.680933E+01	3.534596E-03
24780.00	-77.000	148.755	-191.911	1.514809E+07	1.495000E+01	3.274020E-03
24785.00	-72.000	142.750	-202.719	1.340642E+07	1.323111E+01	3.022979E-03
24790.00	-67.000	136.746	-213.528	1.180166E+07	1.164733E+01	2.781495E-03
24795.00	-62.000	130.741	-224.336	1.032841E+07	1.019335E+01	2.549594E-03
24796.20	-60.800	129.300	-226.930	9.993800E+06	9.863114E+00	2.495366E-03
24800.00	-57.000	124.606	-235.379	8.981310E+06	8.863864E+00	2.327079E-03
24805.00	-52.000	118.429	-246.497	7.755030E+06	7.653620E+00	2.114195E-03
24810.00	-47.000	112.253	-257.615	6.644110E+06	6.557227E+00	1.911052E-03
24815.00	-42.000	106.076	-268.732	5.643072E+06	5.569279E+00	1.717686E-03
24820.00	-37.000	99.900	-279.850	4.746421E+06	4.684353E+00	1.534135E-03
24825.00	-32.000	93.724	-290.968	3.948648E+06	3.897013E+00	1.360443E-03
24828.50	-28.500	89.400	-298.750	3.446081E+06	3.401018E+00	1.244751E-03
24830.00	-27.000	87.483	-302.200	3.247699E+06	3.205229E+00	1.155835E-03
24832.10	-24.900	84.800	-307.030	2.993371E+06	2.954228E+00	1.043823E-03
24835.00	-22.000	81.417	-313.120	2.675280E+06	2.640296E+00	9.480002E-04
24840.00	-17.000	75.583	-323.620	2.194770E+06	2.166069E+00	8.000548E-04
24840.50	-16.500	75.000	-324.670	2.151085E+06	2.122955E+00	7.863879E-04
24845.00	-12.000	70.055	-333.571	1.784360E+06	1.761026E+00	6.945711E-04
24849.60	-7.400	65.000	-342.670	1.455159E+06	1.436130E+00	6.065882E-04
24850.00	-7.000	64.568	-343.448	1.428610E+06	1.409929E+00	5.994706E-04
24855.00	-2.000	59.162	-353.178	1.122655E+06	1.107974E+00	5.136666E-04
24857.00	0.	57.000	-357.070	1.013250E+06	1.000000E+00	4.809994E-04

TABLE 6-R356397

DATE 01/13/72.

NEPTUN

NOMINAL NEPTUNE ATMOSPHERE,

MEAN MOLECULAR MASS = 2.680 GRAMS/MOLE

INITIAL PRESSURE = 1.013250E+06 DYNES/SQCM AT 24857.00 KM RADIUS

PRINT INTERVAL = 5 KM, GAS CONSTANT = 8.31430000E+07 JOULES/(MOLE.DEG KELVIN)

ONE ATMOSPHERE = 1.01325000E+06 DYNES/CM2, MU = 6.79657494E+06 KM3/SEC2

GREF = 1.10000000E-02 KM/SEC2

ALTITUDE IS ABOVE 24857.0 KM RADIUS

RADIUS KM	ALTITUDE KM	TEMPERATURE		PRESSURE		DENSITY GM/CM3
		KELVIN	FAHREN	DYNE/CM2	ATMOSPHERES	
24860.00	3.000	53.691	-363.026	8.623075E+05	8.510314E-01	4.342512E-04
24865.00	8.000	48.176	-372.952	6.439979E+05	6.355765E-01	3.609099E-04
24870.00	13.000	42.662	-382.879	4.644805E+05	4.584066E-01	2.934158E-04
24870.60	13.600	42.000	-384.070	4.453900E+05	4.395658E-01	2.857175E-04
24875.00	18.000	42.652	-382.897	3.272356E+05	3.229564E-01	2.074648E-04
24876.00	19.000	42.800	-382.630	3.052519E+05	3.012602E-01	1.930140E-04
24880.00	23.000	43.438	-381.482	2.316992E+05	2.286693E-01	1.443539E-04
24885.00	28.000	44.236	-380.046	1.651048E+05	1.529458E-01	1.010095E-04
24890.00	33.000	45.033	-378.510	1.183812E+05	1.168332E-01	7.114180E-05
24892.30	35.300	45.400	-377.950	1.017887E+05	1.004577E-01	6.067616E-05
24895.00	38.000	45.814	-377.204	8.538791E+04	8.427132E-02	5.042507E-05
24900.00	43.000	46.581	-375.823	6.194369E+04	6.113367E-02	3.595941E-05
24905.00	48.000	47.349	-374.442	4.518549E+04	4.459461E-02	2.579319E-05
24910.00	53.000	48.116	-373.061	3.313773E+04	3.270439E-02	1.860545E-05
24911.20	54.200	48.300	-372.730	3.078487E+04	3.038231E-02	1.721659E-05
24915.00	58.000	48.878	-371.689	2.442655E+04	2.410713E-02	1.350114E-05
24920.00	63.000	49.639	-370.320	1.809159E+04	1.785501E-02	9.848334E-06
24925.00	68.000	50.400	-368.950	1.346174E+04	1.328571E-02	7.218790E-06
24929.60	72.600	51.100	-367.690	1.029722E+04	1.016256E-02	5.447123E-06
24930.00	73.000	51.161	-367.580	1.006182E+04	9.930240E-03	5.316276E-06
24935.00	78.000	51.928	-366.200	7.553637E+03	7.454860E-03	3.932664E-06
24940.00	83.000	52.694	-364.820	5.694997E+03	5.620525E-03	2.922246E-06
24945.00	88.000	53.461	-363.440	4.311570E+03	4.255189E-03	2.180929E-06
24950.00	93.000	54.227	-362.061	3.277411E+03	3.234553E-03	1.634585E-06
24955.00	98.000	54.994	-360.681	2.501100E+03	2.468393E-03	1.230166E-06
24960.00	103.000	55.760	-359.301	1.915971E+03	1.890916E-03	9.295236E-07
24965.00	108.000	56.527	-357.922	1.473194E+03	1.453929E-03	7.051003E-07
24970.00	113.000	57.293	-356.542	1.136843E+03	1.121977E-03	5.368955E-07
24972.00	115.000	57.600	-355.990	1.025905E+03	1.012489E-03	4.819445E-07
24975.00	118.000	58.072	-355.140	9.803955E+02	8.688828E-04	4.102370E-07
24980.00	123.000	58.860	-353.723	6.842021E+02	6.752550E-04	3.145693E-07
24985.00	128.000	59.647	-352.306	5.335603E+02	5.265830E-04	2.420848E-07
24990.00	133.000	60.434	-350.889	4.174802E+02	4.120210E-04	1.869593E-07
24995.00	138.000	61.221	-349.472	3.277210E+02	3.234355E-04	1.448324E-07
25000.00	143.000	62.009	-348.055	2.580789E+02	2.547041E-04	1.126511E-07
25005.00	148.000	62.796	-346.638	2.038665E+02	2.012006E-04	8.787588E-08
25010.00	153.000	63.583	-345.221	1.615291E+02	1.594169E-04	6.876755E-08
25015.00	158.000	64.370	-343.804	1.283617E+02	1.266831E-04	5.398125E-08
25019.00	162.000	65.000	-342.670	1.070245E+02	1.056250E-04	4.457357E-08
25020.00	163.000	65.155	-342.392	1.022983E+02	1.009606E-04	4.250227E-08
25025.00	168.000	65.928	-340.999	8.175658E+01	8.068747E-05	3.356234E-08
25030.00	173.000	66.702	-339.607	6.551945E+01	6.466267E-05	2.657954E-08
25035.00	178.000	67.475	-338.214	5.264814E+01	5.195968E-05	2.110904E-08
25040.00	183.000	68.249	-336.822	4.241643E+01	4.186176E-05	1.681074E-08
25045.00	188.000	69.023	-335.429	3.426079E+01	3.381277E-05	1.342378E-08
25050.00	193.000	69.796	-334.037	2.774263E+01	2.737984E-05	1.074747E-08

TABLE 5-R356397

DATE 01/13/72.

NEPTUN

NOMINAL NEPTUNE ATMOSPHERE,

MEAN MOLECULAR MASS = 2.680 GRAMS/MOLE

INITIAL PRESSURE = 1.013250E+06 DYNES/SQCM AT 24857.00 KM RADIUS

PRINT INTERVAL = 5 KM, GAS CONSTANT = 8.31430000E+07 JOULES/(MOLE.DEG KELVIN)

ONE ATMOSPHERE = 1.01325000E+06 DYNES/CM2, MU= 6.79657494E+06 KM3/SEC2

GREF = 1.10000000E-02 KM/SEC2

ALTITUDE IS ABOVE 24857.0 KM RADIUS

RADIUS KM	ALTITUDE KM	TEMPERATURE		PRESSURE		DENSITY GM/CM3
		KELVIN	FAHREN	DYNE/CM2	ATMOSPHERES	
25055.00	198.000	70.570	-332.644	2.251958E+01	2.222510E-05	8.626910E-09
25060.00	203.000	71.343	-331.252	1.832366E+01	1.808404E-05	6.942201E-09
25065.00	208.000	72.117	-329.859	1.494446E+01	1.474903E-05	5.600258E-09
25070.00	213.000	72.891	-328.467	1.221638E+01	1.205653E-05	4.528607E-09
25072.00	215.000	73.200	-327.910	1.127719E+01	1.112972E-05	4.162508E-09
25075.00	218.000	73.657	-327.087	1.000857E+01	9.877687E-06	3.671407E-09
25080.00	223.000	74.420	-325.715	8.217233E+00	8.109778E-06	2.983553E-09
25085.00	228.000	75.182	-324.342	6.760554E+00	6.572148E-06	2.429870E-09
25090.00	233.000	75.944	-322.970	5.573445E+00	5.500562E-06	1.983177E-09
25095.00	238.000	76.707	-321.598	4.603969E+00	4.543764E-06	1.621399E-09
25100.00	243.000	77.469	-320.226	3.810580E+00	3.760750E-06	1.329328E-09
25105.00	248.000	78.231	-318.854	3.159972E+00	3.118650E-06	1.091664E-09
25110.00	253.000	78.993	-317.482	2.625384E+00	2.591052E-06	8.982641E-10
25115.00	258.000	79.756	-316.110	2.185264E+00	2.156688E-06	7.405612E-10
25120.00	263.000	80.518	-314.738	1.822224E+00	1.798395E-06	6.117073E-10
25125.00	268.000	81.280	-313.365	1.522198E+00	1.502293E-06	5.062170E-10
25130.00	273.000	82.043	-311.993	1.273790E+00	1.257133E-06	4.196865E-10
25133.00	276.000	82.500	-311.170	1.145596E+00	1.130616E-06	3.753649E-10
25135.00	278.000	82.813	-310.606	1.067748E+00	1.053786E-06	3.485523E-10
25140.00	283.000	83.597	-309.195	8.965600E-01	8.348359E-07	2.899561E-10
25145.00	288.000	84.381	-307.785	7.540803E-01	7.442194E-07	2.416526E-10
25150.00	293.000	85.164	-306.374	6.352876E-01	6.269801E-07	2.017375E-10
25155.00	298.000	85.948	-304.964	5.350741E-01	5.290640E-07	1.687015E-10
25160.00	303.000	86.731	-303.554	4.530731E-01	4.471484E-07	1.413109E-10
25165.00	308.000	87.515	-302.143	3.835205E-01	3.785053E-07	1.185615E-10
25170.00	313.000	88.299	-300.733	3.251425E-01	3.208907E-07	9.963464E-11
25175.00	318.000	89.082	-299.322	2.760656E-01	2.724555E-07	8.386170E-11
25180.00	323.000	89.866	-297.912	2.347430E-01	2.316734E-07	7.059548E-11
25185.00	328.000	90.649	-296.501	1.998960E-01	1.972820E-07	5.968741E-11
25190.00	333.000	91.433	-295.091	1.704652E-01	1.682361E-07	5.046911E-11
25195.00	338.000	92.216	-293.680	1.455718E-01	1.436682E-07	4.273753E-11
25200.00	343.000	93.000	-292.270	1.244853E-01	1.228575E-07	3.624293E-11

TABLE 5-R356397

DATE 01/13/72.

NEPTUN

NOMINAL NEPTUNE ATMOSPHERE,

MEAN MOLECULAR MASS = 2.680 GRAMS/MOLE

INITIAL PRESSURE = 1.013250E+06 DYNES/SQCM AT 24857.00 KM RADIUS

PRINT INTERVAL = 5 KM, GAS CONSTANT = 8.31430000E+07 JOULES/(MOLE.DEG KELVIN)

ONE ATMOSPHERE = 1.013250E+06 DYNES/CM2, MU= 6.79657494E+06 KM3/SEC2

GREF = 1.10000000E-02 KM/SEC

TEMPERATURE PROFILE INPUTS

BASE KM	ALTITUDE KFT	KINETIC KELVIN	TEMPERATURE RANKINE	MOLEC KELVIN	SCALE TEMP RANKINE	MOLEC WT G/GMOLE
-182.000	-597.113	270.000	486.000	269.021	484.238	2.690
-109.000	-357.612	187.000	336.600	186.989	336.580	2.680
-95.600	-313.648	170.900	307.620	170.795	307.431	2.682
-90.600	-297.244	165.000	297.000	164.508	296.114	2.688
-82.200	-269.685	155.000	279.000	155.571	280.027	2.670
-60.800	-199.475	129.300	232.740	129.094	232.369	2.684
-28.500	-93.504	89.400	160.920	89.239	160.629	2.685
-24.900	-81.693	84.800	152.640	92.436	166.385	2.459
-16.500	-54.134	75.000	135.000	88.172	158.709	2.280
-7.400	-24.278	65.000	117.000	77.326	139.187	2.253
0.	0.	57.000	102.600	67.902	122.223	2.250
13.600	44.619	42.000	75.600	50.247	90.445	2.240
19.000	62.335	42.800	77.040	50.978	91.760	2.250
35.300	115.814	45.400	81.720	54.074	97.334	2.250
54.200	177.822	48.300	86.940	57.637	103.746	2.246
72.600	238.189	51.100	91.980	60.934	109.682	2.247
115.000	377.297	57.600	103.680	68.615	123.507	2.250
162.000	531.495	65.000	117.000	77.395	139.312	2.251
215.000	705.381	73.200	131.760	87.328	157.191	2.246
276.000	905.512	82.500	148.500	98.376	177.076	2.248
343.000	1125.328	93.000	167.400	110.714	199.286	2.251

H.

REFERENCES

1. NASA Space Vehicle design criteria document for the planet Jupiter (1970), NASA SP-8069, dated August 1971 (See SOW (b(6) (B))
2. NASA Space Vehicle design criteria document for the planet Saturn (1970) (See SOW (C(4) (B))
3. JPL Section Document 131-17 Preliminary Model Atmospheres for the Planets Uranus and Neptune, dated 4 November 1971
4. Constants and Related Information for Astrodynamic Calculations, 1968, by Melbourne, Mulholland, Sjogren, and Sturms, (JPL) NASA technical report 32-1306, dated July 15, 1968
5. Memo from Ken Ledbetter, describing telecon with D. Wiksten and F. Palluconi of JPL, dated 14 January 1972

APPENDIX F

ATTITUDE CONTROL SUBSYSTEM
ANALYSIS

E. A. Berkery

June 9, 1972

ATTITUDE CONTROL SUBSYSTEM ANALYSIS

1. Separation

Separation with Initial Spin - The location of the significant vectors is determined by assuming the probe's initial position is correct and the momentum vector is composed of the nominal spin rate along the k (spin) axis and a transverse rate equal to the tipoff rate.

$$\bar{P} = I_s \bar{W}_s + I_t \bar{W}_t$$

$$\tan^{-1} \theta_1 \approx \theta_1 = \frac{W_t I_t}{W_s I_s} = \frac{W_t}{W_s (1 + \lambda)}$$

W_s = spin rate

\bar{P} = momentum vector

P_s = spin momentum

I_s = spin moment of inertia

I_t = transverse moment of inertia

$\lambda = I_s/I_t - 1$

W_t = tip off rate

The motion then consists of nutation around the momentum vector with half cone angle θ_1 .

Separation without Spin - There are two types of errors associated with this mode of operation: the initial drift error and the error developed during spinup caused by the combined tipoff and spinup rates.

The drift error is

$$\theta_2 = W_t t_D$$

The error developed during spinup may be analyzed as follows:

$$\frac{\dot{P}}{P} = m \hat{k}$$

m = torque

$$\dot{\hat{k}} = \frac{\bar{p}}{I_t} \times \hat{k}$$

$$\ddot{\bar{p}} = \frac{\bar{p} \times \dot{\bar{p}}}{I_t}$$

$$\bar{p} = \hat{x}p_x + \hat{y}p_y + \hat{z}p_z$$

Assume

$$\dot{p}_z = m \quad p_z = mt$$

Then

$$\ddot{p}_x = \frac{m}{I_t} (p_y - t\dot{p}_y)$$

$$\ddot{p}_y = \frac{m}{I_t} (t\dot{p}_x - p_x)$$

$$\ddot{\ddot{p}}_x = \left(\frac{m}{I_t}\right)^2 (tp_x - t^2\dot{p}_x)$$

$$\ddot{\ddot{p}}_y = \left(\frac{m}{I_t}\right)^2 (tp_y - t^2\dot{p}_y)$$

Assuming

$$p_x = \sum_{n=0}^{\infty} a_n t^n \quad p_y = \sum_{n=0}^{\infty} b_n t^n$$

and

$$p_x(0) = W_T I_T, \dot{p}_x(0) = 0, \ddot{p}_x(0) = 0, \ddot{\ddot{p}}_x(0) = 0$$

$$p_y(0) = 0, \dot{p}_y(0) = 0, \ddot{p}_y(0) = -\frac{m}{I_t} p_x(0), \ddot{\ddot{p}}_y(0) = 0$$

The solutions

$$p_x = p_x(0) \left[1 + \sum_{n=1}^{\infty} (-1)^{n+1} \left(\frac{p_s^2}{mI_t} \right)^{2N} \frac{(4N-2)!}{(4N)! (2N-1)! 2^{2N-1}} \right]$$

$$p_y = p_x(0) \sum_0^{\infty} \frac{(-1)^{n+1} 4N!}{(4N+2)! (2N)! 2^{2N}} \left(\frac{p_s^2}{mI_t} \right)^{2N+1}$$

This solution is valid for small displacements of the momentum vector (i.e., $p_x, p_y \ll p_s$). Although it is absolutely convergent, if the value of p_s^2/mI_t is much greater than unity, many terms must be evaluated. For the purpose of simplification, it is sufficient to evaluate the series for a point in time at which the spin momentum becomes considerably greater than the tipoff momentum.

$$\begin{aligned} m &= 3 \text{ ft-lb} & t &= 2 \text{ seconds} & I_s &= 9 \text{ slug-ft}^2 & W_t &= \frac{1}{2} \text{ deg/sec} \\ \dot{W}_s &= 1/3 \text{ rad/sec}^2 & W_s &= 2/3 \text{ rad/sec} & p_s^2/mI_t &= 1.6 & 1 + \lambda &= 1.2 \end{aligned}$$

$$\theta_x(p) = \frac{p_x}{p} = 0.625 \left[1 + \frac{2.56}{24} - \frac{6.55}{2688} + \frac{16.78}{506880} \dots \right] = 0.693^\circ$$

$$\theta_y(p) = \frac{p_y}{p_s} = 0.625 \left[-\frac{1.6}{2} + \frac{4.1}{240} - \frac{10.49}{54560} \dots \right] = -0.489^\circ$$

Total momentum displacement

$$\theta(p) = \sqrt{\theta_x^2 + \theta_y^2} = 0.85^\circ$$

The location of the \hat{k} spin axis may be determined by $\hat{k} = \frac{\dot{\vec{p}}}{m}$

$$\theta_x(\hat{k}) = 1.25 \left[\frac{5.12}{24} - \frac{26.2}{2688} + \frac{100.68}{506880} \dots \right] = 0.255^\circ$$

$$\theta_y(\hat{k}) = 1.25 \left[-\frac{1.6}{2} + \frac{12.3}{240} - \frac{52.45}{54560} \dots \right] = -0.938^\circ$$

For small angles, the nutation half angle may be determined by taking the difference of the component angles

$$|\theta_x(N)| = 0.438^\circ \quad |\theta_y(N)| = 0.449^\circ$$

Nutation half cone angle $\theta(N) = 0.628^\circ$

Since torquing will continue for another 28 seconds to reach a final spin rate of 10 rad/sec, there may be some additional movement of the momentum vector; however, it should be an order of magnitude less than the initial error of the first few seconds. Taking into account the drift error accumulation from separation to spinup (0.25°), the total pointing error becomes

$$\theta(p) = 1.06^\circ$$

$$\theta(N) = 0.63^\circ$$

Error Caused by Spin Jet Misalignment - This error and the remaining errors to be discussed are derived from Reference JPL TR-32-644. The displacement of the angular momentum vector is

$$\theta(p) = K_3\gamma + K_4W_s$$

$\gamma = m_t/m_s$ ratio of transverse torque to axial torque caused by jet misalignment

K_3 = coefficient from reference (see discussion below)

K_4 = coefficient from reference (see discussion below)

The coefficient K_4 is a Fresnel integral which is plotted in the reference. Although the computer plot in the reference is with respect to some specific vehicle parameters, they are combined in a manner such that the curves may be normalized and applied to all vehicles. The coefficient K_3 is a double Fresnel integral which does not yield to attempts to normalize; however, the value of K_3 is bounded and approximate solutions may be obtained.

Subsequent to the delta velocity impulse event, the attitude control subsystem maneuvers to the final orientation. The accuracy of the final maneuver is a function of the sensor reference and is required to be two or three degrees depending on the specific mission.

Velocity Dispersion - The velocity dispersion caused by coning occurs because of two sources: initial nutation and misalignment of the delta velocity thrust vector. The error due to nutation is

$$\theta(V,N) \approx \frac{\theta_o(N)^\pi}{W_s t_F} W_s t_F > 4\pi$$

$\theta(N)$ = initial nutation

W_s = spin velocity

t_F = period of thrusting

The thrust misalignment error is developed in the reference Eq [67] and is based on the usual Euler angle approximations. This equation is subject to interpretation and does not agree with results of computer simulation and other approximations. An estimate of this error based on several approximate methods is

$$\theta(V,F) = \frac{Fr}{2\lambda I_s W_s^2}$$

r = moment arm (offset) of thrust

Attitude Maneuver - Probe studies at Martin Marietta have considered a number of attitude control systems appropriate to probe missions. The fundamental ACS problem here is to enable a probe to fire a delta velocity impulse and then orient the spin axis to the entry attitude without contact or supervision from the spacecraft or ground station. The economy of the design is a strong influencing factor for system selection. Methods considered consisted of stored momentum systems, offset thruster or radial thrusters to enable separation in the entry attitude, and open loop systems. None of these were feasible or sufficiently accurate and reliable for this application. Two approaches received more serious consideration.

ACS Design - Simple Closed Loop - Single-Axis Maneuver - This approach uses a sun sensor that provides a measurement of solar aspect as well as Sun crossing time. The maneuver sequence would consist of firing a preprogrammed set of precession impulses immediately following the delta velocity impulse maneuver. These

pulses could be offset in phase so that essentially a two-axis maneuver could be achieved, although only the maneuver angle with respect to the Sun line (i.e., solar aspect angle) could be measured. Subsequent to the initial maneuver, some time (order of several hours) would elapse while the damper removed residual nutation. A measurement of solar aspect angle would then provide information for further maneuvers.

ACS Design - Closed Loop - Two-Axis Maneuver - This design approach makes use of a Sun sensor to measure solar aspect angle and Sun crossing time, and a Jupiter sensor to measure Jupiter crossing time. The sequence of the maneuver would be similar to the single-axis system described above. Immediately following the delta velocity impulse maneuver, a preprogrammed series of pulses would orient the probe near its final position. Then, after a waiting period of several damper time constants, measurements are made of solar aspect angle (clock angle) and the angle between the Sun and Jupiter measured about the spin axis of the probe (cone angle). These measurements are then used to develop subsequent precession programs to finalize the probes position. Because of residual nutation, it is not considered desirable to continuously drive the probe to minimize the final error. For this reason the maneuver will take place in a series of steps as described above. With this approach there are certain constraints on the relative position of the Sun and Jupiter as discussed below. This system, using attitude sensors may also be used to trim probe attitude before the delta velocity impulse. Since it represents a minor increment in complexity over a single-axis system and has inherent greater flexibility and capability, it has been the system that has received the major consideration. For missions in which the single axis system may be considered a preferred choice, it would be a minor consideration to reduce the two-axis maneuver system to a single-axis maneuver system.

Application of this approach to the Saturn mission does not require modification of the system although the stored maneuver angles would be changed. The Uranus mission would require some change in functional procedure since the Sun is only 4° away from the spin axis when the probe is in the entry attitude. The system for the Uranus mission will be programmed to point the spin axis directly at the sun initially. The 4-deg maneuver to the final position will then be implemented by sector logic control based on a Uranus sensor pulse. Control of the magnitude of the maneuver will be open loop, i.e., the number and duration of the attitude impulses will be preprogrammed. Because of the small angle of the maneuver, little error may be expected.

Reference System Geometry - The reference system for the probe attitude control consists of the spin axis, the Sun, and a planet. The geometry is illustrated in Figure F-1. The solar aspect sensor measures the angle (α) between the spin axis and the Sun-probe line. The location of the spin axis on this surface is then determined by measuring the angle (β) between the spin axis/Sun plane and the spin axis/planet plane. This measurement is influenced by the planet/probe/Sun angle (ϕ) for which *a priori* knowledge is programmed into the probe. The angle θ locates the probe on the conical surface and may be determined by the following relationship.

$$\tan \beta = \frac{\sin \alpha \sin \theta}{\sin \alpha \cos \theta \cos \phi - \cos \alpha \sin \phi}$$

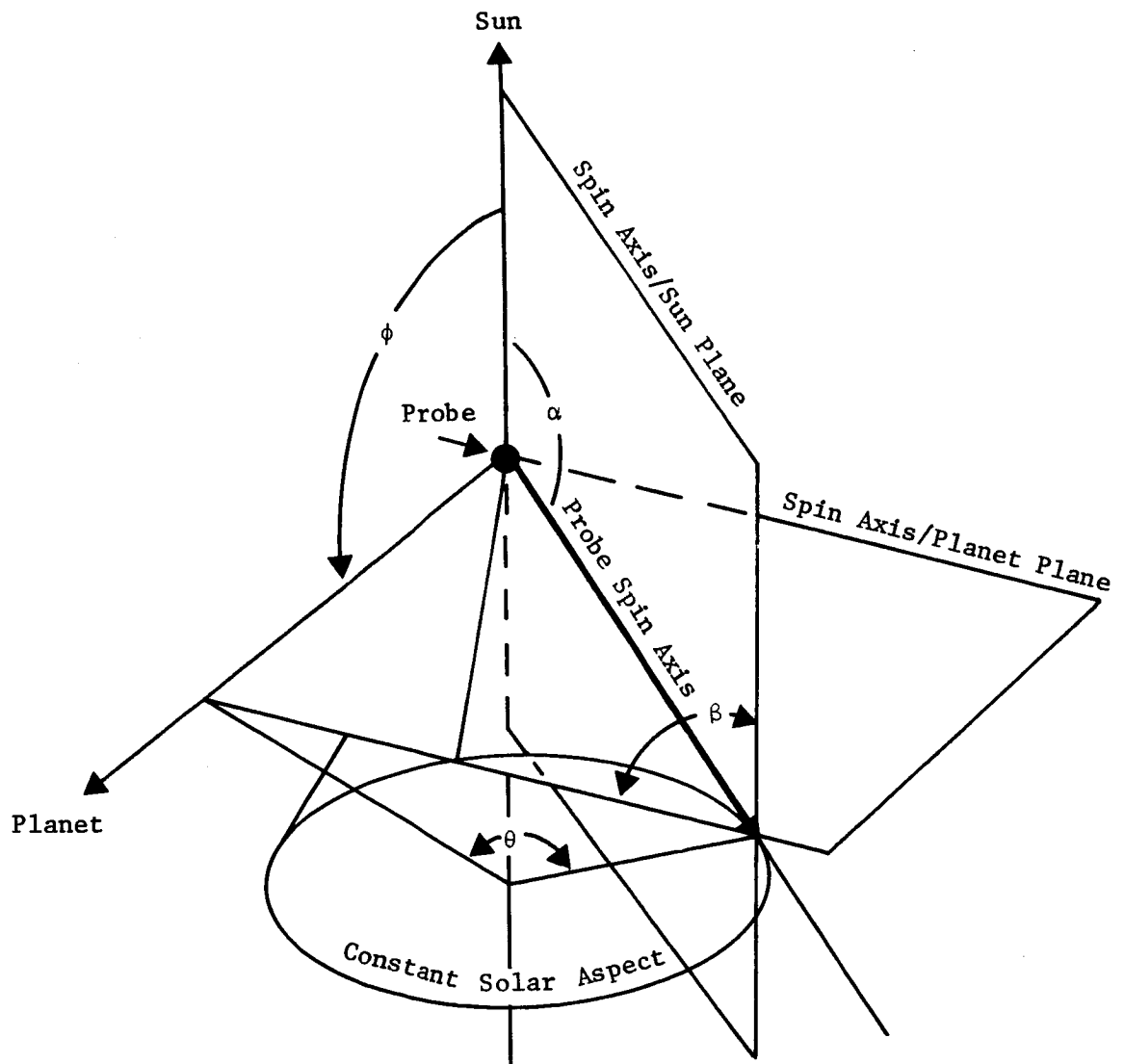


Figure F-1 Reference System Geometry

The angle θ would not be evaluated in the probe because with knowledge of ϕ and α , the measurement of β would be compared directly to a predetermined stored value. When the probe-planet vector lies within the conical surface, θ is a double valued function (i.e., there are two positions on the cone which will result in equal values for β). This could occur during trim maneuvers prior to velocity impulse thrusting. However, the two values of θ are sufficiently far apart not to constitute a problem. For the entry attitude, this condition does not occur. Another undesirable condition occurs when the Sun/probe vector approaches the spin vector as it does in the Uranus mission profile. This represents a singularity in the control processing and creates a sensing problem caused by the finite width of the sensitive angle of the sensor. A slightly different approach must be used on the Uranus mission, as discussed.

2. ACS - Design - Sensors

The problem is the three-axis attitude determination for a spin-stabilized spacecraft at approximately 10^7 km from Jupiter. In the missions discussed, the probe is relatively near the line between Jupiter and the Sun. Jupiter will be nearly full-phase with approximately 0.4 degrees apparent diameter, as seen from the probe. Accuracy of angular measurements within 0.5 degrees is considered adequate.

The design approach uses two sensors: one to obtain two-axis information from the Sun, and the other to furnish third-axis information by sensing Jupiter.

The Sun sensor will measure the angle between the spacecraft spin axis and the Sun. This can be a 9-bit digital output (with the Adcole Corporation instrument), or linear analog output (with the Honeywell Radiation Center instrument). The second axis is determined by the direction of the Sun when the plane containing the instrument's optical axis and the spacecraft spin axis crosses the Sun. This is indicated by a pulse output from the Sun sensor. This sun sensor and its electronics will weigh a maximum of 3.5 lb with a maximum power requirement of 2 watts, if the instrument is to cover the whole celestial sphere on each revolution about the spacecraft spin axis. These numbers can be lowered, if miniaturized integrated circuitry is used, and if the spin-axis-to-Sun angle is constrained within certain limits.

3. ACS Design Jupiter Sensor

The electromagnetic radiation emanating from the planet Jupiter, consists mainly of the following three classifications:

- 1) Reflected light from the Sun, essentially in the wavelength and from 0.3 to 1.5 microns, with peak at approximately 0.5 micron. This is in the visual and near-infrared region. The apparent shape of Jupiter in this radiation will vary from thin-crescent to fully illuminated disc, as a function of the phase angle between the line of sight from the instrument to Jupiter and the line from Jupiter to the Sun.
- 2) Energy radiated by the planet, as a "black body," resulting from its own temperature. Since Jupiter has a significant atmosphere and a high rotational speed (approximately 10 hours per revolution), the temperature over the entire apparent surface of Jupiter is relatively constant at approximately 130 °K. Its black-body radiation is essentially in the wavelength band from 5 to 30 microns, peaking at about 11 microns; it is relatively constant from about 8 to 14 microns. Jupiter's apparent shape in this radiation will be the nearly circular shape of an oblate spheroid.
- 3) Radio-frequency radiations in the wavelength band longer than 3 centimeters. This radiation seems to be associated with varying but discrete sources on the planet, and is therefore not suitable for sensing the planet for determination of its center.

Sensors that can detect the reflected solar radiation are many, and their relative usefulness depends upon the specific purpose of the instrumentation as well as their own intrinsic properties. Some of the more frequently used materials are tabulated.

At least three materials are sensitive in the range of Jupiter's black-body radiation: mercury-doped germanium, operating at 28 °K; gold-doped germanium, at 60°K; copper-doped germanium, at 4.2°K. Zinc-doped germanium at 4.2°K covers the desired range at lower sensitivity; it is more useful at somewhat longer wavelengths. The disadvantage common to these materials is that they must be operated at very low temperatures. This often adds prohibitive amounts of weight for spacecraft applications, but the lower temperatures available in space can conceivably be used to advantage for these detectors.

<u>Material</u>	<u>Wavelength at Peak Response (μ)</u>	<u>Remarks</u>
S-1	1	
S-11	0.3	
S-20	0.42	Highest response
Others		
Silicon	1	Photo conductive and photovoltaic
Selenium	0.8	
Gallium arsenide	0.8	
Copper- cupric oxide	0.5	
Cadmium sulphide	(visual)	

Based on the above, the device selected for a Jupiter sensor will consist of a silicon sensitive element and possibly a lens system.

The Sun sensor requirements for the Saturn mission appear to be within the requirements of available sensors. At Uranus distance from the Sun, an additional lens system may be necessary. Planet sensors for Saturn and Uranus will require additional lenses as compared to the Jupiter sensor; however, these sensors have a very simple function and the modification would be minor.

4. ACS Design - Electronics

The functional block diagram illustrated in Figure F-2 is representative of the electronics for all missions requiring an attitude control system. The functions required of the ACS electronics follow.

- 1) Process the solar aspect angle information. The data output of the solar aspect sensor is generally analog or digital gray code. In either case, this output should be converted to binary digital for processing in the logic. The solar aspect output may be used as a measure of nutation as described in the paragraph on logic.

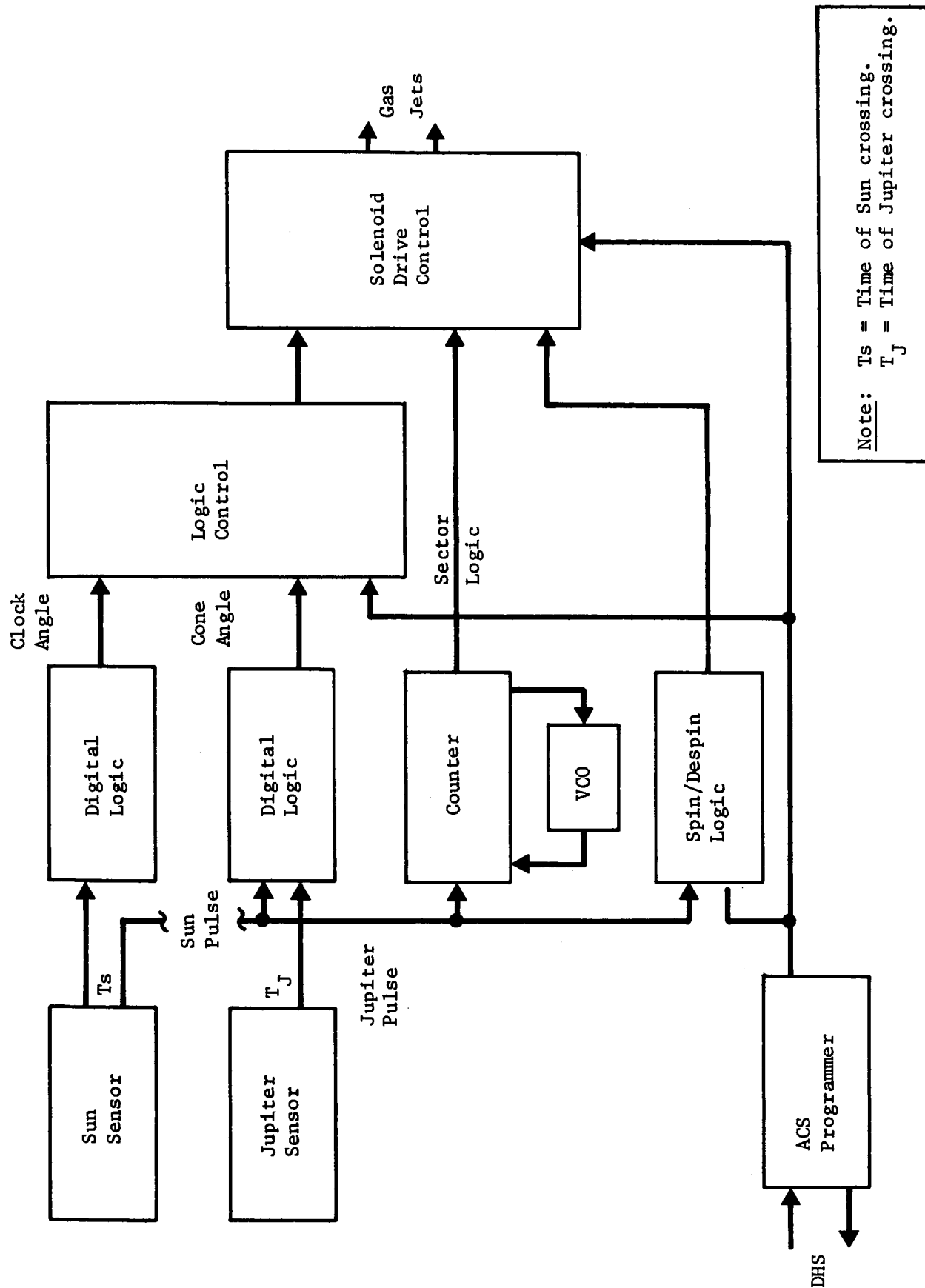


Figure F-2 ACS Block Diagram

- 2) The pulse output from the Sun sensor is generated when the Sun crosses the sensor's optical axis. Processing of this pulse will consist of establishing the center of the pulse by selecting the point at which the derivative (slope) is equal to zero (maximum amplitude) or averaging the time between preselected amplitudes. Some study must be made of the effect of the greatly increased solar range on this pulse. It is distinctly possible that the solar intensity near Jupiter may be decreased by factors other than range as recent data from the Mariner flights indicate a discrepancy between measured and expected illumination. The Sun pulse is used to control the sector logic (discussed below) as well as provide attitude information in combination with a similar Jupiter pulse.
- 3) The pulse derived from the Jupiter sensor when the planet crosses the optical axis of the sensor is essentially similar to the Sun pulse described above and processing will be the same.
- 4) Sector logic will be used to establish correct precession jet firing intervals. There are two obvious approaches to this logic. A counter may be used to measure the period of revolution. Simple binary division and addition processing may then be used to establish the angular position of the probe at any time during the next revolution on the basis of the content of the register. Since the measured period of rotation will be updated every revolution, the basic timing oscillator would have no critical nominal frequency requirements and reasonable drift requirements resulting in a simple economical design for this element. However, the digital processing would be increased over the voltage controlled oscillator approach. The use of a VCO would enable the sector logic to be hard wired. This system generates the proper sector logic by driving the oscillator so that the count register approaches a fixed value for every revolution. The angular position of the probe is determined when this counter reaches a preset value. This is the preferred approach for this function since the required development is decreased.
- 5) A nominal functional block diagram of the solar aspect precession is shown in Figure F-3. At predetermined intervals, a series of solar aspect angles will be measured and the maximum and minimum selected. This is necessary since nutation will be present if the difference between these angles is too great, indicating excessive nutation and another mating interval will be initiated. If the difference between the maximum

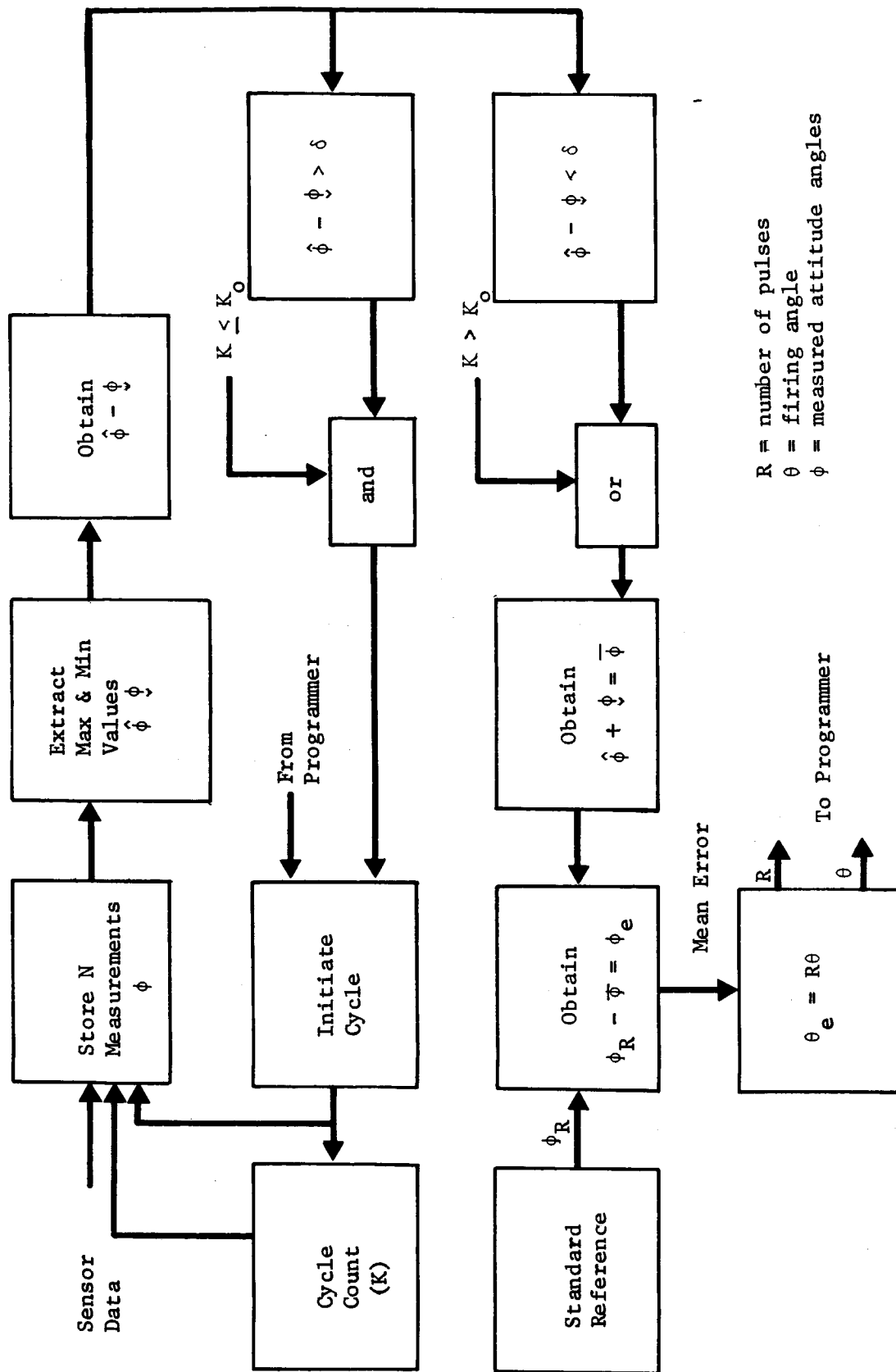


Figure F-3 Precession Logic

and minimum angle is sufficiently small, the attitude evaluation will be performed. The evaluation will consist of summing the maximum and minimum measurements to obtain a measurement related to the mean value which is representative of the position of the angular momentum vector. This value is then compared to a preset attitude command and the sign and magnitude of the error is established. A similar function provides an evaluation of the spin axis cone angle. The difference in the content of the revolution period count register between the Sun and Jupiter pulse is compared with the total revolution period. This provides a measurement of the angle (β) through which the probe rotates between pulses, and establishes the position of the probe on the space cone defined by the solar aspect angle. An averaging similar to that provided by the solar aspect logic is performed and the results compared with a present command. The resultant angular errors are then used to program the timing of the precession events and pulse width. When the indicated error decreases below the allowable maximum error, the ACS signals the data management system that the maneuver is complete and the pre-cost shutdown sequence is initiated.

The attitude control logic may be implemented by COSMOS if the state of the art permits. Since this is a critical maneuver, and with this design there is no method by which the success of the maneuver may be evaluated and readjusted by spacecraft or ground command, it is recommended that 100% redundant majority logic be used. The use of COSMOS will alleviate the power penalty that might otherwise be incurred. The Jupiter range at which this maneuver takes place is sufficient to ignore the effects of the Jupiter radiation belts.

The precession pulses will be implemented by pneumatic jets driven by appropriate power amplifiers. The design of these amplifiers should be such that they require low power during the standby conditions.

The required vehicle maneuver is relatively simple and consequently the electronics presents no design problem. Some further studies may be required to evaluate the effects of nutation on subsystem performance.

ACS Design - Damper - A viscous ring damper was selected because of its mechanical simplicity and its advantages of no mechanical moving parts, no threshold of performance, insensitivity to change in spin rate, mass properties and temperature, and it does not effect probe static or dynamic balance, or have critical mounting

or geometry requirements. Its principal disadvantages are size and weight which are inversely related to rather long-time constants. In the eventuality that the viscous ring damper proves impractical, a tuned wheel which is much smaller but would increase cost may be used. The performance of the viscous damper has been analyzed and the time constant is given by

$$\tau = \frac{2\pi I_s}{F(\gamma) m R^2 (1 + \lambda)^2 W_s}$$

I_s = spin moment of inertia

I_t = transverse moment of inertia

$F(\gamma)$ = function of wobble Reynolds number λ

m = mass of fluid

R = radius of ring

$$\lambda = I_s / I_t - 1$$

W_s = angular rate of probe

With the constants appropriate to the various probes with dynamic attitude control, it appears that time constants of the order of one hour are feasible with a 12-cm diameter damper. Since the period during which the ACS system needs to be active may be as long as six hours, this would appear adequate. With a vehicle operating at 5 rpm, the damping period would extend out to twenty hours. This does not present a problem since there is no attitude control system dependent on the damping on missions with this vehicle angular rate. Furthermore, initial nutation would be due only to tipoff rates and approximately seven days are available for damping.

5. Summary and Results

The structural tolerances used in evaluating disturbances to the probe are listed.

Structural Tolerances (3σ)

Nozzle/flange, cm	0.0254
Flange, cm	0.0762
Mounting surface, deg	0.1
Cg location, cm	0.038
Thrust vector, deg	0.1
Axial thrust offset (RSS) cm	0.144
Spin Thrust offset (RSS) cm	0.102

Probe Parameters

Spin rate, W_s , rad/sec	10 (0.5 Pioneer mission)
Spin torque, m, Newton-Meters	4.07
Spin inertia, I_s , kg-m ²	12.2
Thrust, F, Newtons	810
Thrust period, t_F , sec	15
Tipoff rate, W_t deg/sec	0.5
Drift period, t_D , sec	0.5
$I_s/I_t - 1$	0.2

Error Source

		Value (deg)
1. Tipoff error (at 0.5 rad/sec)	$\frac{W_t I_t}{W_s I_s}$	0.8
2. Drift error	$W_t t_D$	0.25
3. Spin-up (tipoff error) (P vector)		0.85
4. Combined 2. & 3.		1.06
5. Spinup (tipoff error) (nutation)		0.63
6. Spinup (misalignment) (P vector)		0.125
7. Spinup (misalignment) (nutation)		0.125

<u>Error Source</u>	<u>Value (deg)</u>
8. Combined 5. & 7. (nutation) RSS	0.66
9. Velocity dispersion (nutation)	0.014
10. Velocity dispersion (misalignment)	0.902
11. Velocity dispersion (combined 9. & 10.)	0.905
12. Velocity dispersion (combined 11. & 4.) RSS	1.39
13. Velocity dispersion (combined 11. & 0.5 deg ACS error) RSS	1.040

Items 13 and 12 express expected errors with and without an ACS trim maneuver before delta velocity impulse thrusting. The velocity dispersions have significant effects on trajectory dispersions and result in higher communication power and longer acquisition time. Since one degree is the nominal error budget contribution of this subsystem to the velocity dispersion, the trim maneuver is included in the mission profile

The tipoff rate specified is not necessarily critical if the trim maneuver before delta velocity thrust is included in the mission sequence or the mission uses the spacecraft deflect mode. The value ($W_T = 1/2$ deg/second) was selected based on expected and present state of the art. Vela I, II, III, and IV, and OGOI (launches 1963/1964) apparently achieved near this capability at higher separation rates with the use of matched springs. This design parameter is discussed in more detail in Volume II, Section V.B.11 of this report.

APPENDIX G

ELECTRICAL POWER AND PYROTECHNIC SUBSYSTEMS
ANALYSIS

E. A. Berkery

June 9, 1972

ELECTRICAL POWER AND PYROTECHNIC SUBSYSTEMS

Power requirements for the probe components are listed in Table G-1. The subsystem design approach for all missions is essentially the same. The functional block diagram of the power and pyrotechnic subsystem is illustrated in Figure G-1. It should be noted that there are two power subsystems: (1) post separation power subsystem consisting of a primary power source, power conditioning, and essentially hard wire distribution; (2) entry power subsystem consisting of a primary power source, separation power filters, and relay power distribution. In addition to the above, there are two long-life low-drain Hg-Zn batteries to provide power for the Accutron timer and the initial preentry pyrotechnic event. The power and pyrotechnic subsystem configuration was based on an evaluation of a study of outer planet probe requirements. Batteries were evaluated on the basis of a nominal Jupiter mission time and temperature profile; this evaluation would not be valid for the application of secondary cells to Saturn and Uranus. Primary batteries were selected and will fly in the dry state until used. The evaluation for the remote activated cells is considered valid for Saturn and Uranus.

Table G-1 Nominal Power Requirements

SUBSYSTEM ELEMENTS	POWER(W)	SUBSYSTEM ELEMENTS	POWER(W)
Data Management	6.9	ACS Electronics	2.0
Memory	12.0	Sun Sensor	2.0
Pyrotechnics	0.5	Planet Sensor	1.0
Instrument Engineering	1.0	Mass Spectrometer	14.0
Vehicle Engineering	1.0	Accelerometer	2.8
Accutron Timer	14 μ (a)	Temperature Gage	1.4
Nutation Damper	(b)	Pressure Gage	1.3
RF Subsystem	14-122		
Power Subsystem Efficiency		(a) Self Contained Hg-Zn Battery	
Postseparation	80%		
Entry	90%	(b) No Power Required	

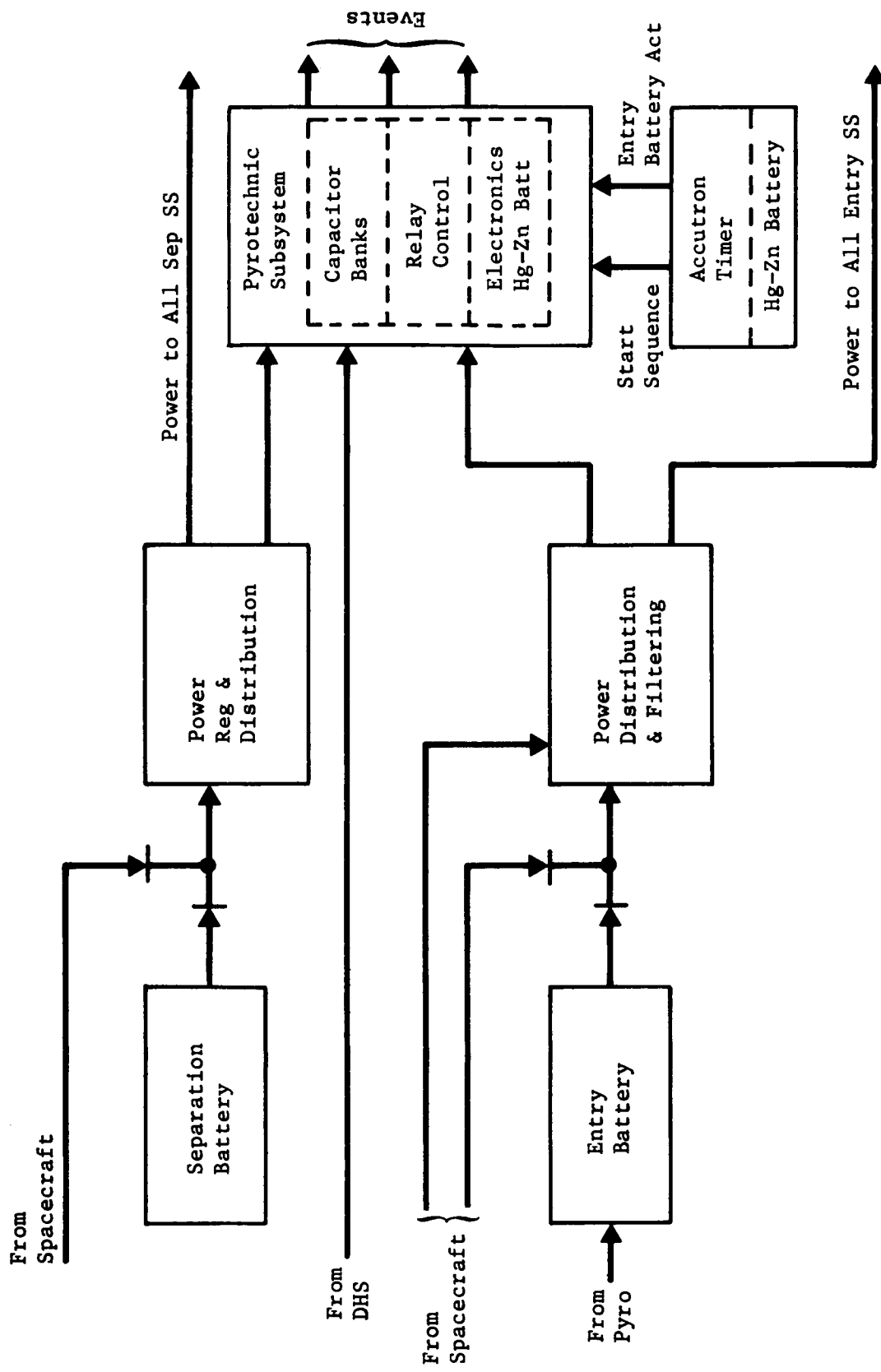


Figure G-1 Power & Pyrotechnic Subsystems

A. POWER SUBSYSTEM

1. Postseparation Power Subsystem

This subsystem provides power for the attitude control, data handling, and pyrotechnic subsystems for the approximate 6-hr post-separation period allowed for the probe attitude control maneuver. The power subsystem consists of a power source, conversion and regulating equipment. It is activated by the spacecraft before separation. The subsystem will also be activated by spacecraft power during preseparation checkout.

2. Entry Power Subsystem

This subsystem provides power to the data handling, communication, science, and pyrotechnic subsystems. The distribution system consists of relays and power-isolation filters to deliver unregulated battery power to various components. Power conditioning and regulation will be implemented in the individual components as required. This approach is used for the entry configuration to minimize the possibility of common-mode failure and to permit use of lower-power transistors that tend to be less sensitive to radiation.

3. Power Source

There are three fundamentally different power source requirements: Probe bus power source, Accutron timer power source, and preentry pyrotechnics power source. Power for the Accutron timer is provided by a Hg-Zn battery which is required to supply approximately 8 microamperes at 1.6 volts for 30 days. A 40-volt Hg-Zn battery is required to charge two pyrotechnic capacitor banks, hold the charge against leakage for approximately twenty minutes, provide power to operate two or three (detail design dependent) latching relays and some minor pyrotechnic logic. Initial drain of the 40-volt Hg-Zn battery is expected to be approximately 40 milliamperes, dropping rapidly to less than one milliampere as the capacitors charge and leakage decreases. The current will rise again to approximately 10 milliamperes for a fraction of a second at the end of the 20-minute soak period. The Hg-Zn battery size and weight are based on standard catalog cells degraded at 7% per year. Approximately 15% increase in volume and weight was allowed for packaging. The Hg-Zn batteries are located near the RTG heaters where the temperature control is more effective and protection against local temperature conditions is provided. The probe bus power source is required to meet much higher power requirements but has an active life of less than 6.5 hr. Selection of battery type to supply probe power is discussed below.

4. Probe Bus Power Source

Although consideration has been given to various power sources such as RTGs, solar cells, and gas generators for the probe, the choice rapidly narrows to some type of battery. An evaluation of various types has been made and is based on the following mission/test profiles.

- 1) Ni-Cd Secondary - Discharged (Table G-2)
 - a) Fly discharged 526 days at 50 to 80°F
 - b) Condition battery at C/10 or greater
 - c) Hold open circuit at less than 70°F for 20 days
 - d) Discharge between 40 and 110°F for 2 hours or less
 - e) System design to 80% depth of discharge
- 2) Ni-Cd Secondary - Charged
 - a) Float charge for 526 days at C/100 or greater (loss of 40% expected at temperatures less than 68°F)
 - b) Hold charged on open circuit at less than 70°F for 20 days
 - c) Discharge between 40 and 100°F for 2 hr or less
 - d) System design to 80% depth of discharge
- 3) Ag-Zn Remotely Activated - Conventional Design
 - a) Assume two batteries, postseparation battery (6-hr life) and entry battery (40-min life); tubular-reservoir standard gas generator activator; common manifold fill
 - b) Standard design capable of satisfying requirements for up to 24-hour activated life.
- 4) Ag-Zn Remotely Activated - Pile Construction
 - a) Assumptions as above, but diaphragm activator mechanism
 - b) Design capable of satisfying requirement for 6-hour activated life; some development needed if activated life is to be significantly extended.
- 5) Ag-Zn Secondary (Table G-3)

In all probability, the only cell design that meets the requirement requires irradiated and cross-linked separator

Table G-2 Ni-Cad Secondary Battery (Float Charge)

Cell Type Rsn#	Cell, amp-hr	New Cells, watt-hr	New Cells, watt-hr/lb (80% DOD)	Degraded watt-hr/lb Discharge/Cruise 20% pkg Wt	Degraded watt-hr/lb Float Charge 20% pkg Wt
3	3.2	84	8.1	6.5	3.2
6	6.0	168	9.3	7.4	3.7
8	8	224	8.1	6.5	3.2
9	9	252	8.8	7.0	3.5
12	12	336	10.0	8.0	4.0
14	14	392	10.0	8.0	4.0
15	15	420	9.1	7.3	3.6
20	25	700	10.4	8.3	4.2
21	20	560	10.1	8.1	4.0
22	22	616	10.6	8.5	4.2
36	36	1010	12.3	9.9	4.9
Note: Basis of Curves for Figure G-2 (Eagle Picher Cell Design 28 volt, 24 Cell Systems).					

Table G-3 Ag-Zn Secondary Battery

Cell, amp-hr	Cells, watt-hr	Cells, watt-hr/lb Rated Cells	Cells, watt-hr/lb New Cells	New Battery, watt-hr/lb	Battery Float, watt-hr/lb	Battery Open CKT watt-hr/lb	Battery D/C Stored watt-hr/lb
.8	22	24	31.2	25	5.3	12.2	14.5
1.5	42	30	39	31.2	6.6	15.3	18.1
3.0	84	38	49.5	40	8.4	19.6	23.2
5.3	147	42	54.6	43.7	9.1	21.4	25.3
8.0	223	48	62.4	50	10.5	24.5	29.0
11.5	322	50	65	52	10.9	25.5	30.2
20.0	560	60	78	62.4	13.1	30.5	36.2
30.0	480	63	82	65.6	13.8	32.1	38
45.0	1260	66	86	68.8	14.4	33.7	39.9
Note: Basis of curves for Figure G-2.							

Probe Power Source Capability

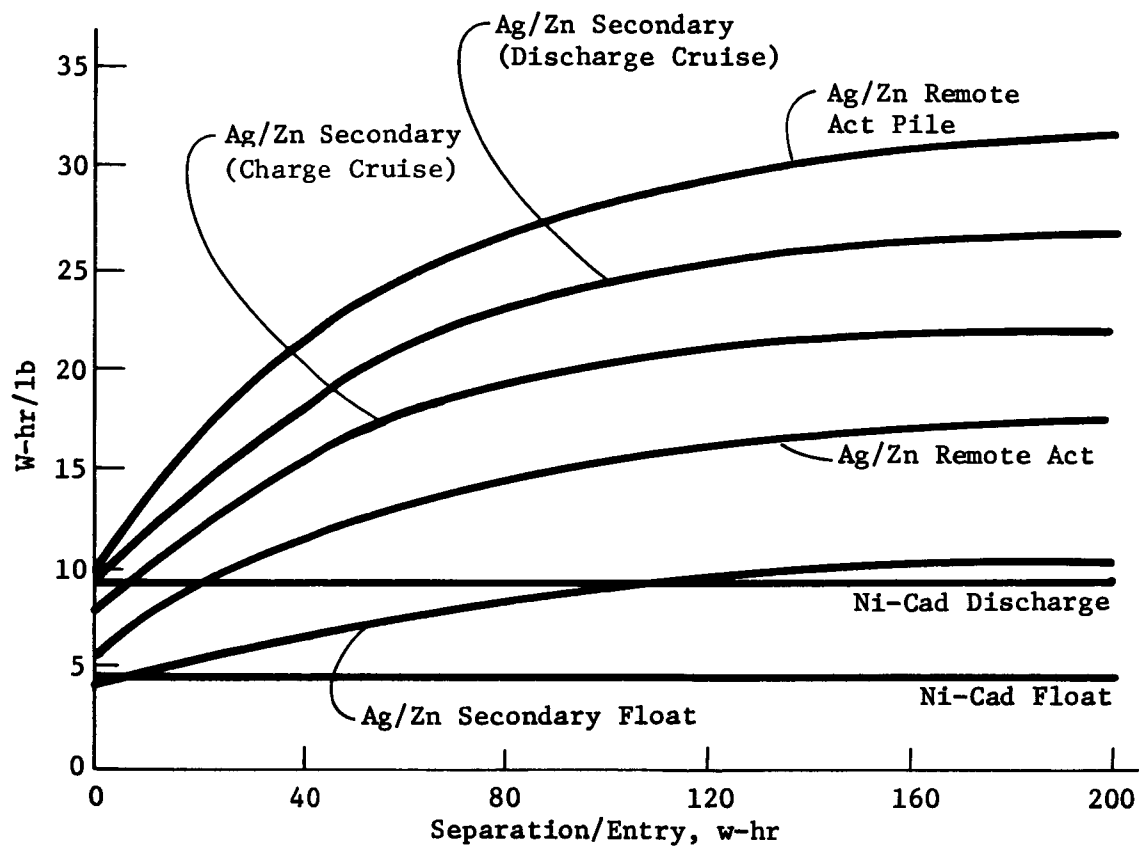


Figure G-2 Power Source Evaluations

material. General Electric Test Report 67SD337(G5) offers the best data to date. Venus Planetary Explorer tests (by Martin Marietta) will be performed on similar cells.

- 6) Ag-Zn Secondary - Float Charge
 - a) High decay rate, expect a loss of approximately 3% per month (approximately 54% total)
 - b) During a 30-day charge stand, expect a 5% loss.
 - c) System design to 80% depth at discharge
- 7) Ag-Zn Secondary - Open Circuit Stand
 - a) Assumed charge at launch and left open circuit at 50°F for 526 days
 - b) Battery would lose all capacity and need recharge
 - c) Expect a permanent loss of 26% on recharge
 - d) Expect 5% loss during 30-day charged stand.
 - e) System design to 80% depth at discharge
- 8) Ag-Zn Discharge Stand
 - a) Expect a loss of 17% on recharge
 - b) Expect a 5% loss after 30-day charge stand
 - c) System design to 80% depth at discharge

5. Evaluation

Based on the above decay and degradation rates, tests, and Reference 1 and 2, the curves in Figure G-2 were generated. It should be noted that all Ag-Zn secondary batteries would need separator development for this application. The pile construction battery would need known minor modifications and packaging for life beyond approximately 6 hour. The Ni-Cd batteries have the highest reliability but are excessively heavy. With these considerations and the need for critical recharge and conditioning control for secondary batteries, the remotely activated Ag-Zn battery was selected for this application. Consideration of standard versus pile construction indicated approximately 50% weight could be saved with the latter. The state of the art indicates that all development necessary for this application should be completed and available for the pile construction battery by 1975. Based on the above, considerations, the pile construction battery is recommended for this application and the weights indicated in Figure G-2 have been used in the current estimates.

The remote activated Ag-Zn battery requires no significant development to meet the electrical requirements; however, a nine-day unused open circuit requirement subsequent to discharge presents a concern with respect to gassing. Silver-zinc couples generate oxygen and hydrogen during any wet stand operation. Hydrogen is by far the major contributor to the evolved gas and results from thermodynamically unstable zinc in contact with KOH and the negative plate potential being above the hydrogen potential. In addition, internal and external shorts will contribute to the gassing.

The battery design will include the following features to greatly reduce the gassing and also provide the capability of storing the gasses generated to safe internal pressure.

- 1) Additives to the negative plate - 2-4% mercuric oxide
- 2) High KOH concentration - 40-45%
- 3) Ion exchange irradiated separators. For example: Permion 307, to provide 7-day wet stand life
- 4) Flap valve on each cell that permits activation, but prevents low resistance intercell leakage and allows gasses to filter into the manifold.

The cooling gasses of the gas generator subsequent to activation reduces the working pressure of the battery during discharge below the activator design pressure. The gasses by the cells work into the electrolyte container area pushing back the activator and gradually increasing the internal pressure of the battery. The design pressure will not be exceeded and the battery can be hermetically sealed.

Long-Life Remotely Activated Batteries

An alternative approach would use standard remotely activated batteries with some modifications for longer life. This would

eliminate a significant problem of energizing pyrotechnics after postseparation coast. The degradation and life characteristics are, in general, applicable to all primary Ag-Zn designs. The fill manifold is a development for standard construction.

7. Remotely Activated Ag-Zn Oxide Batteries

Current designs of remotely activated batteries for space application generally employ an electrolyte reservoir separated from the dry cells by a frangible diaphragm. Activation is accomplished by initiating a trigger mechanism or explosive squib that introduces pressurized gas to the electrolyte compartment, thus forcing the electrolyte into the battery cell compartment.

Typically, separator materials used in standard designs are not semipermeable membranes that permit long activated life, but hydrophilic nonwoven materials capable of fast activation. Activated stand life exceeding 24 hours should not be expected.

Dry Stand Loss - Losses usually result from loss of peroxide on the positive, which is accelerated at high temperature. Figure G-3 shows the effect of temperature and indicates capacity, at any temperature, will decay to a minimum of 50% of rated value, depending on storage time. Dry storage loss is a function of humidity control, temperature, plate processing, and particularly cell materials and fabricating techniques. Most battery manufacturers are aware of these problems and have solved them. Typical data on the Poseidon missile program indicates no loss of capacity during a 91-month storage.

Activated Stand Life - There are two major problems in extending activated stand life of remotely activated batteries.

1) *Electrolyte Paths* - Standard designs use a manifold across the cells that permits simultaneous activation of all cells. After activation, the manifold may remain flooded and, at best, high-resistance electrolyte all paths exist between cells. Resulting potentials between cells are high enough to permit Zn precipitation along the electrolyte paths, resulting in massive shorts and subsequent discharge of the battery.

2) *Separator Material* - Absorbent separators in remotely activated batteries serve two major purposes: activation times of less than 2 sec; higher current density (i.e., voltage current

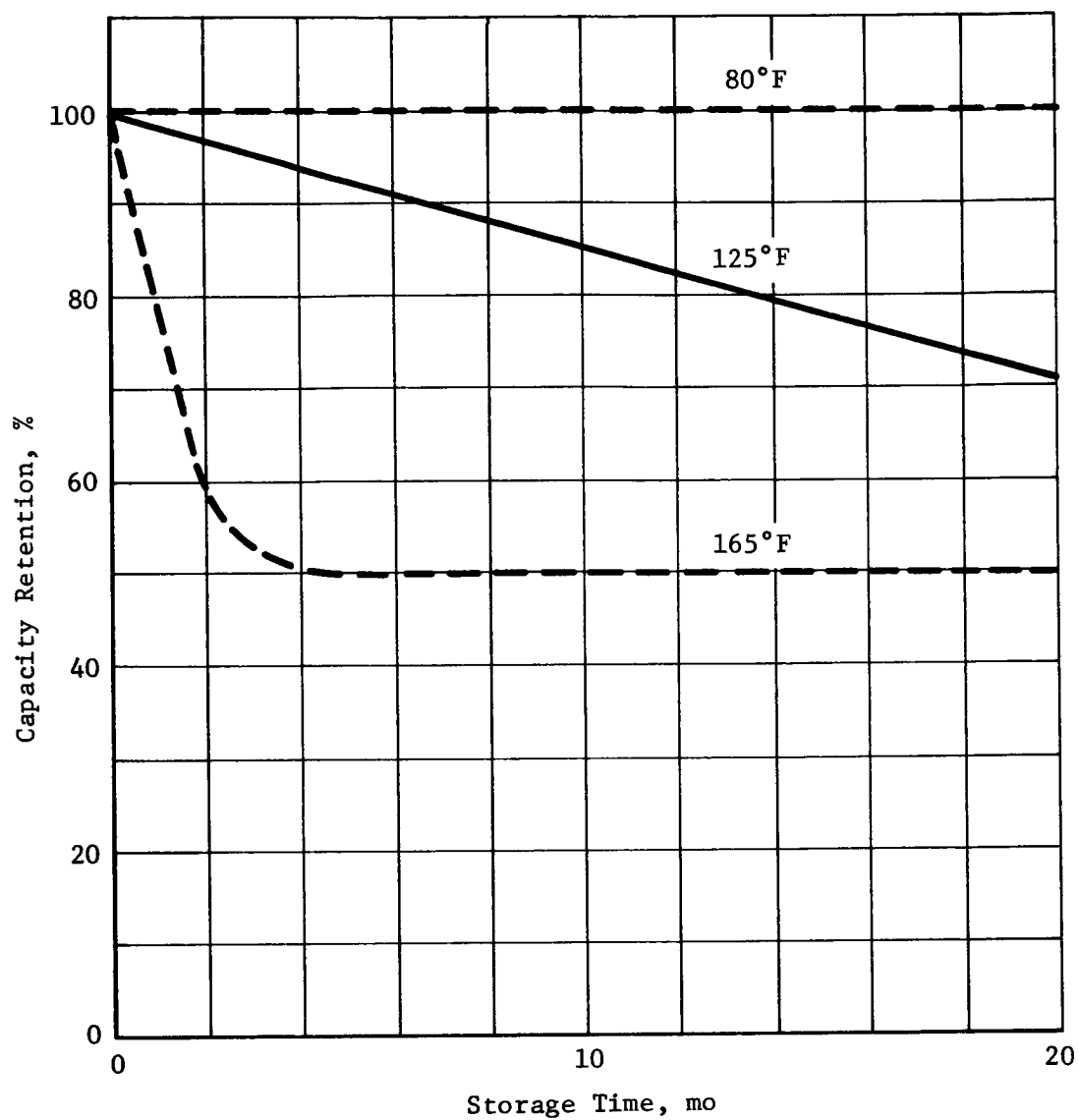


Figure G-3 Dry-Storage Charge-Retention Characteristics

characteristics). The major disadvantage is that it is not a semi-permeable membrane and oxidation occurs at a high rate, resulting in self-discharge.

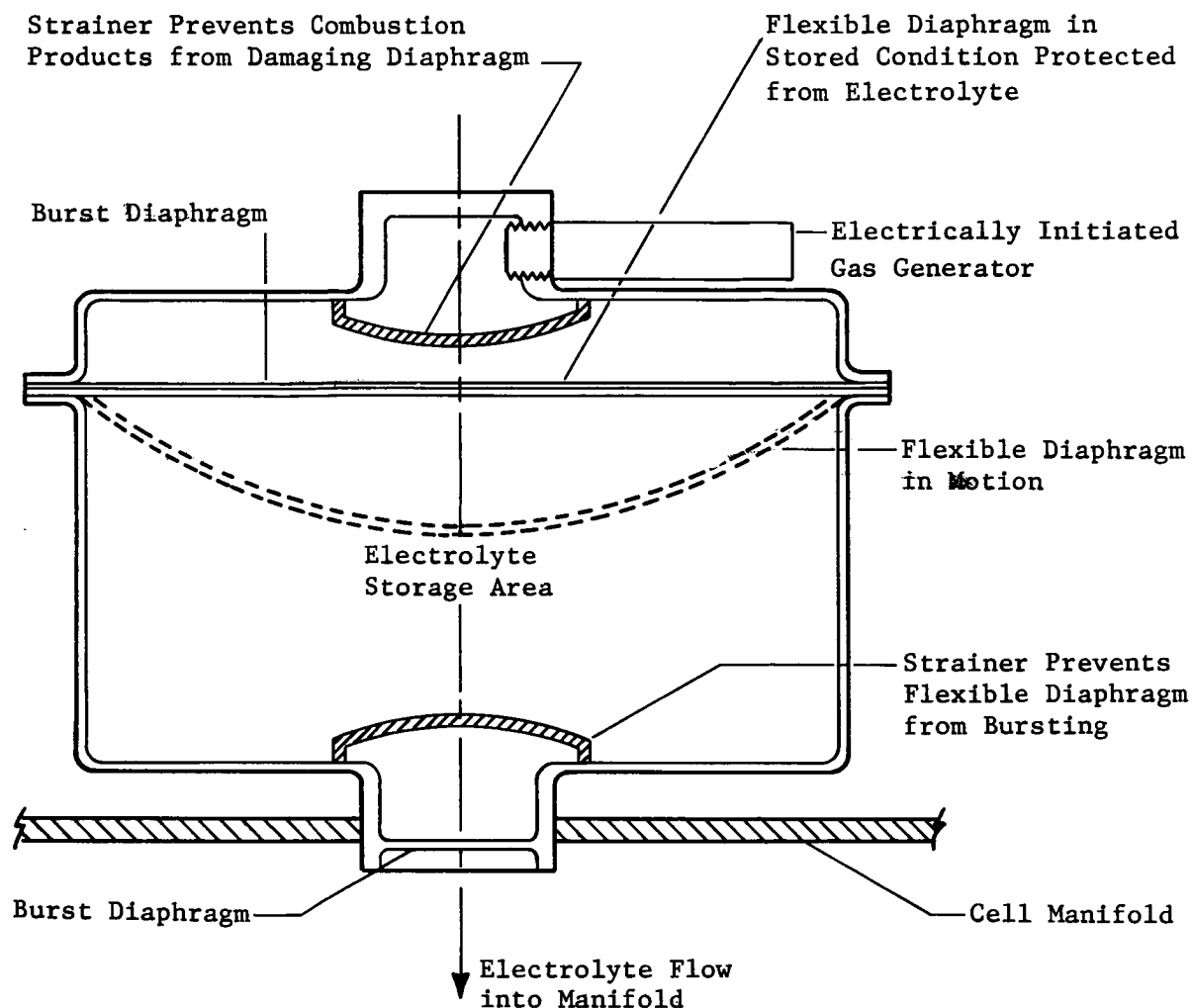
Weight Shift Due to Activation - Upon activation, electrolyte transfers from the reservoir to the cells. The quantity of electrolyte varies with capacity and separator material. As a rule of thumb, 4.2 ml/A-h/cell or 5.9 gm/A-h/cell can be used (e.g., 20 A-h 20-cell battery - 2360 gm KOH). The weight shift depends on the battery design. With a tubular reservoir wrapped around the cell pack, as described in the Eagle Picher data (Ref G-3), electrolyte would transfer from the periphery to the center of the black box. In case of a higher-energy-density design, as shown in Figure G-4, transfer approximates a shift from the top half of the black box to the bottom half.

Design Concepts for Long Wet Stand - A 7-day wet-stand life has been achieved with the design shown in Figure G-5 and G-6. Figure G-5 shows a high energy density design in which the cell case is a half shell. High energy density is achieved by elimination of the double cell wall resulting from normal cell construction. The center wall also can be as thin as 0.0254 cm (0.01 in.).

The half shells are assembled so that the flexible member is directly below the open section. Design tolerances provide a crude seal at this point. When the battery is activated through the manifold, activation pressures deflect the flexible member, permitting electrolyte to enter the cell. At equilibrium conditions, a pressure balance occurs across the flexible member and the joint closes causing very high resistance paths between cells, thus minimizing electrolyte shorts.

To eliminate cell degradation caused by separator breakdown, a semipermeable membrane would be included in the cell pack. Activation times would increase to 20 seconds and wet-stand life to 7 days.

Figure G-6 shows a more conservative design that increases energy density, but eliminates intercell shorting. Electrolyte enters tube A and the first cell at the level of tube B. It travels up tube B across to the next cell and down tube A of the second cell. This process is repeated until the last cell is filled. Excess electrolyte continues to move into a final compartment where it is centrifuged into an absorbent material. The activation mechanism is designed so activating gasses follow through with the electrolyte

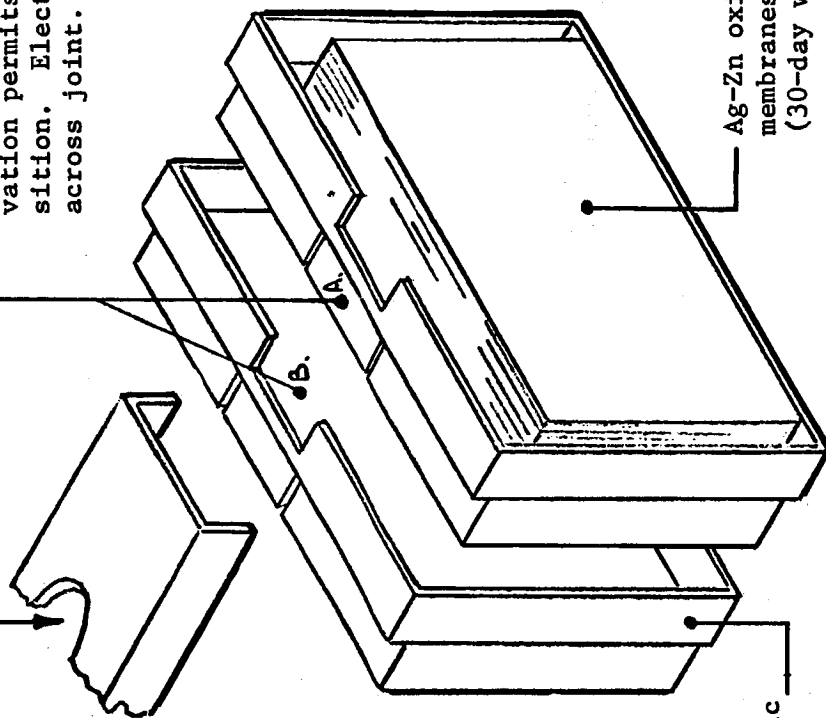


Note: Gas generated by initiator increases internal pressure of mechanism until burst diaphragms open. Electrolyte flows into manifold under pressure of distending flexible diaphragm.

Figure G-4 High Energy Density Activation Mechanism for Ag-Zn Batteries

Electrolyte forced under pressure into common manifold. Activation mechanism not shown.

Flexible member A fits tightly under slot B when interlocking cells assembled. Electrolyte deflects A under pressure & activates cells. Pressure balance after activation permits A to return to original position. Electrolyte resistance path high across joint. Proven 7-day capability.



Ag-Zn oxide plates with ion exchange membranes & absorbant separator. (30-day wet-stand capability)

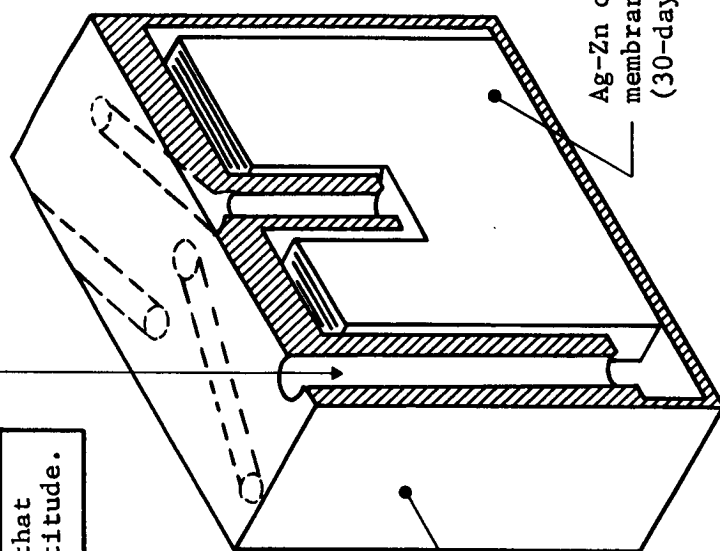
Moulded lightweight plastic interlock cell cases

Note: System designed & qualified for 7-day wet-stand requirement.

Figure G-5 Remotely Activated 30-Day Wet-Stand Design Concept 1

Electrolyte forced under pressure from activation mechanism. Fills first cell & overflows through center tube into down tube of second cell. Electrolyte cascades until last cell filled, then flows over into sump. Activation gases follow through leveling electrolyte to center tube level & clear fill tubes.

Note: Center fill tube designed so that battery can perform in any attitude.



Monoblock battery
construction

Ag-Zn oxide plates with ion exchange
membranes & absorbant separator.
(30-day wet-stand capability)

Note: System designed & developed for 7-day wet-stand requirement.

Figure G-6 Remotely Activated 30-Day Wet-Stand Design Concept 2

and purge the tubes and intertall paths of electrolyte. This design, like the other, will operate in any attitude. As before, separator material would be changed to a semipermeable membrane.

Both designs were developed for the Royal Aircraft Establishment, England, for a 7-day activated mission. It is expected that the design in Figure G-6 could exceed this requirement, but a 30-day stand would be a marginal concept. Conceptually, a revised design would be capable of providing a 30-day wet stand with a high degree of confidence.

Watt-Hour Design Margins - If it is assumed that electrolyte leakage paths can be eliminated, and the whole design concept is based on this assumption, the following margins can be applied when sizing the battery.

With up-to-date design methods, a 40 W-h/lb (pile type) battery can be manufactured.

Start with 40 W-h/lb.

Apply degradation rates:

- a) Dry stand loss 3% per year below 90°F; it would be undesirable to fly the battery at a higher temperature;
- b) Activated stand loss 0.5% per day;
- c) If sterilization is required, loss is 25%, with no further loss because of a dry-charged stand.

Items a) and b) can be supported by characteristics of primary Ag-Zn batteries like those used on Titan III and Biosatellite, and Coppo batteries. Item c) causes loss of peroxide, which in a normal design would be 50%. However, because this loss is known, the Zn plate capacity would be reduced accordingly, and the weight gained would be transferred to the positive plate.

Temperature Performance Activated - Normal operating temperatures should be 30 to 80°F. However, if load requirements are known, the battery could be designed to perform at lower temperatures around 10°F. The high-temperature restraint is not required on discharge, but has a degrading factor on the stand.

B. PYROTECHNIC SUBSYSTEM

The pyrotechnic subsystem is similar to designs already applied to several space vehicles such as Mariner and Viking. Specific

constraints and devices considered for outer planet probe designs were principally derived from Viking, which has severe restrictions on weight and a radiation environment. The pyrotechnic subsystem consists of power conditioning equipment, relay switching control, control logic, and capacitor banks for high pulse discharge.

The pyrotechnic control system derives power and initiating signal from several sources.

- 1) *Separation events* - Initial charging of the capacitor banks and initiation signal are provided by the spacecraft. After the postseparation battery has been activated, power is then derived from the probe postseparation battery.
- 2) *Postseparation events* - Power is derived from the probe postseparation battery and initiation signals from the probe data management system.
- 3) *Preentry battery event* - Power is derived from a 40-volt Hg-Zn battery. This is the only function for this battery, which must maintain the capacitors on charge for about 20 minutes. The initiation signal is derived from the electromechanical (Accutron) timer.
- 4) *Preentry events* - Power is derived from the probe preentry battery. Initiation signals are provided by the data management system.

1. Power

Except for the entry battery pyro event, all power conditioning required in the pyrotechnic control subsystem is provided by an internal power supply. Outputs are not regulated and have a tolerance of $\pm 10\%$. The outputs consist of two 40-volt windings completely isolated from each other and from all other windings. Voltages provided for internal use are tabulated.

Capacitor charging	+40
Relay switching	+28
Logic circuitry	+5
Digital interface circuitry	<u>+5</u>

The supply has an output capability of approximately 50 W and a standby power dissipation of 450 mW. Because the supply is essential in the standby condition at all times, except for approximately 5 seconds after each event, the assumed average power requirement is 0.5 W.

2. Relay Assembly

Magnetic latching relays are used for pyro firing functions as well as for safing and arming. This is a deviation from the Viking approach, which uses SCRs for firing. The modification results from the susceptibility of SCRs to the high-radiation environment near Jupiter. The relay selected for this purpose and for estimated weight and size is Potter Bromfield Type HL 4125 (MIL-R-5757). The relays weigh 0.29 kg (0.063 lb) with a volume of 11.12 cm³. The present configuration assumes one relay for each side of the redundant squib and one for safing and arming in the common lead. This approach requires three relays for each event.

Considerations to be evaluated for this design are the effect of contact bounce on the operation of the squib, possible fusing of contacts (which would leave the capacitor banks connected to the squib circuit), and testing problems. The contact fusing problem could be eliminated by adding another relay for each event and performing safing and arming directly in series with the contacts of the initiator relay. An alternative configuration could use the common-lead relay for firing. However, this would accentuate the effects of contact bounce on the performance reliability. Testing may be a severe problem because the first operation is likely to cause significant damage to relay contacts. A simulated test that measures contact bounce and contact resistance may be sufficient. The effect on the squibs cannot be predicted at this time. The relay manufacturers are reluctant to reduce the specification on contact bounce below 2 msec. Firing time of the squib is approximately 0.4 msec and further study will be required to evaluate this problem. Present Viking design calls for operation of the relay with 8 to 18 volts applied across the coil. A 1600-ohm coil design ensures that sufficient power is available to operate the relay from the low-energy Hg-Zn battery, which initiates the pre-entry phase of the mission.

3. Capacitor Banks

Each capacitor bank contains six 82 μ f capacitors rated at 50 volts. These wet-slug tantalum capacitors are required to deliver 150 mJ in 5 msec into a 1-ohm circuit. Each capacitor bank is required to fire six initiators, one at a time. No two initiators can be

fired by a capacitor bank within a 12-second period. The design is planned to permit charging all capacitor banks from either side of the power supply through charging resistors. Failure of one or several banks will not produce a serious load on the power supply. One possible exception to the resistive cross connection may be the capacitor banks that fire the entry battery pyrotechnics because these are energized by a low-capacity long-life Hg-Zn battery.

The design application of the pyrotechnic subsystem does not depart significantly from state-of-the-art designs, in particular, the Viking design. One aspect that must be given further consideration, because of the nature of the probe mission profile, is the conditioning of the pyrotechnic capacitor banks. Because the various probe designs will have been electrically quiescent for approximately 18 months before separation, the capacitor banks will require reconditioning for approximately 1 hour. A more critical requirement will occur after the quiescent coast period. This represents a significant problem because of the lack of available power. The design approach is to provide a 40-volt Hg-Zn battery that will provide charging current and maintain charge for approximately 20 minutes on two capacitor banks. These capacitor banks will then provide the energy to fire the first entry pyrotechnic. The actuator that initiates the capacity charging and provides the firing control will be mechanically closed contacts in the electromechanical (Accutron) timer. A 40-volt battery will be used to avoid the need for power conditioning. The only function of this battery is to provide charge current to the capacitor banks, leakage current during the conditioning period, and power to operate the relay initiator logic.

4. Interface

Except for the entry battery pyrotechnic event, all pyrotechnic event control will be provided through the data management subsystem. The control signal will be in the form of parallel digital address, enable, fire, and safe commands. The pyrotechnic subsystem will be enabled by applying power through a power control relay in the power distribution control.

C. REFERENCES

- G-1 *Evaluation Program for Spacecraft Secondary Cell.* Prepared for GSFC Contract W12,297, Quality Evaluation Laboratory NAD, Crane, Indiana.
- G-2 C. F. Palandati: *Electron Radiation on Effects on Silver Zinc Cells.* X-716-68-136. GSFC, 1968.
- G-3 E. M. Morse: *Eagle-Pincher Silver Zinc Automatically Activated Batteries.* Bulletin No. 101, Eagle-Picher.
- G-4 J. A. Sanders: *Remote Activated Batteries.* Memo 0455-71-95, September 9, 1971.
- G-5 J. A. Sanders and D.R. Seals: *Test Report on Heat Sterilizable Silver-Fine Batteries.* General Electric Co., 67SD337.

APPENDIX H

DATA HANDLING SUBSYSTEM ANALYSIS AND DEFINITION

E. A. Berkery

June 20, 1972

DATA HANDLING SUBSYSTEM (DHS)

The principal problem in developing a rigorous evaluation of data handling subsystems for a system level study is that the detail requirements which provide the major constraints on the DHS are generally absent. The most significant interfaces (science instruments) lack detail in the sense of synchronization requirements, internal (instrument) processing capability, diagnostic and control requirements. The data that are available, such as science bit rate, measurement duration, intrascience requirements (i.e., simultaneous measurements), are subject to change with changing definition of mission profiles and instrument configurations. Consequently, some generalizations have been made and arbitrary interface descriptions have been assumed where it is necessary to provide a definitive interface. It is understood that the ultimate specifications of the various subsystems could perturb this evaluation; however, the performance required of the DHS is well within the state of the art and no serious obstacle is expected in a detail design of this subsystem.

Sequence of Events - An approximate sequence of events which is applicable to all missions, is shown in Table H-1. During the pre-separation period the probe DHS is controlled by the spacecraft. The primary function during this period will be to decode the serial digital commands from the spacecraft, verify the commands, perform the commands (component turn on, warmup timing, diagnostics), and relay the resulting data to the spacecraft. Since command loop time delay between the ground station and the spacecraft is approximately 1.5 hr, a reasonably automated checkout is desirable. Checkout may be performed at any time before separation; however, it is desirable to limit the number of times the probe is powered up. A pre-separation checkout period of six hours would allow for several probe revision and checkout cycles. The modification to the probe subsystems at this time will consist of switching out components that exhibit catastrophic failure symptoms, assuming a partial data return is still achievable. The Accutron timer will be started before separation at some time $t = E - \tau$. This timer is set for period τ before launch and cannot be reprogrammed in flight. The only function for the Accutron timer is to initiate the entry phase by activating the entry battery. During the immediate (≈ 6 hr) post-separation sequence, the DHS sequencing logic controls the probe. The ACS subsystem is enabled for the entry orientation maneuver by the DHS. When the maneuver is completed (attitude error less than 3°), the ACS provides a signal that initiates the shutdown of that subsystem by

Table H-1 Nominal DHS Sequence of Events

TIME	FUNCTION	COMMAND SOURCE
S - 6 hr	Energize probe power bus and DHS	S/C DHS
	Start timer	S/C DHS
	Exercise probe functions/checkout	S/C DHS, Probe DHS
S - 1 min	Activate probe battery	S/C DHS
S - 0	Separate	S/C DHS
S + 0		
	Perform spinup, V ACS maneuver	DHS
	Engineering measurements, RF transmission	
S + 6 hr	Initiate coast shutdown sequence	ACS logic
S + 6 + hr	Complete coast shutdown sequence	DHS
E - 85 min	Charge pyrotechnic banks	Coast timer
E - 65 min	Activate descent battery	Coast timer
	Activate DHS timer/sequencer	Bus voltage sensor
E - 45 min	Initiate Pre-entry sequence	DHS
E + 20 sec	Initiate descent sequence (100 g)	G-switch
	Measure/store science/engineering data	DHS
E + 3 min	Resume transmission of measurements and stored data	DHS

the DHS. Obviously, the ACS electronic functions could be included in the DHS; however, it is preferable for overall mission reliability to keep them separate, as will be discussed below. Subsequent to the ACS maneuver, the transmitter is energized and data stored during the post-separation activity is transmitted to the spacecraft. When the transmission is completed, the various subsystems are shut down. The DHS shuts itself down by removing its own power. Delay and signal verification approaches will be used for the shutdown sequence since it constitutes a lock-down mode.

During the coast period, the Accutron timer is the only active electronic component. Power ($\approx 10 \mu$ watts) is supplied by a mercury-zinc battery. The mechanical contacts of the timer provide two events: (1) initiation of capacitor bank charging and (2) firing the pyrotechnics to activate the entry battery. The activation of the entry battery initiates a sequence that enables the DHS. All subsequent events are controlled by the DHS timing and sequencing. During the entry phase, the trajectory uncertainties are removed by sensing deceleration and initiating the descent program.

Configuration Alternatives - The configuration of the data handling subsystem was based on studies of probe requirements for Venus and the outer planets. Consideration was given to a programmable processor controlled system and a hard-wired system. These approaches are exemplified by an Adaptive Control and Data Processing Group (ACDPG) and Control and Data Processing Unit (CDPU). The ACDPG (Figure H-1) consists of a computer and a Processor Interface Unit (PIU) that includes all the functional blocks except the computer. The selected computer is a nonredundant version of the Advanced Onboard Processor (AOP) which is being considered by Martin Marietta for outer planet spacecraft. It employs a plated wire memory and bipolar (non-MOS) LSI circuits. An increase of approximately 12 lb and 4.0 watts over the CDPU version could be traded off against savings in weight and power in attitude control and the instruments by the use of a system like the ACDPG. Since the AOP computer is designed for a redundant configuration and some of the electronics is dedicated to redundancy functions, it may be expected that an additional 10 to 30% decrease in weight and power could be achieved for the computer.

The evaluation of the CDPU (Fig. H-2) involved a rather pragmatic evaluation of mission viability that considered the fluctuating instrument designs with consequent changes in interface requirements, development costs, schedule, and practical reliability

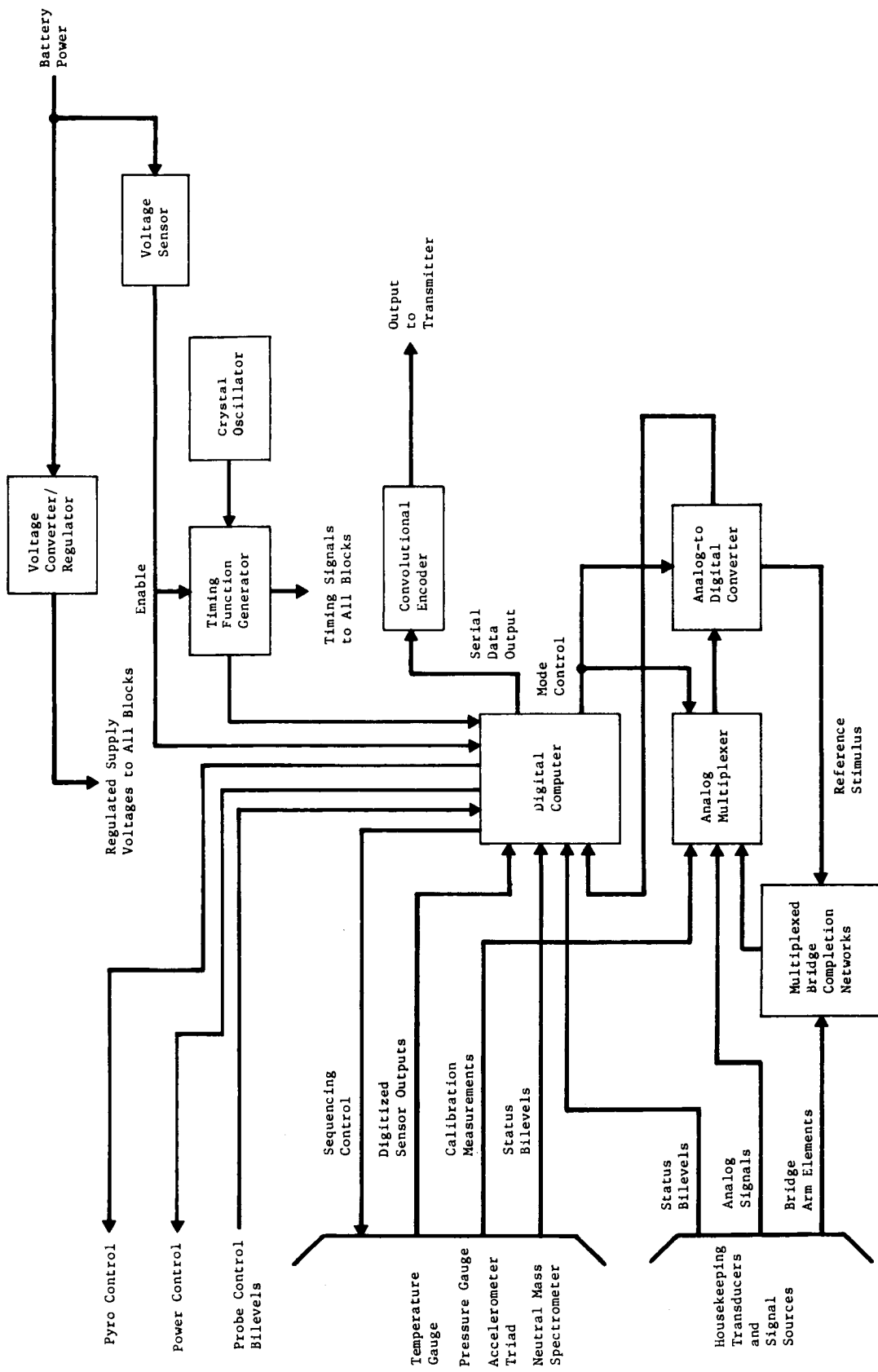


Figure H-1 Data Handling Subsystem, General Purpose Approach

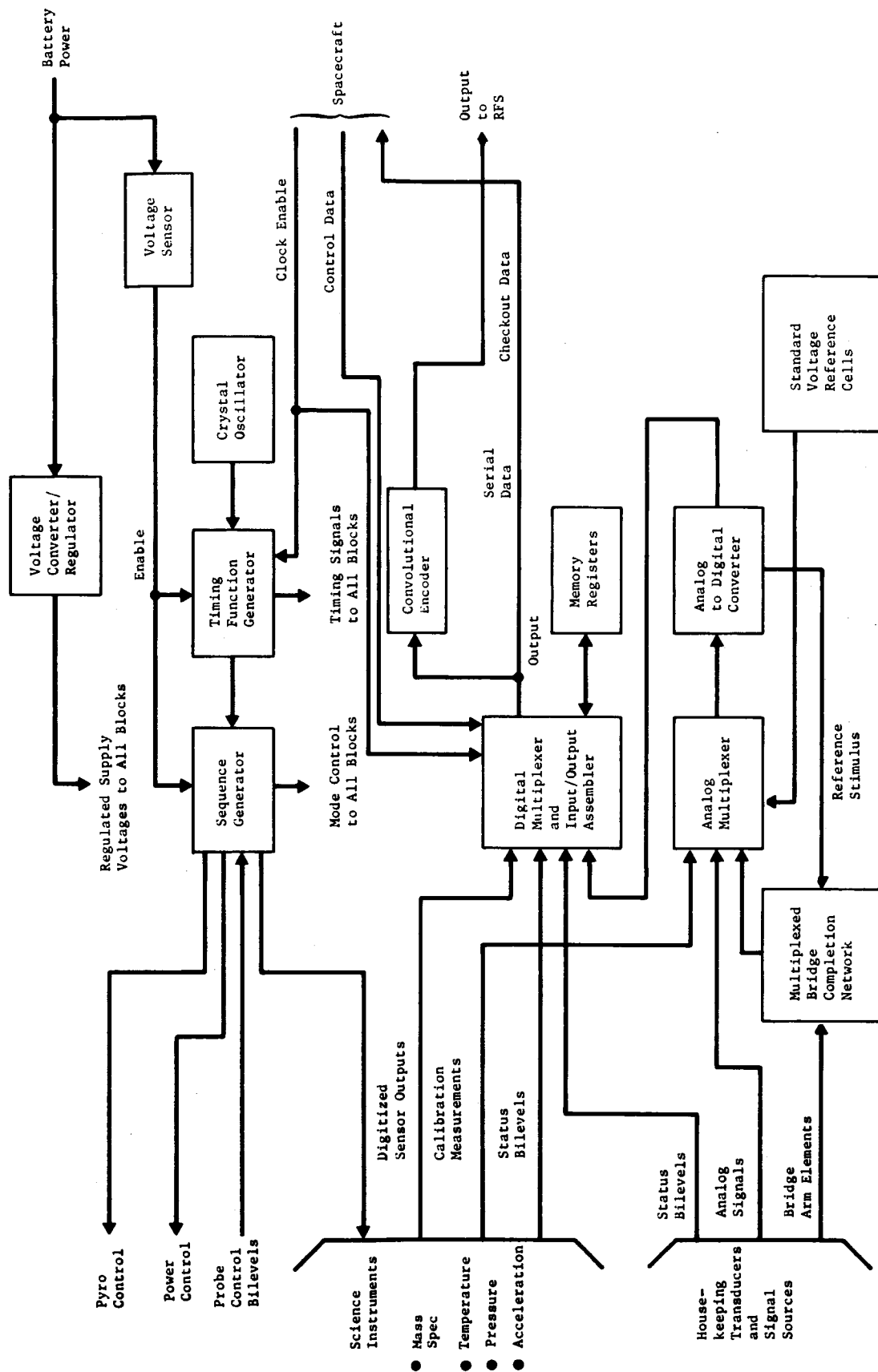


Figure H-2 Data Handling Subsystem Diagram, Special Purpose Approach

aspects. The major functional requirements of the data management subsystem are shown in Table H-2. Except for the entry accelerometer instrument, there are no significant storage requirements. For any specific atmosphere, there is a fixed sequence and format. Consequently, the decision-making capability and processing complexity of the subsystem tend to be minimized. The decision as to the locale of the various functions must consider the fluctuation of the science processing requirements during the development of the instruments as well as the significant differences between instruments. The high radiation, g-stress and long life environment and the value of partial data return provide a basis for a decentralized DHS. The remaining functions, which are necessarily common to all subsystems (i.e., formatting and sequencing), should be well protected from failure by redundancy. A decentralized subsystem should be cost and schedule effective through the development program.

The design of a DHS, which primarily serves to provide formatting, sequencing and encoding, may be implemented from available qualified components, integrated circuits and piece parts. Selection of such devices will be heavily influenced by established reliability and radiation resistance.

Consideration of atmospheric uncertainties indicate a need for adaptive functions in the subsystem that could conceivably optimize the data return. With the present instrument package, the advantages of optimization with respect to the data return and probe design do not appear to be significant. Furthermore, the information available (i.e., temperature and pressure) are not sufficiently well known to make a valid format decision at the required altitudes.

As a result of the above considerations and comparisons the recommended approach is the special purpose CDPU. The alternative configuration may be reconsidered if there is extensive elaboration of the instrument payload or a flexible inflight programmable system is required.

Selected Configuration - The functional block diagram of the special purpose DHS is shown in Figure H-2. The DHS performs only the necessarily centralized functions of timing, sequencing, and formatting. The subsystem is energized twice, by the spacecraft before pre-separation checkout and by the coast timer/bus voltage sensor during the pre-entry period. The probe bus voltage sensor has an additional function in that it provides controls so that

Table H-2 Data Management Functional Requirements

Function	Application	Function Locale	Comments
Timing	Sequencing	DHS	Hardwire/Programmable
	Synchronization	DHS	Sync Bus
Data Storage	Accelerometer	DHS	Blackout Data
	Engineering	DHS	Probe Readiness
Data Processing	Accelerometer	DHS/Inst	Turbulence
	NMS	Inst	A/D
	Pressure	DHS/Inst	A/D
	Temperature	DHS/Inst	A/D
	Engineering	DHS	A/D
Sequencing/ Format	Pre-entry Probe Readiness	DHS	Coast Timer/Battery Initiate
	Data Transmission	DHS	Engineering Data
	Post-Entry Blackout	DHS	G-Switch Initiate
	Probe Readiness	DHS	Engineering/Accelerometer Data
	Data Transmission	DHS	Descent Format

the DHS is disabled until full power is on the bus, and signals are available to ensure that the internal states of the DHS are properly set. Once energized the timer and sequence generator control the probe functions. The DHS receives two additional commands: (1) the accelerometer signals the presence of significant g-level to prevent overloading the science data storage memory with useless pre-entry acceleration data; (2) g-switches provide signals to initiate the descent format.

It is assumed that the science instruments will have ten- or 12-bit buffer storage output to hold the measurements and signal the state of the instrument. Information is shifted from these buffers into the appropriate DHS memory registers. Although this procedure produces some redundancy in the electronics, it facilitates the simultaneous measurements that must be made by the science instruments and will also reduce design schedule interference between probe engineering design and changing science objectives. The bridge completion networks, analog multiplexer and A/D converter, are provided for engineering measurements. Standard voltage cells (chemical cells or zenor diodes) are provided for calibration and measurement purposes. (The difficulty of maintaining a voltage standard for as much as eight years is recognized; however, the probe may be calibrated during pre-separation checkout. This will ensure that probe accuracy is approximately equal to the accuracy of the spacecraft.) The data in the DHS buffer storage is then sequenced into the data stream and convolutionally encoded.

In addition to the science instruments, the DHS controls vehicle pyrotechnics, power, ACS, and RF transmission. Their functions are indicated by the "pyro" and "power" control interfaces. Incoming commands from the accelerometer and g-switches are indicated by the "probe control bilevels."

The physical characteristics were based on estimates of devices required for each function. Included in this estimate were 14-lead flat packs, LSI packages, hybrids, transistors, diodes, resistors, capacitors (small and large tantulum) coils, and transformers. Card surface area was allocated for each device and total surface area calculated. Board thickness of 0.75 cm and a density of 0.93 gm/cm³ were assumed. These estimates resulted in the following physical characteristics: volume 2320 cm³, weight 2.13 kg, power, 6.9 W.

The weight of the memory was based on an estimate from Electronic Memories (Division of Electronics Memories and Magnetics Corp). The estimate for a 7 kb bipolar, IC memory (8 kb card) follows: volume/6.5 x 11.4 x 0.64 cm, weight 0.23 kg, power 6 watts. These data have been used as a basic building block for the cost of memory capacity.

The resulting physical and electrical definition of the nominal Jupiter probe DHS and is volume 2575 cm³, weight 2.59 kg, power 18.9 watts.

Redundancy and Coding - The use of redundancy has not received significant attention in the probe electronics design; however, it is realistic to assume that with the long-life, radiation environment and volatile bipolar IC memory electronics, some efforts will be required in this area. Redundancy techniques may involve the design of the DHS to a greater extent than other systems because of the central control function. While passive (majority vote logic, derating, etc.) redundancy techniques may be applied effectively to many types of circuitry, technologies such as power subsystems require failure sensing circuitry and switching. Inasmuch as the DHS already controls power switching, the failure detection/correction functions may be more effectively and reliably implemented in the DHS subsystem.

Reliability improvement internal to the DHS would primarily use passive approaches particularly in the critical timing and sequencing counters and logic which provide common control functions. The power requirements of the blackout data storage memories would tend to constrain a reliability improvement approach to the use of a parity bit per word; the relatively low capacity buffer memories would use passive techniques.

The data encoding requirements arise because of relay link requirements rather than probe requirements. A noncoherent FSK system and especially a binary system will give poor performance when compared to that attainable according to the Shannon Theory. In order to offset this deficiency error correcting codes are used.

Convolutional codes are easiest to implement and provide the best performance; therefore, only convolutional codes were considered in this study. Either long or short constraint length codes may be used, depending upon the amount of processing, if any, to be

done on the spacecraft. Spacecraft options range from digitally sampling the received signal and recording the data for relay to Earth, to fully detecting and decoding the signal onboard the spacecraft. It was decided, therefore, to assume use of a short constraint length $\kappa = 8$ and rate $\frac{1}{2}$ code to be compatible with any of the available spacecraft signal processing options.

APPENDIX I

MONTE CARLO DEFLECTION
DISPERSION ANALYSIS

E. D. Vogt

June 15, 1972

A Monte Carlo computer program is used to compute the dispersions in communication and entry parameters caused by errors and uncertainties at the time of the deflection maneuver. The deflection maneuver itself is defined in detail in subsection IV.D.1 of Volume II of this report. A summary of the Monte Carlo technique is supplied in this appendix.

A. ERROR SOURCES

Two distinct types of errors are identified as causing dispersions from the nominal entry parameters. First, because of errors in the guidance and navigation process prior to the deflection maneuver, there are uncertainties in the spacecraft state at deflection. Secondly, there will be execution errors made by the spacecraft and probe in the implementation of the required maneuver.

1. Guidance and Navigation Uncertainties

Quantitative measures of the uncertainties in the spacecraft state at the deflection point are provided by the control and knowledge covariances* at that point. The control covariance P_c is a 6×6 matrix defined by

$$P_c = E \left[(X_{act} - X_{nom})(X_{act} - X_{nom})^T \right]$$

where E is the expectation operator and X_{act} is the random variable vector describing the actual state (6 vector of position and velocity) of the spacecraft and X_{nom} is the nominal state of the spacecraft. P_c thus gives a measure of the probabilistic deviation of the actual deflection state from the nominal state.

The generation of the control covariance proceeds as follows. It is assumed that the control errors result solely from errors at the last midcourse correction prior to deflection. A further assumption is made that the last midcourse correction is small enough that the execution errors are dominated by the knowledge errors at the time of the correction. A large *a priori* knowledge covariance is assumed at 25 days prior to the last midcourse maneuver when the tracking for that midcourse is initiated. The *a priori* knowledge covariance is reduced by processing simulated measurements for 25 days to determine the knowledge covariance at the midcourse. This covariance is then simply propagated (processing no measurements) over the last 13 days to generate the control covariance at the deflection point.

*The control and knowledge covariances referred to in this report correspond to the correlation matrix X of the actual deviation vector and the correlation rating E of the estimated errors in Battin's notation of Reference 1. General analytic details of the formulation of these mathematical tools may be found in this reference.

The knowledge covariance P_k at any point is defined mathematically as:

$$P_k = E \left[(X_{\text{est}} - X_{\text{act}})(X_{\text{est}} - X_{\text{act}})^T \right]$$

where X_{est} is the random variable representing possible estimated states if X_{act} is the actual state. Thus, P_k provides a quantitative measure of the estimation error to be expected at the time of deflection.

The knowledge covariance is generated similarly to the control covariance. Tracking begins at 38 days prior to deflection and measurement processing continues to one day prior to deflection. The knowledge covariance at that time (the deflection maneuver computation time) is then simply propagated to the nominal deflection time.

Thus, the knowledge and control uncertainties are really functions of the approach orbit determination (OD) processes. Since the orbit determination process is highly dependent upon the detection of the gravitational effects of Jupiter, the knowledge and control uncertainties decrease as the deflection maneuver is performed nearer Jupiter.

Figure I-1 presents a summary of the control and knowledge covariance computations. The pertinent data used in generating the uncertainties is supplied in Figure I-1C along with a pictorial representation of the process. Deflection radii of 10-, 30-, and 50-million kilometers were studied. These radii correspond to time intervals of approximately 8, 25, and 44 days before encounter. For any of the deflection radii, the tracking was initiated 38 days before deflection tracking through 25 days to generate the midcourse knowledge covariance. That covariance was then propagated forward to deflection to generate the deflection control covariance. Tracking was reinitiated on the midcourse knowledge covariance and carried through to one day prior to deflection. This was then simply propagated over the final day to generate the deflection knowledge covariance.

The dominant part of the deflection covariance matrix is the upper left 3×3 partition defining position uncertainties. This may be rotated into the standard RST coordinate system. Then the one sigma uncertainty in the spatial miss or the impact parameter B is defined in the TR plane as indicated in Figure I-1A. The one-sigma uncertainty in the S direction divided by the hyperbolic excess velocity produces the one-sigma time of flight uncertainty given in Figure I-1B.

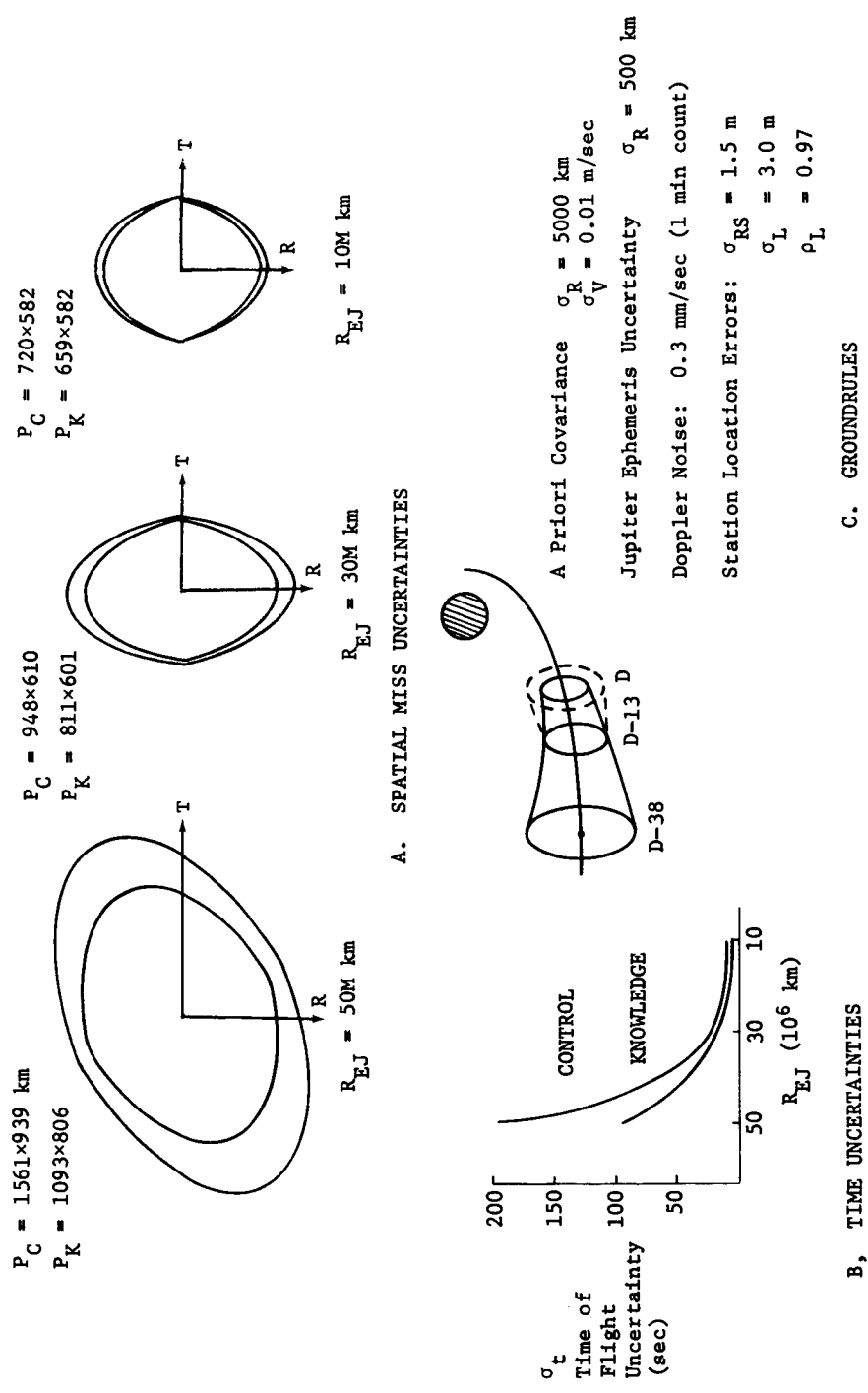


Figure I-1 Knowledge and Control Uncertainties at Deflection

The net effect of decreasing the deflection radius on the knowledge and control covariances is evident. Decreasing the deflection radius from 50- to 30-million kilometers reduces the uncertainties by approximately one-third. Decreasing the deflection radius from 30 to 10 million kilometers produces a decrease in uncertainties of approximately one-fourth.

An intuitive feeling for the exact use of knowledge and control covariances may be gained by referring to section B which describes the analytical technique used in the Monte Carlo dispersion analysis program.

2. Execution Errors

The second source of errors analyzed results from execution errors made in implementing the actual maneuvers required. The types of maneuvers encountered in the three modes identified earlier are:

- 1) Probe deflection maneuver;
- 2) Spacecraft deflection maneuver;
- 3) Probe release and/or orientation.

The error models used to analyze each of these maneuvers are described in the following paragraphs.

The purpose of the probe or spacecraft deflection maneuvers is to add a commanded velocity increment Δv to the current probe or spacecraft state. The actual velocity increment imparted to the body will differ from the commanded value by an amount $\delta\Delta v$ that represents the contribution due to execution errors. The execution error model used in this study is defined by four independent error sources.

The first error source is called the proportionality error and is in the direction of the velocity correction, Δv , with magnitude determined by the proportionality factor, k :

$$\underline{\delta\Delta v_k} = k \underline{\Delta v}$$

A second error source in the direction of Δv but independent of its magnitude, is the resolution error, s , that corresponds to a thrust tailoff error from the thrusters:

$$\frac{\delta \Delta v}{s} = \frac{s}{\Delta v} \Delta v$$

The other error sources are pointing direction errors. The first of these is a pointing error angle, α , measured in a plane parallel to the ecliptic plane (for Jupiter missions, approximately the orbital plane), and along a vector orthogonal to the velocity correction vector, Δv . If \underline{i} , \underline{j} , \underline{k} form the unit triad in the ecliptic system, then for small angles, α , the velocity error caused by the in-plane pointing error is given by

$$\delta \Delta v_{\alpha} = c \Delta v \alpha \left[\Delta v_y \underline{i} - \Delta v_x \underline{j} \right]$$

where $\Delta v = \Delta v_x \underline{i} + \Delta v_y \underline{j} + \Delta v_z \underline{k}$ and $c = (\Delta v_x^2 + \Delta v_y^2)^{-1/2}$. The second pointing error, called the out-of-plane error defines the velocity error that is orthogonal to both $\delta \Delta v_{\alpha}$ and the velocity increment vector, Δv . Again, for small angles, β , the velocity error resulting from this pointing error, referenced to the ecliptic system, is given by

$$\delta \Delta v_{\beta} = \beta c \left[\Delta v_x \Delta v_z \underline{i} + \Delta v_y \Delta v_z \underline{j} - \frac{1}{c^2} \underline{k} \right]$$

Then the total execution error resulting from a proportionality error, k , resolution error, s , and pointing errors, α and β , is given by the sum of these errors

$$\delta \Delta v = \delta \Delta v_k + \delta \Delta v_s + \delta \Delta v_{\alpha} + \delta \Delta v_{\beta}$$

The mathematical model used to describe velocity increment errors is the same for either spacecraft or probe. The individual magnitudes of the execution error sources, k , s , α , and β , may be varied, however, for individual characteristics of the probe or spacecraft. In general, the Pioneer pointing accuracy is 5% of the angle rotated off Earth lock, the TOPS error is considered to be 1 degree (3σ).

The probe release and/or orientation error is essentially involved with simply aligning the probe axis for its zero degree relative angle of attack at entry. This corresponds to the maneuver by which the probe is released from the spacecraft in the Mode 3/Deflect Spacecraft sequence or to the probe self-reorientation maneuver in the Mode 1/Deflect Probe scheme. The current mathematical model for this type of maneuver is based on a single pointing error referenced to the desired direction.

Let \underline{u}_D denote the desired direction for the probe axis. Define

$$\underline{v}_1 = \frac{\underline{r} \times \underline{u}_A}{|\underline{r} \times \underline{u}_A|}$$

$$\underline{v}_2 = \underline{u}_A \times \underline{v}_1$$

Then \underline{v}_1 and \underline{v}_2 are unit vectors in the plane normal to the desired direction \underline{u}_A . An arbitrary unit vector in that plane may then be written.

$$\underline{x} = \underline{v}_1 \cos \theta + \underline{v}_2 \sin \theta$$

where θ is a random variable chosen from a uniform distribution over the interval $(0, 2\pi)$. If the orientation pointing error is to be of magnitude δ , then the actual pointing direction resulting from the error is given by

$$\underline{u}_A = \underline{u}_D \cos \delta + \underline{x} \sin \delta$$

B. ANALYTICAL TECHNIQUE

A Monte Carlo technique is used to convert the errors associated with the deflection maneuver into dispersions in the critical mission parameters. The Monte Carlo procedure will be defined in detail for the Mode 1/Deflect Probe deflection scheme. The modifications for the Mode 2/Shared Deflection and Mode 3/Deflect Spacecraft schemes are then easily explained.

The Monte Carlo technique used in this study consists of generating a large number of sample probe and spacecraft trajectories consistent with assumed statistics of the knowledge and control uncertainties and execution errors. These trajectories are then propagated to certain mission time points (probe acquisition by spacecraft, entry, and selected intermediate points), and the critical mission parameters are evaluated. Because each sample spacecraft and probe trajectory will differ from the nominal (errorless) ones, the critical parameters will also differ. The data in dispersions in critical mission parameters are then analyzed by empirical formulas, assuming normal distributions

to establish mean and three sigma deviations in each critical parameter for each selected time point. The computational flow, outlined in Figure I-2, may be broken up into three main components that are discussed in detail.

1. Preliminary Computations

The preliminary computations generally comprise the determination of the nominal trajectories and preparation for the selection of the perturbed trajectories. The nominal deflection maneuver is first computed, which for the given hyperbolic excess velocity (equivalently the given launch date/arrival date) and desired deflection radius satisfies the desired entry conditions and communication geometry. The knowledge and control covariances, P_k and P_c , are then computed from an orbit determination program in which the procedure described in section A is used. Finally, the execution error uncertainties, σ_k , σ_s , σ_α , σ_β , σ_δ , are selected on the basis of the spacecraft used, the nominal geometry involved (such as the rotation off Earth lock required to implement the maneuver), and the magnitude of errors requiring analysis.

2. The Sampling Procedure

The bulk of the dispersion analysis is concerned with the generation of the statistically consistent ensemble of spacecraft-probe trajectory samples. For each sample, the first problem (listed in Figure I-2) is to generate reasonable deviation vectors, δX_k and δX_c , from the knowledge and control covariances, P_k and P_c . This sampling is done as follows.

Let P represent P_k or P_c . Then, since P is positive definite, it may be diagonalized.

$$P = T^T D T$$

where $D = \text{diag} (d_1^2, d_2^2, \dots, d_6^2)$, T is the orthonormal matrix of the eigenvectors of P , and the superscript T denotes the matrix transpose operation. The elements of D are written as squares to indicate they are necessarily positive numbers.

I. PRELIMINARY COMPUTATIONS

- A. Read in nominal spacecraft deflection state X_{nom} , desired entry angle, γ , and lead angle, λ , knowledge and control covariance matrices, P_k and P_c , execution error model uncertainties, σ_k , σ_s , σ_α , σ_β , σ_δ .
- B. Compute nominal deflection maneuver and parameters

II. SAMPLING PROCEDURE

Generate large number ($N \geq 100$) of sample off-nominal cases.
For each case --

- A. Sample knowledge and control covariances to obtain the deviation vectors, δX_k and δX_c .
- B. Form the actual and estimated spacecraft states

$$X_{act} = X_{nom} + \delta X_c$$

$$X_{est} = X_{act} + \delta X_k$$

- C. Compute the commanded velocity increment, Δv_c , based on the estimated state, X_{est} , and the desired γ and λ .
- D. Sample the execution errors, generate the resulting error in velocity increment, Δv . Compute the post-deflection probe state as

$$Y_{act} = X_{act} + \begin{bmatrix} 0 \\ -\Delta v_c \\ -\delta \Delta v \end{bmatrix}$$

$$Y_{est} = Y_{act} + \delta X_k + u$$

- E. Compute the desired orientation of the probe at entry, \underline{u}_α , using Y_{est} . Generate a sample orientation error and compute the corresponding actual probe orientation, \underline{u}_A .
- F. Propagate the actual probe and spacecraft to probe entry using conic formula. Store the dispersions in critical mission parameters at each timepoint.

III. STATISTICAL ANALYSIS OF DISPERSION DATA

Using the dispersion data generated for each sample case, compute the mean and standard deviation for each critical mission parameter for each selected timepoint.

Figure I-2 Computational Flow Chart of Monte Carlo Analysis Program

T defines a transformation from the original Cartesian coordinate system to a new system in which the covariance matrix is uncorrelated, thereby allowing the individual components to be sampled independently. A vector random variable from a distribution of mean zero and covariance, D, is given by

$$Z = (e_1 d_1, e_2 d_2, \dots, e_6 d_6)^T$$

where each e_i is a scalar random variable sampled from a normal distribution of mean zero and standard deviation unity. The e_i are computed from the formula

$$e_i = \sqrt{-2 \ln \alpha_i} \cos (2\pi \beta_i)$$

where α_i and β_i are random numbers generated from a uniform distribution over the interval (0, 1). The correlated deviation vector in the original Cartesian coordinate system may now be computed using the transformation matrix, T, as

$$\delta X = T \delta Z$$

Therefore, for each sample case, the knowledge and control covariances may be sampled as above to produce knowledge and control state deviation vectors, δX_k and δX_c . The "actual" spacecraft state for the sample is given by

$$X_{act} = X_{nom} + \delta X_c.$$

The "estimated" state of the spacecraft at deflection is given by

$$X_{est} = X_{act} + \delta X_k.$$

Furthermore, at the end of a large number of samples ($N \geq 100$), the ensemble of deviations, δX_c and δX_k , should obey the empirical formulas

$$E \left(\delta X_c \delta X_c^T \right) \rightarrow P_c \text{ as } N \rightarrow \infty$$

$$E \left(\delta X_k \delta X_k^T \right) \rightarrow P_k \text{ as } N \rightarrow \infty.$$

These approximations are checked at the end of the sampling process to ensure that a statistically consistent set of data has been generated.

Having obtained the estimated state of the spacecraft for a sample, the next task is to determine the commanded velocity increment, Δv_c , to be added to the probe at deflection. The vector, Δv_c , is computed as a function of the estimated spacecraft state at deflection, the desired probe flight path angle at entry, γ_c , and the desired lead angle, λ_c . The lead angle is the angle between the radius vector to the probe at entry and the radius vector to the spacecraft at the time of entry. The lead angle is negative when the probe leads the spacecraft. The deflection velocity is determined by iterating on the value of $\Delta\theta$, the true anomaly increment of the probe in going from deflection to entry. The true anomaly of the probe at entry, f_{PE} , can be expressed as:

$$f_{PE} = f(\gamma_c, R_{EJ}, \Delta\theta, R_A)$$

where R_{EJ} is the radius of the bus at deflection and R_A is the radius of the atmosphere. f_{PE} , R_{EJ} , $\Delta\theta$, R_A are used to compute the time of flight, T , from deflection to probe entry using the universal form of Kepler's equation as presented in Reference 1. The spacecraft state is then propagated forward for time T , again using the universal form of Kepler's equation, and the angle, λ , is computed from the state of the spacecraft and the state of the probe at time T . The angle, λ , is compared with the desired λ_c and the $\Delta\theta$ which causes λ to be within 0.01 degrees of λ_c , is found. Since the orbital elements of the probe are known, the required deflection velocity vector may be calculated. The commanded deflection velocity is in the spacecraft plane of motion.

The deviations in the implemented deflection velocity from the commanded are generated using the model described in subsection A2. This model assumes the implementation error is given by three sources: proportionality error, K ; resolution error, S ; and pointing angle errors, α , β . These errors are assumed uncorrelated and normally distributed. The standard deviation of each error σ_K , σ_S , σ_α , σ_β is input to the program. The error used in each Monte Carlo sample is generated by

$$K, S, \alpha, \beta = e_1 \sigma_K, e_2 \sigma_S, e_3 \sigma_\alpha, e_4 \sigma_\beta$$

where each e_i is a scalar random variable sampled from a normal distribution of mean zero and standard deviation unity. The execution error, $\delta\Delta v$, is then the sum of these errors.

The actual state of the probe at deflection is then the actual position vector of the probe and the sum of velocity of the spacecraft and the actual deflection, Δv , given to the probe.

$$Y_{act} = X_{act} + \begin{bmatrix} 0 \\ -\Delta v_c + \delta\Delta v \end{bmatrix}$$

Now that the actual states of the probe and spacecraft are known, the time histories of these two point masses may be computed using conic models.

The attitude of the probe is a crucial parameter, however, as this determines such mission critical parameters as angle of attack at entry and probe aspect angle. Using the nominal trajectory, the desired probe attitude is computed, \underline{u}_q . A pointing error caused by imperfections in the attitude control system is computed in a similar statistical fashion as described above. Once the "actual" probe axis is computed, it is assumed to hold that orientation throughout the mission. No errors are added to the spacecraft axis since it is assumed that the spacecraft can hold the Earth lock with essentially no error.

For each sample probe and space trajectory and probe attitude, the critical entry and communication parameters may be computed as functions of time. The resulting collection of data must then be analyzed by the techniques described in the next subsection.

3. Statistical Analysis of Dispersion Data

The empirical computation of the standard deviations of scalar parameters such as entry angle, lead angle, or lead time may be computed in the following way. Let α_i be the value of any such parameter for the i^{th} case. Suppose that there are N samples to be analyzed. Then the mean and standard deviation of the distribution of α are given by

$$\bar{\alpha} = \frac{1}{N} \sum_{i=1}^N \alpha_i$$

$$\sigma_{\alpha}^2 = \left[\sum_{i=1}^N \frac{\alpha_i^2}{N} \right] - \frac{\bar{\alpha}^2}{N}$$

These formulas must be extended for vector quantities. The probe entry site dispersions are given in terms of the two vectors of latitude and longitude (LAT, LON). The spacecraft-probe look direction is conveniently described in terms of the two vectors of cone angle and clock angle (CA, CLA) referenced to Earth and Canopus. Equivalently, these dispersions may be defined in terms of cone angle and cross-cone angle (CA, CCA).

Let Z_i represent the vector describing the actual values achieved for a vector quantity on the i^{th} sample. Then, the vector of mean values and the covariance matrix describing uncertainties and correlations of the vector are given by the formulas

$$\bar{Z} = \frac{1}{N} \sum_{i=1}^N Z_i$$

$$\begin{aligned} P_Z &= E(ZZ^T) - E(Z)E(Z)^T \\ &= \frac{1}{N} \left[\sum_{i=1}^N ZZ^T \right] - \frac{\bar{Z} \bar{Z}^T}{N} \end{aligned}$$

These formulas are used to compute the covariance matrices of the critical mission vector quantities as well as to reconstruct the original knowledge and control covariances from the deviation vectors generated.

For the entry site dispersions (LON, LAT) and the spacecraft-probe look directions (CA, CLA) or (CA, CCA), the 2×2 covariances are further analyzed. Let any such covariance matrix be denoted P . Then since P is positive definite it may be diagonalized to produce

$$P = TDT^T = T \begin{bmatrix} \lambda_A & 0 \\ 0 & \lambda_B \end{bmatrix} T^T$$

Where λ_A and λ_B are the (positive) eigenvalues of the covariance matrix P , and T is the orthonormal matrix of the eigenvectors of P . Let

$$T = \begin{bmatrix} t_A \\ -\frac{t_A}{t_B} \end{bmatrix}$$

Then t_A is the unit eigenvector associated with the eigenvalue, λ_A . Then the angle between the vector, t_A , and the u_x unit vector (longitude direction for (LON, LAT), cone angle direction for (CA, CLA) or (CA, CCA) is defined by

$$\theta = \cos^{-1} (t_A \cdot u_x) \quad 0 \leq \theta \leq \pi$$

The uncertainty ellipse may now be easily constructed: λ_A represents one semiaxis; λ_B the other.

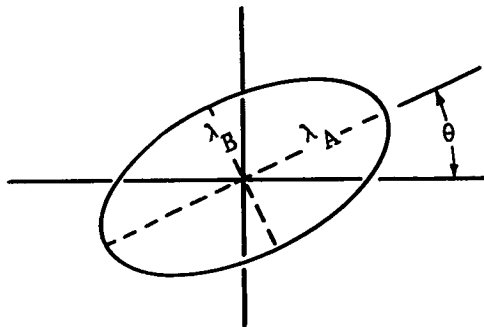


Figure I-3 Two-Dimensional Uncertainty Ellipse

4. Procedures for Alternative Deflection Modes

The procedure for Mode 1/Deflect Probe has been described in detail. A comparison of the procedures for the Mode 2/Shared Deflection and Mode 3/Deflect Spacecraft is provided in Figure IV-3 of Volume II of this report.

For each sample in each mode, the initial task is to determine the control and knowledge deviations, δX_c and δX_k , by sampling the control and knowledge covariances. The actual state of the spacecraft is then defined by $X_{act} = X_{nom} + \delta X_c$; the estimated state of the spacecraft is $X_{est} = X_{act} + \delta X_k$, where X_{nom} is the nominal spacecraft deflection state.

In Mode 1/Deflect Probe the estimated state, X_{est} , is used to determine the commanded probe deflection, Δv . This velocity increment is then degraded by an execution error, $\delta \Delta v$, determined by sampling from possible execution errors. The probe axis orientation throughout the mission is computed as the nominal orientation corrupted by an orientation pointing error, δ . The deflection states for the probe and spacecraft are then propagated to a series of time points at which the sample deviations are recorded. These dispersions are then analyzed to yield mean and standard deviation values.

In the study of the Mode 1/Deflect Probe deflection scheme, it was discovered that the knowledge and control uncertainties did not significantly affect the critical mission parameters. Therefore, to simplify the Mode 2/Shared Deflection analysis, it was assumed that the knowledge and control uncertainties were zero so that the spacecraft correction, Δv , could be precomputed and simply read in. At probe deflection, the probe is commanded to be aligned in the direction of both the Δv and zero angle of attack orientation. Because of the in-plane and out-of-plane pointing errors, the correct direction is not achieved. The incorrect orientation is then used for both the Δv addition and the probe longitudinal axis. Following the probe deflection, the spacecraft correction is implemented with the execution error model described in subsection A2. The resulting sample deviations are then collected and analyzed to determine the mean and standard deviations.

For Mode 3/Deflect Spacecraft deflection analysis, the knowledge and control uncertainties are again considered. The probe is oriented at release using the input orientation pointing error, δ , and keeps that attitude throughout the mission. The estimated state of the spacecraft, X_{est} , is used to compute the deflection,

Δv . Spacecraft execution errors are then sampled to determine the error, $\delta \Delta v$. The erroneous velocity increment is then added to the spacecraft and the spacecraft is then propagated to the selected time points. The critical mission parameter deviations are then recorded and analyzed to determine the important statistical data.

C. REFERENCE

1. R. H. Batten: *Astronautical Guidance*, McGraw-Hill Book Company, New York, N.Y., 1964

APPENDIX J

MULTILAYER INSULATION CONDUCTIVITY EVALUATION

C. Webb

June 15, 1972

To evaluate insulation performance accurately, two applicable data sources on multilayer insulation were obtained. The first source represented laboratory guarded hot plate test data (Ref 1), the second source represented thermal conductivity test data from an actual hardware mockup where fiberglass standoffs penetrated the insulation blanket and seams and joints were present (Ref 2). Figure J-1 presents a comparison between these two sets of data. In addition, an analytical curve fit is shown for each set where the expression representing the thermal conductivity considered both the linear conduction and the radiation associated with multilayer insulation. The expression, therefore, includes the influence of the mean insulation temperature and, in addition, the nonlinear influence of the actual boundary temperatures. The expression used for the multilayer insulation follows:

$$k = aT_M + b(T_H^2 + T_C^2)(T_H + T_C) \quad [J-1]$$

where,

k = effective thermal conductivity

a & b = influence coefficients

T_M = insulation mean temperature

T_H = hot boundary temperature

T_C = cold boundary temperature

and

$$Q_{leak} = \frac{kA}{t} (T_H - T_C) \quad [J-2]$$

where

Q_{leak} = Blanket heat leak

A = insulation surface area

t = insulation thickness.

The importance of this expression is that it more precisely determines the thermal conductivity as a function of boundary temperature and thus insulation thickness variations.

For outer planet entry probe system thermal analyses, the Skylab conductivity data was selected to determine the baseline influence coefficients of Equation [J-1] and thus the multilayer insulation performance.

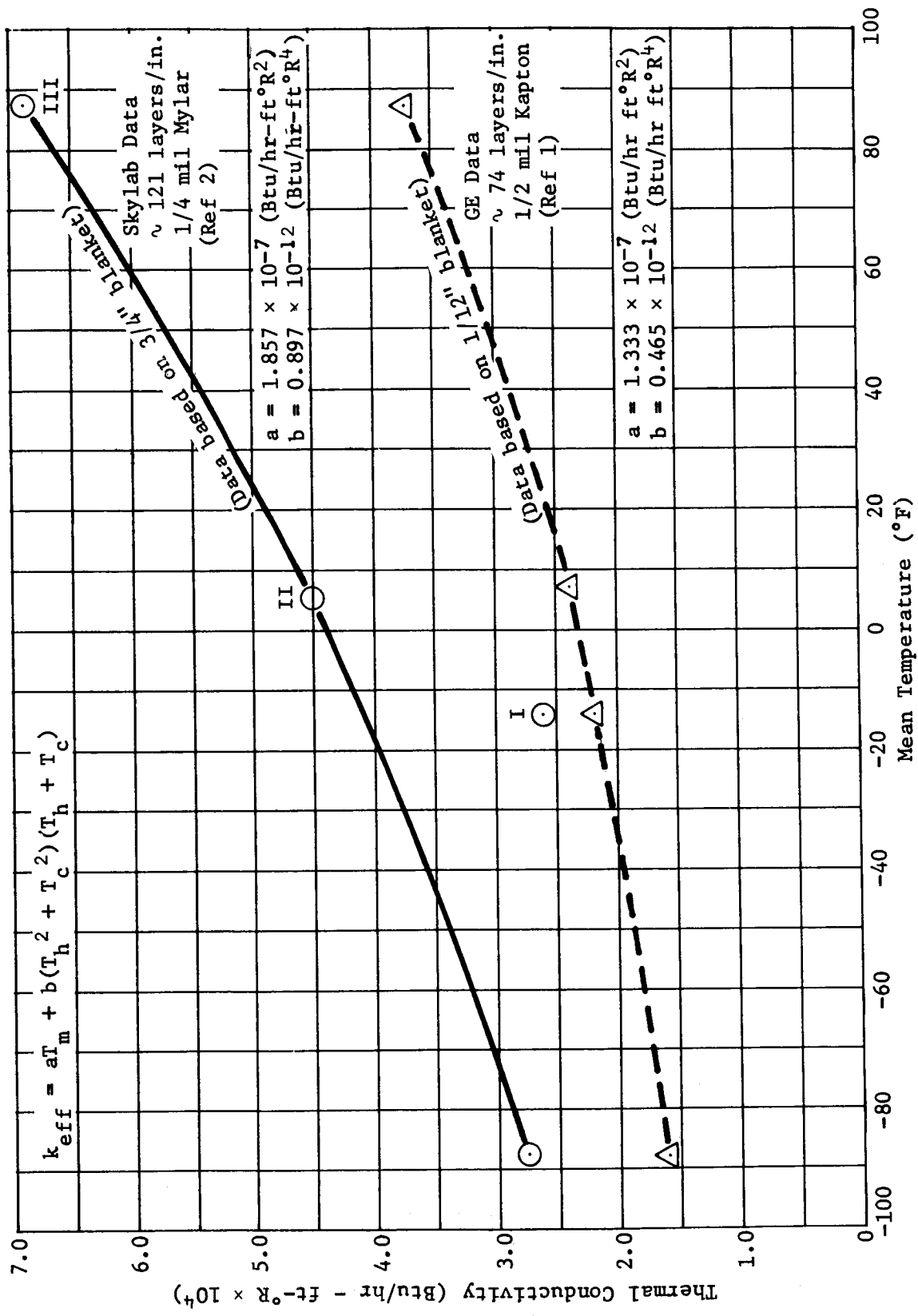


Figure J-1 Multilayer Insulation Thermal Conductivity

REFERENCES:

1. E. Fried and G. Karp, et al.: - *Measurement of Thermal Conductance of Multilayer and Other Insulation Materials*. Final Report Contract NAS9-3685, General Electric Co., Valley Forge Space Technology Center, Philadelphia, Pa, 29 September 1967.
2. D.K. Ong: - *Technical Summary Report MDA Thermal Component Wall Test*, Skylab Program Payload Integration Contract NAS8-24000, Martin Marietta Corporation, Denver, Colo.

APPENDIX K

NH_3 AND H_2O CLOUD MODELS FOR THE OUTER PLANETS

W. S. Cook

May 1, 1972

Report No. D-72-48740-005

NH₃ - H₂O CLOUD MODELS

FOR

THE OUTER PLANETS

Report Date: May 1972

Note: This Report is issued under
Task Authorization 48740

Distribution:

Author

W. F. Butler

A. R. Barger

R. R. Falce

P. C. Carney

K. W. Ledbetter

M. W. Kuethe

J. W. Hungate

R. S. Wiltshire

R. J. Richardson

J. H. Romig

E. G. Howard

R. L. Hulstrom

L. G. Wolfert

J. E. Vandrey

H. D. Greyber

Technical Library

Dept. File

Task Audit Center File

Author

W. S. Cook

W. S. Cook

Cognizant Engineer

A. R. Barger

A. R. Barger

Section Head

Gentry Lee

Gentry Lee

Department Head

& Technology

Panel Chairman

R. J. Farrell

R. J. Farrell

Program Manager IRAD

L. R. Soderberg

L. R. Soderberg

FOREWORD

This report was prepared by the Denver Division of the
Martin Marietta Corporation, Systems Analysis Department.
The Task Authorization was 48740.

ABSTRACT

Ammonia and water cloud structures are calculated for the outer planets. This report presents the theory, the computational procedures, and the results. The results are based on the atmospheric models provided in References 3, 4, and 5.

TABLE OF CONTENTS

	Page
FOREWORD.	i
ABSTRACT.	ii
TABLE OF CONTENTS	iii
I. INTRODUCTION.	1
II. THEORY.	2
III. COMPUTATIONAL PROCEDURES.	8
IV. RESULTS	13
V. REFERENCES.	24

I. INTRODUCTION

Radio attenuation in the atmospheres of the outer planets is dependent upon cloud structures. John Lewis (Ref. 1) has published the theory necessary for predicting ammonia-water clouds; and with the help of the empirical formulas provided by C. Haundenschild (Ref. 2) the cloud structures for the outer planets were predicted.

II. THEORY

From the first law of thermodynamics, conservation of energy for a molar parcel of atmosphere undergoing an adiabatic expansion, gives

$$\bar{C}_v dT + Pdv + \sum_i \lambda_i dX_i = 0 \quad \text{Eq. 1}$$

where \bar{C}_v is the mean molar specific heat at constant volume, dT is a differential change in the absolute temperature, P is the total pressure, dv is the differential change in the molar volume, λ_i is the molar heat of condensation of the i^{th} gas component, and dX_i is the differential change in the number of moles of condensible gas present in the atmosphere. The equation of state of the bulk gas is

$$Pv = RT \quad \text{Eq. 2}$$

where R is the universal gas constant thus

$$Pdv = RdT - vdp \quad \text{Eq. 3}$$

substituting Eq. 3 into Eq. 1

$$\bar{C}_p dT - vdp + \sum_i \lambda_i dX_i = 0 \quad \text{Eq. 4}$$

where $\bar{C}_p = \bar{C}_v + R$.

The variation of the vapor pressure of any condensate j with temperature is given by the Clausius-Clapeyron equation for evaporation or sublimation

$$dp_j = \frac{\lambda_j P_j}{RT^2} dT \quad \text{Eq. 5}$$

The equation of state for the j^{th} the component of the condensable gas is

$$P_j V = X_j RT \quad \text{Eq. 6}$$

Equation 5 is for the case where the molar volume of the solid or liquid is neglected with respect to the molar volume of a gas; therefore, from equation 5 and 6 holding the molar volume constant

$$dp_j = \frac{\lambda_j P_j}{RT^2} dT = \frac{X_j R dT}{V} + \frac{RT}{V} dX_j \quad \text{Eq. 7}$$

and solving for dX_j

$$dX_j = X_j \left(\frac{\lambda_j}{RT^2} - \frac{1}{T} \right) dT \quad \text{Eq. 8}$$

The equation for hydrostatic equilibrium is

$$\boxed{dp = - \frac{\bar{\mu} G}{RT} dz} \quad \text{Eq. 9}$$

where $\bar{\mu}$ is the molecular weight, G is the gravitational acceleration, and dz is a vertical height increment.

Substituting Eq's 8 and 9 into Eq. 4 for the case in which only a single condensate is condensing

$$\bar{C}_p dT + \bar{\mu} G dz + \left[\lambda_j X_j \left(\frac{\lambda_j}{RT^2} - \frac{1}{T} \right) \right] dT = 0 \quad \text{Eq. 10}$$

thus the wet adiabatic temperature lapse rate is

$$\frac{\partial T}{\partial z} = - \frac{\bar{\mu} G}{\bar{C}_p + \lambda_j X_j \left[\frac{\lambda_j}{RT^2} - \frac{1}{T} \right]} \quad \text{Eq. 11}$$

We now need to modify Eq. 11 for a system of two condensates, water and ammonia. Let us imagine an isothermal process in which dX_B moles of solution with constant molar ammonia concentration are evaporated. Then

$$dX_A = C dX_B \quad \text{Eq. 12}$$

where dX_A is the change in the number of moles of ammonia in solution, and C is the molar concentration of ammonia present in solution, then

$$dX_W = (1 - C) dX_B \quad \text{Eq. 13}$$

where dX_W is the change in the number of moles of water in solution. Using Eq. 6 for the isothermal case

$$dP_W = RT dX_W = (1 - C) dP_B \quad \text{Eq. 14}$$

From equation 5 considering only the condensation of H₂O

$$dP_W = P_W \frac{\lambda_W}{RT^2} dT \quad \text{Eq. 15}$$

Since actually we are evaporating water plus ammonia, the latent heat for the bulk solution should be employed;

$$\lambda_B = C\lambda_A + (1 - C) \lambda_W \quad \text{Eq. 16}$$

and equation 15 can be rewritten for the bulk solution

$$dP_B = \frac{P_W}{(1-C)} \frac{\lambda_B}{RT^2} dT \quad \text{Eq. 17}$$

From Eq. 6 we proceed as in Eq. 7

$$\frac{P_W}{(1-C)} \frac{\lambda_B}{RT^2} dT = \frac{X_B R dT}{V} + \frac{RT}{V} dX_B \quad \text{Eq. 18}$$

thus

$$dX_B = X_W \left(\frac{\lambda_B}{(1-C) RT^2} - \frac{X_B}{X_W T} \right) dT \quad \text{Eq. 19}$$

We then combine Eq.'s 9 and 19 to get

$$\bar{C}_P dT + \bar{\mu} G dz + \lambda_B X_W \left[\frac{\lambda_B}{(1-C) RT^2} - \frac{X_B}{X_W T} \right] dT = 0 \quad \text{Eq. 20}$$

The wet adiabatic lapse rate for an ammonia-water systems

$$\frac{\partial T}{\partial Z} = \frac{-\bar{\mu} G}{\bar{C}_P + \lambda_B X_W \left[\frac{\lambda_B}{(1-C) RT^2} - \frac{X_B}{X_W T} \right]} \quad \text{Eq. 21}$$

Equation 21 was derived under the assumption that water was the prime condensate and some ammonia was condensing out at the same time. For the region of Jupiter's atmosphere where ammonia clouds are forming then ammonia is the prime condensate. Equation 11 must then be modified in a similar way as was done when water was the prime condensate; the resulting lapse rate is

$$\frac{\partial T}{\partial Z} = \frac{-\bar{\mu} G}{\bar{C}_P + \lambda_B X_A \left[\frac{\lambda_B}{C RT^2} - \frac{X_B}{X_A T} \right]} \quad \text{Eq. 22}$$

C. Haudenschild (Ref. 2) has formulated empirical analytic equations for predicting the partial pressures of ammonia and water for the various phases. These equations are presented in Table I and the phase boundaries are graphically presented in Figure 1.

TABLE I. ANALYTIC EXPRESSIONS FOR THE $\text{HN}_3 - \text{H}_2\text{O}$ SYSTEM

<u>SYMBOL</u>	<u>UNITS</u>	<u>DEFINITION</u>	<u>SYMBOL</u>	<u>UNITS</u>	<u>DEFINITION</u>
T	K°	Temperature	P ₂	Torr	H ₂ O partial vapor pressure
C	0.0 < C < 1.0	Molar Concentration of NH ₃ in solution.	P ₃	Torr	NH ₃ partial vapor pressure
			log		logarithm base 10

<u>Région</u>	<u>Equation</u>	
Solid H ₂ O	$\log P_2 = 10.447 - 267.01/T$	Eq. 1
Solid NH ₃	$\log P_3 = 10.312 - 1691.77/T$	Eq. 2
(NH ₃) ₂ H ₂ O	$2/3 \log P_3 + 1/3 \log P_2 = 9.777 - 2051.185/T$	Eq. 3
NH ₃ H ₂ O	$1/2 \log P_3 + 1/2 \log P_2 = 9.790 - 2219.28/T$	Eq. 4
	$\log P_2 = \log (1-C) + 9.488 - 1.743C^2 \left[\frac{2406.2 + 878.192C^2}{T} \right]$	Eq. 5
Solution	$\log P_3 = \log C + 9.906 + 1.743(C^2 - 2C) - \left[\frac{2149.65 + 878.192(C^2 - 2C)}{T} \right]$	Eq. 6

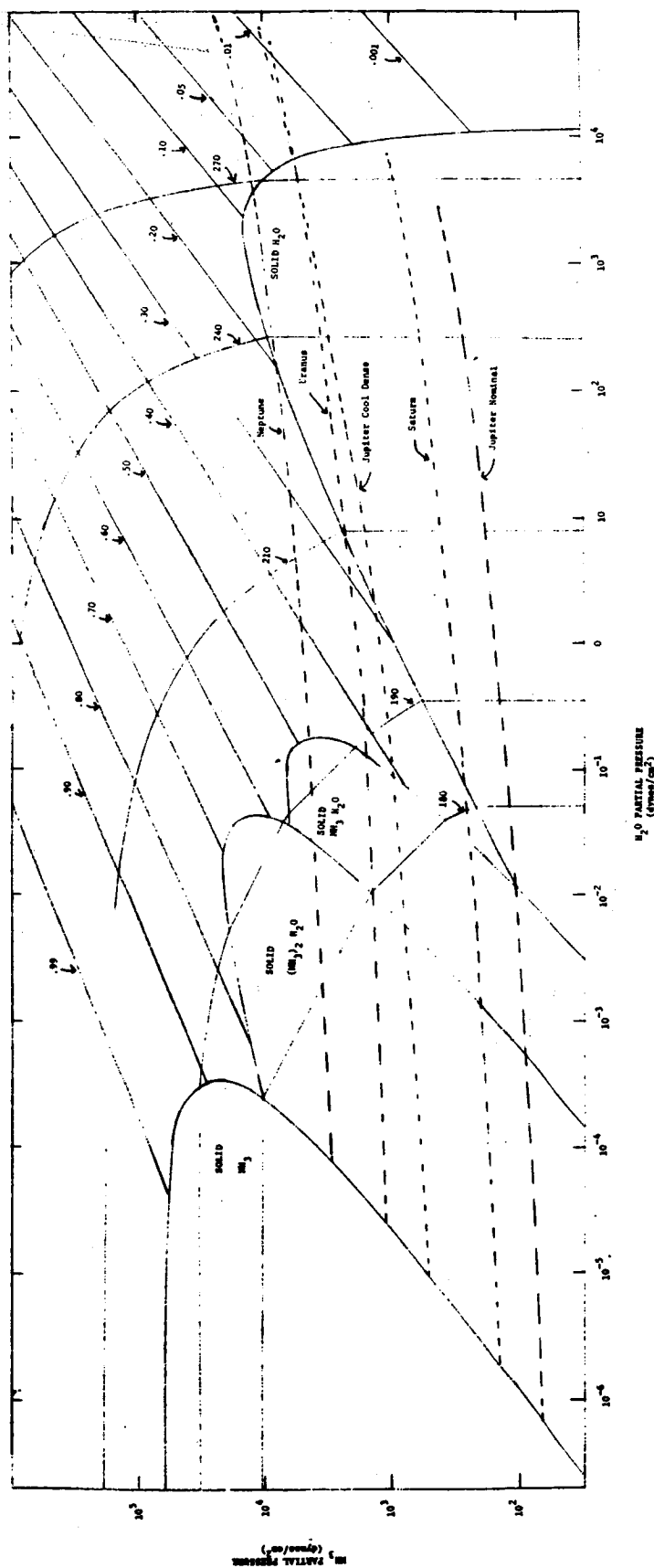


Figure 1. Phase diagram of the $\text{NH}_3 - \text{H}_2\text{O}$ system. The scalloped line running from far left to bottom right is the freezing point line of aqueous NH_3 solutions. The family of diagonal straight lines are lines of constant ammonia concentration in solution. The family of curves intersecting the constant concentration lines are curves of constant temperature. The dashed lines are cloud composition tracks for the different model atmospheres.

III. COMPUTATIONAL PROCEDURES

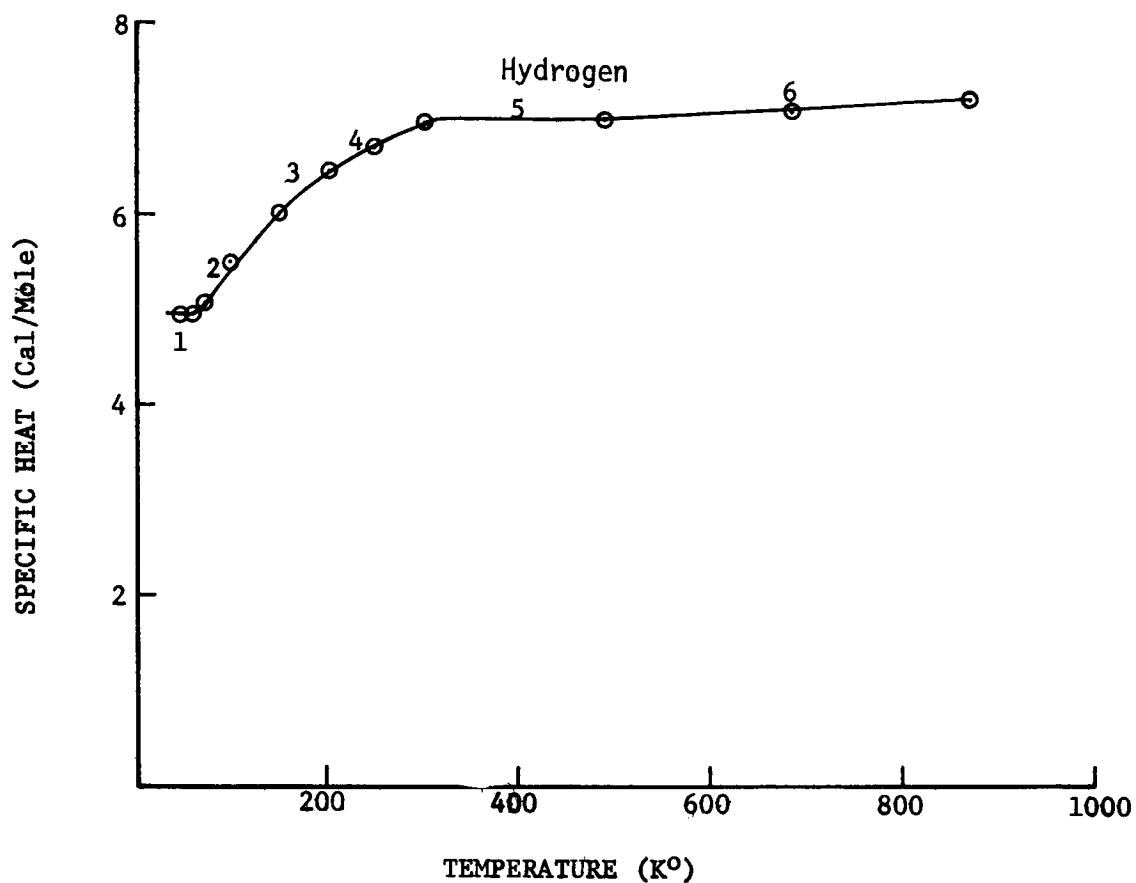
Given the formulas found in Table I and Eqs. 9, 21, and 22, along with the parameters presented in Table II and Figures 2 and 3, the cloud structures for the outer planets were determined. The computational procedure is as follows:

- 1) Specify a reference pressure and temperature deep within the troposphere, below the water-ammonia clouds. The reference pressures and temperatures were provided by NASA (Ref.'s 3, 4, and 5) and are included in Table II.
- 2) Beginning with the reference pressure and temperature, the temperature and pressure are calculated in one Km altitude increments in the positive altitude direction; and after each increment a check is made to see if condensation has occurred. At the base of the lowest-lying solution clouds, the vapor pressures of NH_3 and H_2O are in the same ratio to each other as the $\text{NH}_3/\text{H}_2\text{O}$ abundance ratio in the lower dry atmosphere. The ammonia concentration in solution at the cloud base can be determined from equations 5 and 6 in Table I. With the knowledge of the ammonia concentration P_2 is calculated and compared with the partial pressure of H_2O in the atmosphere. If the partial pressure of H_2O is greater than or equal to P_2 then condensation will occur. At the cloud base there is a possibility that the condensate freezes; therefore a check for freezing has to be made. Freezing occurs when $\bar{P}_2 < P_2$ where \bar{P}_2 is P_2 of Eq. 1 in Table I.
- 3) The incremental changes in the temperature and pressure are calculated in the following manner; where J corresponds to the previous altitude and I corresponds to the present altitude:
 - a) below the level of condensation

$$T_I = T_J - \frac{\mu G x 10^5}{C_{p_J}} \quad \text{Eq. 23}$$

TABLE II. PARAMETERS USED IN NASA'S MODEL ATMOSPHERES FOR JUPITER, SATURN, URANUS, AND NEPTUNE (Ref's 1, 3, 4)

PARAMETER	JUPITER 'COOL' MODEL	JUPITER NOMINAL MODEL	SATURN NOMINAL MODEL	URANUS NOMINAL MODEL	NEPTUNE NOMINAL MODEL
Composition (Molar fraction)	H ₂ 0.68454	0.86578	0.88572	0.88572	0.88572
	He 0.31057	0.13214	0.11213	0.11000	0.11000
	CH ₄ 0.00145	0.00062	0.00063	0.03000	0.03000
	NH ₃ 0.00035	0.00015	0.00015	0.00015	0.00015
	H ₂ O 0.00240	0.00102	0.00105	0.00100	0.00100
	Ne 0.00031	0.00013	0.00013	0.00013	0.00013
	Others 0.00038	0.00016	0.00019	0.00019	0.00019
$\bar{\mu}$ (grams/mole)	2.70	2.30	2.27	2.68	2.68
G (cm/sec ²)	2700	2500	1050	810	1100
Reference Temperature (K°)	405.3	398.169	292.173	351	378
Reference Pressure (ATM)	100.77	10.906	8.366	9.0	27.7
Reference Altitude (Km). Zero altitude is a one atmos- phere.	-133	-52	-156	-331	-282



REGION	EQUATION	DOMAIN
1.	$C_p = 4.96$	$T \leq 60$
2.	$C_p = .011T + 4.38$	$60 < T \leq 150$
3.	$C_p = 7.4 \times 10^{-3}T + 4.92$	$150 < T \leq 200$
4.	$C_p = 5.5 \times 10^{-3}T + 5.3$	$200 < T \leq 300$
5.	$C_p = 6.96$	$300 < T \leq 473$
6.	$C_p = 6.75 \times 10^{-4}T + 6.641$	$T > 473$

Figure 2. Specific Heat, for Hydrogen. The specific heat for He is 4.98 cal/mole and the specific heat for the Jupiter 'cool' atmosphere is 8.94 cal/mole.

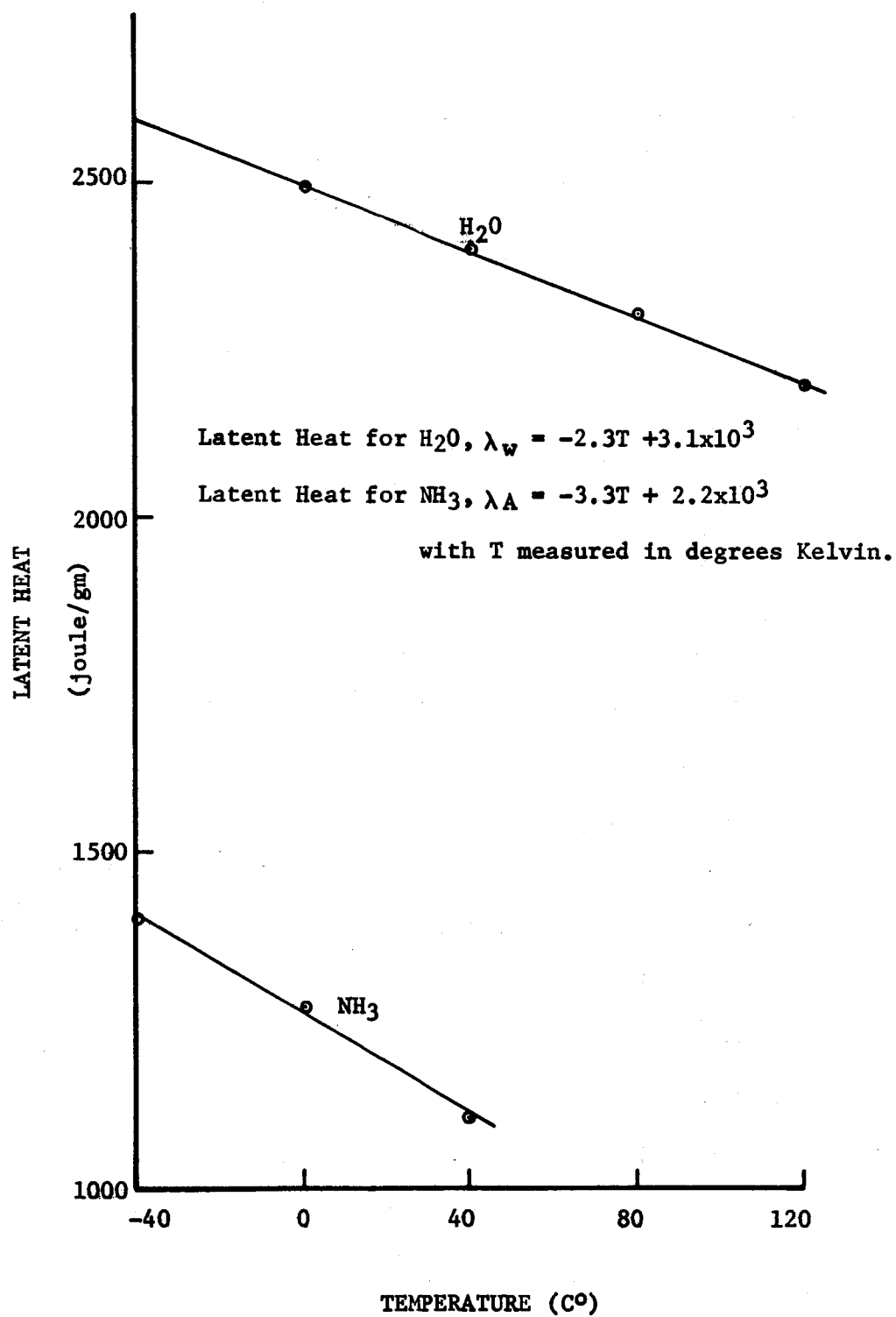


Figure 3. Latent Heat Release of Condensation for Water and Ammonia

cgs units are used and 10^5 is the altitude increment in centimeters.

$$P_I = P_J \text{ EXP } \left[\frac{-\mu G x 10^5}{RT} \right] \quad \text{Eq. 24}$$

where $\bar{T} = 1/2 (T_I + T_J)$

b) after condensation has occurred but below the ammonia clouds:

$$T_I = T_J - \frac{\mu G x 10^5}{C_{PJ} + \lambda_{BJ} \left[\frac{\lambda_{BJ} x_{WJ}}{(1-C_J) RT_J^2} - \frac{x_{BJ}}{T} \right]} \quad \text{Eq. 25}$$

where $x_B = x_W + x_A$

c) for the ammonia clouds

$$T_I = T_J - \frac{\mu G x 10^5}{C_{PJ} + \lambda_{BJ} \left[\frac{\lambda_{BJ} x_{AJ}}{C_J RT_J^2} + \frac{x_{BJ}}{T} \right]} \quad \text{Eq. 26}$$

4) Calculate ammonia concentration in solution.

a) for region where water is the prime condensate x_A is almost constant, thus

$$P_{AI} = x_{AJ} P_I \quad \text{Eq. 27}$$

where P_{AI} is the partial pressure of ammonia. Then the ammonia concentration is calculated with the use of Equation 6, Table I where $P_3 = P_{AI}$.

b) for the region where ammonia is the prime condensate x_W is almost constant, thus

$$P_{WI} = x_{WJ} P_I \quad \text{Eq. 28}$$

The ammonia concentration in solution is calculated with the use of Eq. 5 - Table I where $P_2 = P_{WI}$.

- 5) Calculate water and ammonia vapor pressures in solution and check for freezing. The vapor pressure of water is calculated from Eq. 5 - Table I. Now calculate the concentration of water in the atmosphere by $\chi_W = P_2/P$. Now, a better calculation of the vapor pressure of ammonia can be calculated with the use of Equation 19.

$$P_A = \chi_A P = P \left[\frac{\lambda_B \chi_W^C}{(1-C) K T^2} - \frac{\chi_B}{T} \right] \quad \text{Eq. 29}$$

Theoretically if the above partial pressures are greater than the partial pressures predicted by Eq's 1, 2, 3, or 4 in Table I, then the system is in one of the frozen states. As it turns out the equations in Table I do not give accurate enough predictions to predict the phases in the above manner; therefore, the phases were determined by checking to see if the coordinates defined by $\chi_W P$ and $\chi_A P$ are within the scalloped curves as illustrated in Figure 1. When the $H_2O - NH_3$ system is within one of the solid phases, χ_W and χ_A are determined by the appropriate equations in Table I.

- 6) The cloud density, D , was determined in the following manner:

$$D = \left[\frac{(\chi_{AJ} - \chi_{AI}) + (\chi_{WJ} - \chi_{WI})}{Gd} \right] \bar{P} \quad \text{Eq. 30}$$

where d is the altitude increment and $\bar{P} = 1/2(P_I + P_J)$.

IV. Results

Pertinent results specifying the cloud structures are presented in Tables III through VII. The altitude values found in the tables correspond with a particular cloud base which also coincides with the maximum cloud density. The prominent clouds are illustrated in Figures 4 through 8.

TABLE III. JUPITER NOMINAL CLOUD MODEL

Atmos. Comp.	Ref. Temp - 305 (°K)	Gravitational Accel - 2500 (cm/sec ²)
H ₂ - 86.58%		
He - 13.24%	Ref. Pres - 4.53 x 10 ⁶ (dynes/cm ²)	Molecular Weight - 2.3 (gm/mole)
CH ₄ - 0.06%	Ref. Alt - -52 (Km)	
NH ₃ - 0.01%		
H ₂ O - 0.10%		

ALT (1)	PRESSURE (dynes/cm ²)	TEMP (°K)	CLOUD DENSITY (gm/liter)	PHASE
-30	2.65x10 ⁶	260.4	1.2x10 ⁻³	Solid H ₂ O
12	6.90x10 ⁵	171.4	5.0x10 ⁻⁸	Solid (NH ₃) ₂ H ₂ O
17	5.61x10 ⁵	160.0	1.6x10 ⁻⁹	Solid (NH ₃) ₂ H ₂ O
24	4.09x10 ⁵	144.2	6.5x10 ⁻⁵	Solid NH ₃

(1) Zero altitude at one atmosphere.

TABLE IV. JUPITER 'COOL' CLOUD MODEL

Atmos. Comp.

H ₂ - 68.49%	Ref. Temp - 405 (°K)	Gravitational Accel - 2700 (cm/sec ²)
He - 31.10%	Ref. Pres - 1.02x10 ⁸ (dynes/cm ²)	Molecular Weight - 2.7 (gm/mole)
CH ₄ - 0.14%	Ref. Alt - -133 (Km)	Specific heat - 8.94 (cal/mole)

NH₃ - 0.03%H₂O - 0.24%

Alt (1) (Km)	PRESSURE (dynes/cm ²)	TEMP (°K)	CLOUD DENSITY (gm/liter)	PHASE
-83	2.99x10 ⁷	308.7	2.2x10 ⁻²	(0.8 - 2.7)% Solution (2)
-63	1.65x10 ⁷	272.6	3.1x10 ⁻³	Solid H ₂ O
-26	4.26x10 ⁶	201.6	4.9x10 ⁻⁶	(29.1 - 39.8)% Solution (2)
-16	2.72x10 ⁶	182.2	2.3x10 ⁻⁷	Solid (NH ₃)H ₂ O
-11	2.13x10 ⁶	172.5	1.2x10 ⁻⁸	Solid (NH ₃) ₂ H ₂ O
- 2	1.33x10 ⁶	155.3	3.1x 10 ⁻⁴	Solid NH ₃

(1) Zero altitude at one atmosphere.

(2) Percentage of ammonia in solution.

TABLE V. SATURN CLOUD MODEL

Atmos. Comp.	Ref. Temp - 292 °K	Gravitational Accel - 1050 (cm/sec ²)
H ₂ - 88.59%		
He - 11.23%	Ref. Pres - 8.48x10 ⁶ (dynes/cm ²)	Molecular Weight - 2.27 (gm/mole)
CH ₄ - 0.06%	Ref. Alt - -156 (Km)	
NH ₃ - 0.01%		
H ₂ O - 0.11%		

ALT (1) (Km)	PRESSURE (dynes/cm ²)	TEMP (K°)	CLOUD DENSITY (gm/liter)	PHASE
-134	6.79x10 ⁶	273.7	3.0x10 ⁻³	Solid H ₂ O
- 27	1.78x10 ⁶	181.5	2.5x10 ⁻⁷	(33.4 - 36.4)% Solution (2)
- 21	1.62 x10 ⁶	176.0	1.2x10 ⁻⁷	Solid (NH ₃) H ₂ O
- 10	1.35x10 ⁶	165.8	4.2x10 ⁻⁹	Solid (NH ₃) ₂ H ₂ O
7	9.95x10 ⁵	149.9	1.7x10 ⁻⁴	Solid NH ₃

(1) Zero altitude at one atmosphere.

(2) Percentage of ammonia in solution.

TABLE VI. URANUS CLOUD MODEL

Atmos. Comp.

H₂ - 85.87% Ref. Temp - 351 (K°) Gravitational Accel - 810 (cm/sec²)He - 11.02% Ref. Pres - 9.29×10^7 (dynes/cm²) Molecular Weight - 2.68 (gm/mole)CH₄ - 3.00% Ref. Alt - -331 (Km)NH₃ - 0.01H₂O - 0.10

Alt ⁽¹⁾ (Km)	PRESSURE (dynes/cm ²)	TEMP (K°)	CLOUD DENSITY (gm/liter)	PHASE
-274	5.93×10^7	306.1	2.8×10^{-2}	(0.9 - 2.9) % Solution ⁽²⁾
-231	4.04×10^7	273.5	4.5×10^{-3}	Solid H ₂ O
-154	1.78×10^7	210.8	2.1×10^{-5}	(26.8 - 42.3) % Solution ⁽²⁾
-127	1.25×10^7	188.0	6.6×10^{-7}	Solid (NH ₃) H ₂ O
-115	1.06×10^7	177.6	4.3×10^{-8}	Solid (NH ₃) ₂ H ₂ O
- 98	8.17×10^6	162.9	1.4×10^{-3}	Solid NH ₃

(1) Zero altitude at one atmosphere.

(2) Percentage of ammonia in solution.

TABLE VII. NEPTUNE CLOUD MODEL

Atmos. Comp.		Ref. Temp. - 378 (K°)		Gravitational Accel - 1100 (cm/sec ²)	
H ₂ - 85.87%					
He - 11.02%					
CH ₄ - 3.00%					
NH ₃ - 0.01%					
H ₂ O - 0.10%					
		Ref. Press - 2.87x10 ⁸ (dynes/cm ²)		Molecular Weight - 2.68 (gm/mole)	
		Ref. Alt - -282 (Km)			
Alt (1) (Km)	PRESSURE (dynes/cm ²)	TEMP (K°)	CLOUD DENSITY (gm/liter)	PHASE	
-233	1.77x10 ⁸	326.0	7.4x10 ⁻²	(0.9 - 7.3)% Solution (2)	
-174	8.89x10 ⁷	265.3	2.5x10 ⁻³	Solid H ₂ O	
-146	5.91x10 ⁷	233.3	2.7x10 ⁻⁴	(20.7 - 47.6)% Solution (2)	
-109	3.21x10 ⁷	191.2	7.3x10 ⁻⁷	Solid (NH ₃) H ₂ O	
-103	2.87x10 ⁷	184.3	1.3x10 ⁻⁷	Solid (NH ₃) 2H ₂ O	
- 89	2.17x10 ⁷	167.9	3.1x10 ⁻³	Solid NH ₃	

(1) Zero altitude at one atmosphere.

(2) Percentage of ammonia in solution.

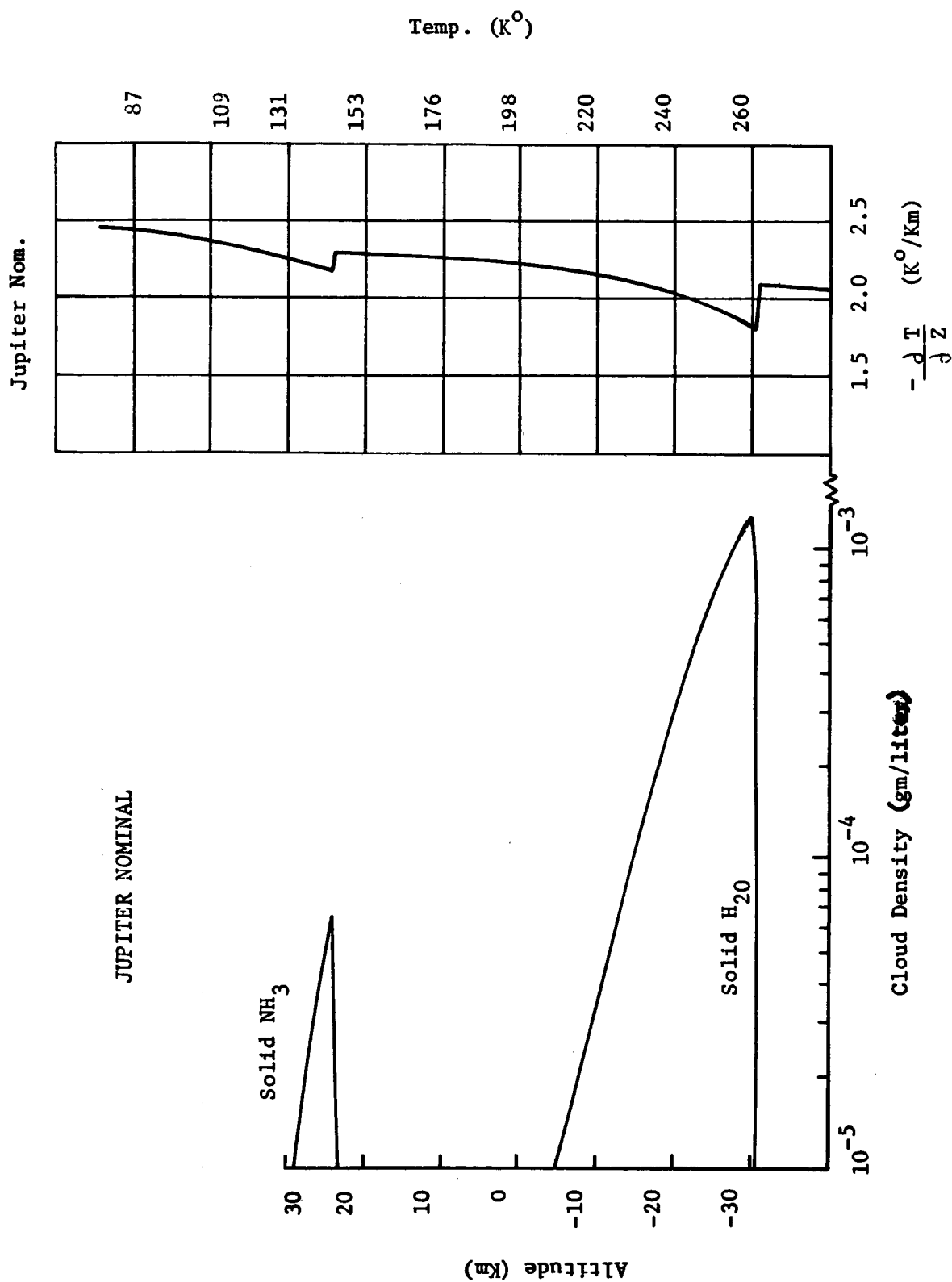
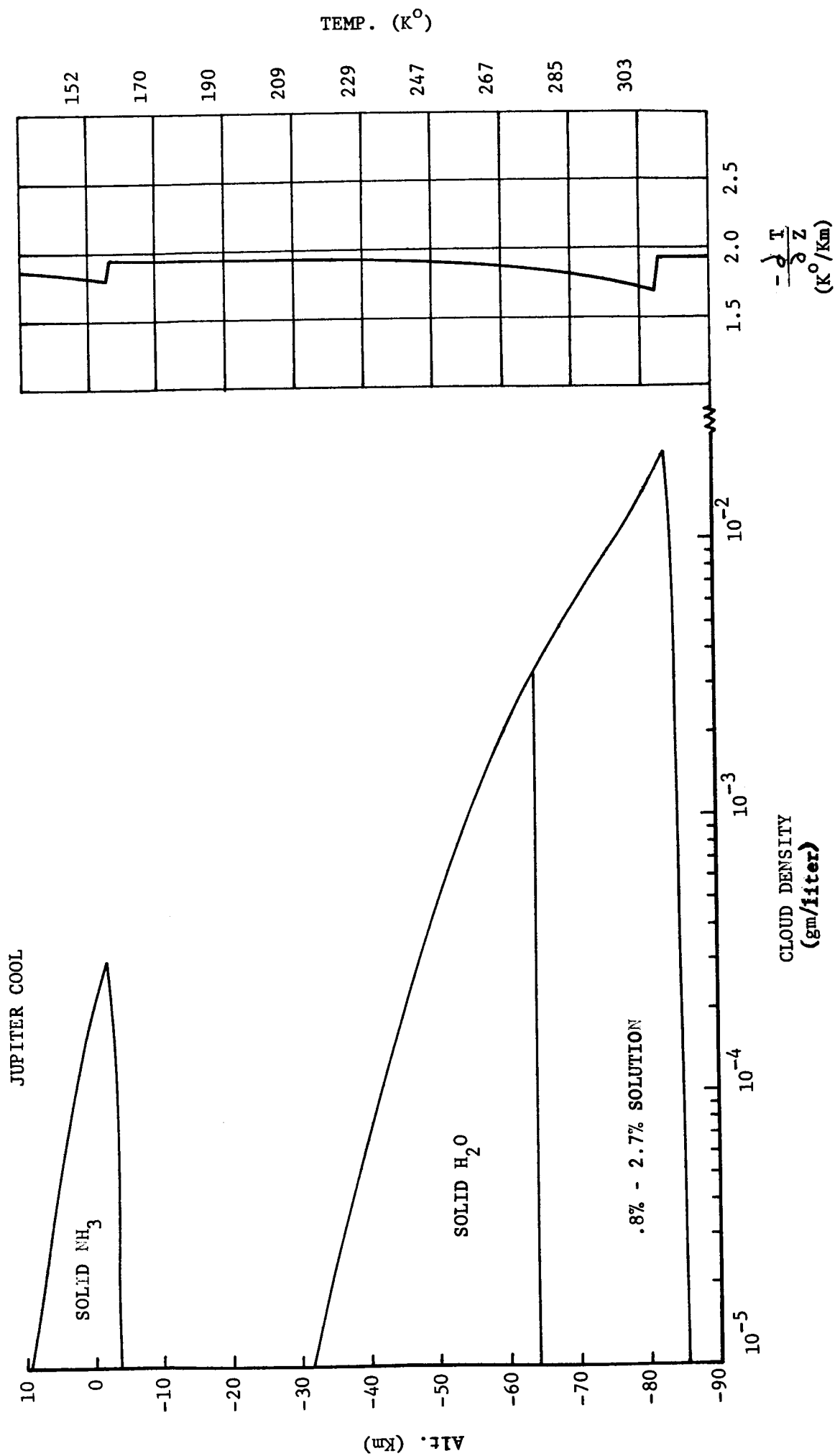


Figure 4. Cloud densities and the wet-adiabatic lapse rate for Jupiter nominal model atmosphere.



SATURN NOM. ATMOS.

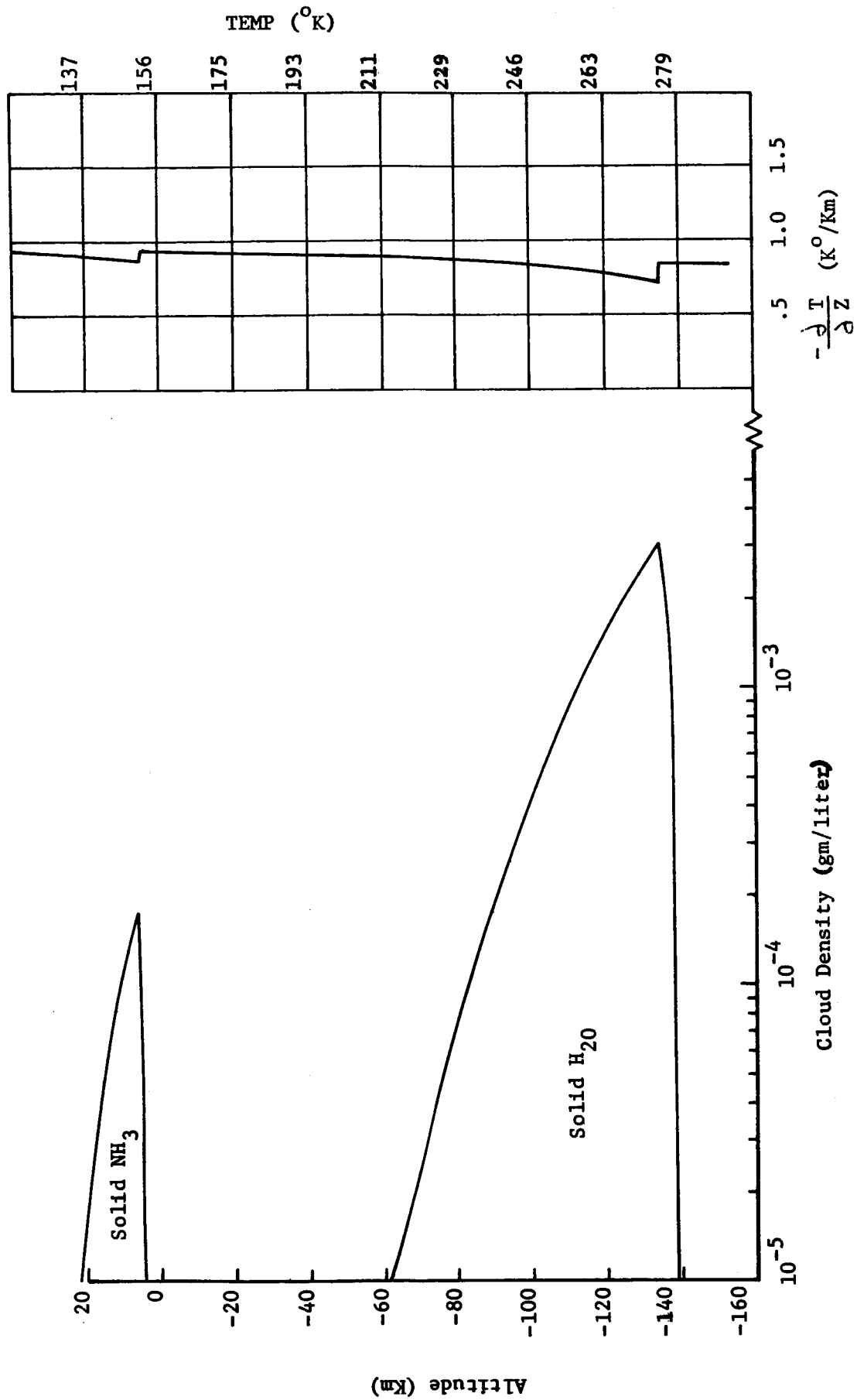


Figure 6. Cloud densities and the wet-adiabatic lapse rate for Saturn nominal model atmosphere.

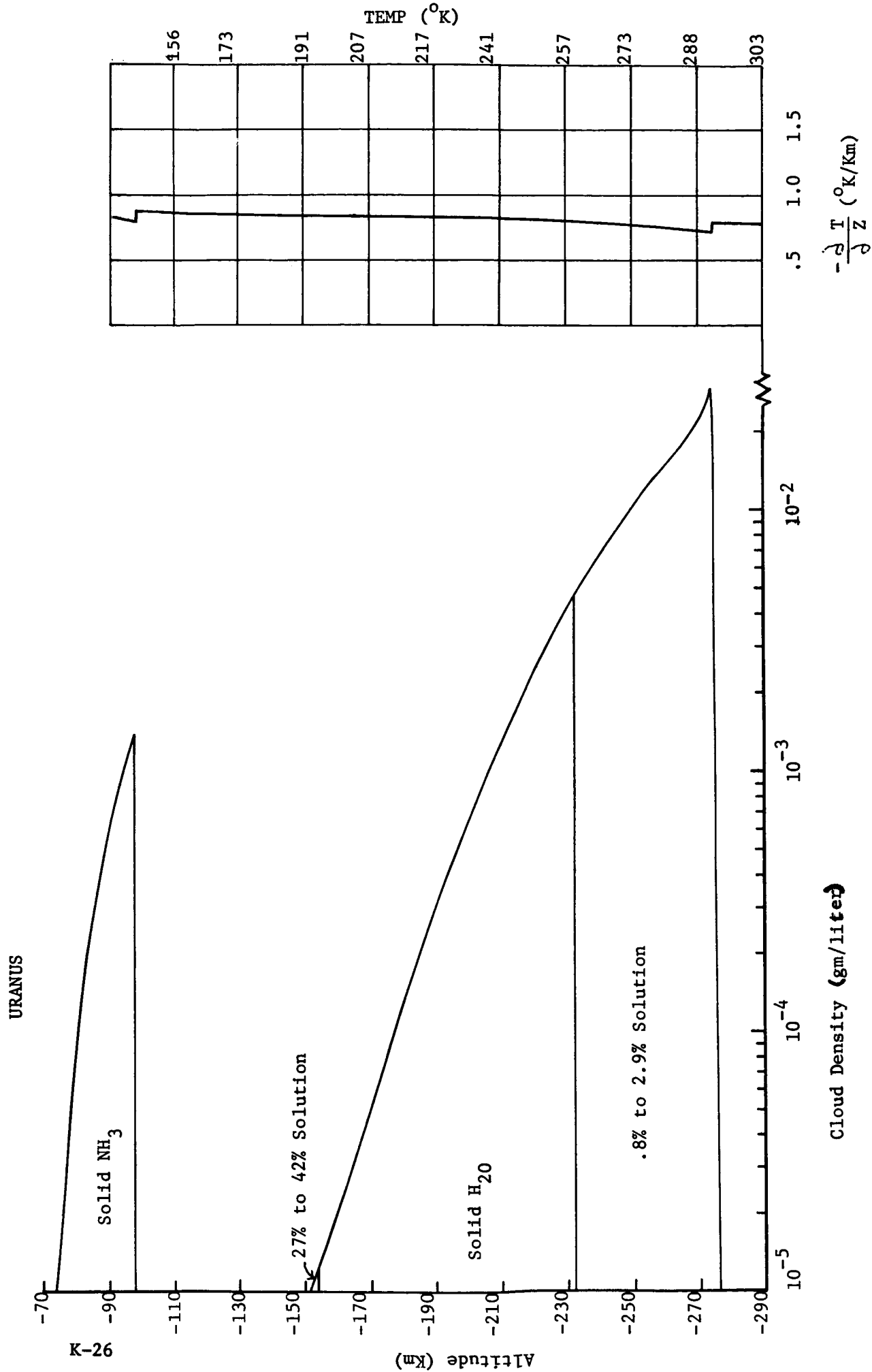


Figure 7. Cloud densities and the wet-adiabatic lapse rate for Uranus nominal model atmosphere.

NEPTUNE

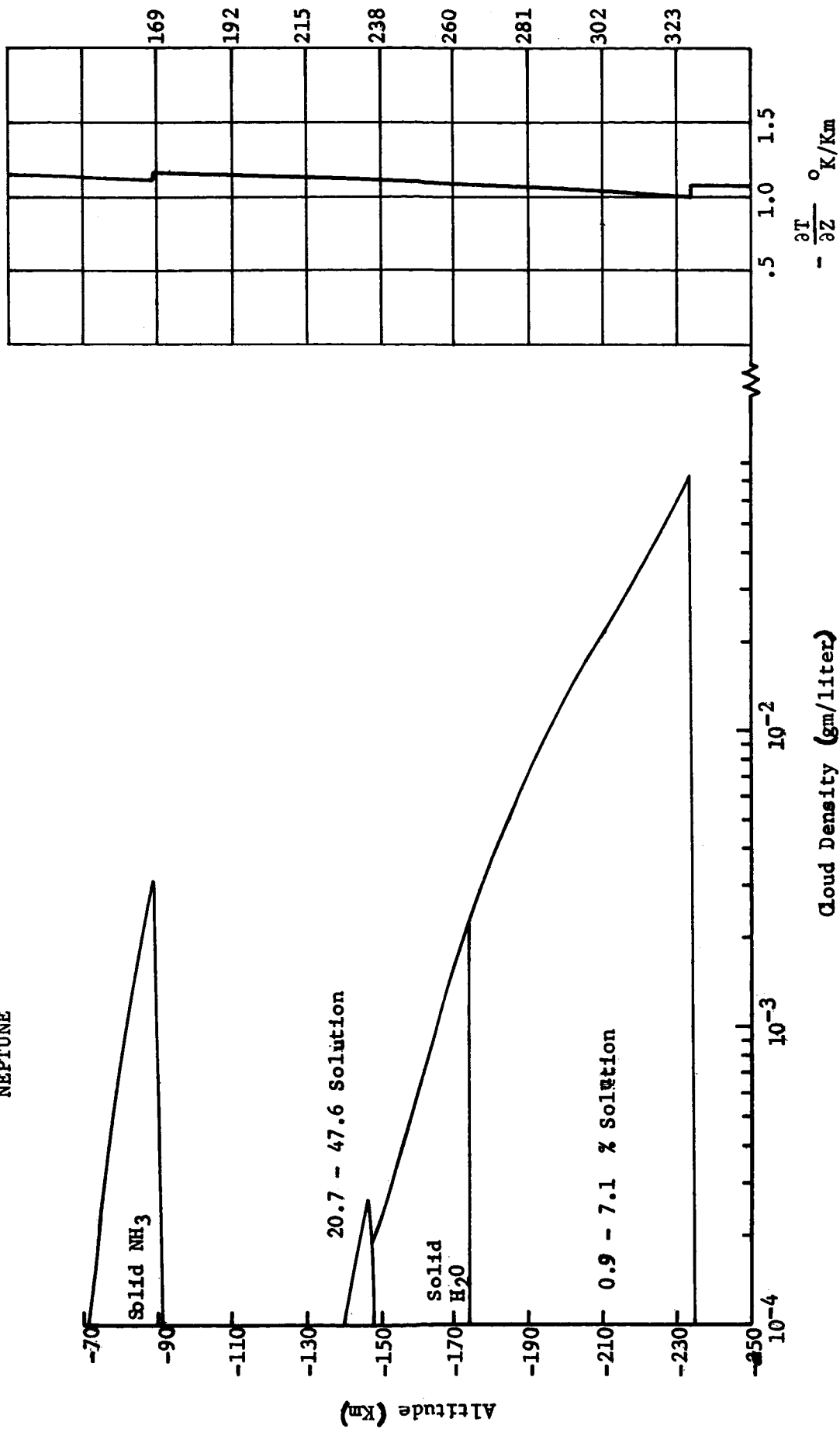


Figure 8. Cloud densities and the wet-adiabatic lapse rate for Neptune nominal model atmosphere.

V. REFERENCES

- 1) John S. Lewis, "The Clouds of Jupiter and the $\text{NH}_3\text{-H}_2\text{O}$ and $\text{NH}_3\text{-H}_2\text{S}$ Systems", Icarus, 10, 365 (1969).
- 2) C. Haudenschild, "Multi-phase Ammonia Water System", JPL Space Programs Summary 37-64 Vol. III.
- 3) "The Planet Jupiter (1970)", NASA SP-8069 (Dec. 1971).
- 4) "Preliminary Model Atmospheres for the Planets Uranus and Neptune", JPL Section Document 131-17 (Nov. 1971).
- 5) "The Planet Saturn (1970)", NASA Space Vehicle Design Criteria (Environment) Preliminary Information.

APPENDIX L

VERTICAL DESCENT PROGRAM FOR SCIENCE INSTRUMENT SIMULATION (DATAT)
DESCENT RUNS FOR JUPITER AND SATURN

K. W. Ledbetter
and
A. R. Barger

June 8, 1972

```

PAINFT
  TITLE=50NSURVIVABLE JUPITER PROBE TASK 3 DESCENT RUNS
  WNOTS=50M RAL. COEF. 0.55/0.09/1.50      SEP 10 BARS
  PS=0.00,
  IAMP=1,
  RSTART=71454.,      TSTART=0,
  RSTCF=71337.,      TSTCO=1.0E+08,
  DP=3.,
  STORC= 6R00.,
  FREQ=2.4E+09,      FZA=25.,
  VNAME=6H TEMP,6H PRESS,6H TEMP,6H PRESS,6H ACCEL,6H ACCEL,
  6H ACCEL,6H ACCEL,6H SPEC,6H SPEC,6H SPEC,6H SPEC,
  DTI(1,1)=3.,3.5,4.,5.,7.,8.,10.,15.,30.,45.,50.,60.,
  DTI(1,2)=3.,3.5,4.,5.,7.,8.,10.,15.,30.,45.,50.,60.,
  APS(1,1)=10.,10.,10.,10.,10.,10.,10.,10.,10.,10.,10.,10.,
  APS(1,2)=10.,10.,10.,10.,10.,10.,10.,10.,10.,10.,10.,10.,
  NSTAR=2,
  WCHG(2)=1.50,
  RCHG(2)=71372.,
  ?

```


SURVIVABLE JUPITER PROBE TASK 3 DESCENT RUNS
 JPL MICROGRAPH JUPITER COOL/CENSE ATMOSPHERE
 BALLISTIC COEFFICIENT = .090, INITIAL TIME = 0. SECONDS AT 71454.000 KM RADIUS

CAL. CCEF. 0.65/0.09/1.50 SEP 10 BARS

SAMPLE INTERVALS (SECONDS)									
TEMP	PRESS	TEMP	PRESS	ACCEL	ACCEL	ACCEL	ACCEL	M SPEC	M SPEC
3.000	3.500	4.000	5.000	7.000	8.000	10.000	15.000	30.000	60.000
10.000	16.000	10.000	10.000	30.000	30.000	30.000	400.000	400.000	400.000
NO OF PREVIOUS MEASUREMENTS									
TEMP	PRESS	TEMP	PRESS	ACCEL	ACCEL	ACCEL	ACCEL	M SPEC	M SPEC
0.	0.	0.	0.	0.	0.	0.	0.	0.	0.

REQUIREC BIT RATE = 61.7262 BITS/SECOND

ENTRY DATA IN STORAGE = 6400.0 BITS

SURVIVABLE JUPITER PROBE TASK 3 DESCENT RUNS
JPL MICROGRAPH JUPITER COOL/DENSE ATMOSPHERE

BALLISTIC COEFFICIENT = .090, INITIAL TIME = 0. SECONDS AT 71454.000 KM RADIUS

EAL. CCEF. 0.65/0.09/1.50 SFP 10 BARS

RADIUS 71454.000 KM ALTITUDE 32.000 KM PRESSURE .093324 BARS TEMPERATURE 100.000 KELVIN
-265.270 FAHRENHEIT
TIME 0. SEC VELOCITY 104.987 KFT DYN P .092103 ATM
0. MIN 164.870 METER/SEC DYN P .002015 BARS
0. HRS 540.912 FT/SEC DOPPLER 1.15523E+03 CPS
PACH NO .233422

INSTRUMENTS TEMP PRESS TEMP PRESS ACCEL ACCEL ACCEL ACCEL M SPEC M SPEC M SPEC M SPEC
NC OF W/FAS 1.00 1.00 1.00 1.00 1.00 1.00 1.00 1.00 1.00 1.00 1.00 1.00
KM/MEAS .42971 .57040 .65081 .81087 .122789 1.20409 1.55592 2.35574 4.50772 5.84404 7.11163 8.31721
MEAS/KM 2.0420 1.7532 1.5365 1.2332 .8866 .7783 .6266 .4243 .2218 .1711 .1486 .1202
BARS/MEAS .00378 .00442 .00506 .00634 .00834 .01025 .01250 .01966 .04128 .05660 .07284 .08991
MEAS/MAR 264.4353 226.2841 197.6717 157.6170 111.0475 59.5477 77.5328 50.8652 24.2726 17.6673 13.7287 11.1217
DECK/MEAS 0. 0. 0. 0. 0. 0. 0. 0. 0. 0. 0. 0.
MEAS/DECK 0. 0. 0. 0. 0. 0. 0. 0. 0. 0. 0. 0.
MEAS/PSCHT 25.17476 21.61300 19.94305 15.20392 10.93039 9.59482 7.72487 5.23101 2.73481 2.10943 1.73340 1.40212

RADIUS 71451.000 KM ALTITUDE 29.000 KM PRESSURE .119026 BARS TEMPERATURE 100.000 KELVIN
-265.270 FAHRENHEIT
TIME 19.349 SEC VELOCITY 95.144 KFT DYN P .117479 ATM
.32249 MIN 145.908 METER/SEC DYN P .002015 BARS
.305375 HRS 1.4102 MB/SEC DOPPLER 1.05840E+03 CPS
PACH NO .206694

INSTRUMENTS TEMP PRESS TEMP PRESS ACCEL ACCEL ACCEL ACCEL M SPEC M SPEC M SPEC M SPEC
NC OF W/FAS 7.45 6.53 5.84 4.87 3.76 3.42 2.93 2.29 1.54 1.48 1.39 1.32
KM/MEAS .43432 .50574 .57714 .71934 1.00180 1.14119 1.41629 2.05797 4.03132 5.24088 6.36371 7.49508
MEAS/KM 2.3035 1.9773 1.7327 1.3902 .9987 .8764 .7051 .4767 .2481 .1908 .1564 .1334
BARS/MEAS .00427 .00499 .00571 .00715 .01087 .01154 .01451 .02208 .04605 .06307 .08093 .09962
MEAS/MAR 234.3778 200.6007 175.2687 139.8056 95.2814 86.6198 68.6971 45.2799 21.7159 15.8555 12.3570 10.0305
DECK/MEAS 0. 0. 0. 0. 0. 0. 0. 0. 0. 0. 0. 0.
MEAS/DECK 0. 0. 0. 0. 0. 0. 0. 0. 0. 0. 0. 0.
MEAS/PSCHT 28.39636 24.37520 21.35930 17.13697 12.81125 10.60313 8.65161 5.87574 3.05776 2.35204 1.92789 1.64457

RADIUS 71448.000 KM ALTITUDE 26.000 KM PRESSURE .151034 BARS TEMPERATURE 100.000 KELVIN
-265.270 FAHRENHEIT
TIME 41.202 SEC VELOCITY 85.302 KFT DYN P .148846 ATM
.68869 MIN 129.267 METER/SEC DYN P .002015 BARS
.011445 HRS 1.5926 MB/SEC DOPPLER 9.37247E+02 CPS
PACH NO .183021

INSTRUMENTS TEMP PRESS TEMP PRESS ACCEL ACCEL ACCEL ACCEL M SPEC M SPEC M SPEC M SPEC
NC OF W/FAS 14.73 12.77 11.30 9.24 6.89 6.15 5.12 3.75 2.37 2.03 1.82 1.69
KM/MEAS .38478 .44833 .51172 .63801 .88866 1.01304 1.25592 1.86653 3.60162 4.69401 5.74803 6.77335
MEAS/KM 2.5909 2.2305 1.9582 1.5674 1.1253 .9271 .7637 .5358 .2777 .2130 .1742 .1476
BARS/MEAS .00481 .00562 .00644 .00807 .01135 .01301 .01634 .02482 .05153 .07030 .09086 .11121
MEAS/MAR 207.7079 177.8040 155.3765 123.9793 85.1003 75.8897 61.1973 40.2832 19.4088 14.2094 11.1039 8.9921
DECK/MEAS 0. 0. 0. 0. 0. 0. 0. 0. 0. 0. 0. 0.
MEAS/DECK 0. 0. 0. 0. 0. 0. 0. 0. 0. 0. 0. 0.
MEAS/PSCHT 32.03463 27.49374 24.08805 19.32002 13.87066 12.16766 9.78334 6.60377 3.42230 2.62582 2.14728 1.81975

0. SECONDS AT 71454.000 KM RADIUS

SEP 10 BARS

108.000 KELVIN
-265.270 FAHRENHEIT

- 003015 BARS
- 290911E+02 CFS
- 162057

Spec	M Spec	M Spec
2.65	2.32	2.10
21656	5.15193	6.14064
.2372	.1926	.1628
0.7893	.10091	.12359
.6656	9.5094	8.0312
2.2313	3.18386	5.04013
.8209	3.141	1.984
9.2535	2.36435	2.02610

108.000 KELVIN
-265.270 FAHRENHEIT

.003815 BARS
 .348244E+02 CPS
 .143493

	SPEC	M SPEC	M SPEC
1	3.34	2.88	2.56
2	8.192	4.70170	5.57016
3	2.623	.2127	.1795
4	0.6707	.11047	.13451
5	.4856	9.0525	7.4341
6	34398	0.07170	9.75790
7	1576	.1239	.1025
8	31239	2.70569	2.30049

112.767 KELVIN
-256.690 FAHRENHEIT

.309717 AIF
 .003215 BARS
 .662411E+02 CFS
 .127321

	SPEC	M SPEC	M SPEC
1	4.12	3.50	3.08
2	4.063	4.31211	5.11504
3	.2865	.2319	.1955
4	0.0459	0.1977	.14556
5	.5719	8.3492	6.8699
6	77847	8.37351	9.93408
7	1475	1.194	.1007
8	7657	3.09327	2.62423

SURVIVABLE JUPITER PROBE TASK 3 DESCENT RUNS

JPL MCO3PAC4 JUPITER CON/LENSE ATMOSPHERE

BALLISTIC COEFFICIENT = .090, INITIAL TIME = 0. SECONDS AT 71454.000 KM RADIUS

REL. COEFF. 0.0570.09/1.5P SEP 10 BARS

RADIUS 71436.000 KM		ALTITUDE 14.000 KM		PRESSURE		TEMPERATURE		110.553 KELVIN		-246.213 FAHRENHEIT	
TIME	158.688 SEC	VELOCITY	84.112 METER/SEC	DYN P	COEFF P	MACT NO	110.553 KELVIN	110.553 KELVIN	110.553 KELVIN	110.553 KELVIN	110.553 KELVIN
	2.64080 MIN		2.4490 METER/SEC								
	0.044163 HRS		275.957 FT/SEC								

INSTRUMENTS		TEMP		PRESS		BOCEL		ACCEL		M SPEC		M SPEC		M SPEC		M SPEC	
NO OF MEAS	54.00	46.43	40.75	32.40	23.71	20.87	16.90	11.60	6.30	2.43765	3.21528	3.21528	3.21528	3.21528	3.21528	3.21528	
KPA/MEAS	25143	29315	33483	41804	58680	83117	1.23554	1.23554	1.23554	1.23554	1.23554	1.23554	1.23554	1.23554	1.23554	1.23554	
MEAS/KM	3.5773	3.4112	2.9866	2.1921	1.7127	1.5004	1.2031	1.0067	0.8102	0.63740	0.51379	0.41379	0.33379	0.27430	0.22430	0.18160	
BARS/MEAS	0.0737	0.0451	0.0384	0.1272	0.1729	0.1578	0.1278	0.1067	0.0874	0.07140	0.05740	0.04640	0.03740	0.03040	0.02440	0.01940	
MEAS/PAE	135.5315	115.1856	101.5012	81.1834	57.8492	50.5575	40.3456	26.7406	13.1379	9.7410	7.7050	6.3495	5.3495	4.5495	3.8495	3.2495	
CECK/MEAS	4.8819	56921	65914	81170	1.13369	1.29412	1.81369	2.40678	3.13310	4.73310	6.24300	7.72643	9.18160	1.089	1.089	1.089	
MEAS/MECK	2.0484	1.7569	1.5341	1.2320	0.821	0.7727	0.6156	0.4155	0.2113	0.1602	0.1294	0.1089	0.089	0.074	0.062	0.052	
MEAS/PSCHT	52.02705	46.26556	40.52117	32.47755	23.28455	20.41178	16.38962	11.02622	5.66064	4.31793	3.51149	2.97324	2.57324	2.22324	1.92324	1.67324	

RADIUS 7143.000 KM		ALTITUDE 11.000 KM		PRESSURE		TEMPERATURE		124.418 KELVIN		-235.718 FAHRENHEIT	
TIME	196.201 SEC	VELOCITY	77.319 METER/SEC	DYN P	COEFF P	MACT NO	124.418 KELVIN	124.418 KELVIN	124.418 KELVIN	124.418 KELVIN	124.418 KELVIN
	3.27001 MIN		2.6644 METER/SEC								
	0.054500 HRS		253.671 FT/SEC								

INSTRUMENTS		TEMP		PRESS		BOCEL		ACCEL		M SPEC		M SPEC		M SPEC		M SPEC	
NO OF MEAS	56.40	57.06	50.05	40.24	29.03	25.53	20.62	14.08	7.54	2.25003	2.97142	2.97142	2.97142	2.97142	2.97142	2.97142	
KPA/MEAS	23122	26962	30797	38457	53727	61339	78516	1.14189	0.8757	0.4444	0.3365	0.2718	0.2205	0.18994	0.16994	0.14994	
MEAS/KM	4.3248	3.7089	3.2470	2.6003	1.8413	1.6303	1.3069	1.0060	0.8026	0.64246	0.51106	0.4022	0.3222	0.26994	0.22994	0.19994	
BARS/MEAS	0.0802	0.0636	0.0570	0.1339	0.1879	0.2150	0.2693	0.3460	0.4360	0.54246	0.67106	0.8422	1.0222	1.22994	1.42994	1.62994	
MEAS/PAE	124.7126	106.8401	92.4358	74.6698	53.2235	46.5217	37.1395	24.6310	12.1271	9.0038	7.1315	5.8845	4.9845	4.2845	3.6845	3.1845	
CECK/MEAS	4.4496	52351	59803	74719	1.84459	1.49283	1.40836	2.22208	3.48019	5.78504	7.16463	8.52022	9.87022	1.174	1.174	1.174	
MEAS/MECK	2.2274	1.0102	1.6722	1.3343	0.9573	0.8323	0.6719	0.4500	0.2243	0.1729	0.1396	0.1174	0.0974	0.0824	0.0674	0.0524	
MEAS/PSCHT	51.46826	52.75620	46.15962	37.02035	26.59960	23.25117	18.66126	12.54092	6.41855	4.88692	3.96717	3.35343	2.85343	2.45343	2.10343	1.80343	

RADIUS 71410.000 KM		ALTITUDE 8.000 KM		PRESSURE		TEMPERATURE		130.258 KELVIN		-225.215 FAHRENHEIT	
TIME	216.602 SEC	VELOCITY	71.353 METER/SEC	DYN P	COEFF P	MACT NO	130.258 KELVIN	130.258 KELVIN	130.258 KELVIN	130.258 KELVIN	130.258 KELVIN
	3.64337 MIN		2.8877 METER/SEC								
	0.065723 HRS		234.098 FT/SEC								

INSTRUMENTS		TEMP		PRESS		BOCEL		ACCEL		M SPEC		M SPEC		M SPEC		M SPEC	
NO OF MEAS	76.47	58.60	60.15	49.32	34.80	30.58	24.66	16.77	8.49	2.08366	2.75457	2.75457	2.75457	2.75457	2.75457	2.75457	
KPA/MEAS	21346	24893	28435	35511	49625	56682	70696	1.05597	0.8479	0.4799	0.3630	0.2929	0.2460	0.2060	0.1760	0.1460	
MEAS/KM	4.8947	4.0173	3.5167	2.8160	2.0151	1.7644	1.4145	1.0472	0.8479	0.6799	0.5430	0.4460	0.3660	0.2960	0.2460	0.2060	
BARS/MEAS	0.0869	0.1014	0.1159	0.1451	0.2035	0.2327	0.2815	0.4392	0.5495	0.6905	0.8430	1.0008	1.1608	1.3208	1.4808	1.6408	
MEAS/PAE	115.1144	98.6276	86.2555	68.9403	45.1518	42.9680	34.3109	22.7689	11.2303	8.3476	6.6191	5.4678	4.5678	3.8678	3.2678	2.7678	
CECK/MEAS	4.1672	4.8478	55378	69159	96644	1.10349	1.37685	2.05597	3.40592	5.36619	6.65237	7.91036	9.16036	1.063	1.063	1.063	
MEAS/MECK	2.4055	2.0624	1.8058	1.4460	1.0347	0.9082	0.7263	0.4864	0.2464	0.1864	0.1503	0.1263	0.1063	0.0863	0.0663	0.0463	
MEAS/PSCHT	65.72131	59.80500	52.76737	41.95464	30.85421	26.33526	21.12863	14.18603	7.24171	5.50459	4.46169	3.76590	3.16590	2.66590	2.26590	1.96590	

AL. CCEF. 0.65/0.09/1.50

US/PSCHT	78.61705	67.42052	59.03884	47.20185	33.86659	25.67113	23.70740	15.96578	8.13183	6.17258	4.95640	4.21179
----------	----------	----------	----------	----------	----------	----------	----------	----------	---------	---------	---------	---------

075822
WACT MD
201.419 FT/SEC

Year	1998	1999	2000	2001	2002	2003	2004	2005	2006	2007	2008	2009	2010	2011	2012	2013	2014	2015	2016	2017	2018	2019	2020	2021	2022	2023	2024	2025	2026	2027	2028	2029	2030	2031	2032	2033	2034	2035	2036	2037	2038	2039	2040	2041	2042	2043	2044	2045	2046	2047	2048	2049	2050	2051	2052	2053	2054	2055	2056	2057	2058	2059	2060	2061	2062	2063	2064	2065	2066	2067	2068	2069	2070	2071	2072	2073	2074	2075	2076	2077	2078	2079	2080	2081	2082	2083	2084	2085	2086	2087	2088	2089	2090	2091	2092	2093	2094	2095	2096	2097	2098	2099	2100
1998	1999	2000	2001	2002	2003	2004	2005	2006	2007	2008	2009	2010	2011	2012	2013	2014	2015	2016	2017	2018	2019	2020	2021	2022	2023	2024	2025	2026	2027	2028	2029	2030	2031	2032	2033	2034	2035	2036	2037	2038	2039	2040	2041	2042	2043	2044	2045	2046	2047	2048	2049	2050	2051	2052	2053	2054	2055	2056	2057	2058	2059	2060	2061	2062	2063	2064	2065	2066	2067	2068	2069	2070	2071	2072	2073	2074	2075	2076	2077	2078	2079	2080	2081	2082	2083	2084	2085	2086	2087	2088	2089	2090	2091	2092	2093	2094	2095	2096	2097	2098	2099	2100	

[illegible]

Model	Log-likelihood	AIC	BIC	Bayes factor
Model 1	-100.00	202.00	204.00	1.00
Model 2	-98.50	201.00	203.00	1.50
Model 3	-97.00	200.00	202.00	2.00
Model 4	-95.50	199.00	201.00	3.00
Model 5	-94.00	198.00	200.00	4.00
Model 6	-92.50	197.00	199.00	6.00
Model 7	-91.00	196.00	198.00	10.00
Model 8	-89.50	195.00	197.00	20.00
Model 9	-88.00	194.00	196.00	40.00
Model 10	-86.50	193.00	195.00	100.00
Model 11	-85.00	192.00	194.00	200.00
Model 12	-83.50	191.00	193.00	500.00
Model 13	-82.00	190.00	192.00	1000.00
Model 14	-80.50	189.00	191.00	2000.00
Model 15	-79.00	188.00	190.00	5000.00
Model 16	-77.50	187.00	189.00	10000.00
Model 17	-76.00	186.00	188.00	20000.00
Model 18	-74.50	185.00	187.00	50000.00
Model 19	-73.00	184.00	186.00	100000.00
Model 20	-71.50	183.00	185.00	200000.00
Model 21	-70.00	182.00	184.00	500000.00
Model 22	-68.50	181.00	183.00	1000000.00
Model 23	-67.00	180.00	182.00	2000000.00
Model 24	-65.50	179.00	181.00	5000000.00
Model 25	-64.00	178.00	180.00	10000000.00
Model 26	-62.50	177.00	179.00	20000000.00
Model 27	-61.00	176.00	178.00	50000000.00
Model 28	-59.50	175.00	177.00	100000000.00
Model 29	-58.00	174.00	176.00	200000000.00
Model 30	-56.50	173.00	175.00	500000000.00
Model 31	-55.00	172.00	174.00	1000000000.00
Model 32	-53.50	171.00	173.00	2000000000.00
Model 33	-52.00	170.00	172.00	5000000000.00
Model 34	-50.50	169.00	171.00	10000000000.00
Model 35	-49.00	168.00	170.00	20000000000.00
Model 36	-47.50	167.00	169.00	50000000000.00
Model 37	-46.00	166.00	168.00	100000000000.00
Model 38	-44.50	165.00	167.00	200000000000.00
Model 39	-43.00	164.00	166.00	500000000000.00
Model 40	-41.50	163.00	165.00	1000000000000.00
Model 41	-40.00	162.00	164.00	2000000000000.00
Model 42	-38.50	161.00	163.00	5000000000000.00
Model 43	-37.00	160.00	162.00	10000000000000.00
Model 44	-35.50	159.00	161.00	20000000000000.00
Model 45	-34.00	158.00	160.00	50000000000000.00
Model 46	-32.50	157.00	159.00	100000000000000.00
Model 47	-31.00	156.00	158.00	200000000000000.00
Model 48	-29.50	155.00	157.00	500000000000000.00
Model 49	-28.00	154.00	156.00	1000000000000000.00
Model 50	-26.50	153.00	155.00	2000000000000000.00
Model 51	-25.00	152.00	154.00	5000000000000000.00
Model 52	-23.50	151.00	153.00	10000000000000000.00
Model 53	-22.00	150.00	152.00	20000000000000000.00
Model 54	-20.50	149.00	151.00	50000000000000000.00
Model 55	-19.00	148.00	150.00	100000000000000000.00
Model 56	-17.50	147.00	149.00	200000000000000000.00
Model 57	-16.00	146.00	148.00	500000000000000000.00
Model 58	-14.50	145.00	147.00	1000000000000000000.00
Model 59	-13.00	144.00	146.00	2000000000000000000.00
Model 60	-11.50	143.00	145.00	5000000000000000000.00
Model 61	-10.00	142.00	144.00	10000000000000000000.00
Model 62	-8.50	141.00	143.00	20000000000000000000.00
Model 63	-7.00	140.00	142.00	50000000000000000000.00
Model 64	-5.50	139.00	141.00	100000000000000000000.00
Model 65	-4.00	138.00	140.00	200000000000000000000.00
Model 66	-2.50	137.00	139.00	500000000000000000000.00
Model 67	-1.00	136.00	138.00	1000000000000000000000.00
Model 68	0.50	135.00	137.00	2000000000000000000000.00
Model 69	2.00	134.00	136.00	5000000000000000000000.00
Model 70	3.50	133.00	135.00	10000000000000000000000.00
Model 71	5.00	132.00	134.00	20000000000000000000000.00
Model 72	6.50	131.00	133.00	50000000000000000000000.00
Model 73	8.00	130.00	132.00	100000000000000000000000.00
Model 74	9.50	129.00	131.00	200000000000000000000000.00
Model 75	11.00	128.00	130.00	500000000000000000000000.00
Model 76	12.50	127.00	129.00	1000000000000000000000000.00
Model 77	14.00	126.00	128.00	2000000000000000000000000.00
Model 78	15.50	125.00	127.00	5000000000000000000000000.00
Model 79	17.00	124.00	126.00	10000000000000000000000000.00
Model 80	18.50	123.00	125.00	20000000000000000000000000.00
Model 81	20.00	122.00	124.00	50000000000000000000000000.00
Model 82	21.50	121.00	123.00	100000000000000000000000000.00
Model 83	23.00	120.00	122.00	200000000000000000000000000.00
Model 84	24.50	119.00	121.00	500000000000000000000000000.00
Model 85	26.00	118.00	120.00	1000000000000000000000000000.00
Model 86	27.50	117.00	119.00	2000000000000000000000000000.00
Model 87	29.00	116.00	118.00	5000000000000000000000000000.00
Model 88	30.50	115.00	117.00	10000000000000000000000000000.00
Model 89	32.00	114.00	116.00	20000000000000000000000000000.00
Model 90	33.50	113.00	115.00	50000000000000000000000000000.00
Model 91	35.00	112.00	114.00	100000000000000000000000000000.00
Model 92	36.50	111.00	113.00	200000000000000000000000000000.00
Model 93	38.00	110.00	112.00	500000000000000000000000000000.00
Model 94	39.50	109.00	111.00	1000000000000000000000000000000.00
Model 95	41.00	108.00	110.00	2000000000000000000000000000000.00
Model 96	42.50	107.00	109.00	5000000000000000000000000000000.00
Model 97	44.00	106.00	108.00	10000000000000000000000000000000.00
Model 98	45.50	105.00	107.00	20000000000000000000000000000000.00
Model 99	47.00	104.00	106.00	50000000000000000000000000000000.00
Model 100	48.50	103.00	105.00	100000000000000000000000000000000.00
Model 101	50.00	102.00	104.00	200000000000000000000000000000000.00
Model 102	51.50	101.00	103.00	500000000000000000000000000000000.00
Model 103	53.00	100.00	102.00	1000000000000000000000000000000000.00
Model 104	54.50	99.00	101.00	2000000000000000000000000000000000.00
Model 105	56.00	98.00	100.00	5000000000000000000000000000000000.00
Model 106	57.50	97.00	99.00	10000000000000000000000000000000000.00
Model 107	59.00	96.00	98.00	20000000000000000000000000000000000.00
Model 108	60.50	95.00	97.00	50000000000000000000000000000000000.00
Model 109	62.00	94.00	96.00	100000000000000000000000000000000000.00
Model 110	63.50	93.00	95.00	200000000000000000000000000000000000.00
Model 111	65.00	92.00	94.00	500000000000000000000000000000000000.00
Model 112	66.50	91.00	93.00	1000000000000000000000000000000000000.00
Model 113	68.00	90.00	92.00	2000000000000000000000000000000000000.00
Model 114	69.50	89.00	91.00	5000000000000000000000000000000000000.00
Model 115	71.00	88.00	90.00	10000000000000000000000000000000000000.00
Model 116	72.50	87.00	89.00	20000000000000000000000000000000000000.00
Model 117	74.00	86.00	88.00	50000000000000000000000000000000000000.00
Model 118	75.50	85.00	87.00	100000000000000000000000000000000000000.00
Model 119	77.00	84.00	86.00	200000000000000000000000000000000000000.00
Model 120	78.50	83.00	85.00	500000000000000000000000000000000000000.00
Model 121	80.00	82.00	84.00	1000000000000000000000000000000000000000.00
Model 122	81.50	81.00	83.00	2000000000000000000000000000000000000000.00
Model 123	83.00	80.00	82.00	5000000000000000000000000000000000000000.00
Model 124	84.50	79.00	81.00	100.00
Model 125	86.00	78.00	80.00	200.00
Model 126	87.50	77.00	79.00	500.00
Model 127	89.00	76.00	78.00	1000.00
Model 128	90.50	75.00	77.00	2000.00
Model 129	92.00	74.00	76.00	5000.00
Model 130	93.50	73.00	75.00	100.00
Model 131	95.00	72.00	74.00	200.00
Model 132	96.50	71.00	73.00	500.00
Model 133	98.00	70.00	72.00	1000.00
Model 134	99.50	69.00	71.00	2000.00
Model 135	101.00	68.00	70.00	5000.00
Model 136	102.50	67.00	69.00	100.00
Model 137	104.00	66.00	68.00	200.00
Model 138	105.50	65.00	67.00	500.00
Model 139	107.00	64.00	66.00	1000.00
Model 140	108.50	63.00	65.00	2000.00
Model 141	110.00	62.00	64.00	5000.00
Model 142	111.50	61.00	63.00	100.00
Model 143	113.00	60.00	62.00	200.00
Model 144	114.50	59.00	61.00	500.00
Model 145	116.00	58.00	60.00	1000.00
Model 146	117.50	57.00	59.00	2000.00
Model 147	119.00	56.00	58.00	5000.00
Model 148	120.50	55.00	57.00	100.00
Model 149	122.00	54.00	56.00	200.00
Model 150	123.50	53.00	55.00	500.00
Model 151	125.00	52.00	54.00	1000.00
Model 152	126.50	51.00	53.00	2000.00
Model 153	128.00	50.00	52.00	5000.00
Model 154	129.50	49.00	51.00	100.00
Model 155	131.00	48.00	50.00	200.00
Model 156	132.50	47.00	49.00	500.00
Model 157	134.00	46.00	48.00	1000.00
Model 158	135.50	45.00	4	

SURVIVABLE JUPITER PROBE TASK 3 (FSCENT RUNS
JPL MONOGRAPH JUPITER COOL/DENSE ATMOSPHERE
BALLISTIC COEFFICIENT = .090, INITIAL TIME = 0. SECONDS AT 71454.000 KM RADIUS

EAL. COEF: 0.65/8.09/1.50 SEP 10 9ARS

RADIUS 71418.000 KM		ALTITUDE -4.000 KM		PRESSURE 1.264212 BARS		TEMPERATURE 153.505 KELVIN		-183.361 FAHRENHEIT	
TIME	432.335 SEC	VELOCITY	53.431 METER/SEC	DYN P	0.03618 BARS	ACCEL	1.247710 ATM	M SPEC	M SPEC
	7.20559 MIN		7.20559 MIN	COEFLER	3.87356E+02 CFS				
	.120053 HRS		175.297 FT/SEC	PACH NO	.063453				
INSTRUMENTS	TEMP	PRESS	TEMP	PRESS	BOEFL	ACCEL	ACCEL	M SPEC	M SPEC
NC OF MEAS	145.11	124.52	109.08	87.47	62.76	55.04	44.23	11.81	9.65
KM/MEAS	.16081	.10662	.21322	.26636	.87247	.42543	.53117	1.97532	2.08068
MEAS/KM	6.2487	5.3585	4.6500	3.7542	2.6848	2.3505	1.8826	.6348	.4788
BARS/MEAS	.01160	.01353	.01547	.01935	.02712	.03102	.03842	.15800	.19864
MEAS/BARS	86.2297	73.8893	64.6340	51.6766	36.8682	32.2407	25.7821	17.1243	11.742
DECK/MEAS	.31281	.36391	.41577	.51941	.72832	.82560	1.03578	1.54517	2.07187
MEAS/DECK	3.2050	2.7479	2.4052	1.9253	1.3768	1.2054	.9555	.6455	.3255
MEAS/PSCHT	105.51451	93.91310	82.21202	65.83047	47.10861	41.25799	33.06714	22.14552	11.82247

RADIUS 71415.000 KM		ALTITUDE -7.968 KM		PRESSURE 1.455814 BARS		TEMPERATURE 159.357 KELVIN		-172.828 FAHRENHEIT	
TIME	490.359 SEC	VELOCITY	50.051 METER/SEC	DYN P	0.03815 BARS	ACCEL	1.476521 ATM	M SPEC	M SPEC
	8.17266 MIN		4.1216 M/SEC	COEFLER	3.628852E+02 CFS				
	.136211 HRS		154.208 FT/SEC	PACH NO	.058337				
INSTRUMENTS	TEMP	PRESS	TEMP	PRESS	BOEFL	ACCEL	ACCEL	M SPEC <td>M SPEC</td>	M SPEC
NC OF MEAS	154.45	141.10	123.59	99.07	71.05	62.29	51.04	13.26	11.81
KM/MEAS	.14291	.17485	.19978	.24959	.34905	.39870	.45785	1.47812	1.98083
MEAS/KM	6.6706	5.7192	5.0056	4.0065	2.8649	2.5081	2.0026	.6765	.5100
BARS/MEAS	.01238	.01445	.01652	.02066	.02695	.03310	.04142	.12558	.16832
MEAS/BARS	80.7253	69.2174	60.5491	44.4334	34.5641	30.2100	24.1623	16.0521	12.558
DECK/MEAS	.29264	.34132	.38997	.48121	.68137	.77829	.97164	1.45393	2.08537
MEAS/DECK	2.4172	2.9298	2.5543	2.0525	1.6676	1.2849	1.0290	.6878	.5613
MEAS/PSCHT	121.32406	104.03558	91.06921	72.91626	52.16994	45.68667	36.61004	24.50762	12.40419

RADIUS 71412.000 KM		ALTITUDE -10.000 KM		PRESSURE 1.759118 BARS		TEMPERATURE 165.213 KELVIN		-162.287 FAHRENHEIT	
TIME	592.228 SEC	VELOCITY	46.995 METER/SEC	DYN P	0.03215 BARS	ACCEL	1.736314 ATM	M SPEC	M SPEC
	9.20380 MIN		4.3900 M/SEC	COEFLER	3.407384E+02 CFS				
	.153357 HRS		154.184 FT/SEC	PACH NO	.053797				
INSTRUMENTS	TEMP	PRESS	TEMP	PRESS	BOEFL	ACCEL	ACCEL	M SPEC <td>M SPEC </td>	M SPEC
NC OF MEAS	185.08	158.74	139.06	111.45	79.89	70.03	56.22	19.41	14.81
KM/MEAS	.14078	.16421	.18762	.23441	.32786	.37452	.42770	1.36590	1.84465
MEAS/KM	7.1032	6.0899	5.3300	4.2660	3.0501	2.6701	2.1381	.7195	.5421
BARS/MEAS	.01319	.01539	.01759	.02200	.03082	.03525	.04410	.13357	.17894
MEAS/BARS	75.8473	64.9928	56.8549	45.6519	32.4414	28.3725	22.8781	15.0811	10.4866
DECK/MEAS	.27481	.32054	.36624	.45758	.64080	.73107	.91257	1.36619	2.71217
MEAS/DECK	3.6388	3.1198	2.7304	2.1854	1.5625	1.3678	1.0593	.7320	.5686
MEAS/PSCHT	133.91670	114.82928	100.51370	80.47187	57.56683	50.48897	40.32761	27.02628	13.65373

RADIUS 71412.000 KM		ALTITUDE -10.000 KM		PRESSURE 1.759118 BARS		TEMPERATURE 165.213 KELVIN		-162.287 FAHRENHEIT	
TIME	592.228 SEC	VELOCITY	46.995 METER/SEC	DYN P	0.03215 BARS	ACCEL	1.736314 ATM	M SPEC	M SPEC
	9.20380 MIN		4.3900 M/SEC	COEFLER	3.407384E+02 CFS				
	.153357 HRS		154.184 FT/SEC	PACH NO	.053797				
INSTRUMENTS	TEMP	PRESS	TEMP	PRESS	BOEFL	ACCEL	ACCEL	M SPEC <td>M SPEC </td>	M SPEC
NC OF MEAS	185.08	158.74	139.06	111.45	79.89	70.03	56.22	19.41	14.81
KM/MEAS	.14078	.16421	.18762	.23441	.32786	.37452	.42770	1.36590	1.84465
MEAS/KM	7.1032	6.0899	5.3300	4.2660	3.0501	2.6701	2.1381	.7195	.5421
BARS/MEAS	.01319	.01539	.01759	.02200	.03082	.03525	.04410	.13357	.17894
MEAS/BARS	75.8473	64.9928	56.8549	45.6519	32.4414	28.3725	22.8781	15.0811	10.4866
DECK/MEAS	.27481	.32054	.36624	.45758	.64080	.73107	.91257	1.36619	2.71217
MEAS/DECK	3.6388	3.1198	2.7304	2.1854	1.5625	1.3678	1.0593	.7320	.5686
MEAS/PSCHT	133.91670	114.82928	100.51370	80.47187	57.56683	50.48897	40.32761	27.02628	13.65373

SURVIVABLE JUPITER PROBE TASK 3 DESCENT RUNS

JPL PHOTOGRAPH JUPITER COOL/HEAT ATMOSPHERE

BOLLOTTIC COEFFICIENT = .050, INITIAL TIME = 0.

SECONDS AT 71454.000 KM RADIUS

EAL. COEF. 1.6570.09/1.50

SEP 10 BARS

RADIUS 71400.000 KM ALTITUDE -13.000 KM PRESSURE 2.057145 BARS TEMPERATURE 171.065 KELVIN
 -42.651 KFT 2.030244 ATM -151.745 FAHRENHEIT

TIME 618.045 SEC VFLCITY 44.223 METER/SEC CYN P 0.031815 BARS
 10.30076 MIN 4.6655 M/S 3.20643E+02 CFS
 .171670 HRS 145.090 FT/SEC .046751

INSTRUMENTS TEMP DPSS DPSS ACCEL ACCEL ACCEL M SPEC M SPEC M SPEC M SPEC
 NC OF MEAS 207.02 177.58 155.51 124.61 89.26 78.26 62.80 42.20 21.60 16.45 13.36 11.30
 KM/MEAS .13250 .15454 .17454 .20067 .22067 .24067 .26067 .28067 .30067 .32067 .34067 .36067
 MEAS/KM 7.5474 6.4707 5.6631 4.5324 3.2403 2.8465 2.2712 1.5174 .7636 .5751 .4620 .3866
 PARS/MEAS .01401 .01635 .01869 .02137 .02322 .02507 .02692 .02877 .03062 .03247 .03432 .03617
 MEAS/PAR 71.7672 61.1584 53.5019 42.7827 30.5322 26.7039 21.3444 14.1585 7.0530 5.2669 4.1955 3.4813
 DECK/MEAS .2864 .3016A .3116A .3216A .3316A .3416A .3516A .3616A .3716A .3816A .3916A .4016A
 MEAS/DECK 2.8664 3.3148 2.8011 2.3219 1.6596 1.4531 1.1635 .8546 1.2844 2.55639 3.35416 4.22503 5.04917
 MEAS/PSCHT 147.3127126.3112110.66032 88.50917 63.40779 55.83232 44.40662 29.70549 15.00351 11.32750 9.12157 7.65068

RADIUS 71400.000 KM ALTITUDE -16.000 KM PRESSURE 2.393053 BARS TEMPERATURE 176.925 KELVIN
 -52.493 KFT 2.361760 ATM -141.204 FAHRENHEIT

TIME 617.917 SEC VFLCITY 41.700 METER/SEC CYN P 0.032815 BARS
 11.46659 MIN 4.6943 M/S 3.02344E+02 CFS
 .19108 HRS 136.811 FT/SEC .046128

INSTRUMENTS TEMP DPSS DPSS ACCEL ACCEL ACCEL M SPEC M SPEC M SPEC M SPEC
 NC OF MEAS 231.31 197.55 172.98 134.58 86.27 86.27 69.76 46.86 23.93 18.20 14.76 12.47
 KM/MEAS .12495 .14575 .16575 .20838 .23253 .25253 .27253 .29253 .31253 .33253 .35253 .37253
 MEAS/KM 8.0332 6.8613 6.0048 4.8058 3.4354 3.0072 2.4077 1.6083 .8089 .6090 .4891 .4091
 PARS/MEAS .01486 .01734 .01982 .02479 .03473 .03571 .04567 .07466 .15022 .20108 .25234 .30399
 MEAS/PAR 67.2015 57.6568 50.4483 40.3425 28.7030 25.1837 20.1309 12.3678 6.6571 4.6731 3.5629 3.2895
 DECK/MEAS .2891 .28450 .28508 .30619 .30621 .30621 .30621 .30621 .30621 .30621 .30621 .30621
 MEAS/DECK 4.0899 3.5149 3.0762 2.4610 1.7595 1.5405 1.2334 .8279 .4144 .3120 .2505 .2096
 MEAS/PSCHT 161.51157138.4991421.22498 97.04082 66.40185 60.76464 48.67250 32.5046 16.42566 12.36423 9.97508 8.36207

RADIUS 71400.000 KM ALTITUDE -19.000 KM PRESSURE 2.770166 BARS TEMPERATURE 182.782 KELVIN
 -62.336 KFT 2.733042 ATM -130.663 FAHRENHEIT

TIME 761.645 SEC VFLCITY 39.306 METER/SEC CYN P 0.033815 BARS
 12.69909 MIN 5.2381 M/S 2.85335E+02 CFS
 .211651 HRS 129.251 FT/SEC .046275

INSTRUMENTS TEMP DPSS DPSS ACCEL ACCEL ACCEL M SPEC M SPEC M SPEC M SPEC
 NC OF MEAS 254.98 218.70 191.49 153.39 103.85 96.24 77.19 51.80 26.40 20.05 16.24 13.70
 KM/MEAS .11806 .13771 .15735 .19662 .22506 .23424 .25424 .27424 .29424 .31424 .33424 .35424
 MEAS/KM 8.4705 7.2617 6.3552 5.0860 3.6355 3.1922 2.5476 1.7015 .8554 .6438 .5168 .4322
 PARS/MEAS .01836 .01836 .02098 .02622 .03622 .04203 .05203 .07500 .15887 .21259 .26670 .32119
 MEAS/PAR 63.5689 54.4776 47.6501 38.1133 27.2038 23.7546 19.1217 12.6590 6.2045 4.7039 3.7496 3.1135
 DECK/MEAS .21045 .26881 .30716 .38281 .53694 .61342 .76622 1.18724 2.28216 3.03211 3.77528 4.51237
 MEAS/DECK 4.2393 3.7201 3.2556 2.6055 1.8624 1.6309 1.3051 .8717 .4392 .3298 .2649 .2216
 MEAS/PSCHT 176.65584151.41142132.52200106.07941 75.85800 66.41378 53.15182 35.56240 17.93227 13.52430 10.07926 9.11568

SURVIVABLE JUPITER PROBE TASK 3 DESCENT RUNS
 JPL MCNOSPARE JUPITER COOL/CEASE ATMOSPHERE
 BALLISTIC COEFFICIENT = .090, INITIAL TIME = 0. SECONDS AT 71454.000 KM RADIUS
 RAL. COEF. 0.6570.00/1.50 SEP 10 BARS

RADIUS 71400.000 KM		ALTITUDE -22.000 KM		PRESSURE		3.151084 BARS		TEMPERATURE		188.629 KELVIN		-120.138 FAHRENHEIT	
TIME 040.274 SEC		VELOCITY 37.284 METER/SEC		DYN P		0.03223 BARS							
14.00349 MIN		5.5397 MB/SEC		COEFF		2.703254E+02 CFS							
.233398 HRS		122.324 FT/SEC		MACH NO		.035544							
INSTRUMENTS	TEMP	PRESS	ACCEL	ACCEL	ACCEL	ACCEL	ACCEL	M SPEC	M SPEC	M SPEC	M SPEC	M SPEC	M SPEC
NC OF MEAS	281.09	241.07	211.06	169.05	121.03	106.03	85.02	57.02	29.01	22.01	17.80	15.00	15.00
KP/MEAS	.11174	.13034	.14894	.16611	.18038	.19747	.21556	.23464	.25372	.27280	.29188	.31096	.32904
MEAS/KM	8.9493	7.6721	6.7143	5.7732	4.8406	3.9140	2.9811	2.0482	1.1153	.7795	.4437	.1079	.0000
BARS/MEAS	.01662	.01940	.02217	.02492	.02767	.03042	.03317	.03592	.03867	.04142	.04417	.04692	.04967
MEAS/BARS	60.1575	51.5544	45.1029	39.0701	32.5211	25.7470	18.8047	11.9270	5.9615	2.9840	1.0063	.2813	.0000
DECK/MEAS	.21738	.25357	.28974	.32591	.36208	.39825	.43442	.47059	.50676	.54293	.57910	.61527	.65144
MEAS/DECK	4.6003	3.9437	3.4514	2.9591	2.4668	1.9745	1.4822	.9899	.4976	.2488	.1244	.0622	.0311
MEAS/PSCHT	192.52126165	0.6175144	4.6711115	6.3460	8.230573	10.1151	12.0000	13.8849	15.7698	17.6547	19.5396	21.4245	23.3094

RADIUS 71397.000 KM		ALTITUDE -25.000 KM		PRESSURE		3.662215 BARS		TEMPERATURE		194.465 KELVIN		-109.633 FAHRENHEIT	
TIME 022.886 SEC		VELOCITY 39.344 METER/SEC		DYN P		0.03223 BARS							
15.39144 MIN		5.8443 MB/SEC		COEFF		2.56234E+02 CFS							
.256357 HRS		115.959 FT/SEC		MACH NO		.037297							
INSTRUMENTS	TEMP	PRESS	ACCEL	ACCEL	ACCEL	ACCEL	ACCEL	M SPEC	M SPEC	M SPEC	M SPEC	M SPEC	M SPEC
NC OF MEAS	304.63	264.68	231.72	195.58	162.84	130.16	97.42	64.68	32.16	24.07	19.46	15.38	15.38
KP/MEAS	.10593	.12357	.14120	.15884	.17647	.19410	.21173	.22936	.24699	.26462	.28225	.30000	.31763
MEAS/KM	9.4398	8.0925	7.0020	5.9674	4.8866	3.8058	2.7250	1.6442	.8531	.4620	.2510	.1300	.0690
BARS/MEAS	.01754	.02046	.02338	.02630	.02922	.03214	.03506	.03798	.04090	.04382	.04674	.04966	.05258
MEAS/BARS	57.0224	48.4687	42.7575	34.1922	26.4079	19.3503	12.2928	5.2352	2.1776	1.0200	.4624	.2051	.0977
DECK/MEAS	.20508	.24030	.27469	.30908	.34347	.37786	.41225	.44664	.48103	.51542	.54981	.58420	.61859
MEAS/DECK	4.8524	4.1599	3.6404	3.1212	2.6020	2.0828	1.5636	.9444	.4252	.2060	.1030	.0515	.0258
MEAS/PSCHT	205.32778179	0.6735157	0.7201125	7.1452	8.88591	10.6270	12.3680	14.1090	15.8500	17.5910	19.3320	21.0730	22.8140

RADIUS 71394.000 KM		ALTITUDE -28.000 KM		PRESSURE		4.164724 BARS		TEMPERATURE		200.301 KELVIN		-99.128 FAHRENHEIT	
TIME 1010.107 SEC		VELOCITY 31.556 METER/SEC		DYN P		0.03223 BARS							
16.83345 MIN		6.1559 MB/SEC		COEFF		2.433125E+02 CFS							
.280557 HRS		110.099 FT/SEC		MACH NO		.034022							
INSTRUMENTS	TEMP	PRESS	ACCEL	ACCEL	ACCEL	ACCEL	ACCEL	M SPEC	M SPEC	M SPEC	M SPEC	M SPEC	M SPEC
NC OF MEAS	337.67	289.57	253.50	203.00	145.29	127.25	102.00	89.33	34.67	26.25	21.20	17.83	17.83
KP/MEAS	.10059	.11734	.13409	.15084	.16759	.18434	.20109	.21784	.23459	.25134	.26809	.28484	.30159
MEAS/KM	6.9415	5.9225	5.0583	4.2444	3.4806	2.7168	1.9529	1.1891	.6152	.3413	.1874	.1035	.0596
BARS/MEAS	.01947	.02155	.02363	.02571	.02779	.02987	.03195	.03403	.03611	.03819	.04027	.04235	.04443
MEAS/BARS	54.1354	46.3952	40.5900	32.4627	24.1744	16.2022	10.7501	5.3721	2.4990	1.2051	.5874	.2754	.1234
DECK/MEAS	.19568	.22827	.26084	.29341	.32598	.35855	.39112	.42369	.45626	.48883	.52140	.55397	.58654
MEAS/DECK	5.1103	4.3489	3.8338	3.3186	2.8034	2.2882	1.7730	.9151	.4000	.2051	.1077	.0551	.0276
MEAS/PSCHT	227.04148194	0.65052170	0.7529136	7.34675	8.88591	10.4270	11.9680	13.5090	15.0500	16.5910	18.1320	19.6730	21.2140

SURVIVABLE JUPITER PROBE TASK 3 DESCENT RUNS
 JPL MCMGPAK JUPITER COOL/SENSE ATMOSPHERE
 BALLISTIC COEFFICIENT = .090, INITIAL TIME = 0. SECONDS AT 71456.000 KM RADIUS
 BAL. COEFF. 0.06570.09/1.50 SEP 10 BARS

RADIUS 71382.000 KM ALTITUDE -40.000 KM PRESSURE 6.08111 BARS TEMPERATURE 223.646 KELVIN
 -131.234 KFT 6.75128 ATM -57.107 FAHRENHEIT
 TIME 1405.174 SEC VELOCITY 27.658 METER/SEC DYN P
 23.41556 MIN 7.4717 MB/SEC COPPLER
 .390326 HRS 90.740 FT/SEC PACH NO

INSTRUMENTS TEMP PRESS ACCEL ACCEL ACCEL M SPEC M SPEC M SPEC P SPC
 NC OF MEAS 465.39 402.48 352.29 281.74 176.65 141.52 94.68 47.04 36.13 26.10 26.42
 KM/MEAS .08292 .09673 .11054 .13014 .15382 .17599 .20089 .23156 .26453 1.07710 1.38856 1.63892
 MEAS/KM 12.0598 10.3360 8.0467 5.2389 3.1728 1.7286 1.0236 0.5722 0.3128 0.1715 0.0907 .06102
 EARS/MEAS .02242 .02615 .02990 .03739 .04586 .05586 .06745 .08061 .09544 .11240 .13131 .15386
 MEAS/RAP 44.5967 38.2217 33.4405 26.7467 15.0967 8.7051 4.3592 2.1868 1.188 2.6495 2.2033
 DEGR/MEAS .16131 .18018 .21504 .26174 .31808 .37608 .42571 .46552 1.60404 2.13430 2.65239 3.18634
 MEAS/DECK 6.1991 5.3141 4.6503 3.7211 2.6590 2.3271 1.8625 1.2430 .6234 .4685 .3756 .3136
 MEAS/PSCHT 387.37470263.50757230.60722184.54671131.90605115.45580 92.42557 61.71030 31.01079 23.33364 18.72719 15.65609

RADIUS 71379.000 KM ALTITUDE -43.000 KM PRESSURE 7.729324 BARS TEMPERATURE 229.482 KELVIN
 -141.075 KFT 7.620250 ATM -46.602 FAHRENHEIT
 TIME 1516.134 SEC VELOCITY 26.435 METER/SEC DYN P
 25.24550 MIN 7.8179 MB/SEC COPPLER
 .421148 HRS 86.770 FT/SEC PACH NO

INSTRUMENTS TEMP PRESS ACCEL ACCEL ACCEL M SPEC M SPEC M SPEC P SPC
 NC OF MEAS 506.59 434.18 380.03 304.23 217.50 190.52 152.61 102.08 51.54 38.50 31.32 26.27
 KM/MEAS .07926 .09246 .10566 .13205 .16776 .21115 .26384 .32537 .39843 1.04921 1.31900 1.56780
 MEAS/KM 12.6168 10.8155 9.4645 7.5731 5.4115 4.7359 3.7502 2.5293 1.2693 .5531 .7639 .6378
 EARS/MEAS .02346 .02738 .03129 .03812 .05079 .06263 .07622 .11750 .21588 .31512 .35466 .47452
 MEAS/RAP 42.6206 36.5283 31.9591 25.5823 18.2516 15.9670 12.7666 8.5440 4.2295 3.1734 2.5338 2.1074
 DEGR/MEAS .15419 .17987 .20555 .25688 .35950 .41077 .51326 .76914 1.57381 2.04113 2.54652 3.04999
 MEAS/DECK 6.4855 5.5595 4.8651 3.8928 2.7817 2.4344 1.9483 1.3001 .6520 .4899 .3927 .3279
 MEAS/PSCHT 325.922808282.63904247.52225198.07874141.57183123.91341 99.15160 66.22509 33.26620 25.02524 20.08052 16.78391

RADIUS 71376.000 KM ALTITUDE -46.000 KM PRESSURE 8.658967 BARS TEMPERATURE 235.318 KELVIN
 -150.919 KFT 8.543662 ATM -36.057 FAHRENHEIT
 TIME 1632.158 SEC VELOCITY 25.296 METER/SEC DYN P
 27.20264 MIN 8.1708 MB/SEC COPPLER
 .453377 HRS 82.991 FT/SEC PACH NO

INSTRUMENTS TEMP PRESS ACCEL ACCEL ACCEL M SPEC M SPEC M SPEC P SPC
 NC OF MEAS 545.85 467.53 409.04 327.43 234.17 205.02 164.22 105.61 55.41 41.80 33.64 28.20
 KM/MEAS .07595 .08948 .10111 .12636 .17684 .20307 .25245 .31740 .39473 1.01450 1.25337 1.50136
 MEAS/KM 13.1847 11.3022 9.8903 7.9137 5.6547 4.9488 3.9605 2.6427 1.3250 .5955 .7978 .6661
 EARS/MEAS .02452 .02861 .03270 .04049 .05726 .06545 .08185 .12280 .24645 .32920 .41224 .49559
 MEAS/RAP 40.7780 34.9883 30.5776 24.4578 17.4634 15.2777 12.2177 8.1376 4.0577 3.0377 2.4257 2.0178
 DEGR/MEAS .14755 .17212 .19670 .24593 .34483 .39310 .46121 1.46825 1.95414 2.43630 2.92074 .3424
 MEAS/DECK 6.7774 5.8097 5.0840 4.0679 2.9067 2.5439 2.0358 1.3585 .6911 .5117 .4101 .3424
 MEAS/PSCHT 353.50522303.051444255.20811218.22742151.57884132.7535106.25555 70.94534 35.62438 26.73392 21.45550 17.98810

SUBVARIABLE JUPITER PROBE TASK 3 DESCENT RUNS
 JOL MNCGRAP4 JUPITER COOL/CEASE ATMOSPHERE
 BALLISTIC COEFFICIENT = .090, INITIAL TIME = 0. SECONDS AT 71454.000 KM RADIUS

EAL. COEF. 0.65/0.00/1.50 SEP 10 RAD5

RADIUS 71373.000 KM		ALTITUDE -49.000 KM		PRESSURE 9.66924 BARS		TEMPERATURE 241.155 KELVIN	
		-160.781 KFT		9.545486 ATM		-25.552 FAHRENHEIT	
TIME	1753.344 SEC	VELOCITY	24.231 METER/SEC	DYN P			
	20.22240 MIN		8.5304 MP/SEC	COEFFLER	1.75681E+02 CFS		
	.487640 HRS		79.499 FT/SEC	MACH NO	.02255C		

INSTRUMENTS		TEMP	PRESS	ACCEL	ACCEL	ACCEL	M SPEC	M SPEC	M SPEC	M SPEC
NO OF MEAS	MEAS/KM	MEAS/MEAS	MEAS/MEAS	MEAS/MEAS	MEAS/MEAS	MEAS/MEAS	MEAS/MEAS	MEAS/MEAS	MEAS/MEAS	MEAS/MEAS
585.45	501.06	430.34	351.67	251.48	176.23	117.89	59.44	44.83	36.07	30.22
.07266	.04476	.06846	.12105	.16942	.19359	.32584	.72223	.96268	1.20133	1.43919
13.7634	11.7987	10.3243	9.2609	5.9026	5.1657	4.1340	2.7883	1.8827	1.3388	.8324
.02560	.02987	.03414	.04269	.05978	.06834	.08545	.12828	.25722	.34355	.43017
36.0569	33.4744	29.2876	23.2261	16.7272	14.6328	11.7030	7.7953	3.8877	2.5108	1.9339
.14135	.16489	.18943	.23549	.37058	.47056	.70528	1.40697	1.87279	2.33784	2.80150
7.0749	6.0647	5.3071	4.2464	3.0342	2.6553	2.1250	1.4176	.7107	.5340	.4277
MEAS/PSCHT	378.13777324	16163283.67552227	00456162.23314141	9926613.65152	75.87108	38.08729	28.64114	22.97330	19.19464	

RADIUS 71372.000 KM		ALTITUDE -50.000 KM		PRESSURE 10.02582 BARS		TEMPERATURE 243.100 KELVIN	
		-164.082 KFT		9.894875 ATM		-22.050 FAHRENHEIT	
TIME	1734.006 SEC	VELOCITY	23.892 METER/SEC	DYN P			
	20.91510 MIN		8.6551 MP/SEC	COEFFLER	1.732283E+02 CFS		
	.495585 HRS		78.386 FT/SEC	MACH NO	.022547		

INSTRUMENTS		TEMP	PRESS	ACCEL	ACCEL	ACCEL	M SPEC	M SPEC	M SPEC	M SPEC
NO OF MEAS	MEAS/KM	MEAS/MEAS	MEAS/MEAS	MEAS/MEAS	MEAS/MEAS	MEAS/MEAS	MEAS/MEAS	MEAS/MEAS	MEAS/MEAS	MEAS/MEAS
506.30	513.83	449.73	350.98	257.42	225.36	180.49	120.66	60.83	45.87	36.90
.07164	.08357	.09550	.11936	.16785	.19684	.33052	.71319	.94935	1.18473	1.41936
13.6887	11.9656	10.4708	8.7780	5.9863	5.2389	4.1525	2.7073	1.4022	1.0534	.8441
.02597	.03030	.03463	.04330	.06062	.06531	.08666	.13010	.26086	.34840	.43622
38.6083	33.0044	28.8764	23.0972	16.4925	14.4285	11.5389	7.6862	3.8335	2.8703	1.9072
.13565	.16291	.18616	.23267	.37562	.47209	.69454	1.39020	1.85054	2.30937	2.76672
7.1610	6.1385	5.3716	4.2980	3.0710	2.6876	2.1508	1.4351	.7193	.5404	.4330
MEAS/PSCHT	386.58354331	40088260.01398232	07206165.85822145	15.30116	18.824	77.56173	38.93198	29.27469	23.48019	19.61709

BALLISTIC COEFFICIENT CHANGED FROM .090 TO 1.500

ADDITIONAL BIT RATES REQUIRED TO READ OUT ENTRY DATA
 ONCE 1.788
 TWICE 7.577

SURVIVABLE JUPITER PROBE TASK 3 PERCENT RUNS
 JPL MICROGRAPH JUPITER COOL/CENSE ATMOSPHERE
 HALLISTIC COEFFICIENT = 1.500, INITIAL TIME = 1754.91 SECONDS AT 71372.000 KV RADTUS
 CAL. COEF. 0.65/0.00/1.50 SEP 10 BARS

SAMPLE INTERVALS (SECONDS)			
TEMP	PRESS	ACCEL	ACCEL
3.000	3.500	4.000	7.000
		8.000	10.000
		12.000	15.000
		20.000	30.000
		40.000	50.000
		60.000	80.000

BITT DEEP SAMPLE			
TEMP	PRESS	ACCEL	ACCEL
10.000	10.000	10.000	30.000
		30.000	40.000
		40.000	40.000
		40.000	40.000
		40.000	40.000
		40.000	40.000

NO OF PREVIOUS MEASUREMENTS			
TEMP	PRESS	ACCEL	ACCEL
519.302	513.430	449.726	350.081
		257.415	225.363
		180.491	120.660
		60.430	45.473
		36.698	30.915

RECLIPED BIT RATE = 61.7262 BITS/SECOND

ENTRY DATA IN STORAGE = 6800.0 BITS

```

UNRECOVERABLE JUPITER PROBE TASK 3 PERCENT RUNS
JCL MCAG08APR JUPITER COOL/CFN=CF ATMOSPHERE
BALLISTIC COEFFICIENT = 1.500, INITIAL TIME = 1764.81 SECONDS AT 71372.000 KM RADIUS
EAL. COEF. 0.66/0.39/1.50 SEE 10 PARS

```

[illegible][illegible][illegible]

PEOL. CCEF. 0.65/0.00/1.50

EOL. CCF. 0.65/0.00/1.50

SEP 10 2000

1993

0.65/9.00

703

ASSEMBLY	TEMP	DESS	TEMP	DESS	ACCEL	ACCEL	ACCEL	ACCFL	M SPEC	M SPEC	M SPEC	P SPEC	P SPEC
C OF MPIS	657.12	563.53	493.74	398.07	282.77	287.77	199.54	173.92	67.51	113.13	113.13	41.31	34.76
OF MPIS	279.93	279.93	279.93	279.93	557.69	537.04	557.69	1.50332	2.34337	1.12616	1.12616	4.66017	4.66017
OF MPIS	4.1756	3.5401	3.1733	2.5079	1.7931	1.5659	1.2571	.8401	.4231	.3189	.2583	.2166	.2166
OF MPIS	1.2558	1.5121	1.2861	1.2618	3.0266	3.4641	3.3245	.65180	1.31333	1.75974	2.21084	2.66554	2.66554
OF MPIS	7.7193	6.8131	5.7850	4.5257	3.2008	2.8467	2.3071	1.8342	.7614	.5623	.4524	.3752	.3752
OF MPIS	2.1304	5.9239	6.1937	7.7746	1.08209	1.34662	1.54462	2.1131	4.56099	6.06944	7.57594	9.04956	9.04956
OF MPIS	2.1304	1.4437	1.6136	1.9716	.9235	.8084	.6474	.4327	.2179	.1642	.1320	.1105	.1105
OF MPIS	120.55640111	100.44	97.25090	77.96151	55.70212	48.77729	39.06244	26.15576	13.22213	9.95954	8.05578	6.76224	6.76224

SURVIVABLE JUPITER PROBE TASK 3 DESCENT RUNS
 JPL MCNOSPAP JUPITER COOL/DENSE ATMOSPHERE
 BALLISTIC COEFFICIENT = 1.500, INITIAL TIME = 1758.91 SECONDS AT 71372.000 KM RADIUS

RAL. COEF. 0.65/0.09/1.50 SEP 10 PARS

RADIUS 71372.000 KM		ALTITUDE -68.000 KM		PRESSURE 18.405009 BARS		TEMPERATURE 278.155 KELVIN		41.610 FAHRENHEIT	
TIME 2003.429 SEC		VFLOCITY 77.025 METER/SEC		DYN P 5.584653E+02 CFS		ACCEL 252.45		M SPEC 52.09	
33.333715 MIN		252.708 FT/SEC		COFFLER 5.584653E+02 CFS		ACCEL 252.45		M SPEC 52.09	
.556553 HRS				PACT NO .067954		ACCEL 252.45		M SPEC 52.09	
INSTRUMENTS	TEMP	PRESS	ACCEL	ACCEL	ACCEL	ACCEL	ACCEL	ACCEL	M SPEC
NC OF MEAS	665.86	502.90	4.0272	286.23	252.45	202.36	135.57	68.79	52.09
KM/MEAS	.23075	.26914	.30752	.34422	.37440	.40128	.42816	.45504	42.07
MEAS/KM	4.3337	3.7155	3.2518	2.8027	2.4602	2.1304	1.8044	1.4788	3.76395
BARS/MEAS	.13451	.15696	.17943	.20439	.23145	.26054	.29178	.32416	.2657
MEAS/BAR	7.4345	6.3709	5.5732	4.9565	4.4445	3.9954	3.5954	3.2416	2.8156
DECK/MEAS	.44806	.52261	.59713	.67406	.75133	.82899	.90712	.98574	.4364
MEAS/DECK	2.2319	1.9135	1.6747	1.4304	.9583	.8389	.7118	.5869	7.30865
MEAS/PSHT	137.33065117	75544.103	82.52002	50.02965	51.68887	41.41172	27.70866	14.00469	10.57815

RADIUS 71351.000 KM		ALTITUDE -71.000 KM		PRESSURE 20.214791 BARS		TEMPERATURE 283.921 KELVIN		51.455 FAHRENHEIT	
TIME 2003.257 SEC		VFLOCITY 74.266 METER/SEC		DYN P 5.384631E+02 CFS		ACCEL 252.45		M SPEC 52.09	
34.05429 MIN		243.855 FT/SEC		COFFLER 5.384631E+02 CFS		ACCEL 252.45		M SPEC 52.09	
.567571 HRS				PACT NO .064844		ACCEL 252.45		M SPEC 52.09	
INSTRUMENTS	TEMP	PRESS	ACCEL	ACCEL	ACCEL	ACCEL	ACCEL	ACCEL	M SPEC
NC OF MEAS	683.09	585.79	512.81	410.65	293.89	257.41	206.33	138.22	70.11
KM/MEAS	.22250	.25953	.29653	.33050	.36924	.40292	.43252	.45808	42.87
MEAS/KM	4.4644	3.8532	3.3723	2.9990	2.6990	2.4690	2.2890	2.1490	3.63360
BARS/MEAS	.13052	.16281	.19511	.22774	.26113	.29522	.32992	.36512	.2752
MEAS/BAR	7.1675	6.1422	5.3732	4.7966	4.30683	3.8918	3.5243	3.2012	2.86128
DECK/MEAS	.43204	.50393	.57579	.64942	.72490	.80237	.88089	.95944	.4212
MEAS/DECK	2.3146	1.9844	1.7367	1.5000	.9937	.8699	.7555	.6454	8.43198
MEAS/PSHT	145.3858124	65991.109	87.35316	62.48190	54.70560	43.82833	29.31976	14.81035	11.18247

RADIUS 71348.000 KM		ALTITUDE -74.000 KM		PRESSURE 22.155585 BARS		TEMPERATURE 289.806 KELVIN		61.960 FAHRENHEIT	
TIME 2004.384 SEC		VFLOCITY 71.658 METER/SEC		DYN P 5.062753 BARS		ACCEL 252.45		M SPEC 52.09	
34.733574 MIN		235.100 FT/SEC		COFFLER 5.062753 BARS		ACCEL 252.45		M SPEC 52.09	
.578665 HRS				PACT NO .061935		ACCEL 252.45		M SPEC 52.09	
INSTRUMENTS	TEMP	PRESS	ACCEL	ACCEL	ACCEL	ACCEL	ACCEL	ACCEL	M SPEC
NC OF MEAS	696.79	597.54	523.10	418.88	299.77	262.55	210.44	140.96	71.48
KM/MEAS	.21470	.25043	.28615	.32574	.36913	.41624	.46614	.51884	43.69
MEAS/KM	4.6576	3.9931	3.4947	3.0769	2.7369	2.4613	2.2313	2.0413	3.51005
BARS/MEAS	.14481	.16875	.19289	.21822	.24512	.27349	.30344	.33504	.2849
MEAS/BAR	6.9152	5.9260	5.1842	4.6156	4.1456	3.7369	3.3769	3.0613	2.76170
DECK/MEAS	.41696	.48636	.55574	.62494	.69436	.76404	.83404	.90436	.4068
MEAS/DECK	2.3983	2.0561	1.7994	1.6401	1.4895	.9012	.7215	.5820	8.81753
MEAS/PSHT	153.73672131	61780.115	92.36369	66.86087	57.84120	46.33363	30.95000	15.64557	11.80897

RADIUS 71348.000 KM		ALTITUDE -74.000 KM		PRESSURE 22.155585 BARS		TEMPERATURE 289.806 KELVIN		61.960 FAHRENHEIT	
TIME 2004.384 SEC		VFLOCITY 71.658 METER/SEC		DYN P 5.062753 BARS		ACCEL 252.45		M SPEC 52.09	
34.733574 MIN		235.100 FT/SEC		COFFLER 5.062753 BARS		ACCEL 252.45		M SPEC 52.09	
.578665 HRS				PACT NO .061935		ACCEL 252.45		M SPEC 52.09	
INSTRUMENTS	TEMP	PRESS	ACCEL	ACCEL	ACCEL	ACCEL	ACCEL	ACCEL	M SPEC
NC OF MEAS	696.79	597.54	523.10	418.88	299.77	262.55	210.44	140.96	71.48
KM/MEAS	.21470	.25043	.28615	.32574	.36913	.41624	.46614	.51884	43.69
MEAS/KM	4.6576	3.9931	3.4947	3.0769	2.7369	2.4613	2.2313	2.0413	3.51005
BARS/MEAS	.14481	.16875	.19289	.21822	.24512	.27349	.30344	.33504	.2849
MEAS/BAR	6.9152	5.9260	5.1842	4.6156	4.1456	3.7369	3.3769	3.0613	2.76170
DECK/MEAS	.41696	.48636	.55574	.62494	.69436	.76404	.83404	.90436	.4068
MEAS/DECK	2.3983	2.0561	1.7994	1.6401	1.4895	.9012	.7215	.5820	8.81753
MEAS/PSHT	153.73672131	61780.115	92.36369	66.86087	57.84120	46.33363	30.95000	15.64557	11.80897

BALLISTIC COEFFICIENT = 1.500, INITIAL TIME = 1754.91 SECONDS AT 71372.000 KM RADIUS

SEP 10 9ARS

RADIUS	71345.000 KM	ALTITUDE	-77.000 KM	PRESSURE	24.247770 BARS	TEMPERATURE	295.633 KELVIN
			-252.625 KFT		23.930880 ATM		77.460 FAHRENHEIT

[illegible]

ALTIMETER	-80.000 KM	26.88320 BARS	301.460 KELVIN
ALTITUDE	-262.467 KFT	26.139574 ATM	62.957 FAHRENHEIT

[illegible]

ALTITUDE	83.000 KM	28.82281 BAR	307.227 KELVIN
ALTITUDE	71339.000 KM	28.50517 ATM	93.446 FAHRENHEIT

[illegible]

SURVIVABLE JUPITER PROBE TASK 3 DESCENT RUNS
 JPL MONTANA JUPITER COOL/DENSE ATMOSPHERE
 BALLISTIC COEFFICIENT = 1.500, INITIAL TIME = 1794.91 SECONDS AT 71372.000 KM RADIUS

EAL. COEFF. (.6570.00/1.50 SEP 10 PARS

RADIUS 71337.000 KM		ALTITUDE -85.000 KM		PRESSURE 30.572251 BARS		TEMPERATURE 311.172 KELVIN		100.429 FAHRENHEIT	
TIME 2248.029 SEC		VELOCITY -278.871 KFT		DYM P		ACCEL		M SPEC	
37.46715 MIN		63.226 METER/SEC		COEFLEP		ACCEL		M SPEC	
.524452 HRS		54.6088 METER/SEC		MACH NO		ACCEL		M SPEC	
		207.435 CT/SEC							
INSTRUMENTS	TEMP	DRESS	TEMP	DRESS	ACCEL	ACCEL	ACCEL	M SPEC	M SPEC
AC OF MEAS	751.34	644.29	564.01	451.51	373.15	283.00	226.80	151.87	76.93
KP/MEAS	.18548	.22102	.25255	.31558	.44151	.50441	.63008	.64350	1.87738
MEAS/KM	5.2776	4.5244	3.9595	3.1687	2.2549	1.9825	1.5871	1.0590	1.0810
BARS/MEAS	.16396	.19132	.21869	.27346	.37310	.43759	.54786	.62322	1.65438
MEAS/BARS	6.0991	5.2269	4.5727	3.6569	2.6103	2.2822	1.8252	1.2147	2.21422
DECK/MEAS	.36820	.42949	.49076	.51324	.55794	.60016	1.22436	1.83338	3.64810
MEAS/DECK	2.7159	2.3284	2.0377	1.6307	1.1656	1.0202	.8168	.5854	4.84780
MEAS/PSCT	196.96182160	20646140	20744112	208278	209026	70.30070	56.30127	37.63521	19.96849
									14.30139
									11.50088
									9.63366

ADDITIONAL PIT RATES REQUIRED TO READ OUT ENTRY DATA

CNCF 1.025
 TIME 6.050

```

P$INPT
TITLE=50H SURVIVABLE SATURN PROBE TASK 4 DESCENT RUNS
XNOTE=50H BAL. COEF. 0.65/0.70/1.50 SEP 30 BARS
DS=0.70,
IATM=1,
$RSTART=59900., TSTART=0,
RSTOP=59480., TSTOP=1.0E+08,
DR=5.,
STORD=7850.,
FREQ=2.4E+09, EZA=25.,
XNAME=6H TEMP, 6H PRESS, 6H TEMP, 5H PRESS, 6H ACCEL, 6H ACCEL,
        6H ACCEL, 6H ACCEL, 6H SPEC, 6H SPEC, 6H SPEC, 6H SPEC, 6H SPEC,
DTI(1,1)=3., 3., 3., 4., 5., 7., 8., 10., 15., 30., 40., 50., 60.,
DTI(1,2)=3., 3., 3., 4., 5., 7., 8., 10., 15., 30., 40., 50., 60.,
BPS(1,1)=10., 10., 10., 10., 30., 30., 30., 30., 400., 400., 400.,
BPS(1,2)=10., 10., 10., 10., 30., 30., 30., 30., 400., 400., 400.,
NSTAG=2,
BCHG(2)=1.50,
RCHG(2)=59484.0,
$

```

SURVIVABLE SATURN PROBE TASK 4 DESCENT RUNS
JP. MONOGRAPH SATURN NOMINAL ATMOSPHERE

BALLISTIC COEFFICIENT = .700, INITIAL TIME = 0. SECONDS AT 59900.000 KM RADIUS

BAL. COEF. 0.65/0.70/1.50 SEP 30 BARS

SAMPLE INTERVALS (SECONDS)

TEMP	PRESS	TEMP	PRESS	ACCEL	ACCEL	ACCEL	ACCEL	ACCEL	M SPEC	M SPEC	M SPEC	M SPEC
3.000	3.500	4.000	5.000	7.000	8.000	10.000	10.000	15.000	30.000	40.000	50.000	60.000

BITS PER SAMPLE

TEMP	PRESS	TEMP	PRESS	ACCEL	ACCEL	ACCEL	ACCEL	ACCEL	M SPEC	M SPEC	M SPEC	M SPEC
10.000	10.000	10.000	10.000	30.000	30.000	30.000	30.000	30.000	400.000	400.000	400.000	400.000

NO OF PREVIOUS MEASUREMENTS

TEMP	PRESS	TEMP	PRESS	ACCEL	ACCEL	ACCEL	ACCEL	ACCEL	M SPEC	M SPEC	M SPEC	M SPEC
0.	0.	0.	0.	0.	0.	0.	0.	0.	0.	0.	0.	0.

REQUIRED BIT RATE = 61.7262 BITS/SECOND

ENTRY DATA IN STORAGE = 7850.0 BITS

SURVIVABLE SATURN PROBE TASK 4 DESCENT RUNS
JP MONOGRAPH SATURN NOMINAL ATMOSPHERE

BALLISTIC COEFFICIENT = .700, INITIAL TIME = 0. SECONDS AT 5900.000 KM RADIUS

BAL. COEF. 0.65/0.70/1.50 SEP 30 BARS

RADIUS 5900.000 KM										TEMPERATURE 77.000 KELVIN -321.070 FAHRENHEIT									
TIME		0.	SEC	ALTITUDE	100.000 K4	PRESSURE	0.68489 BARS	0.47855 ATM	0.11521 BARS	TEMPERATURE		77.000 KELVIN	-321.070 FAHRENHEIT						
0.		MIN	VELOCITY	328.084 KFT	365.969 METER/SEC	DYN P	0.65344E+03 CPS	0.576276	0.11521 BARS										
0.		HRS		1200.684 FT/SEC		MACH NO													
INSTRUMENTS																			
NO OF MEAS	TEMP	PRESS	TEMP	PRESS	ACCEL	ACCEL	ACCEL	ACCEL	ACCEL	M SPEC	M SPEC	M SPEC	M SPEC	M SPEC	M SPEC	M SPEC	M SPEC	M SPEC	M SPEC
1.00	1.00	1.00	1.00	1.00	1.00	1.00	1.00	1.00	1.00	1.00	1.00	1.00	1.00	1.00	1.00	1.00	1.00	1.00	1.00
1.00687	1.26590	1.44434	1.79945	2.50273	2.85036	3.54073	5.22747	9.99212	12.94934	15.75253	18.41690								
.9201	.7900	.6924	.5557	.3996	.3508	.2824	.1913	.1001	.0772	.0635	.0543								
.00200	.00233	.00267	.00335	.00472	.00541	.00681	.01039	.02178	.02994	.03855	.04760								
500.8449	429.5737	374.3725	298.4959	211.7939	184.7037	146.7920	96.2769	45.9085	33.3998	25.9425	21.0077								
DEGK/MEAS	0.	0.	0.	0.	0.	0.	0.	0.	0.	0.	0.								
MEAS/DEGK																			
MEAS/PSGHT	24.78203	21.27714	18.64843	14.95816	10.76190	9.44735	7.60682	5.15219	2.69520	2.07960	1.70945								

RADIUS 59895.000 KM										TEMPERATURE 77.000 KELVIN -321.070 FAHRENHEIT									
TIME		14.317 SEC	ALTITUDE		95.000 K4	PRESSURE		.058380 BARS	.057617 ATM		.011521 BARS		.011521 BARS						
.23861 MIN		.003977 HRS	VELOCITY		311.680 KFT	333.555 METER/SEC		DYN P	2.418428E+03 CPS		2.525236								
			1094.341 FT/SEC					MACH NO											
INSTRUMENTS																			
NO OF MEAS	TEMP	PRESS	TEMP	PRESS	ACCEL	ACCEL	ACCEL	ACCEL	ACCEL	M SPEC	M SPEC	M SPEC	M SPEC	M SPEC	M SPEC	M SPEC	M SPEC	M SPEC	
5.77	5.09	4.58	3.86	3.05	2.79	2.43	1.95	1.48	1.36	1.29	1.24								
.99148	1.15497	1.31796	1.64247	2.28563	2.60444	3.23634	4.78438	9.17814	11.91995	14.52882	17.01705								
1.0086	.6658	.7587	.5088	.4375	.3840	.3090	.2090	.1090	.0839	.0688	.0588								
.00219	.00256	.00293	.00367	.00517	.00593	.00746	.01135	.02371	.03251	.04176	.05146								
456.7412	390.6918	341.5063	272.3705	193.3689	163.6836	134.1364	88.0908	42.1739	30.7573	23.9449	19.4321								
0.	0.	0.	0.	0.	0.	0.	0.	0.	0.	0.	0.								
MEAS/DEGK																			
MEAS/PSGHT	27.16166	23.31684	20.43319	16.39601	11.78108	10.33987	8.32092	5.62844	2.33378	2.25885	1.85316								

RADIUS 59890.000 KM										TEMPERATURE 77.000 KELVIN -321.070 FAHRENHEIT									
TIME		30.024 SEC	ALTITUDE	90.000 K4	PRESSURE	0.70292 BARS	0.69373 ATM	0.11521 BARS	0.11521 BARS	TEMPERATURE		77.000 KELVIN	-321.070 FAHRENHEIT						
.50041 MIN		.008340 HRS	VELOCITY	295.276 KFT	304.008 METER/SEC	DYN P	2.204196E+03 CPS	2.478709	0.11521 BARS										
			997.401 FT/SEC			MACH NO													
INSTRUMENTS																			
NO OF MEAS	TEMP	PRESS	TEMP	PRESS	ACCEL	ACCEL	ACCEL	ACCEL	ACCEL	M SPEC	M SPEC	M SPEC	M SPEC	M SPEC	M SPEC	M SPEC	M SPEC	M SPEC	M SPEC
11.01	9.58	8.51	7.00	5.29	4.75	4.00	3.70	3.00	2.00	1.75	1.50								
.90439	1.05365	1.20250	1.43898	2.08708	2.37874	2.95736	4.37728	8.42529	10.96416	13.38863	15.70855								
1.1057	.9491	.8316	.6671	.4791	.4204	.3381	.2295	.1187	.0912	.0747	.0637								
.00240	.00281	.00321	.00402	.00567	.00639	.00816	.01241	.02583	.03534	.04529	.05570								
416.4823	355.4950	311.4883	248.4958	176.5125	154.0214	122.5394	80.5848	38.7168	28.2997	22.0787	17.9540								
DEGK/MEAS	0.	0.	0.	0.	0.	0.	0.	0.	0.	0.	0.								
MEAS/DEGK																			
MEAS/PSGHT	29.77253	25.55475	22.39138	17.95260	12.90095	11.31910	9.10438	6.15092	3.19544	2.45540	2.01068								

RADARS 59805.000 KM													
TIME	ALTITUDE		85.000 KM		PRESSJRE		.084836 BAKS		TEMPERATURE		77.000 KELVIN		
	278.871 KFT						.083530 ATM		-321.070 FAHRENHEIT				
	VELOCITY		277.073 METER/SEC		DYV P		.011521 BARS						
.78765 MINS		.8712 MB/SEC		DOPPLER		2.008911E+03 CPS							
.013128 HRS		909.034 FT/SEC		MACH NO		.436296							
INSTRUMENTS													
NO OF MEAS	TEMP	PRESS	TEMP	PRESS	ACCEL	ACCEL	ACCEL	ACCEL	M SPEC	M SPEC	M SPEC	M SPEC	
	16.75	14.50	12.81	10.45	7.75	6.31	5.73	4.15	2.58	2.18	1.95	1.79	
	WM/KM/MEAS	.82487	.96113	1.09704	1.35784	1.90540	2.17218	2.70380	4.00359	7.72975	16.07790	12.32785	14.48746
KM/MEAS	1.2123	1.0404	.9115	.7311	.5248	.4804	.3701	.2498	.1294	.0992	.6811	.0690	
	MEAS/KM	.00308	.00352	.00441	.00621	.00711	.00894	.01357	.02815	.03854	.04917	.06035	
	BARS/MEAS	379.7389	325.0747	284.0775	226.5837	161.0969	140.6038	111.9177	73.6859	35.5205	26.0177	20.5386	16.5705
MEAS/BAR	0.	0.	0.	0.	0.	0.	0.	0.	0.	0.	0.	0.	
	DECK/MEAS	0.	0.	0.	0.	0.	0.	0.	0.	0.	0.	0.	
	MEAS/DECK	32.63717	28.01017	24.53990	19.68145	14.12877	12.39347	9.96395	6.72412	3.448243	2.67092	2.18337	1.85783
MEAS/PSGHT													
RADARS 59880.000 KM													
TIME	ALTITUDE		80.000 KM		PRESSJRE		.101911 BAKS		TEMPERATURE		77.000 KELVIN		
	262.467 KFT						.100579 ATM		-321.070 FAHRENHEIT				
	VELOCITY		252.522 METER/SEC		DYV P		.011526 BARS						
65.169 SEC		.9565 MB/SEC		DOPPLER		1.830898E+03 CPS							
1.10282 MIN		.9565 MB/SEC		MACH NO		.397636							
.018380 HRS		828.483 FT/SEC											
INSTRUMENTS													
NO OF MEAS	TEMP	PRESS	TEMP	PRESS	ACCEL	ACCEL	ACCEL	ACCEL	M SPEC	M SPEC	M SPEC	M SPEC	
	23.06	19.91	17.54	14.23	10.45	9.27	7.62	5.41	3.21	2.65	2.32	2.10	
	WM/KM/MEAS	.75228	.87665	1.00073	1.24803	1.73925	1.98319	2.46778	3.66050	7.08782	9.26715	11.34240	13.43518
KM/MEAS	1.3293	1.1407	.9993	.8013	.5750	.5042	.4052	.2732	.1411	.1080	.0882	.0744	
	MEAS/KM	.00289	.00337	.00386	.00484	.00680	.00779	.01485	.03070	.04134	.05342	.06597	
	BARS/MEAS	346.2091	295.4049	259.0524	206.7606	147.0034	123.3313	102.1936	67.3559	32.5690	23.9020	18.7195	15.1578
MEAS/BAR	0.	0.	0.	0.	0.	0.	0.	0.	0.	0.	0.	0.	
	DECK/MEAS	0.	0.	0.	0.	0.	0.	0.	0.	0.	0.	0.	
	MEAS/DECK	35.78030	30.70430	26.89720	21.55739	15.47592	13.57227	10.90705	7.35300	3.79723	2.90728	2.37271	2.00333
MEAS/PSGHT													
RADARS 59875.000 KM													
TIME	ALTITUDE		75.000 KM		PRESSJRE		.122716 BAKS		TEMPERATURE		77.000 KELVIN		
	246.063 KFT						.121111 ATM		-321.070 FAHRENHEIT				
	VELOCITY		230.142 METER/SEC		DYV P		.011526 BARS						
85.918 SEC		1.0497 MB/SEC		DOPPLER		1.668634E+03 CPS							
1.144864 MIN		.755.058 FT/SEC		MACH NO		.362395							
.024144 HRS													
INSTRUMENTS													
NO OF MEAS	TEMP	PRESS	TEMP	PRESS	ACCEL	ACCEL	ACCEL	ACCEL	M SPEC	M SPEC	M SPEC	M SPEC	
	29.97	25.83	22.73	18.38	13.42	11.96	9.69	6.79	3.90	3.17	2.74	2.45	
	WM/KM/MEAS	.68603	.79953	.94278	1.13958	1.58735	1.81034	2.25357	3.34594	6.449596	8.53151	10.54232	12.51270
KM/MEAS	1.4577	1.2507	1.0956	.8783	.6300	.5324	.4437	.2989	.1539	.1172	.0949	.0799	
	MEAS/KM	.00317	.00370	.00423	.00530	.00745	.00954	.01072	.01625	.02350	.04577	.05855	
	BARS/MEAS	315.6152	270.2407	236.2095	188.5672	134.1224	117.1130	93.2951	61.5514	29.8466	21.8507	17.4802	13.9556
MEAS/BAR	0.	0.	0.	0.	0.	0.	0.	0.	0.	0.	0.	0.	
	DECK/MEAS	0.	0.	0.	0.	0.	0.	0.	0.	0.	0.	0.	
	MEAS/DECK	39.22904	33.66038	29.44836	23.63668	16.95403	11.86556	11.94182	8.04298	4.14255	3.15506	2.56359	2.17438
MEAS/PSGHT													

SURVIVABLE SATURN PROBE TASK 4 DESCENT RUNS
JP. MONOGRAPH SATURN NOMINAL ATMOSPHERE

BALLISTIC COEFFICIENT = .700, INITIAL TIME = 0. SECONDS AT 59900.000 KM RADIUS

BAL. COEF. 0.55/0.70/1.50 SEP 30 BARS

RADIJS 59870.000 KM		70.000 KM		PRESSURE		147772 BARS		TEMPERATURE		77.000 KELVIN	
		229.659 KT				.145840 ATM				-321.070 FAHRENHEIT	
TIME	103.685 SEC	VELOCITY	209.742 METER/SEC	DYN P							
	1.52609 MIN		1.1520 MB/SEC	JOPPLER							
	.030460 HRS		688.130 FT/SEC	MACH NO							

INSTRUMENTS		TEMP	PRESS	ACCEL	ACCEL	ACCEL	ACCEL	M SPEC	M SPEC	M SPEC	M SPEC
NO OF MEAS	37.56	32.34	28.42	22.94	16.67	14.71	11.97	8.31	4.66	3.74	3.19
KM/MEAS	.62558	.72914	.83250	1.03862	1.44852	1.65231	2.05750	3.05003	6.01630	7.93579	9.81799
MEAS/KM	1.5995	1.3715	1.2012	.9628	.6904	.5032	.3268	.2060	.1260	.1019	.0857
BARS/MEAS	.00348	.00406	.00464	.00582	.00817	.00936	.01174	.01780	.03659	.06266	.07617
MEAS/BAR	287.7066	243.3665	215.3620	171.3565	122.3529	103.6530	85.1550	56.1877	27.3292	20.2058	15.9528
DECK/MEAS	0.	0.	0.	0.	0.	0.	0.	0.	3.24239	5.23955	7.19791
MEAS/DECK	43.01317	36.30393	32.32199	25.90721	18.57591	16.28482	13.07720	8.79351	4.52008	3.46182	2.82798
MEAS/PSCHT											

RADIJS 59865.000 KM		65.000 KM		PRESSURE		177757 BARS		TEMPERATURE		79.185 KELVIN	
		213.255 KT				.175433 ATM				-317.137 FAHRENHEIT	
TIME	134.483 SEC	VELOCITY	193.946 METER/SEC	DYN P							
	2.24139 MIN		1.2457 MB/SEC	JOPPLER							
	.037356 HRS		636.306 FT/SEC	MACH NO							

INSTRUMENTS		TEMP	PRESS	ACCEL	ACCEL	ACCEL	ACCEL	M SPEC	M SPEC	M SPEC	M SPEC
NO OF MEAS	45.83	39.42	34.62	27.90	20.21	17.91	14.45	9.97	5.48	4.36	3.69
KM/MEAS	.57391	.67619	.77236	.98440	1.34722	1.53802	1.91841	2.86244	5.53844	7.44574	9.22120
MEAS/KM	1.7244	1.4789	1.2947	1.0369	.7423	.5502	.3494	.213	.1774	.1343	.1084
BARS/MEAS	.00375	.00438	.00501	.00627	.00879	.01006	.01260	.01900	.03862	.05204	.06573
MEAS/BAR	266.6141	223.3993	199.7385	159.8137	113.7579	93.4235	79.3680	52.6237	25.8915	19.2154	15.2140
DECK/MEAS	.60337	.70355	.80361	1.00342	1.40173	1.60025	1.99603	2.97826	5.86659	7.74702	9.59431
MEAS/DECK	1.6574	1.4214	1.2444	.9966	.7134	.6249	.5010	.3358	.1705	.1291	.1042
MEAS/PSCHT	47.89082	41.09760	35.00264	28.85959	20.71726	18.16934	14.60253	9.84579	5.08602	3.89431	3.17822

RADIJS 59860.000 KM		60.000 KM		PRESSURE		211762 BARS		TEMPERATURE		84.387 KELVIN	
		136.850 KT				.209993 ATM				-307.773 FAHRENHEIT	
TIME	160.995 SEC	VELOCITY	183.433 METER/SEC	DYN P							
	2.68325 MIN		1.3182 MB/SEC	JOPPLER							
	.044721 HRS		601.879 FT/SEC	MACH NO							

INSTRUMENTS		TEMP	PRESS	ACCEL	ACCEL	ACCEL	ACCEL	M SPEC	M SPEC	M SPEC	M SPEC
NO OF MEAS	54.57	47.00	41.25	33.20	24.00	21.12	17.10	11.73	6.37	5.02	4.22
KM/MEAS	.54873	.63988	.73093	.91278	1.27542	1.45622	1.81679	2.71236	5.35118	7.07311	8.76742
MEAS/KM	1.8224	1.5628	1.3681	1.0956	.7841	.6857	.5504	.3687	.1869	.1414	.1141
BARS/MEAS	.00397	.00463	.00529	.00662	.00929	.01063	.01331	.02006	.04070	.05478	.06911
MEAS/BAR	252.1939	215.0637	188.9625	151.0211	107.6603	94.1104	75.1412	49.8511	24.5701	18.2552	14.4694
DECK/MEAS	.57034	.66577	.76051	.94971	1.32702	1.51514	1.89030	2.82210	5.36770	7.35930	9.12217
MEAS/DECK	1.7515	1.5020	1.3149	1.0530	.7535	.6600	.5290	.3543	.1796	.1359	.1096
MEAS/PSCHT	53.90462	46.23231	40.51304	32.47797	23.29479	20.42434	16.40697	11.04902	5.68837	4.34660	3.54057

BAL. COEF. 0.65/0.70/1.50 SEP 30 BARS

INSTRUMENTS	TEMP	PRESS	TEMP	PRESS	ACCE-	ACCEL	ACCEL	M SPEC	N SPEC	M SPEC	N SPEC
KNO/MEAS	63.99	50.93	48.24	38.80	28.60	24.32	13.60	7.30	5.72	4.78	4.15
KNO/MEAS	52.093	50.749	69.397	86.671	1.21129	1.38313	1.72595	5.09277	8.35550	9.95152	9.95152
MEAS/KM	1.9196	1.6461	1.4410	1.1538	0.8255	0.7230	0.5794	0.1964	0.1484	0.1197	0.1005
BARS/MEAS	0.00418	0.0488	0.0358	0.0698	0.0978	0.1119	0.2111	0.04277	0.05751	0.07249	0.08771
MEAS/BAR	239.319	205.0596	179.3479	143.3518	102.2140	83.3588	71.3618	47.3676	23.3804	17.3890	11.4016
DECK/MEAS	5.8201	5.3207	7.2205	9.0178	1.26030	1.43310	1.79579	2.60288	5.29892	8.61164	10.23077
MEAS/DISK	1.0450	1.3621	1.3849	1.1089	0.7935	0.6949	0.5563	0.1887	0.1435	0.1161	0.0978
MEAS/P3GHT	60.250+0	51.69157	45.27242	35.28352	26.01455	22.00879	18.31093	12.31838	6.32376	4.82390	3.32133

INSTRUMENTS	TEMP	PRESS	TEMP	PRESS	ACCEL	ACCEL	ACCEL	M SPEC	M SPEC	M SPEC	M SPEC
NO OF MEAS	73.81	63.40	55.60	32.20	28.30	15.36	8.28	6.46	5.37	4.64	
KM/H MEAS	4.5597	5.7839	6.6076	.82329	1.31733	2.45654	4.85776	6.43004	7.98087	9.51136	
MEAS/KM	2.0163	1.7289	1.5134	1.2217	.8663	.7531	.6082	.4071	.2059	.1555	.1051
BAR/S/MEAS	.00433	.00512	.00586	.00733	.01023	.01175	.01472	.02216	.03446	.05026	.07591
MEAS/BAR	227.7984	195.4773	170.7115	136.4594	97.3145	85.0820	67.9567	45.1243	22.2974	15.5939	10.8954
DESK/MEAS	.50835	.59197	.67553	.84244	1.17563	1.34352	2.49734	4.93336	6.52842	8.10173	9.65440
MEAS/DESK	1.9672	1.6294	1.4803	1.1870	.8507	.7454	.5977	.4004	.2027	.1532	.1036
MEAS/PSI/H	66.92535	57.41693	50.72824	40.29383	28.87235	20.33092	13.65225	6.99005	5.32226	4.32226	3.65434

[illegible]

SURVIVABLE SATURN PROBE TASK 4 DESCENT RUNS

JP - MNOGRAPH SATURN NOMINAL ATMOSPHERE

BALLISTIC COEFFICIENT = .700, INITIAL TIME = 0. SECONDS AT 59900.000 KM RADIUS

BAL. COEF. 0.0570.70/1.50

SEP 30 BARS

RADIUS 59840.000 KM		ALTITUDE		PRESS		TEMP		PRESS		ACCEL		PRESSURE		BARS		TEMPERATURE		104.942 KELVIN		-270.774 FAHRENHEIT	
TIME	281.678 SEC	VELOCITY	131.234 KFT	131.234 KFT	57.34	41.24	36.21	1.05269	1.20229	1.50091	2.24411	19.78	10.39	8.04	5.8198	7.32119	8.73439	8.73439	8.73439	8.73439	8.73439
NO OF MEAS	94.89																				
KM/MEAS	.45234																				
MEAS/KM	2.2107	1.8953																			
BARS/MEAS	.00482	.00562																			
MEAS/BAR	207.8200	177.9008	155.6114	124.8064	88.7438	77.5994	61.9974	41.1956	20.3973	15.1999	12.0826	10.0055									
DECK/MEAS	.45890	.53520	.61146	.73382	1.06795	1.21971	1.52266	2.27663	4.51048	5.97737	7.42729	8.86098									
MEAS/DECK	2.1791	1.8685	1.6354	1.3092	.9364	.8139	.6567	.5392	.4217	.3173	.2346	.1129									
MEAS/PSCHT	81.18862	69.62120	60.96061	48.83572	34.97854	30.64810	24.58537	16.50129	8.41538	6.39279	5.17856	4.36853									

RADIUS 59835.000 KM		ALTITUDE		PRESS		TEMP		PRESS		ACCEL		PRESSURE		BARS		TEMPERATURE		110.014 KELVIN		-261.644 FAHRENHEIT	
TIME	315.495 SEC	VELOCITY	114.829 KFT	114.829 KFT	46.07	40.44	32.55	1.15225	1.15225	1.63860	2.15152	4.26590	5.65598	7.03120	8.39214	8.39214	8.39214	8.39214	8.39214	8.39214	8.39214
NO OF MEAS	106.17																				
KM/MEAS	.43339																				
MEAS/KM	2.3074	1.9783																			
BARS/MEAS	.00503	.00567																			
MEAS/BAR	198.8570	173.3970	149.0520	119.1691	85.0175	74.3432	59.4042	39.4835	19.5657	14.5879	11.6023	9.6127									
DECK/MEAS	.43967	.51280	.58588	.73191	1.02344	1.16835	1.45944	2.18271	4.32773	5.73796	7.13310	8.51377									
MEAS/DECK	2.2744	1.9501	1.7068	1.3663	.9771	.8535	.6852	.4581	.2311	.1743	.1402	.1175									
MEAS/PSCHT	88.78064	76.14580	65.66964	53.40297	38.24091	33.50270	26.86910	18.02390	9.17701	6.96427	5.63599	4.74997									

RADIUS 59830.000 KM		ALTITUDE		PRESS		TEMP		PRESS		ACCEL		PRESSURE		BARS		TEMPERATURE		115.007 KELVIN		-252.513 FAHRENHEIT	
TIME	350.763 SEC	VELOCITY	98.425 KFT	98.425 KFT	46.07	40.44	32.55	1.15225	1.15225	1.63860	2.15152	4.26590	5.65598	7.03120	8.39214	8.39214	8.39214	8.39214	8.39214	8.39214	8.39214
NO OF MEAS	106.17																				
KM/MEAS	.43339																				
MEAS/KM	2.3074	1.9783																			
BARS/MEAS	.00503	.00567																			
MEAS/BAR	198.8570	173.3970	149.0520	119.1691	85.0175	74.3432	59.4042	39.4835	19.5657	14.5879	11.6023	9.6127									
DECK/MEAS	.43967	.51280	.58588	.73191	1.02344	1.16835	1.45944	2.18271	4.32773	5.73796	7.13310	8.51377									
MEAS/DECK	2.2744	1.9501	1.7068	1.3663	.9771	.8535	.6852	.4581	.2311	.1743	.1402	.1175									
MEAS/PSCHT	88.78064	76.14580	65.66964	53.40297	38.24091	33.50270	26.86910	18.02390	9.17701	6.96427	5.63599	4.74997									

RADIUS 59830.000 KM		ALTITUDE		PRESS		TEMP		PRESS		ACCEL		PRESSURE		BARS		TEMPERATURE		115.007 KELVIN		-252.513 FAHRENHEIT	
TIME	350.763 SEC	VELOCITY	98.425 KFT	98.425 KFT	46.07	40.44	32.55	1.15225	1.15225	1.63860	2.15152	4.26590	5.65598	7.03120	8.39214	8.39214	8.39214	8.39214	8.39214	8.39214	8.39214
NO OF MEAS	106.17																				
KM/MEAS	.43339																				
MEAS/KM	2.3074	1.9783																			
BARS/MEAS	.00503	.00567																			
MEAS/BAR	198.8570	173.3970	149.0520	119.1691	85.0175	74.3432	59.4042	39.4835	19.5657	14.5879	11.6023	9.6127									
DECK/MEAS	.43967	.51280	.58588	.73191	1.02344	1.16835	1.45944	2.18271	4.32773	5.73796	7.13310	8.51377									
MEAS/DECK	2.2744	1.9501	1.7068	1.3663	.9771	.8535	.6852	.4581	.2311	.1743	.1402	.1175									
MEAS/PSCHT	88.78064	76.14580	65.66964	53.40297	38.24091	33.50270	26.86910	18.02390	9.17701	6.96427	5.63599	4.74997									

RADIUS 59830.000 KM		ALTITUDE		PRESS		TEMP		PRESS		ACCEL		PRESSURE		BARS		TEMPERATURE		115.007 KELVIN		-252.513 FAHRENHEIT	
TIME	350.763 SEC	VELOCITY	98.425 KFT	98.425 KFT	46.07	40.44	32.55	1.15225	1.15225	1.63860	2.15152	4.26590	5.65598	7.03120	8.39214	8.39214	8.39214	8.39214	8.39214	8.39214	8.39214
NO OF MEAS	106.17																				
KM/MEAS	.43339																				
MEAS/KM	2.3074	1.9783																			
BARS/MEAS	.00503	.00567																			
MEAS/BAR	198.8570	173.3970	149.0520	119.1691	85.0175	74.3432	59.4042	39.4835	19.5657	14.5879	11.6023	9.6127									
DECK/MEAS	.43967	.51280	.58588	.73191	1.02344	1.16835	1.45944	2.18271	4.32773	5.73796	7.13310	8.51377									
MEAS/DECK	2.2744	1.9501	1.7068	1.3663	.9771	.8535	.6852	.4581	.2311	.1743	.1402	.1175									
MEAS/PSCHT	88.78064	76.14580	65.66964	53.40297	38.24091	33.50270	26.86910	18.02390	9.17701	6.96427	5.63599	4.74997									

RADIUS 59830.000 KM		ALTITUDE		PRESS		TEMP		PRESS		ACCEL		PRESSURE		BARS		TEMPERATURE		115.007 KELVIN		-252.513 FAHRENHEIT	
TIME	350.763 SEC	VELOCITY	98.425 KFT	98.425 KFT	46.07	40.44	32.55	1.15225	1.15225	1.63860	2.15152	4.26590	5.65598	7.03120	8.39214	8.39214	8.39214	8.39214	8.39214	8.39214	8.39214
NO OF MEAS	106.17																				
KM/MEAS	.43339																				
MEAS/KM	2.3074	1.9783																			
BARS/MEAS	.00503	.00567																			
MEAS/BAR	198.8570	173.3970	149.0520	119.1691	85.0175	74.3432	59.4042	39.4835	19.5657	14.5879	11.6023	9.6127									
DECK/MEAS	.43967	.51280	.58588	.73191	1.02344	1.16835	1.45944	2.18271	4.32773	5.73796	7.13310	8.51377									
MEAS/DECK	2.2744	1.9501	1.7068	1.3663	.9771	.8535	.6852	.4581	.2311	.1743	.1402	.1175									
MEAS/PSCHT	88.78064	76.14580	65.66964	53.40297	38.24091	33.50270	26.86910	18.02390	9.17701	6.96427	5.63599	4.74997									

SURVIVABLE SATURN PROBE TASK 4 DESCENT RUNS
JP. MONOGRAPH SATURN NOMINAL ATMOSPHERE

BALLISTIC COEFFICIENT = .700, INITIAL TIME = 0. SECONDS AT 59900.000 KM RADIUS

BAL. COEF. 0.65/0.70/1.50 SEP 30 BARS

RADIUS 59825.000 KM										TEMPERATURE 120.159 KELVIN -243.383 FAHRENHEIT									
ALTIUDE 29.000 KM										PRESSURE .569545 BARS									
82.021 KFT										.562098 ATM									
TIME 387.475 SEC										DYN P .011546 BARS									
VELOCITY 133.561 METER/SEC										DOPP-ER 9.683758E+02 CPS									
6.45792 MIN										MACH NO .168357									
.107632 HRS																			
INSTRUMENTS																			
NO OF MEAS	TEMP	PRESS	TEMP	PRESS	ACCEL	ACCEL	ACCEL	ACCEL	ACCEL	M SPEC	M SPEC	M SPEC	M SPEC	M SPEC	M SPEC	M SPEC	M SPEC	M SPEC	M SPEC
130.16	111.71	97.87	78.50	56.35	49.43	39.75	26.83	13.92	10.69	8.75	7.46								
40.007	.46662	.5315	.66610	.93159	1.06413	1.32882	1.98823	3.94720	5.23768	6.51826	7.78336								
2.4996	2.1431	1.8757	1.5013	1.0734	.9337	.7525	.5030	.2533	.1909	.1535	.1285								
.80545	.00636	.00727	.00909	.01275	.01437	.01824	.02742	.05327	.07406	.09304	.11220								
183.4425	157.1960	137.5111	109.3522	78.4566	68.6143	54.8352	36.4635	18.0937	13.5023	10.7482	8.9127								
.40586	.47339	.54088	.67575	.94503	1.07955	1.34808	2.01705	4.00440	5.31359	6.61070	7.89616								
2.4639	2.1124	1.8489	1.4798	1.0561	.9253	.7418	.4958	.2497	.1882	.1513	.1266								
MEAS/PSCHT 104.97805	90.02930	78.81772	63.12147	45.18275	39.57686	31.72851	21.26370	10.79745	8.18001	6.60901	5.56123								
RADIUS 59820.000 KM										TEMPERATURE 125.232 KELVIN -234.253 FAHRENHEIT									
ALTIUDE 20.000 KM										PRESSURE .640118 BARS									
65.617 KFT										.631747 ATM									
TIME 425.627 SEC										DYN P .011546 BARS									
VELOCITY 128.626 METER/SEC										DOPP-ER 9.325945E+02 CPS									
7.09378 MIN										MACH NO .158819									
.118230 HRS																			
INSTRUMENTS																			
NO OF MEAS	TEMP	PRESS	TEMP	PRESS	ACCEL	ACCEL	ACCEL	ACCEL	ACCEL	M SPEC	M SPEC	M SPEC	M SPEC	M SPEC	M SPEC	M SPEC	M SPEC	M SPEC	M SPEC
142.88	122.61	107.41	85.13	61.80	54.20	43.56	29.38	15.19	11.64	9.51	8.09								
.38533	.44944	.51353	.64161	.89741	1.02513	1.28021	1.91585	3.80585	5.05136	6.28622	7.51060								
2.5982	2.2250	1.9473	1.5586	1.1143	.9755	.7831	.5220	.2628	.1980	.1591	.1331								
.80586	.00661	.00755	.00945	.01324	.01513	.01894	.02847	.05734	.07681	.09646	.11628								
MEAS/BAR 176.6280	151.3576	132.4064	105.8747	75.5529	65.0774	52.8118	35.1247	17.4392	13.0190	10.3674	8.6000								
.39091	.45596	.52097	.65091	.91041	1.03938	1.29878	1.94362	3.86070	5.11718	6.34397	7.56034								
MEAS/DEGK 2.5581	2.1932	1.9195	1.5363	1.0984	.9516	.7700	.5145	.2590	.1954	.1576	.1323								
MEAS/PSCHT 113.56075	97.38590	85.25475	68.27110	48.86110	42.79542	34.30339	22.98036	11.65600	8.82423	7.12470	5.99114								
RADIUS 59815.000 KM										TEMPERATURE 130.298 KELVIN -225.134 FAHRENHEIT									
ALTIUDE 15.000 KM										PRESSURE .716120 BARS									
49.213 KFT										.706755 ATM									
TIME 465.213 SEC										DYN P .011532 BARS									
VELOCITY 124.054 METER/SEC										DOPP-ER 8.994518E+02 CPS									
7.75355 MIN										MACH NO .150167									
.129226 HRS																			
INSTRUMENTS																			
NO OF MEAS	TEMP	PRESS	TEMP	PRESS	ACCEL	ACCEL	ACCEL	ACCEL	ACCEL	M SPEC	M SPEC	M SPEC	M SPEC	M SPEC	M SPEC	M SPEC	M SPEC	M SPEC	M SPEC
156.07	133.92	117.30	94.04	67.45	59.15	47.52	32.01	16.51	12.63	10.30	8.75								
.37157	.43352	.49534	.61090	.86569	.98832	1.23507	1.84857	3.67338	4.87727	6.07138	7.25801								
2.6906	2.3067	2.0188	1.5158	1.1551	1.0112	.8097	.5410	.2722	.2030	.1647	.1378								
.80587	.00685	.00783	.00979	.01373	.01559	.01933	.02992	.05942	.07958	.09990	.12040								
MEAS/BAR 170.3072	145.9450	127.6733	102.0931	72.8586	63.7229	50.9330	33.8800	16.8284	12.5663	10.0095	8.3054								
.36924	.43068	.49210	.61485	.86003	.98246	1.22700	1.83648	3.64937	4.84539	6.03170	7.20858								
MEAS/DEGK 2.7083	2.3219	2.0321	1.6284	.86003	.98246	1.22700	1.83648	3.64937	4.84539	6.03170	7.20858								
MEAS/PSCHT 122.459641	105.01327	91.92847	73.60972	52.67390	46.13141	36.97184	24.75880	12.54453	9.49021	7.65715	6.43473								

SURVIVABLE SATURN PROBE TASK 4 DESCENT RUNS
JP. MONOGRAPH SATURN NOMINAL ATMOSPHERE
BALLISTIC COEFFICIENT = .700, INITIAL TIME = 0. SECONDS AT 5900.000 KM RADIUS

BAL. COEF. 0.65/0.70/1.50 SEP 30 BARS

RADJIS 59810.000 KM ALTITUDE 10.000 KM PRESSURE .797771 BARS TEMPERATURE 135.265 KELVIN
32.808 KFT -216.192 FAHRENHEIT
TIME 505.237 SEC VELOCITY 119.764 METER/SEC DYN P .011552 BARS
6.3729 MIN 2.0260 MB/SEC DOPPLER 8.68348E+02 CPS
.140621 HRS 392.927 FT/SEC MACH NO .142287

INSTRUMENTS TEMP PRESS PRESS ACCEL ACCEL M SPEC M SPEC M SPEC M SPEC
NO OF MEAS 169.75 145.64 127.56 73.32 64.28 51.62 36.75 17.87 13.66 11.12 9.44
KM/MEAS .35685 .41857 .47826 .53758 .59436 1.19272 1.78545 3.54950 4.71410 5.86984 7.01698
MEAS/KM 2.7867 2.3691 2.0909 1.8734 1.6722 .8384 .5601 .2817 .2121 .1704 .1425
BARS/MEAS .00608 .00710 .00811 .01015 .01422 .02034 .03057 .06152 .08236 .10336 .12453
MEAS/BAR 164.3776 140.8658 123.2319 98.3446 70.3306 61.5138 49.1703 32.7125 16.2559 12.1424 9.6747 8.0299
DECK/MEAS .35650 .41583 .47514 .53368 .59047 .94872 1.18493 1.77378 3.52630 4.68329 5.83148 6.97112
MEAS/DECK 2.8050 2.4048 2.1046 1.8444 1.6041 .8439 .5638 .2836 .2135 .1715 .1434
MEAS/PSCHT 131.63506112.67792 98.81004 79.11499 56.60625 49.57223 39.72452 26.59398 13.46228 10.17866 8.20805 6.89395

RADJIS 59805.000 KM ALTITUDE 5.000 KM PRESSURE .885294 BARS TEMPERATURE 140.233 KELVIN
16.404 KFT -207.251 FAHRENHEIT
TIME 549.704 SEC VELOCITY 115.768 METER/SEC DYN P .011552 BARS
9.14507 MIN 2.0953 MB/SEC DOPPLER 8.393737E+02 CPS
.152418 HRS 379.817 FT/SEC MACH NO .135082

INSTRUMENTS TEMP PRESS PRESS ACCEL ACCEL M SPEC M SPEC M SPEC M SPEC
NO OF MEAS 183.90 157.77 138.18 110.74 79.39 65.59 55.87 37.58 19.29 14.72 11.97 10.15
KM/MEAS .34690 .40464 .46236 .52773 .59436 .92330 1.15325 1.72659 3.43383 4.56162 5.68129 6.79306
MEAS/KM 2.8927 2.4713 2.1628 1.8709 1.6331 1.0831 .8671 .5792 .2912 .2192 .1760 .1472
BARS/MEAS .00630 .00735 .00840 .01050 .01471 .01682 .02104 .03162 .06361 .08513 .10682 .12867
MEAS/BAR 158.8535 135.1338 119.0340 95.2382 67.9745 53.4548 47.5271 31.6237 15.7212 11.7452 9.3616 7.7721
DECK/MEAS .34464 .40200 .45934 .51795 .80292 .9127 1.14571 1.71530 3.41138 4.53181 5.63707 6.72999
MEAS/DECK 2.9016 2.4876 2.1770 1.8423 1.6455 1.0902 .8728 .5830 .2931 .2207 .1774 .1486
MEAS/PSCHT 141.13143121.01766105.93232 84.81282 60.67614 53.13339 42.57347 28.49333 14.41211 10.89115 8.77826 7.36929

RADJIS 59800.000 KM ALTITUDE 0. KM PRESSURE .978881 BARS TEMPERATURE 145.200 KELVIN
0. KFT -198.310 FAHRENHEIT
TIME 592.611 SEC VELOCITY 112.038 METER/SEC DYN P .011554 BARS
9.97685 MIN 2.1689 MB/SEC DOPPLER 8.123237E+02 CPS
.154614 HRS 357.577 FT/SEC MACH NO .128473

INSTRUMENTS TEMP PRESS PRESS ACCEL ACCEL M SPEC M SPEC M SPEC M SPEC
NO OF MEAS 198.54 170.32 149.15 119.52 85.65 75.08 60.26 40.51 20.75 15.82 12.85 10.88
KM/MEAS .33575 .39163 .44750 .50917 .78228 .89371 1.11634 1.67151 3.32538 4.41847 5.50420 6.58252
MEAS/KM 2.9784 2.5534 2.2346 1.7884 1.2783 1.1159 .8958 .5983 .3007 .2263 .1817 .1519
BARS/MEAS .00651 .00759 .00868 .01085 .01520 .01738 .02174 .03267 .06570 .08792 .11029 .13281
MEAS/BAR 153.6936 131.7133 115.2261 92.1489 65.7727 57.5302 45.9907 30.5049 15.2199 11.3741 9.0670 7.5293
DECK/MEAS .33006 .38580 .43992 .49970 .76902 .87856 1.09741 1.64318 3.26901 4.34358 5.41091 6.45372
MEAS/DECK 3.0298 2.5974 2.2732 1.9192 1.6304 1.1392 .9112 .6086 .3059 .2302 .1848 .1549
MEAS/PSCHT 150.94709129.43096113.29384 90.70186 64.88235 56.81372 45.51758 30.45581 15.39304 11.62674 9.36658 7.85970

L-28

JP- MONOGRAPH SATURN NOMINAL ATMOSPHERE

0.1. NONLOCALITY COEFFICIENT = 0.700, INITIAL TIME = 0. SECONDS AT 59900.000 KM RADIUS

BAL. COEF. 0.05/0.70/1.50 SEP 30 1965

[illegible]

RADIO		59790.000 KM		ALTITUDE		-10.000 KM		PRESSURE		1.185129 BARS		TEMPERATURE		154.927 KELVIN	
TIME		684.758 SEC		VELOCITY		-32.808 KFT		DYV P		1.169631 ATM		-180.801 FAHRENHEIT			
11.41263 MIN				105.196 METER/SEC				DOPPLER							
.130211 HRS				2.3133 MB/SEC				MACH NO							
				345.130 FT/SEC											
INSTRUMENTS		TEMP	PRESS	TEMP	PRESS	ACCEL	ACCEL	ACCEL	ACCEL	M SPEC	M SPEC	M SPEC	M SPEC	M SPEC	M SPEC
NO OF MEAS	229.25	172.19	137.95	98.82	86.59	69.48	46.65	23.83	18.12	14.70	12.41				
KM/HRS	31528	36777	42024	52513	63399	73471	1.04857	1.57034	3.12583	5.17755	6.19417				
MEAS/KM	3.1178	2.7191	2.3796	1.90483	1.3611	1.1913	.9537	.8368	.8199	.7407	.6161				
BARS/MEAS	0.0093	0.0089	0.00925	.01156	.01620	.02316	.03460	.06994	.10356	.14723					
MEAS/BAR	144.2285	123.6043	108.1362	86.4808	61.7318	53.9978	43.1702	28.7335	14.2975	10.6888	7.0807				
DECK/MEAS	.30197	.35225	.40250	.50286	.70370	.80337	1.00431	1.50406	2.93390	3.97945	4.95902	5.93273			
MEAS/DECK	3.3115	2.8389	2.4845	1.9882	1.4211	1.2436	.9957	.6649	.5340	.42017	.34016				
MEAS/PSCH	171.42890146	38648128.65456	102.99007	73.65903	69.9307	51.66064	34.55054	17.44926	13.45128	10.59397	8.58216				

RADIOS		5975.000 KM		ALTITUDE		-15.000 KM		PRESSURE		1.296301 BARS		TEMPERATURE		159.716 KELVIN	
TIME		733.018 SEC		VELOCITY		-9.213 KFT		DY+ P		1.281323 ATM		-172.161 FAHRENHEIT			
12.21696 MIN								00PP+R		7.399562E+02 CPS					
.203616 HRS								MACH NO		.111583					
INSTRUMENTS		TEMP	PRESS	TEMP	PRESS	ACCEL	ACCEL	ACCEL	ACCEL	ACCEL	ACCEL	M SPEC	M SPEC	M SPEC	M SPEC
NO OF MEAS	295.34	184.25	147.60	105.72	92.53	74.30	59.87	25.43	19.33	15.66	13.22				
KM/MEAS	.30589	.40773	.50951	.71288	.81477	1.01747	1.52391	3.03422	4.03376	5.02756	6.01574				
MEAS/KM	3.2692	2.8025	2.4526	1.9627	1.4023	.9828	.5562	.3296	.2479	.1989	.1662				
BARS/KM	.00715	.00834	.00953	.01192	.01670	.02388	.03587	.07208	.09639	.12085	.14542				
MEAS/BAR	139.8853	113.8835	104.8820	83.9799	59.8775	41.8758	27.8746	13.8740	10.3741	8.2744	6.8747				
DESK/MEAS	.29298	.34176	.39052	.48800	.68273	.97452	1.45959	2.30616	3.46350	4.81536	5.76183				
MEAS/DEGK	3.44132	2.9261	2.5607	1.4645	1.2819	1.0261	.68051	.3441	.2588	.2077	.1736				
MEAS/PSCHT	182.1130156	14431135	.66775109	.40035	78.23797	60.49353	58.86590	36.68740	18.50809	13.96275	11.23523				

SURVIVABLE SATURN PROBE TASK 4 DESCENT RUNS
JP- MONOGRAPH SATURN NOMINAL ATMOSPHERE

BALLISTIC COEFFICIENT = .700, INITIAL TIME = 0. SECONDS AT 59900.000 KM RADIUS

BAL. COEF. 0.6570.70/1.50 SEP 30 BARS

RADIUS 59770.000 KM		ALTITUDE	-20.000 KM	PRESSURE	1.418474 BARS	TEMPERATURE	164.505 KELVIN
			-65.617 KFT		1.399925 ATM		-163.561 FAHRENHEIT
TIME	782.740 SEC	VELOCITY	99.099 METER/SEC	DYN P	.011578 BARS		
	13.04567 MIN		2.4565 M3/SEC	DOPPLER	7.185131E+02 CPS		
	.217428 HRS		325.128 FT/SEC	MACH NO	.106761		

INSTRUMENTS	TEMP	PRESS	TEMP	PRESS	ACCEL	ACCEL	M SPEC	M SPEC	M SPEC	M SPEC
NO OF MEAS	261.91	224.64	196.68	157.55	112.82	98.84	79.27	53.18	27.09	20.57
KM/MEAS	.29704	.34650	.35994	.43478	.69230	.79037	.98815	1.48013	2.34779	3.91948
MEAS/KM	3.3665	2.8860	2.5256	2.0211	1.4445	1.2643	1.0120	.8756	.3392	.2531
BARS/MEAS	.00736	.00859	.00982	.01228	.01720	.02460	.03695	.07421	.09924	.12440
MEAS/BAR	135.7935	115.3776	101.8156	81.4290	58.1300	50.8430	40.6558	27.0649	13.4744	10.0770
DECK/MEAS	.28450	.33187	.37923	.47390	.66308	.75739	.94645	1.41765	2.82337	3.75405
MEAS/DECK	3.5149	3.0132	2.6369	2.1102	1.5081	1.3200	1.0566	.7054	.3542	.2654
MEAS/PSCHT	193.11899165	.37799144	.92222116	.00413	82.95481	72.62637	58.16770	38.88853	19.60878	14.78834

RADIUS 59775.000 KM		ALTITUDE	-25.000 KM	PRESSURE	1.545860 BARS	TEMPERATURE	169.294 KELVIN
			-82.021 KFT		1.525645 ATM		-154.941 FAHRENHEIT
TIME	833.924 SEC	VELOCITY	96.308 METER/SEC	DYN P	.011578 BARS		
	13.89874 MIN		2.5281 M3/SEC	DOPPLER	6.982771E+02 CPS		
	.231646 HRS		315.971 FT/SEC	MACH NO	.102276		

INSTRUMENTS	TEMP	PRESS	TEMP	PRESS	ACCEL	ACCEL	M SPEC	M SPEC	M SPEC	M SPEC
NO OF MEAS	278.97	239.26	209.48	167.78	120.13	103.24	84.39	56.59	28.80	21.85
KM/MEAS	.28869	.33676	.38481	.49089	.67288	.76830	.96048	1.43878	2.86610	3.81143
MEAS/KM	3.4639	2.9695	2.5987	2.0795	1.4862	1.3007	1.0412	.8950	.3489	.2624
BARS/MEAS	.00758	.00884	.01011	.01264	.01771	.02024	.02531	.03802	.07636	.10208
MEAS/BAR	131.9312	113.0684	98.9214	79.1155	56.4802	49.4037	39.5038	26.3001	13.0967	9.7961
DECK/MEAS	.27650	.32254	.36857	.45059	.64448	.73635	.91994	1.37805	2.74512	3.65056
MEAS/DECK	3.6165	3.1004	2.7132	2.1711	1.5515	1.3531	1.0870	.7257	.3643	.2739
MEAS/PSCHT	204.44659175	.28744153	.41799122	.80074	87.60954	76.87478	61.56602	41.15420	20.74164	15.63805

RADIUS 59770.000 KM		ALTITUDE	-30.000 KM	PRESSURE	1.680072 BARS	TEMPERATURE	174.083 KELVIN
			-98.425 KFT		1.658695 ATM		-146.321 FAHRENHEIT
TIME	885.571 SEC	VELOCITY	93.670 METER/SEC	DYN P	.011578 BARS		
	14.77618 MIN		2.5997 M3/SEC	DOPPLER	6.791483E+02 CPS		
	.246270 HRS		307.315 FT/SEC	MACH NO	.098096		

INSTRUMENTS	TEMP	PRESS	TEMP	PRESS	ACCEL	ACCEL	M SPEC	M SPEC	M SPEC	M SPEC
NO OF MEAS	296.52	254.31	222.64	178.31	127.63	111.32	89.66	60.16	30.55	23.16
KM/MEAS	.28079	.32755	.37429	.46775	.65451	.74732	.93430	1.39987	2.78878	3.70911
MEAS/KM	3.5613	3.0530	2.6717	2.1379	1.5279	1.3372	1.0703	.9145	.3586	.2696
BARS/MEAS	.00780	.00910	.01040	.01300	.01821	.02091	.02603	.03910	.07850	.10493
MEAS/BAR	128.2799	103.9400	96.1850	76.9281	54.9203	43.0429	38.4145	25.5767	12.7392	9.5301
DECK/MEAS	.26894	.31372	.35850	.44801	.62683	.71626	.89487	1.34059	2.67107	3.55256
MEAS/DECK	3.7183	3.1873	2.7894	2.2321	1.5952	1.3951	1.1175	.7459	.3744	.2815
MEAS/PSCHT	216.09602185	.27258162	.15499129	.79034	92.80211	81.24326	65.06083	41.48409	21.30666	16.51187

SURVIVABLE SATURN PROBE TASK 4 DESCENT RUNS
 JP. MONOGRAPH SATURN VOMINAL ATMOSPHERE
 BALLISTIC COEFFICIENT = .700, INITIAL TIME = 0. SECONDS AT 59900.000 KM RADIUS

BAL. COEF. 0.65/0.70/1.50 SEP 30 BARS

RADIUS 59765.000 KM		ALTITUDE -35.000 KM		PRESSURE -114.829 K/T		PRESSURE 1.023125 BARS		TEMPERATURE 178.672 KELVIN		TEMPERATURE -137.701 FAHRENHEIT	
TIME	940.680 SEC	VELOCITY	91.172 METER/SEC	DYN P	0.11578 BARS	ACCEL	95.07	ACCEL	63.71	M SPEC	M SPEC
	15.57800 MIN		2.6714 M3/SEC	JOPP-ER	6.610398E+02 CPS						
	.251300 HRS		239.121 FT/SEC	MACH NO	.094194						
INSTRUMENTS	TEMP	PRESS	TEMP	PRESS	ACCEL	ACCEL	ACCEL	ACCEL	ACCEL	M SPEC	M SPEC
NO OF MEAS	314.56	269.77	236.17	183.14	135.39	119.59	95.07	63.71	32.36	24.52	19.81
KM/MEAS	.27332	.31883	.36433	.43531	.63712	.72736	.90951	1.36262	2.71549	3.61210	4.50425
MEAS/KM	3.6588	3.1365	2.7447	2.1963	1.5696	1.3737	1.0995	.7339	.3683	.2768	.2220
BARS/MEAS	.00801	.00935	.01068	.01336	.01871	.02139	.02675	.04017	.08064	.10778	.13500
MEAS/BARS	124.8227	105.9777	93.5941	74.8569	53.4430	45.7512	37.3827	24.8914	12.4004	9.2778	7.4044
DEGR/MEAS	.26178	.30537	.34896	.43609	.61023	.69723	.87112	1.30511	2.60087	3.45964	4.31442
MEAS/DEGR	3.8200	3.2747	2.8657	2.2931	1.6387	1.4342	1.1479	.7652	.3845	.2890	.2318
MEAS/PSCHT	228.06691195	53333171	13315136	97286	97.93248	85.73234	68.65210	45.87829	23.10382	17.40979	13.95312

RADIUS 59760.000 KM		ALTITUDE -40.000 KM		PRESSURE -131.234 K/T		PRESSURE 1.973431 BARS		TEMPERATURE 183.661 KELVIN		TEMPERATURE -129.081 FAHRENHEIT	
TIME	996.252 SEC	VELOCITY	88.804 METER/SEC	DYN P	0.11578 BARS	ACCEL	100.63	ACCEL	67.42	M SPEC	M SPEC
	16.50420 MIN		2.731 M3/SEC	JOPP-ER	6.438704E+02 CPS						
	.276737 HRS		291.352 FT/SEC	MACH NO	.090543						
INSTRUMENTS	TEMP	PRESS	TEMP	PRESS	ACCEL	ACCEL	ACCEL	ACCEL	ACCEL	M SPEC	M SPEC
NO OF MEAS	333.08	285.64	250.06	200.25	143.32	125.53	100.63	67.42	34.21	25.91	20.93
KM/MEAS	.28623	.31056	.35489	.44351	.62063	.70912	.88600	1.32747	2.84592	3.51997	4.39017
MEAS/KM	3.7562	3.2200	2.8178	2.2548	1.6113	1.4102	1.1287	.7533	.3779	.2841	.2276
BARS/MEAS	.00823	.00960	.01097	.01372	.01922	.02137	.02747	.04125	.08279	.11064	.13862
MEAS/BARS	121.5445	104.1689	91.1371	72.8928	52.0421	45.5252	36.5041	24.2413	12.0767	9.0382	7.2141
DEGR/MEAS	.25499	.29745	.33991	.42479	.59443	.67919	.84860	1.27144	2.53424	3.37140	4.20487
MEAS/DEGR	3.9217	3.3619	2.9420	2.3541	1.6823	1.4723	1.1784	.7865	.3946	.2966	.2378
MEAS/PSCHT	240.35324206	06962180	35240144	34826103	20062	90.34136	72.33980	48.33677	24.33311	18.33131	14.73079

RADIUS 59755.000 KM		ALTITUDE -45.000 KM		PRESSURE -147.638 K/T		PRESSURE 2.131804 BARS		TEMPERATURE 188.450 KELVIN		TEMPERATURE -120.461 FAHRENHEIT	
TIME	1053.286 SEC	VELOCITY	86.556 METER/SEC	DYN P	0.11578 BARS	ACCEL	106.33	ACCEL	71.22	M SPEC	M SPEC
	17.55477 MIN		2.8148 M3/SEC	JOPP-ER	6.275692E+02 CPS						
	.292579 HRS		283.976 FT/SEC	MACH NO	.087122						
INSTRUMENTS	TEMP	PRESS	TEMP	PRESS	ACCEL	ACCEL	ACCEL	ACCEL	ACCEL	M SPEC	M SPEC
NO OF MEAS	352.10	301.94	264.32	211.66	151.47	132.56	106.33	71.22	36.11	27.33	22.07
KM/MEAS	.25950	.30271	.34592	.43230	.60495	.69123	.86366	1.29409	2.57980	3.3239	4.28139
MEAS/KM	3.8536	3.3035	2.8908	2.3132	1.6530	1.4457	1.1579	.7727	.3876	.2913	.2336
BARS/MEAS	.00844	.00985	.01126	.01408	.01972	.02254	.02819	.04233	.08494	.11350	.14219
MEAS/BARS	118.4317	101.5017	88.8042	71.0276	50.7115	44.3629	35.5746	23.6237	11.7730	8.8105	7.0331
DEGR/MEAS	.24854	.28994	.33132	.41406	.57943	.66236	.82721	1.23947	2.47092	3.28752	4.10066
MEAS/DEGR	4.0234	3.4490	3.0182	2.4151	1.7258	1.5104	1.2089	.8068	.4047	.3042	.2439
MEAS/PSCHT	252.97295216	88137163	81267151	31648108	60643	93.07210	76.13391	50.85922	25.53454	19.27793	15.46772

SURVIVABLE SATURN PROBE TASK 4 DESCENT RUNS
 JP MONOGRAPH SATURN JONINAL ATMOSPHERE
 BALLISTIC COEFFICIENT = .700, INITIAL TIME = 0. SECONDS AT 59900.000 KM RADIUS
 BAL. COEF. 0.6570.70/1.50 SEP 30 BARS

RADIUS 59750.000 KM		ALTITUDE -50.000 KM		PRESSURE		TEMPERATURE 193.239 KELVIN		TEMPERATURE -111.840 FAHRENHEIT	
TIME	1111.783 SEC	VELOCITY	84.418 METER/SEC	DYN P	0.11578 BARS				
	18.52972 MIN		2.8866 M/SEC	DOPPLER	6.120719E+02 CPS				
	.338829 HRS		276.963 FT/SEC	MACH NO	.083912				
INSTRUMENTS									
NO OF MEAS	TEMP	PRESS	TEMP	PRESS	ACCEL	ACCEL	M SPEC	M SPEC	M SPEC
371.59	318.65	278.95	223.36	159.83	139.37	112.10	75.12	34.06	28.79
25310	.29525	.33739	.42165	.59007	.67422	.84243	1.26233	2.51689	3.34902
3.9511	3.3870	2.9639	2.3716	1.6947	1.4832	1.1870	.7922	.2986	.2394
MEAS/KM	MEAS	MEAS	MEAS	MEAS	MEAS	MEAS	MEAS	MEAS	MEAS
0.0866	.01010	.01155	.01444	.02022	.02312	.02691	.04341	.08709	.11636
MEAS/BAR	115.4722	93.9658	86.5859	69.2542	49.4465	34.5908	23.0363	11.4021	8.5937
DEGK/MEAS	.24241	.28279	.32315	.40385	.56215	.80687	1.20905	2.41065	4.00148
MEAS/DEGK	4.1252	3.5362	3.0945	2.4761	1.7694	1.2394	.8271	.4148	.3118
MEAS/PSCHT	265.90794227	36850193	51391159	67746114	15005	99.92272	80.00441	53.44653	26.88809

RADIUS 59745.000 KM		ALTITUDE -55.000 KM		PRESSURE		TEMPERATURE 198.028 KELVIN		TEMPERATURE -103.220 FAHRENHEIT	
TIME	1171.743 SEC	VELOCITY	82.384 METER/SEC	DYN P	.011578 BARS				
	19.52905 MIN		2.9583 M/SEC	DOPPLER	5.973205E+02 CPS				
	.325484 HRS		270.288 FT/SEC	MACH NO	.080893				
INSTRUMENTS									
NO OF MEAS	TEMP	PRESS	TEMP	PRESS	ACCEL	ACCEL	M SPEC	M SPEC	M SPEC
391.58	335.78	293.94	235.35	168.39	147.47	118.17	79.12	40.06	30.29
24700	.28814	.32927	.41151	.57888	.65832	.82220	1.23209	2.55694	3.26956
MEAS/KM	4.0485	3.4705	2.4301	1.7365	1.5137	1.2162	.8116	.4070	.3059
MEAS/BAR	.00888	.01036	.01184	.02073	.02359	.02963	.04449	.08925	.11923
DEGK/MEAS	112.6549	95.5817	84.4742	67.5658	48.2420	33.7491	22.4770	11.2050	8.3871
MEAS/DEGK	4.2269	3.6234	3.1708	2.5372	1.8130	1.2698	.8474	.4249	.3193
MEAS/PSCHT	279.16413239	33094203	45604167	63117119	8312710	89378	83.98126	56.09778	28.21375

RADIUS 59740.000 KM		ALTITUDE -60.000 KM		PRESSURE		TEMPERATURE 202.817 KELVIN		TEMPERATURE -94.600 FAHRENHEIT	
TIME	1233.166 SEC	VELOCITY	80.445 METER/SEC	DYN P	.011578 BARS				
	20.55276 MIN		3.0302 M/SEC	DOPPLER	5.832621E+02 CPS				
	.342546 HRS		263.927 FT/SEC	MACH NO	.078051				
INSTRUMENTS									
NO OF MEAS	TEMP	PRESS	TEMP	PRESS	ACCEL	ACCEL	M SPEC	M SPEC	M SPEC
412.06	353.33	309.29	247.63	177.17	155.15	124.32	83.21	42.11	31.83
24120	.28137	.32154	.40184	.56237	.64238	.80293	1.20326	2.39977	3.19376
MEAS/KM	4.1460	3.5540	2.4885	1.7782	1.5552	1.2454	.8311	.4167	.3131
MEAS/BAR	.00909	.01061	.01213	.01516	.02123	.02427	.03035	.04557	.09140
DEGK/MEAS	109.9697	94.2507	82.4615	65.3566	47.0939	32.9468	21.5438	10.9406	8.1899
MEAS/DEGK	4.3287	3.7107	3.2471	2.5982	1.8565	1.2448	.8677	.4351	.3269
MEAS/PSCHT	292.74143250	36863213	63902175	77755125	65011103	98526	88.05445	58.81324	29.57152

SURVIVABLE SATURN PROBE TASK 4 DESCENT RUNS

JP. MONOGRAPH SATURN NOMINAL ATMOSPHERE

BALLISTIC COEFFICIENT = .700, INITIAL TIME = 0. SECONDS AT 59900.000 KM RADIUS

BAL. COEF. 0.65/0.70/1.50

SEP 30 BARS

RADIUS 59735.000 KM		ALTITUDE -85.000 KM		PRESSURE -213.255 KFT		PRESSURE 2.850264 BARS		TEMPERATURE 207.606 KELVIN		TEMPERATURE -85.980 FAHRENHEIT	
TIME	1295.051 SEC	VELOCITY	78.595 METER/SEC	DYN P	3.1020 MB/SEC	DOPPLER	5.698491E+02 CPS				
	21.50085 MIN		3.1020 MB/SEC								
	.350014 HRS		257.837 FT/SEC	MACH NO			.075371				
INSTRUMENTS											
NO OF MEAS	TEMP	PRESS	ACCEL	ACCEL	ACCEL	ACCEL	ACCEL	M SPEC	M SPEC	M SPEC	M SPEC
433.02	371.30	325.01	260.21	186.15	163.01	130.61	87.40	33.40	28.92	28.60	28.60
23566	.27431	.31415	.33262	.54947	.62735	.78453	1.17574	2.34517	3.12136	3.89483	4.66562
MEAS/KM	4.2435	3.6375	3.1832	2.5476	1.8199	1.2747	.8505	.4264	.3204	.2568	.2143
BARS/MEAS	.00331	.01085	.01242	.01552	.02174	.03107	.04665	.09356	.12497	.15650	.18814
MEAS/BAR	107.4076	92.0553	80.5410	64.4210	45.9982	32.1812	21.4346	10.6882	8.0016	6.3896	5.3152
DEGR/MEAS	.22571	.26330	.30389	.37605	.52629	.75142	1.12611	2.24619	2.98908	3.72924	4.46684
MEAS/DEGR	4.4305	3.7979	3.3235	2.5592	1.9001	1.3308	.8880	.4452	.3346	.2682	.2239
MEAS/PSCHT	306.63978262	88149230.08277184	11654131.60653115	19713	92.22394	61.59291	30.96138	23.30321	18.70810	15.64453	

RADIUS 59730.000 KM		ALTITUDE -70.000 KM		PRESSURE -229.659 KFT		PRESSURE 3.052197 BARS		TEMPERATURE 212.392 KELVIN		TEMPERATURE -77.364 FAHRENHEIT	
TIME	1369.400 SEC	VELOCITY	76.828 METER/SEC	DYN P	3.1761 MB/SEC	DOPPLER	5.570350E+02 CPS				
	22.57334 MIN		3.1761 MB/SEC								
	.377669 HRS		252.039 FT/SEC	MACH NO			.072842				
INSTRUMENTS											
NO OF MEAS	TEMP	PRESS	ACCEL	ACCEL	ACCEL	ACCEL	ACCEL	M SPEC	M SPEC	M SPEC	M SPEC
454.47	389.69	341.10	273.06	195.34	171.15	137.04	91.69	46.35	35.01	28.21	23.67
23035	.26673	.30710	.33881	.53714	.61377	.76695	1.14943	2.29298	3.05212	3.80872	4.56281
MEAS/KM	4.3410	3.7212	3.2563	2.5055	1.8617	1.2633	1.3039	.4361	.3276	.2626	.2192
BARS/MEAS	.00953	.01112	.01271	.01588	.02225	.03180	.04774	.09572	.12785	.16109	.19244
MEAS/BAR	104.9597	83.9576	78.7360	62.9536	44.9513	31.4495	20.9481	10.4468	7.8216	6.2465	5.1964
DEGR/MEAS	.22044	.25716	.29387	.37228	.51401	.73392	1.09994	2.19423	2.92069	3.64471	4.36632
MEAS/DEGR	4.5363	3.8885	3.4028	2.7227	1.9455	1.3625	.9091	.4557	.3424	.2744	.2290
MEAS/PSCHT	320.95743275	86804240.72598192	64710137.69975120	52859	95.48918	64.43638	32.38311	24.36950	19.56115	16.35543	

RADIUS 59725.000 KM		ALTITUDE -75.000 KM		PRESSURE -246.063 KFT		PRESSURE 3.253491 BARS		TEMPERATURE 217.177 KELVIN		TEMPERATURE -68.751 FAHRENHEIT	
TIME	1425.213 SEC	VELOCITY	75.137 METER/SEC	DYN P	3.220815 ATM	DOPPLER	5.447804E+02 CPS				
	23.77022 MIN		3.2481 MB/SEC								
	.396170 HRS		246.514 FT/SEC	MACH NO			.070450				
INSTRUMENTS											
NO OF MEAS	TEMP	PRESS	ACCEL	ACCEL	ACCEL	ACCEL	ACCEL	M SPEC	M SPEC	M SPEC	M SPEC
476.40	397.55	357.55	285.24	204.74	179.28	143.62	98.08	48.54	36.06	29.52	24.77
22330	.26283	.30035	.37538	.52335	.60030	.75013	1.12427	2.24303	2.98585	3.72628	4.46436
MEAS/KM	4.4385	3.8234	3.2640	1.9035	1.6058	1.3331	.8835	.4458	.3349	.2684	.2240
BARS/MEAS	.00974	.01137	.01300	.01625	.02275	.03251	.04882	.09789	.13073	.16369	.19675
MEAS/BAR	102.6185	87.9514	76.9511	61.3506	43.9500	30.7496	20.4827	10.2158	7.6492	6.1093	5.0827
DEGR/MEAS	.21550	.25151	.28742	.39321	.50273	.71783	1.07586	2.14644	2.85727	3.56582	4.27212
MEAS/DEGR	4.6383	3.9760	3.4793	2.7839	1.9891	1.3931	.9295	.4659	.3530	.2804	.2341
MEAS/PSCHT	335.39452247	52839251.62879201	35934143.92992123	98009100	85029	57.34379	33.83684	25.45983	20.43344	17.08237	

SURVIVABLE SATURN PROBE TASK 4 DESCENT RUNS
 JP. MONOGRAPH SATURN NOMINAL ATMOSPHERE
 BALLISTIC COEFFICIENT = .700, INITIAL TIME = 0. SECONDS AT 59900.000 KM RADIUS
 BAL. COEF. 0.65/0.70/1.50 SEP 30 BARS

RADIUS 59720.000 KM		ALTITUDE -90.000 KM		PRESSURE 3.484364 BARS		TEMPERATURE 221.962 KELVIN		-60.139 FAHRENHEIT	
TIME 1493.490 SEC		VELOCITY 73.520 METER/SEC		DYN P					
24.89150 MIN		3.3201 MB/SEC		DOPPLER					
.414858 HRS		241.206 FT/SEC		MACH NO					
INSTRUMENTS	TEMP	PRESS	ACCEL	ACCEL	ACCEL	M SPEC	M SPEC	M SPEC	M SPEC
NO OF MEAS	438.83	+27.71	374.37	293.70	214.35	187.59	100.37	50.78	38.34
KM/MEAS	.22045	.25718	.29389	.35731	.51407	.58741	.73403	1.10018	2.19519
MEAS/KM	4.5351	3.8884	3.4026	3.0225	1.9453	1.7024	.9089	.4555	.2742
BARS/MEAS	.00996	.01162	.01329	.01661	.02325	.02539	.04991	.10005	.13362
MEAS/BAR	100.3778	85.0312	75.2713	60.2074	42.9915	37.8116	30.0797	20.0371	9.3947
DEGK/MEAS	.21096	.24610	.28124	.35149	.49193	.56212	.70242	1.05280	2.10066
MEAS/DEGK	4.7432	.0634	3.5357	2.8450	2.0328	1.7730	1.4236	.9498	.4760
MEAS/PSCHT	350.252503	00.26380262	77227210.28412150	29762131.55182105	30768	70.31538	35.32266	26.57421	21.32497

RADIUS 59715.000 KM		ALTITUDE -95.000 KM		PRESSURE 3.715033 BARS		TEMPERATURE 226.746 KELVIN		-51.526 FAHRENHEIT	
TIME 1362.232 SEC		VELOCITY 71.970 METER/SEC		DYN P					
25.03713 MIN		3.3922 MB/SEC		DOPPLER					
.433953 HRS		236.122 FT/SEC		MACH NO					
INSTRUMENTS	TEMP	PRESS	ACCEL	ACCEL	ACCEL	M SPEC	M SPEC	M SPEC	M SPEC
NO OF MEAS	521.74	+27.35	391.56	313.45	224.18	196.28	157.22	105.15	53.07
KM/MEAS	.21591	.25175	.28770	.35958	.50325	.57536	.71861	1.07710	2.14934
MEAS/KM	4.6337	3.9720	3.4758	2.7810	1.9671	1.7339	1.3916	.9284	.4653
BARS/MEAS	.01018	.01188	.01358	.01697	.02377	.02717	.03397	.05039	.10222
MEAS/BAR	98.2310	84.1915	73.6820	58.9205	42.0732	35.8034	29.4377	19.6101	9.7826
DEGK/MEAS	.20552	.24092	.27532	.34405	.48158	.55030	.68766	1.03071	2.05678
MEAS/DEGK	4.8422	.1508	3.6322	2.9062	2.0765	1.8172	1.4542	.9702	.4862
MEAS/PSCHT	365.4333313	27422274.15639213	39140156.80282137	24337109.86131	73.35114	36.84956	27.71266	22.23587	18.58464

RADIUS 59710.000 KM		ALTITUDE -90.000 KM		PRESSURE 3.955723 BARS		TEMPERATURE 231.488 KELVIN		-42.991 FAHRENHEIT	
TIME 1632.441 SEC		VELOCITY 70.478 METER/SEC		DYN P					
27.20735 MIN		3.4671 MB/SEC		DOPPLER					
.453456 HRS		231.226 FT/SEC		MACH NO					
INSTRUMENTS	TEMP	PRESS	ACCEL	ACCEL	ACCEL	M SPEC	M SPEC	M SPEC	M SPEC
NO OF MEAS	545.15	+57.41	409.11	327.49	234.21	205.16	164.24	103.83	52.41
KM/MEAS	.21134	.24654	.28174	.35213	.49283	.56315	.70373	1.05483	2.10502
MEAS/KM	4.7317	.0561	3.5493	2.8399	2.0291	1.7757	1.4210	.9480	.4751
BARS/MEAS	.01040	.01213	.01387	.01734	.02428	.02775	.03470	.05209	.10441
MEAS/BAR	96.1630	82.4192	72.1115	57.5806	41.1861	35.0342	28.8188	15.1982	9.5777
DEGK/MEAS	.19359	.22934	.26209	.32756	.45845	.52396	.65464	.98123	1.95816
MEAS/DEGK	5.0855	.3603	3.8155	3.0529	2.1813	1.9019	1.5276	1.0191	.5107
MEAS/PSCHT	380.89384326	52747285.75258228	65797163.42827143	04035114.49843	76.44479	38.38475	26.87025	23.16159	19.35536

[illegible]

SURVIVABLE SATURN PROBE TASK 4 JESCENT RUNS
JP. MONOGRAPH SATURN NOMINAL ATMOSPHERE
BALLISTIC COEFFICIENT = .700, INITIAL TIME = 0. SLUGS AT 59900.000 KM RADIUS

BAL. COEF. 0.55/0.70/1.50 SEP 30 BARS

RADIUS 59900.000 KM		ALTITUDE -110.000 KM		PRESSURE 5.024461 BARS		TEMPERATURE 250.092 KELVIN		-9.505 FAHRENHEIT	
TIME 1923.123 SEC		VELOCITY 65.020 METER/SEC		DYN P		DOPP-EK		MACH NO	
32.113538 MIN		3.7642 M3/SEC		0.11606 BARS		4.714279E+02 CPS			
.535590 HRS		213.322 FT/SEC		.056811					
INSTRUMENTS	TEMP	PRESS	ACCEL	ACCEL	ACCEL	ACCEL	M SPEC	M SPEC	M SPEC
NO OF MEAS	63.71	531.89	483.03	395.62	270.45	193.81	129.54	65.27	49.20
KM/MEAS	.19439	.22747	.25995	.32490	.45474	.51363	.57345	1.34322	2.58771
MEAS/KM	5.1286	4.3962	3.8469	3.0779	2.1991	1.5244	1.0273	.5146	.3864
BARS/KM	.01129	.01317	.01505	.01682	.02635	.03012	.03765	.05652	.11325
MEAS/BAR	88.6037	75.9412	66.4442	53.1486	37.9535	33.2031	26.5572	17.6935	8.8298
DECK/MEAS	.17908	.20692	.23875	.29840	.41765	.47725	.59641	.83405	1.78473
MEAS/DECK	5.5840	4.7865	4.1865	3.3512	2.3944	2.0953	1.6767	1.1185	.5603
MEAS/PSCHT	445.68557382	0.6315334	3.4527257	5.4262191	1.9555167	3.3708133	9.3521	8.93929	4.86304

RADIUS 59685.000 KM		ALTITUDE -115.000 KM		PRESSURE 5.319381 BARS		TEMPERATURE 254.684 KELVIN		-1.239 FAHRENHEIT	
TIME 2003.773 SEC		VELOCITY 63.775 METER/SEC		DYN P		DOPP-EK		MACH NO	
33.442955 MIN		3.8383 M3/SEC		0.11606 BARS		4.623991E+02 CPS			
.557159 HRS		209.236 FT/SEC		.055218					
INSTRUMENTS	TEMP	PRESS	ACCEL	ACCEL	ACCEL	ACCEL	M SPEC	M SPEC	M SPEC
NO OF MEAS	689.59	574.08	502.44	402.15	287.54	201.58	134.72	67.86	51.14
KM/MEAS	.19125	.22312	.25498	.31868	.44604	.50970	.53697	1.30627	2.53862
MEAS/KM	5.2285	4.4820	3.9219	3.1379	2.2419	1.5619	1.0473	.5246	.3939
BARS/KM	.01151	.01343	.01535	.01919	.02687	.03071	.03840	.05764	.11549
MEAS/BAR	86.8789	74.4630	65.1511	52.1144	37.2154	32.5534	26.0411	17.3500	8.6590
DECK/MEAS	.17565	.20492	.23418	.29269	.40965	.46813	.58502	.87639	1.75079
MEAS/DECK	5.6929	4.8800	4.2702	3.4166	2.4410	2.1352	1.7093	1.1403	.5712
MEAS/PSCHT	462.84158396	5.9679347	0.6319277	7.1615198	4.6235173	6.9553139	0.2196	92.79046	6.555863

RADIUS 59680.000 KM		ALTITUDE -120.000 KM		PRESSURE 5.625927 BARS		TEMPERATURE 259.276 KELVIN		7.027 FAHRENHEIT	
TIME 2084.927 SEC		VELOCITY 62.575 METER/SEC		DYN P		DOPP-EK		MACH NO	
34.74878 MIN		3.9126 M3/SEC		0.11606 BARS		4.536985E+02 CPS			
.579146 HRS		205.299 FT/SEC		.053697					
INSTRUMENTS	TEMP	PRESS	ACCEL	ACCEL	ACCEL	ACCEL	M SPEC	M SPEC	M SPEC
NO OF MEAS	695.98	536.69	522.23	417.99	298.85	209.49	140.00	70.50	53.12
KM/MEAS	.18756	.21692	.25018	.31269	.43765	.50013	.562501	1.87064	2.49128
MEAS/KM	5.3288	4.5678	3.9971	3.1980	2.2849	1.5935	1.0673	.5346	.4014
BARS/KM	.01173	.01369	.01565	.01956	.02739	.03131	.03915	.05876	.11773
MEAS/BAR	85.2157	73.0385	63.9049	51.1178	36.5040	31.9372	25.5437	17.0190	8.4943
DECK/MEAS	.17235	.20107	.22978	.29719	.40197	.45934	.57404	.86035	1.71807
MEAS/DECK	5.8020	4.9735	4.3520	3.44820	2.44879	2.1770	1.7420	1.1621	.5820
MEAS/PSCHT	479.32278	11.40924360	0.2408288	0.8486205	0.86857180	1.7597144	0.20630	96.24666	4.828675

SURVIVABLE SATURN PROBE TASK 4, DESCENT RUNS
JP. MONOGRAPH SATURN NOMINAL ATMOSPHERE

BALLISTIC COEFFICIENT = .700, INITIAL TIME = 0. SECONDS AT 5900.000 KM RADIUS

BAL. COEF. 0.65/0.70/1.50 SEP 30 BARS

RADIUS 59675.000 KM		ALTITUDE -125.000 KM		PRESSURE		5.943343 BARS		TEMPERATURE		263.058 KELVIN		15.293 FAHRENHEIT	
TIME 2165.584 SEC		VELOCITY 61.418 METER/SEC		DYN P		5.866610 AT							
36.9307 MIN		3.9670 M3/SEC		DOPPLER		4.4530881+02 CPS							
.601551 HRS		201.503 FT/SEC		MACH NO		.052244							
INSTRUMENTS	TEMP	PRESS	TEMP	PRESS	ACCEL	ACCEL	ACCEL	ACCEL	M SPEC	M SPEC	M SPEC	M SPEC	M SPEC
NO OF MEAS	722.86	519.74	542.40	34.12	310.37	271.70	217.56	145.37	73.19	55.14	44.31	37.09	
KM/MEAS	.18419	.21488	.24556	.30691	.42958	.49030	.51343	.51970	1.33628	2.44562	3.02359	3.66022	
MEAS/KM	5.4292	4.5538	4.0723	3.2582	2.3278	2.0371	1.6300	1.0873	5.446	4.039	3.275	.2732	
BARS/MEAS	.01196	.01395	.01595	.01994	.02792	.03131	.03990	.05988	.11997	.16014	.20041	.24076	
MEAS/BAR	83.5139	71.5649	52.7032	50.1568	35.8180	31.3372	25.0640	15.0097	8.3325	6.2445	4.9899	4.1535	
DEGK/MEAS	.16917	.19735	.22553	.26188	.39455	.45036	.56344	.84469	1.08621	2.24615	2.86454	3.36169	
MEAS/DEGK	5.9113	5.0671	4.4340	3.5476	2.5345	2.2130	1.7748	1.1639	.5929	.4452	.3566	.2975	
MEAS/PSCHT	97.52958	26.50078	373.22918298	54892213.41432186	77850149.48833	99.70800	50.04743	37.61709	30.15878	25.18646			

RADIUS 59670.000 KM		ALTITUDE -130.000 KM		PRESSURE		6.274874 BARS		TEMPERATURE		268.401 KELVIN		23.559 FAHRENHEIT	
TIME 2247.743 SEC		VELOCITY 60.301 METER/SEC		DYN P		6.192819 AT							
37.46243 MIN		4.0615 M3/SEC		DOPPLER		4.3721361+02 CPS							
.624375 HRS		197.839 FT/SEC		MACH NO		.050853							
INSTRUMENTS	TEMP	PRESS	TEMP	PRESS	ACCEL	ACCEL	ACCEL	ACCEL	M SPEC	M SPEC	M SPEC	M SPEC	M SPEC
NO OF MEAS	750.25	543.21	562.94	450.55	32.11	281.37	225.77	150.85	75.92	57.19	45.95	38.46	
KM/MEAS	.18084	.21097	.24110	.30134	.42179	.48139	.50235	.50303	1.40311	2.40153	2.99867	3.59452	
MEAS/KM	5.5295	4.7399	4.1477	3.3185	2.3709	2.0747	1.6602	1.1074	.5546	.4164	.3335	.2782	
BARS/MEAS	.01219	.01422	.01625	.02031	.02844	.03251	.04065	.06101	.12222	.16314	.20414	.24524	
MEAS/BAR	82.0674	70.3396	51.5437	43.2295	35.1561	30.7582	24.6011	16.3916	8.1822	6.1299	4.8985	4.0713	
DEGK/MEAS	.16609	.19377	.22144	.27676	.38738	.44258	.55322	.82938	1.05605	2.20566	2.75405	3.00136	
MEAS/DEGK	6.0207	5.1608	4.5160	3.6132	2.5814	2.2530	1.8076	1.2057	.6038	.4534	.3631	.3029	
MEAS/PSCHT	315.46229	41.87167	365.67870309	40854221.09976193	50325154.86812133	55455	51.34070	38.96205	31.23475	25.08312			

RADIUS 59665.000 KM		ALTITUDE -135.000 KM		PRESSURE		6.617767 BARS		TEMPERATURE		273.053 KELVIN		31.825 FAHRENHEIT	
TIME 2331.421 SEC		VELOCITY 59.224 METER/SEC		DYN P		6.531228 AT							
38.95702 MIN		4.1361 M3/SEC		DOPPLER		4.2939781+02 CPS							
.647617 HRS		194.303 FT/SEC		MACH NO		.049523							
INSTRUMENTS	TEMP	PRESS	TEMP	PRESS	ACCEL	ACCEL	ACCEL	ACCEL	M SPEC	M SPEC	M SPEC	M SPEC	M SPEC
NO OF MEAS	778.14	567.12	583.86	467.28	33.05	292.43	234.14	150.43	78.71	59.29	47.03	39.80	
KM/MEAS	.17751	.20721	.23679	.29596	.41425	.47339	.55161	.56694	1.77107	2.35895	2.94900	3.53103	
MEAS/KM	5.8302	4.8261	4.2231	3.3768	2.4140	2.1124	1.6903	1.1275	.5646	.4239	.3392	.2632	
BARS/MEAS	.01241	.01448	.01655	.02069	.02897	.03311	.04140	.05213	.12447	.16614	.20789	.24973	
MEAS/BAR	80.5742	69.0599	50.4242	48.3342	34.5170	30.1931	24.1541	15.0941	8.0342	6.0192	4.6102	4.0043	
DEGK/MEAS	.16313	.19031	.21748	.27182	.39047	.43478	.54335	.81460	1.02662	2.16655	2.70536	3.23901	
MEAS/DEGK	6.1302	5.2547	4.5981	3.5789	2.5283	2.3300	1.8404	1.2276	.6148	.4616	.3687	.3087	
MEAS/PSCHT	333.72123	45.752219	400.37290320	33389228.92500200	35033160.35579107	40.0632	53.56658	40.33148	32.33030	26.99617			

SURVIVABLE SATURN PROBE TASK 4 DESCENT RUNS

JP. MINOGRAPH SATURN NOMINAL ATMOSPHERE

BALLISTIC COEFFICIENT = .700, INITIAL TIME = 0. SECONDS AT 59900.000 KM RADIUS

BAL. COEF. 0.55/0.70/1.50 SEP 30 BARS

RADIJS 59660.000 KM										TEMPERATURE 277.627 KELVIN 40.059 FAHRENHEIT									
ALTIUDE -140.000 KM										PRESSURE 6.973271 BARS									
VELOCITY 58.180 METER/SEC										DYN P .011620 BARS									
40.27676 MIN										DOPPLER 4.218338E+02 CPS									
.671279 HRS										MACH NO .046248									
INSTRUMENTS		TEMP	PRESS	TEMP	PRESS	ACCEL	ACCEL	ACCEL	ACCEL	M SPEC	M SPEC	M SPEC	M SPEC	M SPEC	M SPEC	M SPEC	M SPEC		
NO OF MEAS		806.34	591.46	605.15	484.32	346.23	303.08	242.60	162.11	31.55	61.42	1.74003	2.31768	2.89415	3.46947	4.04482	4.61915		
KM/MEAS		.17449	.20356	.23262	.26168	.29075	.31982	.34888	.37795	.40702	.43609	.46516	.49423	.52330	.55237	.58144	.61051		
MEAS/KM		5.7311	4.9126	4.2988	3.6850	3.0712	2.4574	1.8436	1.2298	.6160	.00215	.00430	.00645	.00860	.01075	.01290	.01505		
MEAS/MEAS		.01254	.01474	.01694	.01914	.02134	.02354	.02574	.02794	.03014	.03234	.03454	.03674	.03894	.04114	.04334	.04554		
MEAS/BAR		79.1291	67.8214	59.3406	47.4676	33.8983	23.0579	15.8067	9.5551	.00000	.00000	.00000	.00000	.00000	.00000	.00000	.00000		
DECK/MEAS		.15862	.18505	.21148	.23791	.26434	.29077	.31720	.34363	.37006	.39649	.42292	.44935	.47578	.50221	.52864	.55507		
DECK/DECK		6.3042	5.4039	4.7286	3.7833	2.7029	1.8926	1.2624	.8322	.5320	.3320	.2120	.1320	.0820	.0520	.0320	.0220		
MEAS/PSCHT		552.28841473	436.79414	298.07331	50.386236	8.8188207	3.1250165	3.1533110	7.1909	55.52257	41.72327	33.44358	27.92371	23.40382	19.88493	16.36604	12.84715		

RADIJS 59655.000 KM				ALTIUDE -145.000 KM				PRESSURE 7.341683 BARS				TEMPERATURE 282.173 KELVIN			
				-475.722 KFT				7.245678 ATM				48.241 FAHRENHEIT			
TIME 2503.307 SEC				VELOCITY 57.169 METER/SEC				DYN P .011620 BARS							
41.72176 MIN				4.2915 MB/SEC				DOPPLER 4.145002E+02 CPS							
.695363 HRS				167.362 FT/SEC				MACH NO .047020							

RADIJS 59650.000 KM										TEMPERATURE 286.718 KELVIN 56.423 FAHRENHEIT									
ALTIUDE -150.000 KM										PRESSURE 7.723268 BARS									
VELOCITY 56.190 METER/SEC										DYN P .011620 BARS									
43.19217 MIN										DOPPLER 4.074070E+02 CPS									
.719869 HRS										MACH NO .045853									
TIME	2591.530 SEC	TEMP	PRESS	ACCEL	ACCEL	ACCEL	ACCEL	ACCEL	ACCEL	M SPEC	M SPEC	M SPEC	M SPEC	M SPEC	M SPEC	M SPEC	M SPEC	M SPEC	M SPEC
NO OF MEAS	864.84	715.23	625.88	501.66	358.42	313.31	251.33	167.89	84.44	63.58	51.07	42.72	34.0963	2.7769	2.6471	2.5054	2.3516	2.1946	2.0386
KM/MEAS	.1745	.2002	.2298	.25870	.28570	.31950	.35950	.40620	.46020	1.70996	1.70996	1.70996	1.70996	1.70996	1.70996	1.70996	1.70996	1.70996	1.70996
MEAS/KM	5.8324	4.9995	4.3748	3.5002	2.5003	2.1693	1.7510	1.1579	0.5808	0.5808	0.5808	0.5808	0.5808	0.5808	0.5808	0.5808	0.5808	0.5808	0.5808
BARS/MEAS	.01287	.01501	.01716	.02145	.03003	.03932	.04891	.06440	.08490	.12900	.17218	.21594	.25876	.30995	.3687	.4326	.5016	.5756	.6546
MEAS/BAR	77.77281	65.6208	58.2902	46.5275	33.2985	23.1334	15.2566	7.7517	3.0574	1.55451	0.79053	0.40474	0.20985	0.10985	0.05985	0.02985	0.01485	0.00735	0.00385
DECK/MEAS	.15587	.18184	.20780	.23973	.36355	.41544	.51920	.77841	1.55451	1.55451	1.55451	1.55451	1.55451	1.55451	1.55451	1.55451	1.55451	1.55451	1.55451
DECK/DECK	6.5273	5.5951	4.8122	3.9502	2.7507	2.0771	1.5960	1.2847	0.9433	0.6433	0.4233	0.2733	0.1633	0.0933	0.0533	0.0233	0.0133	0.0073	0.0033
MEAS/PSCHT	571.155528489	690.3429	4.9821342	8.9397244	9.6766214	3.8756171	5.9739114	4.9424	57.09925	43.13828	33.57586	28.86706	24.86706	20.86706	16.86706	12.86706	8.86706	4.86706	0.86706

SURVIVABLE SATURN PROBE TASK 4 DESCENT RUNS
JP MONOGRAPH SATURN NOMINAL ATMOSPHERE
BALLISTIC COEFFICIENT = .700, INITIAL TIME = 0. SECONDS AT 59900.000 KM RADIUS

BAL. COEF. 0.65/0.70/1.50 SEP 30 BARS

RADIUS 59630.000 KM		ALTITUDE -170.000 KM		PRESSURE		9.386455 BARS		TEMPERATURE		30.900 KELVIN		89.150 FAHRENHEIT	
TIME 2959.66+ SEC		VELOCITY 52.579 METER/SEC		DYN P		DOPPLER		MACH NO		M SPEC		M SPEC	
49.32806 MIN		172.502 FT/SEC											
.822134 HRS													
INSTRUMENTS													
NO OF MEAS	TEMP	PRESS	TEMP	PRESS	ACCEL	ACCEL	ACCEL	ACCEL	ACCEL	M SPEC	M SPEC	M SPEC	M SPEC
15770	987.55	146.62	740.92	592.94	423.81	370.36	296.97	193.31	39.56	74.99	60.15	50.33	50.33
MEAS/KM	15770	18397	21024	26276	36783	42034	52534	78767	157335	2.09603	2.01784	3.13878	3.13878
MEAS/KM	6.3413	3.4357	4.7564	3.8054	2.7185	2.3730	1.9035	1.2696	.6356	.4771	.3820	.3186	.3186
BARS/MEAS	.01401	.01635	.01868	.02336	.03270	.03738	.04673	.07013	.14044	.18741	.23447	.28160	.28160
MEAS/BAR	71.3707	61.1722	53.5234	42.8150	30.5769	23.7525	14.2594	7.1205	1.53358	4.2650	3.5511	2.85344	2.85344
DEGK/MEAS	14335	16725	19113	23385	33439	38213	47758	71607	1.43032	1.90449	2.37986	2.85344	2.85344
MEAS/DEGK	6.9735	5.3792	5.2320	4.1860	2.9905	2.6159	2.0939	1.3965	.6991	.5248	.4202	.3505	.3505
MEAS/PSCHT	570.44738574	69017502.89475	42.38116287	50847508475201.35392134	434477	67.33539	50.58291	40.53133	33.63021				

RADIUS 59625.000 KM		ALTITUDE -175.000 KM		PRESSURE		9.837753 BARS		TEMPERATURE		309.445 KELVIN		97.332 FAHRENHEIT	
TIME 3055.548 SEC		VELOCITY 51.744 METER/SEC		DYN P		DOPPLER		MACH NO		M SPEC		M SPEC	
50.32580 MIN		169.765 FT/SEC											
.848763 HRS													
INSTRUMENTS													
NO OF MEAS	TEMP	PRESS	TEMP	PRESS	ACCEL	ACCEL	ACCEL	ACCEL	ACCEL	M SPEC	M SPEC	M SPEC	M SPEC
1019.52	374.01	764.89	612.11	437.51	382.34	366.55	204.78	102.85	77.39	62.11	51.93	51.93	51.93
MEAS/KM	15519	18105	20691	25861	36200	41338	51702	77520	1.54846	2.05230	2.57649	3.08923	3.08923
MEAS/KM	6.4435	5.5233	4.8331	3.8668	2.7624	2.4173	1.9342	1.2930	.6458	.4844	.3881	.3237	.3237
BARS/MEAS	.01424	.01662	.01899	.02374	.03324	.03739	.04750	.07128	.14274	.19048	.23830	.28620	.28620
MEAS/BAR	70.2150	60.1818	52.6559	42.1220	30.0821	23.3137	14.0250	7.0057	1.52498	4.1363	3.4944	2.72722	2.72722
DEGK/MEAS	14109	16459	18810	23510	32903	37607	46948	69610	1.37482	1.82536	2.27716	2.72722	2.72722
MEAS/DEGK	7.0879	5.0736	5.3164	4.2534	3.0387	2.6531	2.1300	1.4366	.7274	.5475	.4391	.3667	.3667
MEAS/PSCHT	591.25790592	55346519.52513414	488546296.44	40112534.223247	60614136.51313	69441878	52.14439	41.78044	34.87072				

RADIUS 59620.000 KM		ALTITUDE -180.000 KM		PRESSURE		10.303868 BARS		TEMPERATURE		313.850 KELVIN		103.260 FAHRENHEIT	
TIME 3152.958 SEC		VELOCITY 50.923 METER/SEC		DYN P		DOPPLER		MACH NO		M SPEC		M SPEC	
52.34930 MIN		167.071 FT/SEC											
.875822 HRS													
INSTRUMENTS													
NO OF MEAS	TEMP	PRESS	TEMP	PRESS	ACCEL	ACCEL	ACCEL	ACCEL	ACCEL	M SPEC	M SPEC	M SPEC	M SPEC
1051.99	301.95	789.24	631.59	451.42	395.12	316.30	211.20	106.10	79.82	64.06	53.55	53.55	53.55
MEAS/KM	15273	17818	20363	25451	35625	40712	50882	70292	1.52398	2.03034	2.53586	3.04061	3.04061
MEAS/KM	6.5474	5.6123	4.9110	3.9291	2.8063	2.4253	1.9653	1.3108	.6562	.4925	.3943	.3289	.3289
BARS/MEAS	.01448	.01689	.01930	.02413	.03373	.03852	.04828	.07245	.14509	.19361	.24221	.29088	.29088
MEAS/BAR	69.6779	59.2072	51.6041	41.4399	29.5951	23.8935	20.7114	13.4026	6.8925	5.1651	4.1267	3.4378	3.4378
DEGK/MEAS	13406	15640	17873	22340	31270	35735	44661	66934	1.33768	1.76211	2.22584	2.68687	2.68687
MEAS/DEGK	7.4594	5.3940	5.5950	4.4764	3.1973	2.7984	2.2391	1.4933	.7476	.5611	.4493	.3747	.3747
MEAS/PSCHT	712.26923510	56278534.282394427	49116305.44339267	3035213.9075412	71293	71.51811	53.71928	43.03390	35.92025				

SURVIVABLE SATURN PROBE TASK 4 DESCENT RUNS
JP- MONOGRAPH SATURN IONMAL ATMOSPHERE
BALLISTIC COEFFICIENT = .700, INITIAL TIME = 0. SECONDS AT 59800.00 KM RADIUS
BAL. COEF. 0.65/0.70/L.50 SEP 30 BARLS

[illegible]

RADII'S	59610.003 KM	ALTITUDE	-190.000 KM	PRESSURE	11.282073 BAARS	TEMPERATURE	322.627 KELVIN
			-626.360 MET		11.134540 ATM		121.059 FAHRENHEIT
TIME	3392.460 SEC	VELOCITY	+9.350 METER/SEC	DYN P	.011052 BAARS		
	55.87444 MIN		+9.923 M/M/SEC	JOPP-ER	3.578070E+02 CPS		
	.931241 HRS		131.308 FT/SEC	MACH NO	.037963		
INSTRUMENTS	TEMP	PRESS	TEMP	PRESS	ACCEL	ACCEL	M SPEC
KNO OF MEAS	1118.99	358.885	639.12	671.449	+20.006	336.25	112.75
MEAS/KM	1.301	1.788	1.9734	2.0665	.39455	.49312	.79339
MEAS/HK	6.7561	5.7912	5.0575	4.0543	2.8564	2.0279	1.3525
BARS/MEAS	.31495	.01744	.01993	.02492	.03489	.04985	.07481
MEAS/BAR	66.8493	57.3401	50.1706	46.1334	28.6522	25.0775	20.0589
DECK/MEAS	12.992	1.5157	1.7421	2.1050	.30305	.34263	.64849
MEAS/DEGK	7.6972	5.5978	5.7733	4.5190	3.2682	3.6332	1.29650
MEAS/PSCHT	755.262399647	4.14566565	5.2824453	287.93933	8.6525283	4.2618226	8.0562151
					3.2998	2.3104	.7713
							56.9439
							45.61951
							38.06993

RADIOJS 59505.000 KM		ALTITUDE -195.000 KM		PRESSURE		11.794730 3AKS		TEMPERATURE		327.016 KELVIN	
TIME 3554.572 SEC		VELOCITY -639.784 KET		DYN P		0.11052 3AKS		126.959 FAHRENHEIT			
57.57620 MIN		3.5737 M3/SEC		JOPP-ER		3.523462E+02 CPS					
.959603 HRS		159.437 FT/SEC		MACH NU		.037132					
INSTRUMENTS		PRESS		ACCEL		ACCEL		M SPEC		M SPEC	
1152152		861.64		+32.32		346.46		116.15		87.30	
NM/MEAS		17.004		34.000		.88550		1.93809		58.58	
14576		24289		.00854		.72813		1.55404		2.90285	
MEAS/KM		5.8609		2.9412		2.0593		.6675		.3445	
.01318		.01772		.03544		.05068		.15215		.30495	
MEAS/SEC		55.4464		28.2158		19.7466		6.5723		3.27886	
65.6557		49.3858		24.6859		13.1594		1.27668		2.54794	
DEGR/MEAS		.17357		.34134		.42623		4.9255		3.6778	
127954		.70000		2.9843		.83911		2.12485		.7000	
MEAS/DEGR		5.74254		3.3509		2.3401		.7832		.3925	
777.261426666		.02706466		.88644333		.00513155		78.01728		39.16385	
MEAS/PSCHT		27036593		23713291		.5757233		58.593566		46.93341	

SURVIVABLE SATURN PROBE TASK 4, DESCENT RUNS
JP. MONOGRAPH SATURN NOMINAL ATMOSPHERE

BALLISTIC COEFFICIENT = .700, INITIAL TIME = 0. SECONDS AT 59900.000 KM RADIUS

BAL. COEF. 0.65/0.70/1.50 SEP 30 BARS

RADIJS 59600.000 KM ALTITUDE -200.000 KM PRESSURE 12.323471 BARS TEMPERATURE 331.405 KELVIN
-656.160 KFT 12.162320 ATM 136.850 FAHRENHEIT

TIME 3559.249 SEC VELOCITY 47.864 METER/SEC DYN P .011652 BARS
59.30415 MIN 5.1431 M3/SEC DOPPLER 3.470391E+02 CPS
.988403 HRS 157.035 FT/SEC MACH NO .036330

INSTRUMENTS TEMP PRESS TEMP PRESS ACCEL ACCEL ACCEL ACCEL M SPEC M SPEC M SPEC
NO OF MEAS 1187.00 1017.64 890.56 712.65 509.32 445.70 356.82 238.22 119.61 89.96 72.16 60.30
KM/MEAS .14356 .16748 .19140 .23924 .32480 .38259 .47830 .71719 1.43282 1.90905 2.38460 2.85948
MEAS/KM 6.9656 5.9708 5.2246 4.1800 2.9861 2.6131 2.0908 1.3943 .6979 .5238 .4194 .3497
BARS/MEAS .01542 .01799 .02056 .02571 .03593 .04114 .05143 .07718 .13452 .20618 .25791 .30972
MEAS/BAR 64.8433 55.5780 48.6289 38.9003 27.7819 24.4430 19.4430 12.9573 6.4715 4.8501 3.8772 3.2287
DECK/MEAS .12601 .14701 .16800 .20999 .29394 .33530 .41982 .62950 1.25764 1.67565 2.09306 2.50988
MEAS/DECK 7.9359 5.8024 5.9523 4.7622 3.4021 2.9770 2.3820 1.5886 .7951 .5968 .4778 .3984
MEAS/PSCHT 799.59501685.41343593.77724479.88657342.86865300.05054240.10518160.17799 80.25062 60.26866 48.27942 40.28653

RADIJS 59595.000 KM ALTITUDE -205.000 KM PRESSURE 12.068581 BARS TEMPERATURE 335.793 KELVIN
-672.572 KFT 12.700302 ATM 144.758 FAHRENHEIT

TIME 3663.502 SEC VELOCITY 47.153 METER/SEC DYN P .011652 BARS
61.05836 MIN 5.2277 M3/SEC DOPPLER 3.448792E+02 CPS
1.017639 HRS 154.701 FT/SEC MACH NO .035555

INSTRUMENTS TEMP PRESS TEMP PRESS ACCEL ACCEL ACCEL ACCEL M SPEC M SPEC M SPEC
NO OF MEAS 1222.17 1347.71 916.88 733.70 524.35 458.94 367.35 245.23 123.12 92.59 74.27 62.06
KM/MEAS .14143 .16499 .18856 .23568 .32991 .37701 .47120 .70654 1.41160 1.88082 2.34938 2.81730
MEAS/KM 7.0707 5.0608 5.3034 4.2430 3.0312 2.6525 2.1223 1.4153 .7084 .5317 .4256 .3550
BARS/MEAS .01566 .01827 .02088 .02610 .03655 .04177 .05223 .07837 .13690 .20935 .26187 .31447
MEAS/BAR 63.8582 54.7336 47.8902 38.3095 27.3600 23.9393 19.1479 12.7607 6.3735 4.7768 3.8187 3.1800
DECK/MEAS .12414 .14482 .16550 .20687 .28957 .33032 .41359 .62016 1.23902 1.65087 2.06214 2.47285
MEAS/DECK 8.0556 5.9050 6.0421 4.3340 3.4534 3.0219 2.4179 1.6125 .8071 .6057 .4849 .4044
MEAS/PSCHT 922.26432704.84427615.77922493.48815352.58405308.55152246.90596164.71183 82.31753 61.96885 49.63956 41.41999

RADIJS 59590.000 KM ALTITUDE -210.000 KM PRESSURE 13.430349 BARS TEMPERATURE 340.182 KELVIN
-686.976 KFT 13.254724 ATM 152.658 FAHRENHEIT

TIME 3770.332 SEC VELOCITY 46.451 METER/SEC DYN P .011652 BARS
62.83887 MIN 5.3065 M3/SEC DOPPLER 3.388608E+02 CPS
1.047315 HRS 152.430 FT/SEC MACH NO .034807

INSTRUMENTS TEMP PRESS TEMP PRESS ACCEL ACCEL ACCEL ACCEL M SPEC M SPEC M SPEC
NO OF MEAS 1257.78 1378.24 943.58 753.07 539.62 472.29 378.03 252.36 126.68 95.26 76.41 63.84
KM/MEAS .13935 .16257 .18579 .23222 .32507 .37140 .46429 .69619 1.39096 1.85335 2.31511 2.77626
MEAS/KM 7.1760 6.1511 5.3824 4.3062 3.0763 2.6919 2.1538 1.4364 .7189 .5396 .4319 .3682
BARS/MEAS .01590 .01855 .02120 .02650 .03711 .04241 .05302 .07956 .15928 .21252 .26583 .31922
MEAS/BAR 62.9001 53.9125 47.1718 37.7348 26.9497 23.5793 18.8609 12.5695 6.2782 4.7054 3.7617 3.1326
DECK/MEAS .12332 .14270 .16308 .20383 .28532 .32636 .40752 .61108 1.22090 1.62676 2.03207 2.43643
MEAS/DECK 8.1756 7.8079 6.1321 4.3060 3.5048 3.0669 2.4538 1.6365 .8191 .6147 .4921 .4184
MEAS/PSCHT 945.26994724.56336634.833442507.29151362.44358317.17860253.80762169.31293 84.01807 63.69425 51.01989 42.57026

SURVIVABLE SATURN PROBE TASK 4 DESCENT RUNS
JP- MONOGRAPH SATURN NOMINAL ATMOSPHERE

BALLISTIC COEFFICIENT = .700, INITIAL TIME = 0. SECONDS AT 59900.000 KM RADIUS

BAL. COEF. 0.65/0.70/1.50 SEP 30 BARS

RADIUS 59285.000 KM		ALTITUDE -215.000 KM		PRESSURE 14.009065 BARS		TEMPERATURE 344.571 KELVIN		160.557 FAHRENHEIT	
		-705.381 KFT		13.825872 ATM					
TIME	3873.745 SEC	VELOCITY	45.787 METER/SEC	DYN P	.011652 BARS				
	6.534574 MIN		5.3854 MB/SEC	DOPPLER	3.319782E+02 CPS				
	1.077423 HRS		150.220 FT/SEC	MACH NO	.034083				
INSTRUMENTS									
NO OF MEAS	TEMP	PRESS	TEMP	PRESS	ACCEL	ACCEL	ACCEL	M SPEC	M SPEC
1337.91	1109.21	970.69	775.75	555.11	388.87	259.58	130.59	97.97	78.57
1373.33	16022	18310	22886	32035	36610	45757	63612	1.37087	1.82662
MEAS/KM	7.2815	5.2415	5.4615	4.3695	3.1215	2.7315	2.1855	1.4575	.5475
BARS/MEAS	.01514	.01883	.02152	.02690	.03765	.04305	.05302	.08075	.16187
MEAS/BAR	61.9679	51.1136	46.4728	37.1757	26.5505	23.2301	18.5816	12.3835	6.1855
DEGK/MEAS	.12054	.14063	.16071	.20088	.28113	.32134	.40162	.60224	1.20327
MEAS/DEGK	8.2958	7.1109	6.2222	4.9781	3.5563	3.1120	2.4899	1.6605	.8311
MEAS/PSCHT	368.612427	44.57119651	54027521.29698372	44749325.9321260	81034173.98150	87.15230	65.44492	52.42043	43.73737

RADIUS 59880.000 KM		ALTITUDE -220.000 KM		PRESSURE 14.605019 BARS		TEMPERATURE 348.959 KELVIN		168.457 FAHRENHEIT	
		-721.785 KFT		14.414033 ATM					
TIME	3988.741 SEC	VELOCITY	45.132 METER/SEC	DYN P	.011652 BARS				
	6.607902 MIN		5.4646 MB/SEC	DOPPLER	3.272280E+02 CPS				
	1.107984 HRS		148.070 FT/SEC	MACH NO	.033383				
INSTRUMENTS									
NO OF MEAS	TEMP	PRESS	TEMP	PRESS	ACCEL	ACCEL	ACCEL	M SPEC	M SPEC
1330.58	1140.64	998.19	798.15	570.82	399.97	266.92	133.96	100.72	80.77
1357.37	15793	18048	22559	31578	36037	45102	67632	1.35132	1.80060
MEAS/KM	7.3872	5.3321	5.5408	4.4329	3.1668	2.7711	2.2172	1.4786	.5554
BARS/MEAS	.01638	.01911	.02184	.02730	.03822	.04359	.05462	.08195	.16406
MEAS/BAR	61.0607	52.3360	45.7925	36.5316	26.1620	22.8902	18.3098	12.2025	6.0952
DEGK/MEAS	.11862	.13682	.15841	.19801	.27717	.31675	.39508	.59363	1.18611
MEAS/DEGK	8.4182	7.2141	6.3126	5.0504	3.6079	3.1571	2.5280	1.6846	.8431
MEAS/PSCHT	392.292327	64.86824669	30019535.50490382	59599333.811395267	91429178.71736	89.52027	67.22090	53.84121	44.92136

RADIUS 59375.000 KM		ALTITUDE -225.000 KM		PRESSURE 15.218505 BARS		TEMPERATURE 353.348 KELVIN		176.357 FAHRENHEIT	
		-738.189 KFT		15.019497 ATM					
TIME	4100.325 SEC	VELOCITY	44.494 METER/SEC	DYN P	.011652 BARS				
	6.833875 MIN		5.5439 MB/SEC	DOPPLER	3.225991E+02 CPS				
	1.138973 HRS		145.976 FT/SEC	MACH NO	.032706				
INSTRUMENTS									
NO OF MEAS	TEMP	PRESS	TEMP	PRESS	ACCEL	ACCEL	ACCEL	M SPEC	M SPEC
1367.78	1172.52	1026.08	821.07	586.75	513.24	411.03	274.36	137.68	103.51
1334.6	15569	17793	22240	31132	35577	44453	66677	1.33228	1.77526
MEAS/KM	7.4931	5.4229	5.6202	4.4955	3.2122	2.8108	2.2489	1.4998	.5633
BARS/MEAS	.01652	.01939	.02216	.02770	.03878	.04433	.05542	.08315	.16646
MEAS/BAR	60.1774	51.5790	45.1302	36.1018	25.7837	22.5533	18.0451	12.0262	6.0074
DEGK/MEAS	.11714	.13666	.15618	.19521	.27325	.31237	.39029	.58525	1.16940
MEAS/DEGK	8.5369	7.3175	6.4031	5.1228	3.6595	3.2023	2.5622	1.7087	.8511
MEAS/PSCHT	316.31019785	45499687.31358549	91561392.6893534	3.61833275	1.1963183	5.52091	91.32204	69.02222	55.28226

RADIUS 59375.000 KM		ALTITUDE -225.000 KM		PRESSURE 15.218505 BARS		TEMPERATURE 353.348 KELVIN		176.357 FAHRENHEIT	
		-738.189 KFT		15.019497 ATM					
TIME	4100.325 SEC	VELOCITY	44.494 METER/SEC	DYN P	.011652 BARS				
	6.833875 MIN		5.5439 MB/SEC	DOPPLER	3.225991E+02 CPS				
	1.138973 HRS		145.976 FT/SEC	MACH NO	.032706				
INSTRUMENTS									
NO OF MEAS	TEMP	PRESS	TEMP	PRESS	ACCEL	ACCEL	ACCEL	M SPEC	M SPEC
1367.78	1172.52	1026.08	821.07	586.75	513.24	411.03	274.36	137.68	103.51
1334.6	15569	17793	22240	31132	35577	44453	66677	1.33228	1.77526
MEAS/KM	7.4931	5.4229	5.6202	4.4955	3.2122	2.8108	2.2489	1.4998	.5633
BARS/MEAS	.01652	.01939	.02216	.02770	.03878	.04433	.05542	.08315	.16646
MEAS/BAR	60.1774	51.5790	45.1302	36.1018	25.7837	22.5533	18.0451	12.0262	6.0074
DEGK/MEAS	.11714	.13666	.15618	.19521	.27325	.31237	.39029	.58525	1.16940
MEAS/DEGK	8.5369	7.3175	6.4031	5.1228	3.6595	3.2023	2.5622	1.7087	.8511
MEAS/PSCHT	316.31019785	45499687.31358549	91561392.6893534	3.61833275	1.1963183	5.52091	91.32204	69.02222	55.28226

SURVIVABLE SATURN PROBE TASK 4 DESCENT RUNS
JPL MONOGRAPH SATURN NOMINAL ATMOSPHERE
BALLISTIC COEFFICIENT = .700, INITIAL TVE = 0. SECONDS AT 5900.000 KM RADIUS

BAL. COEF. 0.55/0.70/1.50 SEP 30 BARS

RADIUS 59570.000 KM		ALTITUDE -230.000 KM		PRESSURE -754.533 KFT		TEMPERATURE 357.737 KELVIN	
TIME 4213.500 SEC		VELOCITY 43.872 METER/SEC		DYN P .011652 BARS		184.256 FAHRENHEIT	
70.22500 MIN		5.6234 MB/SEC		DOPPLER 3.180329E+02 CPS			
1.170417 HRS		143.937 FT/SEC		MACH NO .032051			

INSTRUMENTS		TEMP	PRESS	TEMP	PRESS	ACCEL	ACCEL	ACCEL	M SPEC	M SPEC	M SPEC	M SPEC
NO OF MEAS		1483.50	1204.86	1054.37	843.70	602.93	527.59	422.35	281.90	141.45	106.34	85.27
KM/MEAS		.13159	.15352	.17545	.21929	.30697	.35030	.43845	.55747	1.31374	1.75057	2.18688
BARS/KM		7.5993	5.5138	5.0398	4.5601	3.2575	2.8506	2.2808	1.5210	.7612	.5712	.4573
MEAS/KM		.01686	.01967	.02248	.02810	.03935	.04497	.05622	.08436	.16887	.22530	.28180
BARS/BAR		59.3172	50.8417	44.4851	35.5859	25.4153	22.2370	17.7874	11.8546	5.9217	4.4385	3.5486
MEAS/BAR		.11350	.13475	.15399	.19248	.26944	.30791	.38485	.57709	1.15312	1.53655	1.91951
DECK/MEAS		6.6578	7.4212	6.4937	5.1953	3.7114	3.2477	2.5984	1.7328	.8672	.6508	.5210
MEAS/DECK		340.66658806	33189705	58087554	52943403	32778352	95226282	42652188	39216	94.35765	70.84893	56.74363
MEAS/PSCHT												47.34005

RADIUS 59563.000 KM		ALTITUDE -235.000 KM		PRESSURE -770.997 KFT		TEMPERATURE 362.125 KELVIN	
TIME +323.268 SEC		VELOCITY 43.267 METER/SEC		DYN P .011652 BARS		192.156 FAHRENHEIT	
72.13780 MIN		5.7030 MB/SEC		DOPPLER 3.137026E+02 CPS			
1.202297 HRS		141.951 FT/SEC		MACH NO .031415			

INSTRUMENTS		TEMP	PRESS	TEMP	PRESS	ACCEL	ACCEL	ACCEL	M SPEC	M SPEC	M SPEC	M SPEC
NO OF MEAS		1443.76	1237.65	1083.07	863.65	613.32	542.03	433.83	289.55	145.28	109.21	87.57
KM/MEAS		.12378	.15140	.17302	.21627	.30274	.34537	.43241	.56841	1.29566	1.72652	2.15687
BARS/KM		7.7056	5.6050	5.7795	4.5239	3.3032	2.8905	2.3125	1.5422	.7718	.5792	.4636
MEAS/KM		.01710	.01995	.02280	.02850	.03991	.04551	.05702	.08556	.17128	.22851	.28582
BARS/BAR		58.4792	50.1235	43.8567	35.0832	25.0564	21.9230	17.5363	11.6873	5.8383	4.3761	3.4488
MEAS/BAR		.11391	.13283	.15187	.19983	.26573	.30357	.37954	.56914	1.13726	1.51544	1.89317
DECK/MEAS		8.7789	7.5250	6.5846	5.2680	3.7633	3.2931	2.6348	1.7570	.8793	.6599	.5282
MEAS/DECK		365.36203827	439+2724	10245579	34669413	91153362	23303289	83513193	33123	96.82718	72.70107	58.22534
MEAS/PSCHT												48.57481

RADIUS 59560.000 KM		ALTITUDE -240.000 KM		PRESSURE -787.402 KFT		TEMPERATURE 366.514 KELVIN	
TIME 444.633 SEC		VELOCITY 42.676 METER/SEC		DYN P .011652 BARS		200.056 FAHRENHEIT	
74.07721 MIN		5.7828 MB/SEC		DOPPLER 3.094241E+02 CPS			
1.234620 HRS		140.015 FT/SEC		MACH NO .030802			

INSTRUMENTS		TEMP	PRESS	TEMP	PRESS	ACCEL	ACCEL	ACCEL	M SPEC	M SPEC	M SPEC	M SPEC
NO OF MEAS		1482.54	1270.90	1112.16	883.93	635.95	556.58	445.46	297.31	149.15	112.12	89.89
KM/MEAS		.12801	.14934	.17067	.21332	.29861	.34125	.42651	.56359	1.27805	1.70308	2.12761
BARS/KM		7.8121	5.6963	5.6594	4.5874	3.3488	2.9304	2.3446	1.5635	.7824	.5872	.4700
MEAS/KM		.01734	.02023	.02312	.02891	.04047	.04626	.05783	.08677	.17370	.23174	.28984
BARS/BAR		57.6625	43.4235	33.2443	24.7065	21.6170	17.2916	11.5243	5.7570	4.3152	3.4501	2.8734
MEAS/BAR		.11236	.13108	.14980	.19724	.26210	.29953	.37437	.56139	1.12180	1.49486	1.86749
DECK/MEAS		8.9002	7.6290	6.6756	5.3408	3.8153	3.3386	2.6712	1.7813	.8914	.6690	.5355
MEAS/DECK		390.39709848	95803742	87873594	35771+24	64082371	60116297	34563198	33822	99.33066	74.37868	59.72743
MEAS/PSCHT												49.82655

SURVIVABLE SATURN PROBE TASK 4 DESCENT RUNS

JP. MONOGRAPH SATURN VOMINAL ATMOSPHERE

BALLISTIC COEFFICIENT = .700, INITIAL TIME = 0. SECONDS AT 59900.000 KM RADIUS

BAL. COEF. 0.5570.70/1.50 SEP 30 BARS

RADIUS 59555.000 KM ALTITUDE -245.000 K4 PRESSURE 17.853663 BARS TEMPERATURE 370.903 KELVIN
 -803.806 KFT 17.620196 ATM 207.955 FAHRENHEIT

TIME 42.597 SEC VELOCITY 42.101 METER/SEC DYN P
 76.04328 MIN 5.8628 MB/SEC DOPP-ER 3.052531E+02 CPS
 1.257383 HRS 136.127 FT/SEC MACH NO .030206

INSTRUMENTS TEMP PRESS TEMP PRESS ACCEL ACCEL M SPEC M SPEC M SPEC M SPEC
 NO OF MEAS 1521.87 1304.60 114.165 913.52 652.80 571.32 457.26 305.17 153.09 115.06 92.25 77.04
 KM/MEAS .12628 .14732 .16837 .21045 .29459 .33656 .42077 .63098 1.26088 1.68022 2.09908 2.51747
 MEAS/KM 7.9188 5.7877 5.9394 4.7518 3.3945 2.9704 2.3765 1.5848 .7931 .5952 .4764 .3972
 BARS/MEAS .01759 .02052 .02345 .02931 .04104 .04531 .05864 .08799 .17613 .23497 .29388 .35286
 MEAS/BAR 56.8653 43.7412 42.6473 34.1159 24.3655 21.3187 17.0530 11.3654 .56778 4.2559 3.4027 2.8340
 DEGR/MEAS .11084 .12931 .14778 .19472 .25857 .29350 .36933 .55383 1.10672 1.47479 1.84245 2.20968
 MEAS/DEGR 9.0218 7.7332 6.7667 5.4437 3.8674 3.3841 2.7076 1.8056 .9036 .6781 .5428 .4826
 MEAS/PSCHT *15.77226870.70817761.91010609.59280435.51587381.11633304.95816203.41323101.86815 76.48179 61.24992 51.09529

RADIUS 59550.000 KM ALTITUDE -250.000 K4 PRESSURE 18.559244 BARS TEMPERATURE 375.292 KELVIN
 -820.210 KFT 18.316950 ATM 215.855 FAHRENHEIT

TIME 4082.163 SEC VELOCITY 41.540 METER/SEC DYN P
 78.03606 MIN 5.9430 MB/SEC DOPPLER 3.011857E+02 CPS
 1.300601 HRS 136.287 FT/SEC MACH NO .029629

INSTRUMENTS TEMP PRESS TEMP PRESS ACCEL ACCEL M SPEC M SPEC M SPEC M SPEC
 NO OF MEAS 1561.72 1338.76 117.154 937.43 669.88 586.27 469.22 313.14 157.07 118.05 94.64 79.04
 KM/MEAS .12450 .14536 .16812 .20764 .29067 .33217 .41517 .62258 1.24413 1.65792 2.07126 2.48414
 MEAS/KM 8.0257 5.8794 6.0196 4.8160 3.4404 3.0105 2.4086 1.6062 .8038 .6032 .4828 .4026
 BARS/MEAS .01783 .02080 .02377 .02972 .04161 .04736 .05945 .08920 .17856 .23821 .29793 .35772
 MEAS/BAR 56.0930 43.0758 42.0651 33.6502 24.0332 21.0278 16.8204 11.2104 5.6005 4.1980 3.3565 2.7955
 DEGR/MEAS .10337 .12759 .14581 .18226 .25513 .29136 .36441 .54647 1.09202 1.45522 1.81802 2.18042
 MEAS/DEGR 9.1436 7.9376 6.8581 5.4868 3.9195 3.4238 2.7441 1.8299 .9157 .6872 .5500 .4586
 MEAS/PSCHT *41.44880982.75031781.19697625.02228446.53692390.76024312.67280208.55637104.43971 78.41046 62.79285 52.38107

RADIUS 59545.000 KM ALTITUDE -255.000 KM PRESSURE 19.284143 BARS TEMPERATURE 379.680 KELVIN
 -836.614 KFT 19.031969 ATM 223.754 FAHRENHEIT

TIME 4803.335 SEC VELOCITY 40.993 METER/SEC DYN P
 80.05529 MIN 6.0234 MB/SEC DOPP-ER 2.972182E+02 CPS
 1.334260 HRS 134.431 FT/SEC MACH NO .029069

INSTRUMENTS TEMP PRESS TEMP PRESS ACCEL ACCEL M SPEC M SPEC M SPEC M SPEC
 NO OF MEAS 1602.11 1373.38 1201.83 961.67 687.19 501.42 481.33 321.22 161.11 121.08 97.07 81.06
 KM/MEAS .12296 .14345 .16394 .20491 .28684 .32780 .40971 .61439 1.22779 1.63617 2.04411 2.45161
 MEAS/KM 8.1328 5.9712 6.0999 4.8802 3.4862 3.0506 2.4408 1.6276 .8145 .6112 .4892 .4079
 BARS/MEAS .01807 .02109 .02410 .03012 .04218 .04821 .06026 .09042 .18099 .24146 .30199 .36258
 MEAS/BAR 55.3328 47.4268 41.4373 33.1560 23.7083 20.7441 16.5934 11.0592 5.5251 4.1415 3.3114 2.7580
 DEGR/MEAS .10793 .12591 .14389 .17986 .25177 .28772 .35962 .53928 1.07768 1.43613 1.79419 2.15187
 MEAS/DEGR 9.2656 7.9422 6.9496 5.5600 3.9718 3.4756 2.7807 1.8543 .9279 .6963 .5574 .4647
 MEAS/PSCHT *67.54509915.08487800.73971640.63647457.70419403.53130320.489896213.76774107.04539 80.36471 64.35626 53.68391

SURVIVABLE SATURN PROBE TASK 4 DESCENT RUNS
 JP MONOGRAPH SATURN NOMINAL ATMOSPHERE
 BALLISTIC COEFFICIENT = .700, INITIAL TIME = 0. SECONDS AT 59900.000 KM RADIUS
 BAL. COEF. 0.65/0.70/1.50 SEP 30 BARS

RADIJS 59540.000 KM		ALTITUDE -260.000 KM		PRESSURE 20.028660 BARS		TEMPERATURE 384.069 KELVIN	
		-853.018 KFT		19.766751 ATM		231.654 FAHRENHEIT	
TIME	4926.116 SEC	VELOCITY	40.439 METER/SEC	DYN P			
	82.10193 MIN		6.1164 MB/SEC	DOPPLER	2.933470E+02 CPS		
	1.358365 HRS		132.740 FT/SEC	MACH NO	.028526		

INSTRUMENTS		TEMP	PRESS	ACCEL	ACCEL	ACCEL	M SPEC	M SPEC	M SPEC
NO OF MEAS	1643.04	1232.53	985.22	784.73	316.76	493.61	329.41	165.20	124.15
KM/MEAS	.12136	.14158	.20224	.28311	.32354	.40438	.60640	1.21185	1.61434
MEAS/KM	8.2401	7.0631	6.1804	4.9346	3.5322	2.4729	1.6491	.8252	.6192
BARS/MEAS	.01832	.02137	.02442	.03053	.04275	.06108	.09164	.18344	.24471
MEAS/BARS	54.5940	45.7936	40.9433	32.7529	23.3924	16.3720	10.9118	5.4515	4.0864
DECK/MEAS	.10652	.12427	.14202	.17752	.24849	.35494	.53226	1.06368	1.41750
MEAS/DECK	9.3879	8.0470	7.0413	5.6333	4.0242	2.8174	1.8788	.9401	.7055
MEAS/PSGHT	*93.94377937	*71231820	*53871636	*49567469	*01783410	*43108328	*40954219	*04745109	*68523
									82.34459
									65.94016
									55.00382

RADIJS 59535.000 KM		ALTITUDE -265.000 KM		PRESSURE 20.793101 BARS		TEMPERATURE 388.458 KELVIN	
		-869.423 KFT		20.521195 ATM		239.554 FAHRENHEIT	
TIME	5053.587 SEC	VELOCITY	39.938 METER/SEC	DYN P			
	84.17512 MIN		6.1972 MB/SEC	DOPPLER	2.895688E+02 CPS		
	1.402919 HRS		131.030 FT/SEC	MACH NO	.027999		

INSTRUMENTS		TEMP	PRESS	ACCEL	ACCEL	ACCEL	M SPEC	M SPEC	M SPEC
NO OF MEAS	1684.50	1263.63	1011.10	722.50	532.31	506.05	337.70	159.35	127.26
KM/MEAS	.11980	.13976	.15972	.19964	.27943	.39917	.59860	1.18628	1.59422
MEAS/KM	8.3476	7.1552	6.2610	5.0091	3.5783	2.5052	1.6706	.8359	.6273
BARS/MEAS	.01856	.02166	.02475	.03094	.04332	.06190	.09287	.18588	.24798
MEAS/BARS	53.8729	45.1756	40.4026	32.3203	23.0835	16.1559	10.7678	5.3797	4.0326
DECK/MEAS	.10515	.12267	.14019	.17523	.24530	.35037	.52542	1.05002	1.39931
MEAS/DECK	9.5103	8.1519	7.1331	5.7068	4.0767	2.8541	1.9032	.9524	.7146
MEAS/PSGHT	*20.68465960	*53305840	*59436672	*54018480	*47825420	*45839336	*43178224	*39560112	*35929
									84.35014
									67.54459
									56.34085

RADIJS 59530.000 KM		ALTITUDE -270.000 KM		PRESSURE 21.577771 BARS		TEMPERATURE 392.846 KELVIN	
		-885.827 KFT		21.295605 ATM		247.453 FAHRENHEIT	
TIME	5175.512 SEC	VELOCITY	39.429 METER/SEC	DYN P			
	86.27521 MIN		6.2783 MB/SEC	DOPPLER	2.858802E+02 CPS		
	1.437920 HRS		129.361 FT/SEC	MACH NO	.027438		

INSTRUMENTS		TEMP	PRESS	ACCEL	ACCEL	ACCEL	M SPEC	M SPEC	M SPEC
NO OF MEAS	1726.50	1295.13	1036.30	740.50	548.06	518.65	346.10	173.55	130.41
KM/MEAS	.11827	.13798	.15769	.19710	.27591	.39409	.59039	1.18109	1.57339
MEAS/KM	8.4552	7.2475	6.3418	5.0737	3.6244	2.5375	1.6921	.8467	.6353
BARS/MEAS	.01881	.02194	.02508	.03135	.04389	.06272	.09410	.18834	.25125
MEAS/BARS	53.1690	45.5723	39.6747	31.8981	22.7820	15.9333	10.6273	5.3096	3.9601
DECK/MEAS	.10381	.12111	.13841	.17300	.24217	.34591	.51873	1.03668	1.38155
MEAS/DECK	9.6330	8.2571	7.2251	5.7804	4.1293	2.8909	1.9278	.9646	.7238
MEAS/PSGHT	*47.76822983	*84754860	*90703688	*73031492	*08547430	*61521344	*55683229	*81229115	*06763
									86.38138
									69.16958
									57.69501

SURVIVABLE SATURN PROBE TASK 4 DESCENT RUNS

JP. MONOGRAPH SATURN NOMINAL ATMOSPHERE

BALLISTIC COEFFICIENT = .700, INITIAL TIME = 0. SECONDS AT 59900.000 KM RADIIJS

BAL. COEF. 0.65/0.70/1.50 SEP 30 BARS

RADJIS	59525.000 KM	ALTITUDE	-275.000 KM	PRESSURE	22.382977 BAKS	TEMPERATURE	397.23> KELVIN
			-902.231 KFT		22.090281 AT		255.353 FAHRENHEIT
TIME	530+.135 SEC	VELOCITY	38.932 METER/SEC	DYN P	.011676 BAKS		
	88.+0224 MIN		1.3594 M3/SEC	DOPPLER	2.822782E+02 CPS		
	1.473371 HRS		127.731 FT/SEC	MACH NO	.026991		

INSTRUMENTS	TEMP	PRESS	TEMP	PRESS	ACCEL	ACCEL	ACCEL	M SPEC	M SPEC	M SPEC	M SPEC
1769.04	1.16147	1.327.03	1061.03	758.73	564.12	531.41	354.31	177.80	133.60	107.06	89.40
1.1678	1.3624	1.55370	1.9461	2.7233	3.1114	3.6913	3.8355	1.16625	1.5423	1.94184	2.32906
MEAS/KM	8.5631	7.3400	6.4226	5.1384	3.6705	3.2120	2.5698	1.7136	1.6575	1.5434	1.4294
BAR/MEAS	0.1905	0.2223	0.02541	0.03176	0.0447	0.0582	0.0645	0.19080	0.31332	0.5150	0.8294
MEAS/BAK	52.4816	44.9831	39.3593	31.4858	22.4875	13.6787	15.7390	10.4300	5.2411	3.9288	2.6166
DECK/MEAS	10.250	1.1958	1.3666	1.7082	2.3912	2.7327	3.4156	5.1221	1.02366	1.36421	2.04431
MEAS/DECK	9.7559	3.3624	4.7371	5.8541	4.1819	3.6934	2.9278	1.9623	1.7699	1.5867	1.4892
MEAS/PSCHT	*75.19500	*07.35621	*881.47711	*71705.24636	*503.86397	*40.90023	*358.79842	*31.028	*80.43037	*70.81517	*59.06633

RADIIJS	59520.000	KM	ALTITUDE	-280.000	K4	PRESSURE	23.209027	BAKS	TEMPERATURE	401.62*	KELVIN
				-918.635	KFT		22.905529	ATM		263.253	FAHRENHEIT
TIME	5*33.377	SEC	VELOCITY	38.447	METER/SEC	DYN P	.011676	BAKS			
	90.55628	MIN		6.4408	M3/SEC	JOPPER	2.787598E+02	CPS			
	1.509271	HRS		126.139	FT/SEC	WACH NO	.036309				

[illegible]

RADJIS	59515.000	KM	ALTITUDE	-285.000	K4	PRESSURE	24.056230	BAKS	TEMPERATURE	406.012	KELVIN
				-935.039	K5T		23.741654	ATM		271.152	FAHRENHEIT
TIME	556+2.41	SEC	VELOCITY	37.973	METER/SEC	DYN P		.011676	BAKS		
	92.73735	MINS		6.5223	MB/SEC	JOPPER	2.753222	+02	CPS		
	1.545622	HRS		124.584	FT/SEC	MACH NO		.026040			

INSTRUMENTS	TEMP	PRESS	TEMP	PRESS	ACCEL	ACCEL	ACCEL	ACCEL	M SPEC	M SPEC	M SPEC	M SPEC
1855/75	1390.75	1390.78	1392.06	1113.85	795.89	696.33	557.42	371.95	185.47	140.11	112.28	93.74
KNND/MEAS	11330	13288	15186	18382	26572	30357	37955	59519	1.13758	1.51607	1.89420	2.27197
MEAS/KH	8.7734	7.5254	6.5849	5.2881	3.7633	3.2930	2.6347	1.7569	0.8791	0.6596	0.5279	0.4401
BARS/MEAS	0.1955	0.2281	0.2027	0.3258	0.4562	0.5214	0.6518	0.9780	1.9174	3.2654	5.2508	8.2508
MEAS/BAR	51.15+3	43.8455	38.3639	30.5497	21.9491	19.173	15.3412	10.2250	5.1088	3.6298	2.3054	1.99420
DECK/MEAS	0.0938	1.1664	1.3330	1.5661	2.3324	2.6654	3.3315	4.9360	9.9850	1.33071	1.66261	1.99420
MEAS/DECK	10.0023	3.5736	7.5021	6.0019	4.7952	3.7517	3.0017	2.0016	1.0015	0.7515	0.6015	0.5015
MEAS/PSCH	31.38015+58	25775.923	39095730	777472527	7.90857	4.61571	3.1359	5503246.4	7460423.3	33874	92.65970	74.46382
MEAS/PSCH	10.0023	3.5736	7.5021	6.0019	4.7952	3.7517	3.0017	2.0016	1.0015	0.7515	0.6015	0.5015

SURVIVABLE SATURN PROBE TASK 4 DESCENT RUNS
JP. MONOGRAPH SATURN NOMINAL ATMOSPHERE

BALLISTIC COEFFICIENT = .700, INITIAL TIME = 0. SECONDS AT 59900.000 KM RADIUS

BAL. COEF. 0.6570.7071.50 SEP 30 BARS

RADIUS 59510.000 KM		ALTITUDE	-290.000 KM	PRESSURE	24.924899 BARS	TEMPERATURE	410.401 KELVIN
			-931.444 KFT		24.598962 ATM		279.032 FAHRENHEIT
TIME	5695.730 SEC	VELOCITY	37.510 METER/SEC	DYN P	.011676 BARS		
	94.94550 MIN		6.6040 MB/SEC	DOPP-ER	2.719628E+02 CPS		
	1.532425 HRS		123.063 FT/SEC	MACH NO	.025584		

INSTRUMENTS		TEMP	PRESS	ACCEL	ACCEL	M SPEC	M SPEC
NO OF MEAS	1899.91	1528.64	1425.14	814.82	713.09	130.89	143.42
KM/MEAS	.11251	.13126	.15001	.18751	.26248	.29337	.37492
BARS/KM	8.8878	7.6183	6.6652	5.3332	3.8093	3.3337	2.6672
MEAS/MEAS	.01980	.02310	.02640	.03300	.04620	.06601	.09904
MEAS/BAR	50.5133	43.2961	37.8832	30.3052	21.6445	13.9381	15.1490
DECK/MEAS	.09875	.11521	.13157	.15456	.23039	.32909	.49351
MEAS/DECK	10.1258	8.6795	7.5947	6.0761	4.3404	3.0387	2.0263
MEAS/PSCHT	*59.53950*	79.55147	94.73545755	83.302539	98.873742	52.935378	0.8811232

RADIUS 59505.000 KM		ALTITUDE	-295.000 KM	PRESSURE	25.815344 BARS	TEMPERATURE	414.790 KELVIN
			-967.848 KFT		25.477764 ATM		286.952 FAHRENHEIT
TIME	5830.848 SEC	VELOCITY	37.057 METER/SEC	DYN P	.011676 BARS		
	97.18079 MIN		6.6358 MB/SEC	DOPP-ER	2.686788E+02 CPS		
	1.619680 HRS		121.577 FT/SEC	MACH NO	.025141		

INSTRUMENTS		TEMP	PRESS	ACCEL	ACCEL	M SPEC	M SPEC
NO OF MEAS	1944.62	1566.96	1458.71	833.99	729.36	195.36	146.77
KM/MEAS	.11116	.12968	.14820	.18324	.25932	.29635	.37840
BARS/KM	8.9964	7.7114	6.7476	5.3983	3.8563	3.3744	2.6998
MEAS/MEAS	.02003	.02339	.02673	.03341	.04678	.06684	.09904
MEAS/BAR	49.8858	42.7591	37.4134	29.3293	21.3761	13.7033	14.9812
DECK/MEAS	.09757	.11382	.13008	.16259	.22761	.32511	.48756
MEAS/DECK	10.2496	3.7855	7.6075	6.1503	4.3935	3.0758	2.0510
MEAS/PSCHT	*88.34401*	04.34104965	33.882773	13.571552	33.214483	33.101386	7.2944237

RADIUS 59500.000 KM		ALTITUDE	-300.000 KM	PRESSURE	26.727880 BARS	TEMPERATURE	419.178 KELVIN
			-984.252 KFT		26.378367 ATM		294.851 FAHRENHEIT
TIME	5966.596 SEC	VELOCITY	36.614 METER/SEC	DYN P	.011676 BARS		
	99.44326 MIN		6.7678 MB/SEC	DOPP-ER	2.654680E+02 CPS		
	1.657388 HRS		120.124 FT/SEC	MACH NO	.024710		

INSTRUMENTS		TEMP	PRESS	ACCEL	ACCEL	M SPEC	M SPEC
NO OF MEAS	1989.87	1705.74	1492.65	853.37	746.32	139.89	150.16
KM/MEAS	.10983	.12813	.14643	.18303	.25622	.29281	.36598
BARS/KM	9.1052	7.8046	6.8292	5.4636	3.9029	3.4152	2.7324
MEAS/MEAS	.02029	.02368	.02706	.03383	.04735	.06767	.10153
MEAS/BAR	49.2742	42.2341	36.9540	29.5619	21.1137	13.4737	14.7775
DECK/MEAS	.09540	.11246	.12853	.16065	.22489	.32731	.48174
MEAS/DECK	10.3735	3.8918	7.7805	6.2246	4.4463	3.0913	2.0758
MEAS/PSCHT	*17.49415*	29.32688988	2014.2790	6.2578564	8.250349	26.230395	4.7446463

BALLISTIC COEFFICIENT = .700, INITIAL TIME = 0. SECONDS AT 59900.000 KM RADIUS

BAL. COEF. 0.65/0.70/1.50 SEP 30 BARS

RADIIJS	59+95.000	KM	ALTITUDE	-305.000	KM	PRESSURE	27.662823	BAKS	TEMPERATURE	23.007	KELVIN
				-1000.656	KFT		27.301084	ATM		302.751	FAHRENHEIT
TIME	6103.977	SEC	VELOCITY	36.191	METER/SEC	DIV P	.011675	BAKS			
	101.73296	MIN		0.8500	M3/SEC	JOPP_ER	2.632786	0.02	CPS		
	1.635543	HRS		118.704	FT/SEC	MACH NO	.024291				

[illegible]

RADIOS	59490.000 KM	ALTITUDE	-310.000 KM	PRESSURE	28.620486 BARS	TEMPERATURE	427.956 KELVIN
			-1017.060 K ^F		28.246226 ATM		310.001 FAHRENHEIT
TIME	6242.995 SEC	VELOCITY	35.757 METER/SEC	DVP P	.011676 BARS		
	104.34992 MIN		5.9323 M3/SEC	DOPP-ER	2.592560±.02 CPS		
	1.734105 HRS		117.314 FT/SEC	MACH NO	.023883		

[illegible]

RADIIJS	59485.000 KM	ALTITUDE	-315.000 KM	PRESSURE	29.603195 BAKS	TEMPERATURE	432.345 KELVIN
			-1033.485 KFT		29.214108 ATM		318.550 FAHRENHEIT
TIME	6403.651 SEC	VELOCITY	35.343 METER/SEC	DYN P			
	100.39419 MIN		7.0148 MB/SEC	JOPP_ER	.011676 BAKS		
	1.773237 HRS		115.934 FT/SEC	JOPP_NO	2.562505E+02 CPS		
				WACH NO	.023465		

[illegible]

APPENDIX M

PROPULSION SUBSYSTEM ANALYSIS AND DEFINITION

R. Moses
and
R. Fearn

June 19, 1972

PROPULSION SUBSYSTEM ANALYSIS AND DEFINITION (NOMINAL JUPITER PROBE)

The data presented in this appendix were prepared early in this program and are presented here largely unchanged. The data in Volumes I and II include later iterations of design, in some cases, and varies with data in this appendix.

The selected propulsion systems were studied in depth to evolve more accurate definitions of their characteristics. Neither the solid motor nor the cold gas systems exist in their entirety as flight-qualified items that will exactly satisfy the Jupiter probe propulsion requirements, but the design of suitable systems based on existing technology is not an enormous task.

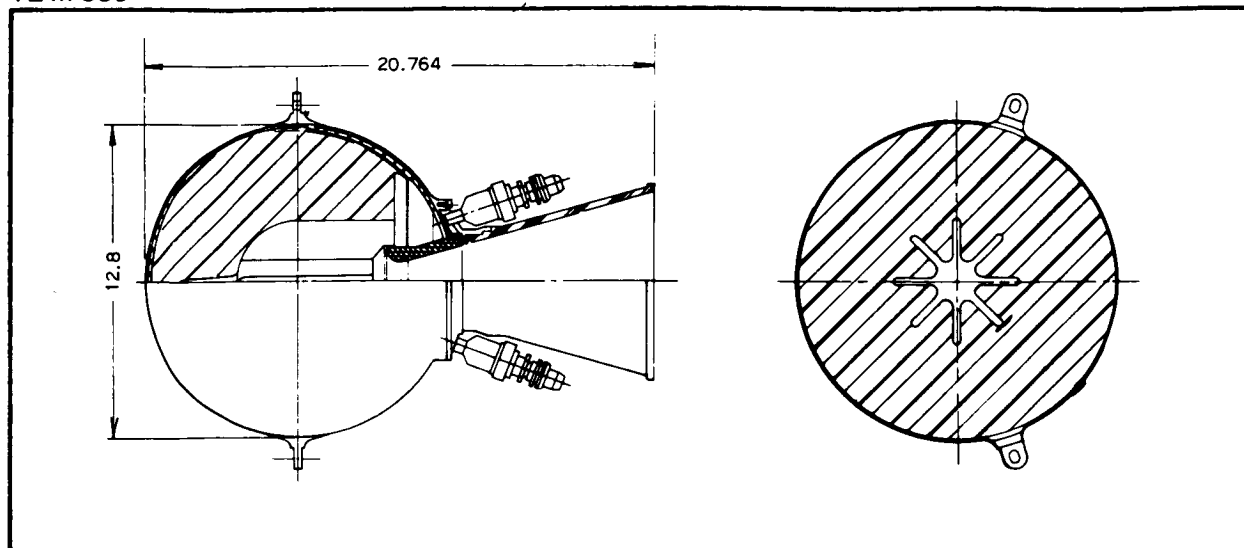
In the case of the solid motor, sizes both larger and smaller than the size (total impulse) required for this application have been developed and flight-qualified so that a new design may be developed by interpolation rather than extrapolation. Any one of the several major solid motor manufacturers in this country is capable of developing the required motor. The principal characteristics of the proposed motor are discussed herein.

The situation with regard to the cold gas system is slightly different in that it would consist of an assembly of individual components, the majority of which already exist in a flight-qualified status. Very likely, the only component to be fabricated specifically for this application would be the gas storage vessel, and even this exists in sizes very close to that required. Identification of specific candidate components for the system is included in the discussion herein.

A. SOLID PROPELLANT MOTOR

1. General Configuration

The general configuration of the motor is anticipated to be spherical, but with two partially submerged nozzles instead of the usual one to preclude plume impingement on the spacecraft after probe separation. Except for the two nozzles, the motor will resemble a scaled-down version of the Thiokol TE-M-385 motor shown in Fig-M-1. It has a high strength titanium alloy case containing a bonded TL-L-305 liner (insulator) and a TP-L-3014A composite propellant grain of an 8-point star configuration. The nozzle is of phenolic construction with a graphite throat insert; a screw-in igniter near the nozzle provides propellant ignition.

**CASE**

Material	Titanium Alloy 6Al4V
Strength, Min. Ultimate, psi	165,000
Strength, Min. Yield, psi	155,000
Pressure, Hydrostatic Test, psi	1,430
Nominal Thickness, in.	0.04

NOZZLE

Material, Body	Vitreous Silica Phenolic
Material, Throat Insert	CGW Graphite
Area, Throat, in. ²	1.86
Ratio, Expansion	23:1

LINER	TL-L-305
--------------	----------

IGNITER

Type and Designation	PYROGEN TE-P-386
Minimum Firing Current, amps	4
Circuit Resistance, ohms	1.00 ± 0.20
No. of Squibs/Igniter	1

CURRENT STATUS	Production
-----------------------	------------

PROPELLANT

Designation	TP-L-3014A
Web, in.	3.79
Density, Loading, Volumetric, %	83.5

MOTOR PERFORMANCE

Time, Action, sec	5.7
Time, Ignition Delay, sec	0.022
Pressure, Chamber, Avg, psia	790
Impulse, Total, lbf-sec	14,000
Thrust, Avg. Action Time, lbf	2,150

WEIGHTS, lbm

Total, Loaded	67.4
Propellant	55.4
Total, Inert	11.84
Mass Ratio	0.823

TEMPERATURE LIMITS, °F

Operation	-20 to 180
Storage	10 to 160

Figure M-1 Thiokol TE-M-385 Motor

2. Propellant

The specific propellant to be used in the probe motor will be determined at a later date, dependent upon the selection of the supplier for the solid motor assembly. Each of the major solid motor manufacturers has his own collection of proprietary propellant formulations from which to choose, several of which will probably provide the required performance. The specific one selected as baseline for this study is a Thiokol modified TP-H-3062 propellant that contains 70% ammonium perchlorate and 16% aluminum in a CTPB binder. It has good physical characteristics, a very high specific impulse (principally the result of the high percentage of aluminum), and a relatively low burning rate that permits operation at a relatively low thrust level. It has a normal storage temperature range of 272 to 322°K (20 to 110°F) and a normal operating range of 283 to 311°K (40 to 90°F). The chamber pressure (and thrust) increase only 0.1% per °F temperature increase, while the burning time decreases a proportionate amount. The delivered total impulse changes only 0.003% per °K (0.005% per °F) temperature change, so that it is possible for the manufacturer to guarantee a 3-σ variation in total impulse of only ±0.75% from nominal. This degree of total impulse control is believed to be adequate for the Jupiter probe application.

The principal disadvantage of the propellant is the large percentage of solids in its exhaust products, leading to a plume impingement problem in some situations. More detailed propellant characteristics are presented in Figure M-2.

3. Motor Size

If the quantity of propellant consumed in accelerating a mass is negligible relative to the mass being accelerated, the total impulse required may be approximated by

$$Ft = \frac{W_I \Delta V}{g} = I_{sp} W_P = \frac{V_e}{g} W_P \text{ lbf-sec, or}$$

$$\frac{W_P}{W_I} = \frac{\Delta V}{V_e},$$

[M-1]

Designation: Modified TP-H-3062

Composition: CTPB/AP/AL Composite

70% AP
16% AL

Characteristic Exhaust Velocity, C^* , 1510 m/sec (5015 fps)

Burn Rate Equation at 70°F, $\left[0.207 \left(P_c / 500\right)^{0.34}\right]$

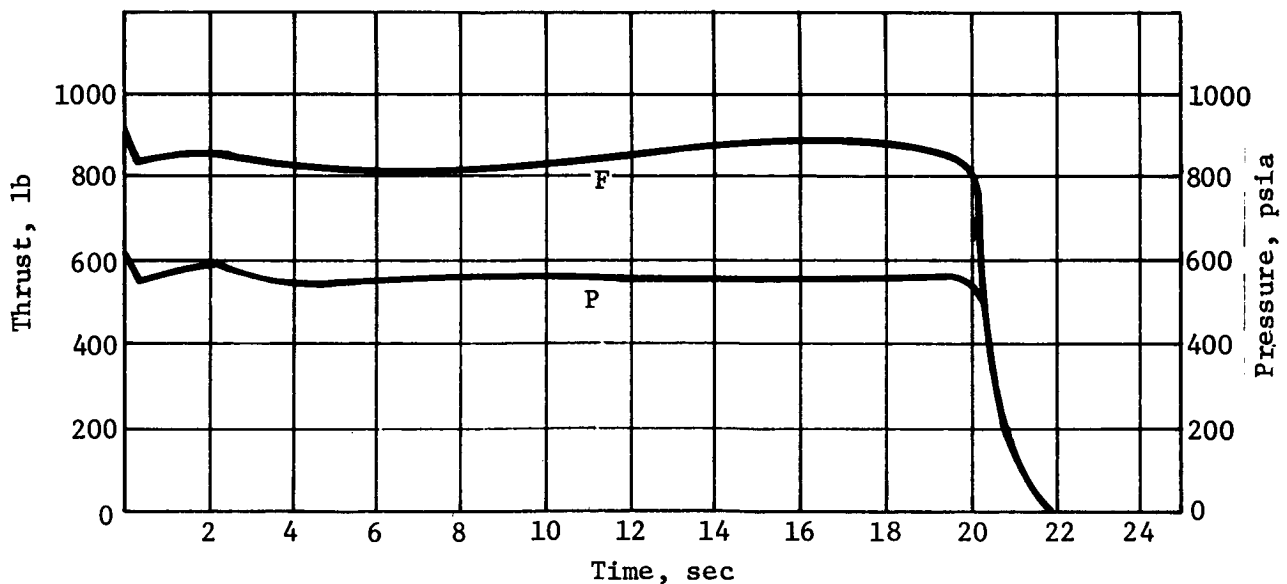
Density, 1740 kg/m³ (0.0628 lbm/in.³)

Ratio of Specific Heats, 1.16

Temperature Sensitivity Coefficient, π_K , %/°F, 1.10

Specific Impulse, I_{sp} , 2820 N sec/kg (287 sec)

Typical F/t Performance



TE-M-345-12 Motor, TP-G-3129 Propellant

Figure M-2 Proposed Jupiter Probe Propellant

where

F = thrust, lbf

t = action time, sec

W_I = mass being accelerated (initial mass), lbm

W_P = quantity of propellant consumed, lbm

I_{sp} = propulsion system specific impulse, sec

Ve = propulsion system effective exhaust velocity, fps

ΔV = velocity increase, fps

If the quantity of propellant consumed is not negligible, it is necessary to use an integral solution of Newton's law based on a constant rate of propellant consumption yielding the following expression for the propellant consumed:

$$\frac{W_P}{W_I} = \frac{W_I / W_F - 1}{W_I / W_F} \quad [M-2]$$

where

$$\frac{W_I}{W_F} = \log^{-1} \frac{\Delta V}{2.303 Ve}$$

Since the difference between W_P / W_I as computed from Equations [M-1] and [M-2] is usually small for typical spacecraft propulsion systems, it is possible to provide a very accurate graphical solution to Equation [M-2] without the need to resort to logarithmic tables. Figure M-3, a plot of the difference between Equations [M-1] and [M-2], provides such a solution. Once the spacecraft ΔV and propellant I_{sp} are specified, $\Delta V / Ve$ may be computed, ($\Delta V / Ve - W_P / W_I$), read from the graph, and W_P / W_I obtained by simple subtraction.

The specific motor to be used on the Jupiter probe will require 12.3K° (27.1 lbm) of propellant, assuming a specific impules of 2820 N sec/kg (287 sec). (This value has been achieved in motors of similar design with TP-H-3062 propellant.) Referring to Figure M-1, for a ΔV of 221 m/sec (725 fps) and a resulting probe-delta-velocity to rocket-motor-effective-exhaust velocity ratio:

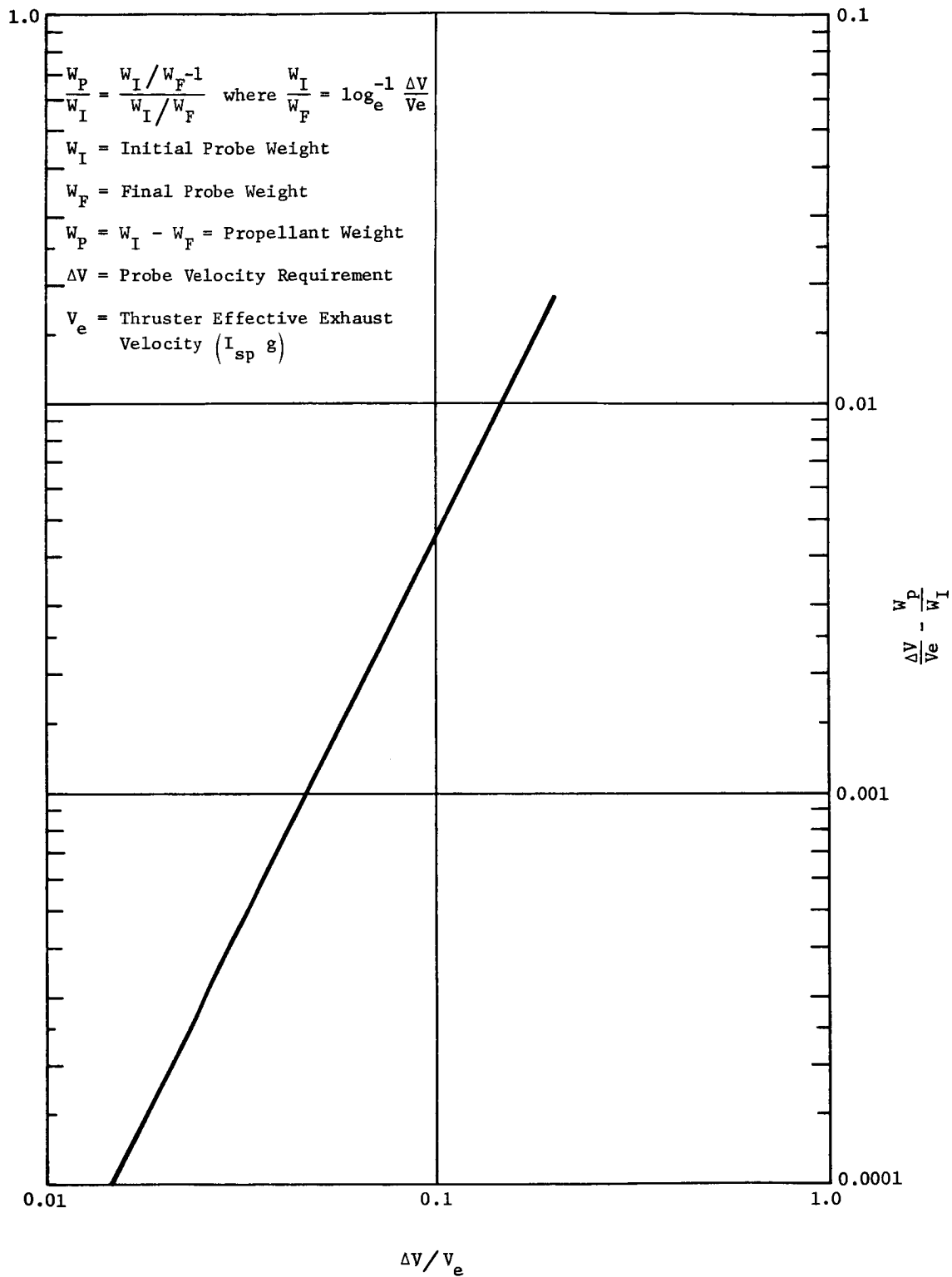


Figure M-3 Probe Propellant Requirements

$$\frac{\Delta V}{V_e} = \frac{221(3.28)}{287(32.2)} = 0.0785,$$

then

$$\frac{W_p}{W_I} = 0.0757,$$

and

W_p (propellant weight) = 11.3 kg (25 lbm) for a probe having an initial weight (W_I) of 149 kg (330 lbm).

However, because of the fact that each nozzle is canted $22\frac{1}{2}^\circ$ from the resultant thrust axis, the net thrust is only 92.4% of the gross thrust, and the total propellant required is 12.3 kg (27.1 lbm) instead of 11.3 kg (25 lbm). This still compares fairly closely with the first cut approximation of 11.3 kg (26 lbm) which used a cruder estimate of the required total impulse, and did not take into account the canted nozzles.

With the propellant load known, the approximate size of the motor (diameter) is also fixed. Using Thiokol data (Fig. M-4), it will be seen that a motor 10 in. in diameter is required to contain the 12.3 kg (27.1 lbm) propellant load in the proposed 8-point star configuration. Further, assuming a burning rate of ~ 0.79 cm/sec (0.2 m/sec) (Fig. M-5), the motor burn time will be ~ 15 sec; therefore, the net motor thrust is predicted to be

$$\frac{287 \times 25}{15} \quad 2135 \text{ N (480 lbf)},$$

Providing a probe acceleration slightly more than 1.5 g. This level of thrust and acceleration appear to be perfectly acceptable to the probe, so there appears to be no reason for considering other alternatives. If this acceleration level proved to be unacceptable, and entirely different motor/propellant grain configuration might have to be developed.

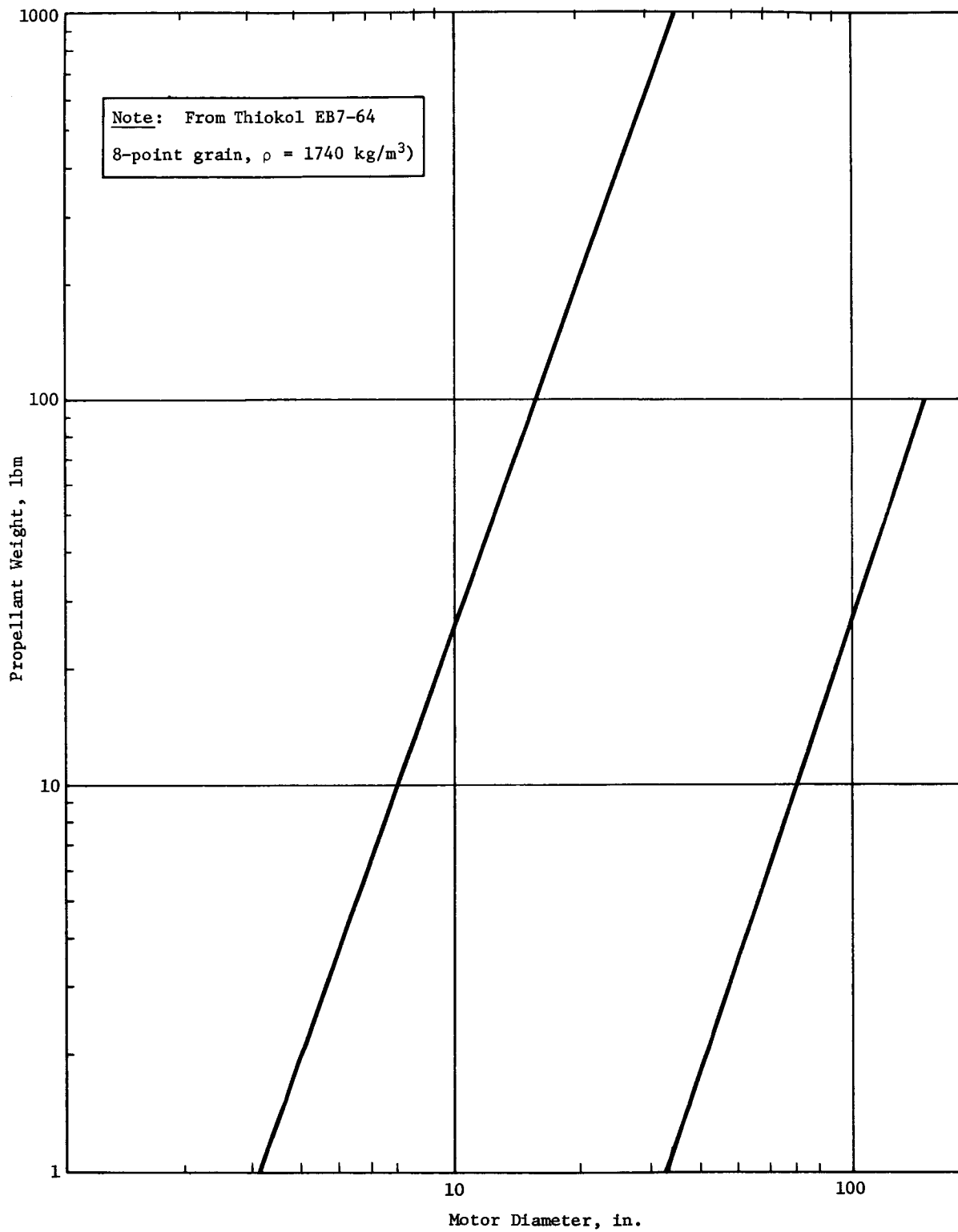


Figure M-4 Motor Diameter versus Propellant Weight

Spherical Motors, 8-pt grain

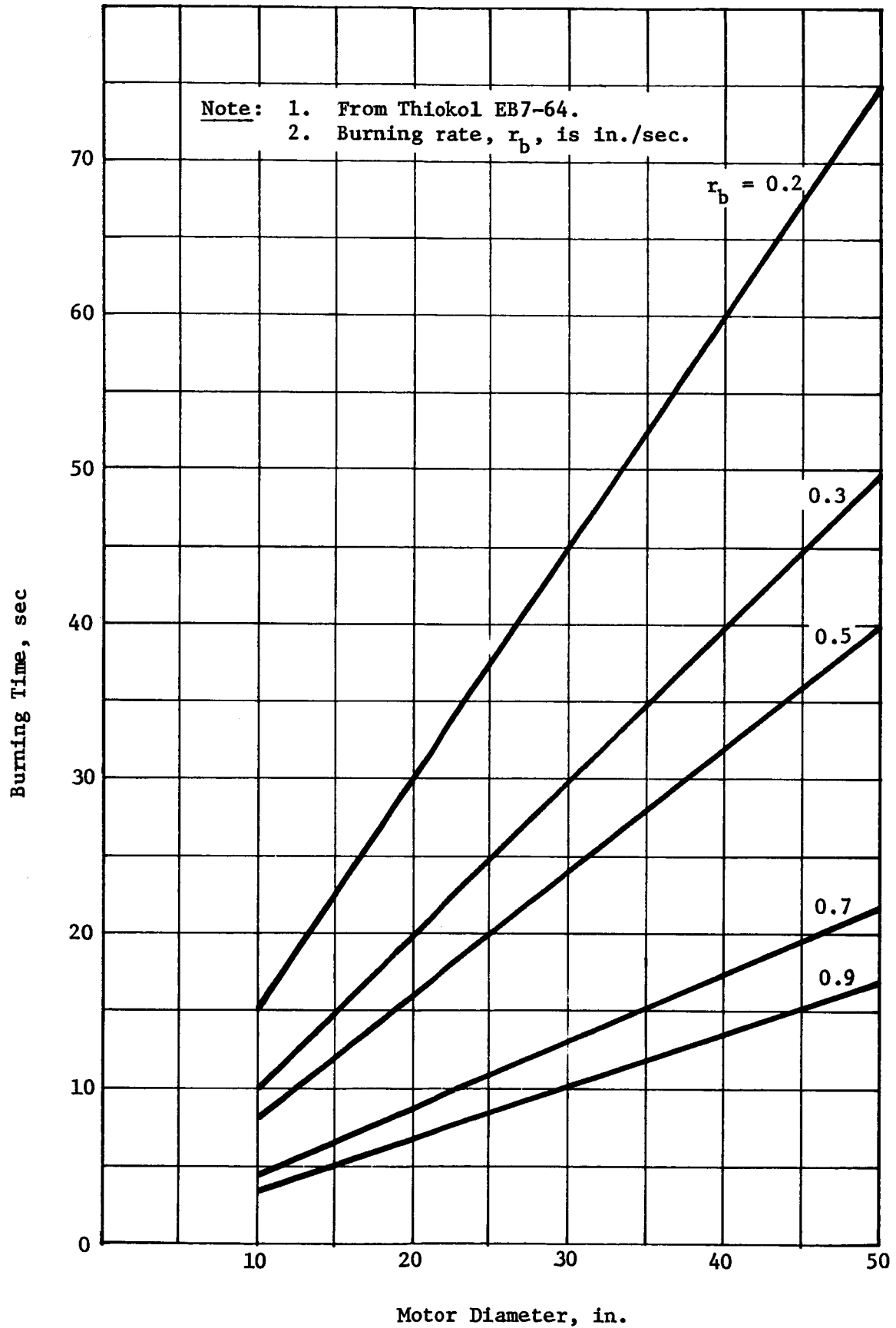


Figure M-5 Burning Time vs Motor Diameter

Although there is some choice in the combustion pressure that can be selected for the motor, the minimum motor weight generally is achieved at a pressure in the range of 3.45×10^6 to 4.13×10^6 N/m² (500 to 600 psia) where the chamber walls need not be excessively heavy, and the nozzle is still relatively small (and light). Assuming for convenience a chamber pressure of 3.8×10^6 N/m² (550 psia) and a nozzle area ratio of 40, a thrust coefficient of ~ 1.78 may be predicted based on known nozzle performance. Then the required nozzle throat area is found to be ~ 0.53 in.² or 0.265 in.² per nozzle. This yields a nozzle throat diameter of 1.47 cm (0.58 in.), an exit diameter of 9.3 cm (3.67 in.), and a divergent nozzle length of 14.4 cm (5.75 in.) assuming a nozzle half-angle of 15° . Then, assuming that the nozzle is $\sim 40\%$ submerged in the spherical chamber, the protruding length will be 8.9 cm (3.5 in.). The foregoing outline configuration is shown in Figure M-6.

Based on previous experience with motors of similar size, and the performance achieved with the high energy propellants such as Thiokol TP-H-3062, there is every reason to believe that a suitable motor can be fabricated with loaded weight < 34 lbm. Assuming that the mass fraction trend established by Thiokol motors TE-M-541 and -516 can be maintained with this new probe motor, a λ of 0.84 should be attainable. This would result in a motor loaded weight of 14.6 kg (32.3 lbm) (for a single nozzle configuration), or a weight of possibly 15.3 kg (33.8 lbm) to account for the additional nozzle.

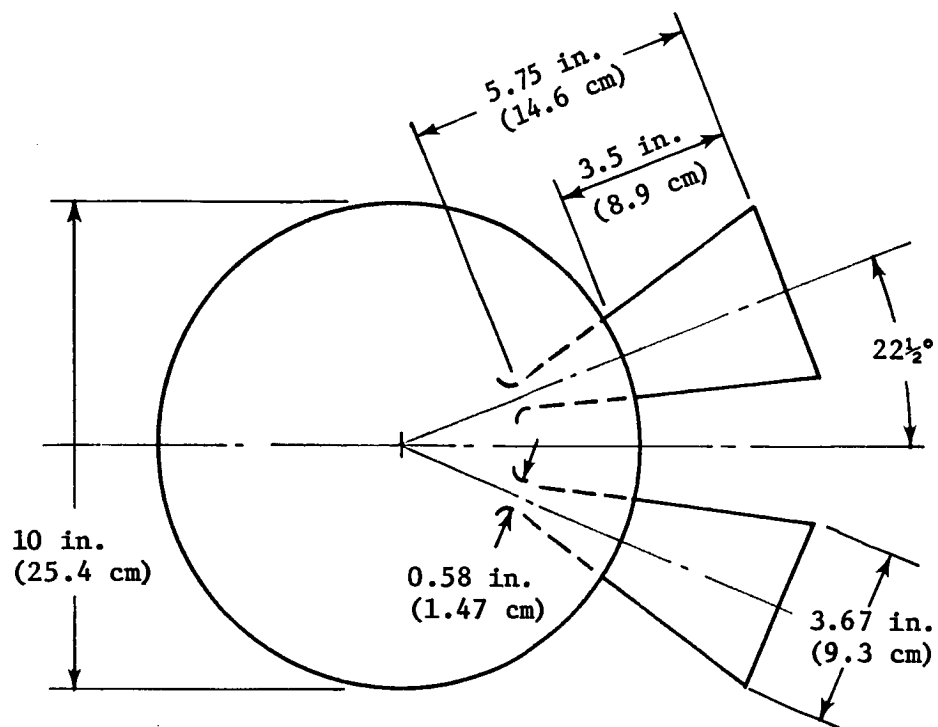


Figure M-6 Nominal Jupiter Probe, Solid Motor Characteristics

Propellant Weight	12.3 kg (27.1 lbm)
Loaded Weight	15.3 kg (33.8 lbm)
Chamber Pressure, avg	3.7×10^6 N/m ² (550 psi)
Burn Time	15 sec
Thrust, gross	2310 N (520 lbf)
Thrust, net	2135 N (480 lbf)
Total Impulse, gross	34,600 N sec (7770 lbf sec)
Total Impulse, net	31,900 N sec (7180 lbf sec)

B. AUXILIARY PROPULSION

The cold gas system has been evolved to accomplish the four auxiliary propulsion functions: spin, despin, precess for the probe, plus deflection of the service module. The system is depicted schematically in Figure M-7. It may be considered to consist of five subsystems, i.e., the four subsystems that accomplish spinup, precession, despin, and module ejection, respectively, plus the gas supply subsystem that provides GN_2 to the thrusters under the proper conditions. This system does not necessarily represent the optimum solution to the propulsion requirements, but it appears to be a good solution in that it has sufficient redundancy to assure a high reliability, yet is not unnecessarily complex and heavy. Redundancy is provided for all valve functions.

It is envisioned that the system will use GN_2 as the working fluid, stored at an initial pressure of $\sim 24.5 \times 10^6 \text{ N/m}^2$ (3500 psi). Fluids other than GN_2 conceivably could be used, but they offer very little advantage in terms of performance and/or system weight. Storage at this pressure level is somewhat arbitrary, but results in a pressure vessel volume that is not too large, and provides a greater selection of system components. A conventional pressure regulator is used to reduce the pressure to $\sim 17 \times 10^4 \text{ N/m}^2$ (25 psia) for use by the thrusters.

The majority of the thruster/valve clusters are located at the periphery of the probe to provide the maximum possible moment arm, and are interconnected to the GN_2 supply system by means of stainless steel tubing. To minimize system leakage, all joints are either welded or brazed. The selection of specific components for the system has not been pursued in depth, but potential suppliers and even candidate components have been identified to some degree. The next step in the evolution of the design would be to evolve a detailed system layout that defines each individual component, the interconnecting line sizes and configurations, and the mounting provisions.

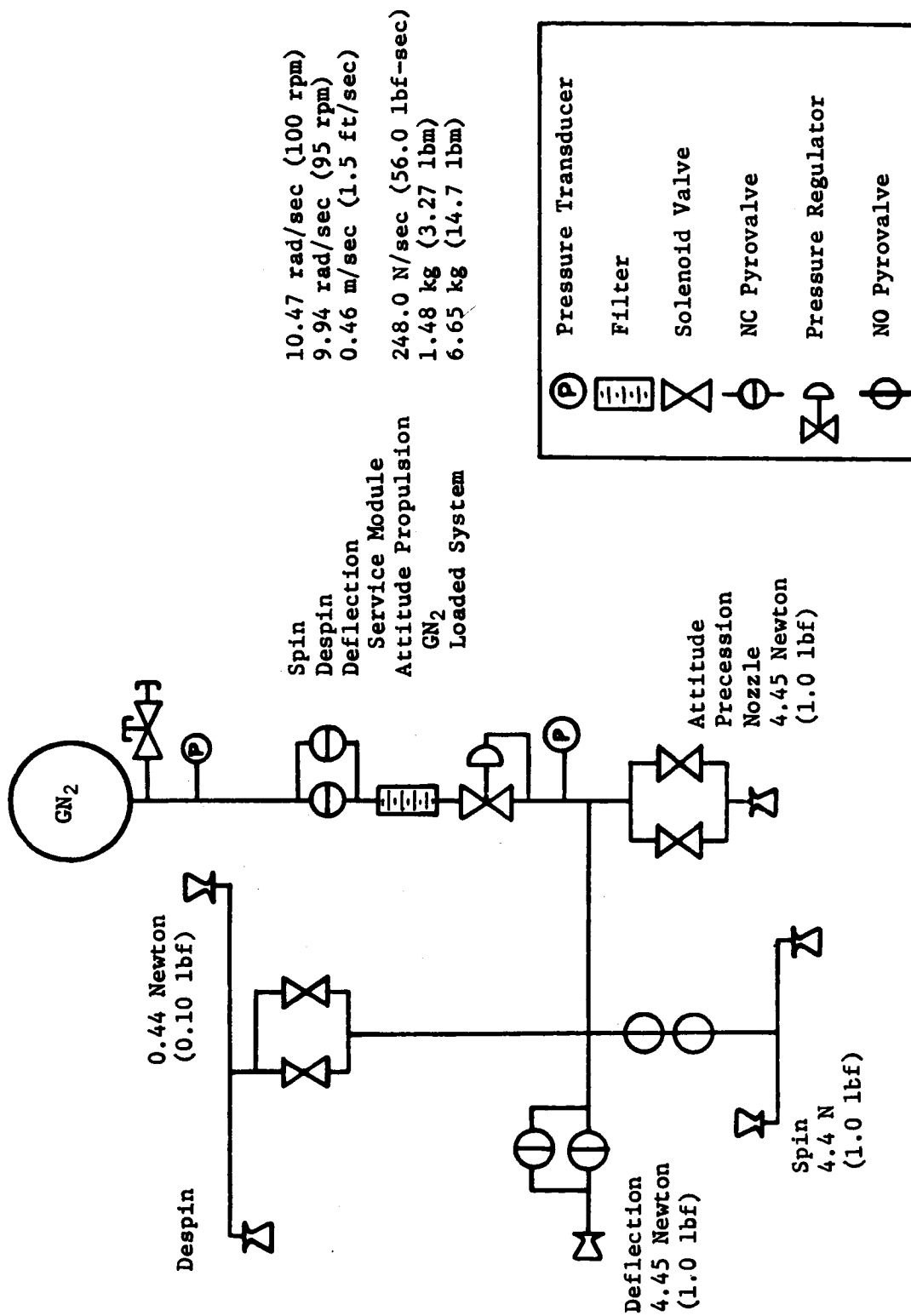


Figure M-7 Auxiliary Propulsion Schematic

1. Spinup Subsystem

The first subsystem to go into operation is the spinup system that accelerates the probe to a rotational velocity of ~ 10.5 rad/sec (100 rpm) before the firing of the ΔV motor. As will be noted on the schematic, the system selected is extremely simple and at the same time highly reliable. The subsystem is not provided with an independent start capability. Instead, the pyro valves in the gas supply subsystem are fired to activate the thrusters, and to provide gas up to the control valves of the other auxiliary subsystems. Then after the required operating period, thrust is terminated by firing the series redundant N/O pyro valves. The elimination of valving to control each of the two thrusters individually will result in a longer thrust tail-off than otherwise, but the tailoff impulse is insignificant compared to the total spinup impulse.

The selection of the thrust level to be used is to some degree arbitrary, but not completely without guidelines. From purely propulsion considerations, a low thrust level is desired because it leads to valves, thrusters, and interconnecting lines that are small and lightweight. On the other hand, as the thrust level decreases and the spin time increases, the pointing accuracy of the probe is degraded rapidly. From a structural standpoint, high thrusts may not be desirable, but the shorter thrust periods are advantageous to the guidance system. The 4.4 N (1 lbf) thrust level appears to represent a reasonable compromise between two extremes, though no real attempt has been made to determine the optimum thrust, if indeed one can be defined. Thruster/valve clusters in the 4.4 N (1 lbs) thrust category are relatively common (and available) and are not excessively heavy, yet provide a spinup time interval that does not appear to be too long. To provide the required 276 N/sec (62.8 lbf sec) impulse with two 4.4 N (1 lbf) thrusters, it is evident that the burn time will be only slightly more than 30 sec.

During the continuous burn of this magnitude, (expelling $\sim 1/4$ of the stored gas), performance (I_{sp}) will decrease slightly as the gas temperature drops. This will result in the consumption of a larger quantity of gas than that previously computed for the spinup maneuver, but the total delivered impulse can still be predicted very accurately. The added GN_2 required has been accounted for in the 30% "pad" provided in the storage gas requirements.

The calculations for the ACS system sizing is presented in this Appendix following the system description.

2. Despin Subsystem

The second auxiliary propulsion function to be performed is the precession of the probe axis to the proper Jupiter entry angle, but the despin maneuver will be discussed first because of its similarity to the spinup maneuver. The despin subsystem provides the same torque to the probe as the spinup subsystem, but it is applied in the opposite direction to reduce the angular velocity of the probe from 10.5 rad/sec (100 rpm) to 52 rad/sec (5 rpm) before atmospheric entry.

The thrusters used in the two subsystems would be of identical designs, but the valving is different because the despin subsystem must have provisions for both start and shutdown. This capability conceivably could be provided by a combination of N/O and N/C pyro valves, but solenoid valves have been tentatively selected because they provide greater operational flexibility. The solenoid valves permit the application of a series of impulses to achieve the proper rpm should this mode of operation be found necessary. A predetermined thrusting interval (achieved with a timer) may not exactly provide the desired final probe rpm so that one or more vernier impulses may be required.

The tentatively selected valve cluster includes only two solenoids in a parallel redundant configuration. Consideration has been given to the use of a quad redundant configuration, but this does not appear to be necessary. The two-valve configuration provides a very high reliability because of the very limited number of operational cycles involved (possibly, only one), the very low probability of failure to close once the valve has opened, and the negligible overall effect of leakage through the valve seat. All the auxiliary propulsion functions will have been accomplished within a few hours after the termination of the despin impulse, so the quantity of gas that could be lost as a result of "normal" valve leakage is insignificant.

Sizing of the despin thruster is not at all critical. Large thrusters would not be appropriate because they would be unnecessarily heavy, but small thrusters could be used without detrimental effects. Adequate time is available to accommodate a prolonged despin maneuver. To minimize the number of different sizes of components, however, 4.4 N (1 lbf) thrusters have been selected to provide the despin function. With thrusters of this

size, despin will be accomplished in slightly less time than spinup (within ~ 30 seconds), consuming 0.376 kg (0.83 lbf) of GN_2 in delivering 267 Nsec (60 lbf sec) impulse.

3. Precession Subsystem

The precession subsystem applies a moment about one transverse axis of the probe to effect precession of the probe about a second axis at 90° to the first, eventually rotating the probe longitudinal axis through an angle of 0.89 rad (51°) for proper Jupiter entry attitude. This torquing of the probe is accomplished by pulsing the precession thruster for a short time, usually once each revolution. A single thruster has been selected to provide the required torquing. This results in the application of a small ΔV to the probe in addition to the moment, but this appears to present no particular problem. The use of a single thruster, of course, results in minimum system complexity and weight.

The one operating requirement that is different for this subsystem is the necessity for repeated pulsing of the thruster. Consequently, it is mandatory to use solenoid valves instead of pyro valves to control the thruster. The selection of parallel redundant valving rather than quad redundant valves follows the same basic logic as for the despin subsystem; i.e., a very high reliability is achieved without resorting to a four-valve configuration.

The choice of thrust level for the precession thruster is somewhat more critical than for other subsystems. Application of a high torque to the probe will produce a pronounced undesirable nutation, though the precession will be accomplished with a relatively small number of pulses and in a short elapsed time. Application of a low torque results in only a very small amount of nutation, but requires a relatively large number of pulses (resulting in lower reliability), and consumes an excessive amount of time. To provide the 249 Nsec (56 lbf sec) impulse required with a single 4.4 N (1 lbf) thruster, it is evident that 56 seconds of thruster operation is required. If each thruster pulse is restricted to 0.78 rad (45°) of probe rotation (1/8 revolution), it is evident that the elapsed time required to accomplish precession will be ~ 7.5 minutes; the total number of pulses required is ~ 750 . The application of thrust must be limited to approximately 1/8 of the probe revolution in order to achieve maximum efficiency. As the angle of rotation during thrust application increases, the effective moment arm decreases, thereby necessitating a greater total impulse and increased consumption of GN_2 . If a 0.44 N (0.1 lbf) thruster were used, the number of pulses would increase to 7500, and the elapsed time to 1.25 hr.

4. Deflection Subsystem

The final function to be performed by the auxiliary propulsion system is to eject the service module (including the auxiliary propulsion system) from the probe just before Jupiter entry. The subsystem is required to provide a minimum impulse to deflect the module a safe distance from the probe, but there is no practical maximum limit to the impulse that can be tolerated. Only a very small total impulse is required, so the gas consumption is also small.

As seen from the system schematic diagram, it is proposed to provide a start capability, but no shutdown capability for the system. Any excess gas remaining in the system will simply be allowed to blowdown through the thruster, thereby providing a ΔV to the service module in excess of the minimum requirement. The simplest most reliable valving for this function appears to be the parallel redundant N/C pyro valves shown. These valves provide a reliability of nearly 1.0 for initiating the thrust; they are not required to provide thrust termination.

The thrust level to be provided for this function is not at all critical. The selection of the 4.4 N (1 lbf) thruster was made simply to achieve uniformity of components, but other thrust levels would accomplish the deflection maneuver equally well. The 4.4 N (1 lbf) thruster will accelerate the 25 kg (55 lbm) service module at a rate <0.02 g, and achieve the desired minimum service module ΔV of 1.5 fps in less than 3 sec, consuming less than 0.02 kg (0.04 lbm GN_2).

5. Gas Supply Subsystem

This subsystem must provide long-term storage for all of the gas to be used for the auxiliary propulsion functions, and subsequently supply the gas to the thrusters under the required conditions of pressure, flowrate and cleanliness. It is envisioned that the subsystem will consist of a pressure vessel for storage of the compressed gas, a fill valve for loading the gas into the system, pyro valves to isolate the gas from the thrusters until needed, a pressure regulator to reduce the pressure from the maximum storage value of 24.6 N/m^2 (3500 psi) to a usable constant level of $17 \times 10^4 \text{ N/m}^2$ (25 psia), a filter to remove particulate contaminants, and transducers to monitor storage and regulated pressures. Since the thruster subsystems do not operate simultaneously, the gas supply components need to be sized to accommodate a maximum flowrate corresponding to the operation of only two 4.4 N (1 lbf) thrusters.

The total amount of gas required by the thrusters is ~ 1.13 kg (2.5 lbm). Since the stored gas is effectively isolated from the thrusters throughout a majority of the mission, leakage can be held to a negligible amount by careful quality control of the welded and brazed joints. Since the thrusters are activated for only the final few days of the mission, they should not contribute a significant amount of leakage even if the valve seats should become contaminated with particulate matter. However, a quantity of gas somewhat greater than 11.3 kg (2.5 lbm) is required to account for some inefficiencies in the thruster outputs, and provide a reasonable safety factor. Normally, it would also be necessary to account for a significant amount of residual unusable gas at the end of the mission, but, in this case, the system will be blown down during the final deflection maneuver so that all the remaining gas is effectively used.

It was noted previously that thruster performance during the long spinup and despin maneuvers will probably fall a few percent below the assumed I_{sp} of 705 Nsec/kg (72 sec). In view of this, it is proposed to provide an initial charge of gas that is 30% greater than the summation of the thruster requirements; i.e., 1.48 kg (3.27 lbm) instead of 1.13 kg (2.5 lbm). It is believed that this will provide an adequate factor of safety for this specific type of mission.

It is proposed to use parallel redundant N/C pyro valves to provide isolation of the stored gas until needed by the thrusters. These valves are very simple, light in weight, and highly reliable. They do not leak before activation, and they exhibit an extremely low failure rate (reliability nearly 1.0).

The presence of the pressure regulator results in a somewhat low reliability for the subsystem, but this is unavoidable. The regulator is absolutely essential to the proper operation of the system. Unfortunately, however, about the best reliability that can be expected is 0.9975, which leads to a subsystem reliability of approximately the same value.

6. Component Selection

It is not intended as part of the current study to make final selections of the components to be used in the auxiliary propulsion system. Final selections would only be made after a more detailed analysis of system requirements had been completed, and an in-depth search for state-of-the-art components had been conducted. However, the current study has proceeded to the point of identifying

Table M-1 Pressure Vessels

MANUFACTURER	VOL. in. ³	PRESSURE, psi	PV(10) ⁻⁶	SIZE OF SPHERE, in.	MATERIAL	WEIGHT, lbm	PART NO.	REMARKS
Menasco	68	4,500	0.306	5.29	6Al-4V	1.8	823000-505	
Menasco	75			5.48	6Al-4V	2.7	782000-503	
Menasco	75	3,000	0.225	5.36	4340	2.1	848000-501	
Tavco	75	3,000	0.225	5.29		1.75	23711407	Emergency brakes for B-58
Tavco	75	3,000	0.225	5.29	4130	2.0	23711546	GN ₂ tank for Agena
Menasco	83	3,000	0.249	5.62	6Al-4V	1.6	730500-501	
Airite	83	3,600	0.299	5.65	6Al-4V		6428	Tank for JPL
PSI	85	6,000	0.510	5.9	6Al-4V	2.57	80075-1	Tank for Mariner Mars
PSI	87.5	6,000	0.525	5.9	Inc 718	3.94	80101-1	CH ₂ tank for Mariner Mars
Brunswick	100	3,000	0.300	6.5	Glass/ Epoxy	2.8	3002	GN ₂ tank for F-106
Fansteel	100	1,600	0.160	5.75	6Al-4V	1.65	4425002	He tank for Saturn
Tavco	100	3,500	0.350	5.95		2.4	23711400	Air/GN ₂ for B-58
Whittaker	100	3,250	0.325	6.17	Glass/ Epoxy	2.4	ASFW100	For aircraft
Fansteel	103	3,250	0.335	5.95	6Al-4V	1.0	4425033	
Fansteel	113	4,000	0.452	6.0	6Al-4V	1.3	107519	Gas for Vela Hotel
PSI	113	10,000	1.13	6.0	6Al-4V	1.67	80094-1	GN ₂ for Mariner Mars Application
Menasco	130	3,670	0.477	6.5	6Al-4V	2.1	806000	
Menasco	157	3,000	0.470	7.31	6Al-4V	3.0	864000-503	
Menasco		3,000		6.34	6Al-4V	3.0		GN ₂ for ACS on OSO
Fansteel	160	6,750	1.08	7.024	Inc 718	7.2	4425038	O ₂ Tank for IOPS

at least the major functional requirements (specifications) for each component, the potential vendors, and in some cases, a specific candidate that appears to be a reasonably good selection. The results of this selection are given in the body of the report.

Since the pressure vessel is by far the largest and heaviest component in the system, it was studied in somewhat greater detail than the others. It sized as follows:

To contain 1.48 kg (3.27 lbm) of gas, the vessel must have a pressure-volume product of at least

$$PV = WRT = 3.27 (55.1) (530) / 95,500 \text{ psf ft}^3 = 1.145 \times 10^6 \text{ psi in.}^3.$$

Since in this application it is proposed to use three pressure vessels to distribute the weight uniformly about the probe axis,

$$PV = 0.382(10)^6 \text{ psi in.}^3 \text{ per vessel.}$$

Then, referring to Table M-1, a tabulation of existing pressure vessels, it will be seen that a reasonable selection is a 15.2 cm (6 in.) diameter titanium alloy vessel manufactured by Fansteel for gas storage on the Vela Hotel Satellite. This vessel ($PV = 0.452(10)^6$) is somewhat larger than actually required, but is probably a good selection because it does provide a comfortable margin of safety. To contain the required amount of GN_2 , it would have to be charged to only $\sim 23.4 \times 10^6 \text{ N/m}^2$ (3400 psi) instead of the design value of $27.6 \times 10^6 \text{ N/m}^2$ (4000 psi). It weighs only 0.58 kg (1.3 lbm), so three of them will weigh less 1.8 kg (4 lbm). This is a storage vessel only 22% greater than the weight of the contained gas, indicating a very good design.

7. Auxiliary Propulsion Impulse & Calculations

SPINUP:

$$I_z = 9.0 \text{ slug ft}^2$$

final angular velocity - 100 rpm

thruster lever arm - 1.5 ft

$$I_{sp} = 72 \text{ lbf sec/lbm}$$

$$Ft = \frac{I_z \Delta\omega}{2L} \text{ lbf sec/thruster}$$

$$\Delta\omega = \frac{100}{60} 2\pi = 10.47 \text{ rad/sec}$$

$$Ft = \frac{9(10.47)}{2(1.5)} = 31.4 \text{ lbf sec/thruster}$$

$$= 62.8 \text{ lbf sec for 2 thrusters}$$

DESPIN:

Assume final angular velocity - 5 rpm

$$\Delta\omega = 0.95(10.47) \text{ rad/sec}$$

$$Ft = 0.95(62.8) = 59.6 \text{ lbf sec}$$

PRECESSION:

Assume precession angle - 51° (at 100 rpm)

$$W_P = \frac{I_z \omega}{I_{sp}} \frac{2\pi\theta}{360} = \frac{9(10.47) 2\pi (51)}{72(1.5) (360)}$$

$$= 0.776 \text{ lbm GN}_2 \text{ required}$$

$$Ft = 0.776(72) = 55.8 \text{ lbf sec}$$

DEFLECTION:

Assume service module mass - 55.8 lbm

service module $\Delta V = 1.5 \text{ fps}$

$$Ft = \frac{W\Delta V}{g} = \frac{55.6(1.5)}{32.2} = 2.6 \text{ lbf sec}$$

TOTAL IMPULSE:

$$F_t = 62.8 + 59.6 + 55.8 + 2.6 = 180.8 \text{ lbf sec}$$

$$\text{GN}_2 \text{ Required} - \frac{180.8}{72} = 2.52 \text{ lbm}$$

$$W_p \text{ (total) including leakage allowance} - 2.52(1.3) = 3.27 \text{ lbm}$$

$$\text{Assume storage bottle weight} - 3.27 (1.3) - 4.25 \text{ lbm}$$

	<u>kg</u>	<u>lbm</u>
Component weights:		
Fill Valves (1)	0.11	0.25
Transducers (2)	0.23	0.50
Squib Valves (6)	0.68	1.50
Filters (1)	0.16	0.35
Regulators (1)	0.18	0.40
Solenoid Valves (8)	0.72	1.60
Thrusters, 1 lbf (6)	0.54	1.2
Lines	<u>0.72</u>	<u>1.6</u>
Component Total	33.4	7.4

$$\text{Loaded System Weight} = 3.27 + 4.26 + 7.4 = 14.93 \text{ lbm}$$

C. RELIABILITY COMPARISONS

1. General

Solid propellant motors inherently possess a high reliability because of their extreme simplicity, and their relatively advanced state of the art. Estimates of reliability for new designs are usually based on the demonstrated reliability of prior designs for which the motor components, materials of construction, and service applications are essentially the same as those for the

proposed design. The observed component failure rates are combined by rss addition to provide a quantitative estimate of failure probability (and reliability). Typical of the reliability estimates made by solid motor fabricators is that provided to Martin Marietta by Aerojet. Based on various component tests ranging in number from 122 to 2878, and a total number of failures of only 5, a best estimate of motor reliability for this particular application is 0.997. To actually attain this level of reliability, however, the proposed design must be subjected to a carefully planned development and qualification program.

Liquid (and gaseous) propellant systems tend to be less reliable than solid propellant motors because of their greater complexity, but this deficiency can usually be compensated for by providing redundancy for the critical system components (principally, valves). Using conventional reliability theory, a reasonably accurate quantitative estimate of system reliability may be made from the vast quantity of available statistical data of individual component failure rates, once the total system is adequately defined.

For the particular case of the proposed monopropellant hydrazine system, a preliminary system schematic (Fig. M-8) was first developed, combining the requirements of the ΔV propulsion and the auxiliary propulsion into a single system. To achieve a high reliability, the system operates in a blowdown mode (no pressure regulator), and redundancy is provided for all valve operations. Then the reliability computations were made as presented herein. It will be noted that the ΔV thruster/valve reliability is estimated to be ~ 0.9997 , which combined with a tank/feed system reliability of essentially 1.0, still provides a reliability > 0.999 for the ΔV portion of the system. The addition of the auxiliary propulsion thrusters and valving to the system reduces the overall system reliability (including the ΔV thruster) to a value slightly less than 0.996.

The cold gas system proposed for the auxiliary propulsion functions was treated in a similar manner to the hydrazine system. A complete system to accomplish the four auxiliary propulsion functions was first evolved, and is shown schematically in Figure M-9. Then the predicted reliability for the system was computed as shown in Section C2 of the Appendix. It will be noted that the reliability of the individual thruster/valve assemblies is very high (generally > 0.9999), but the regulator reliability is estimated to be only ~ 0.9975 , thereby reducing the overall system reliability to ~ 0.997 .

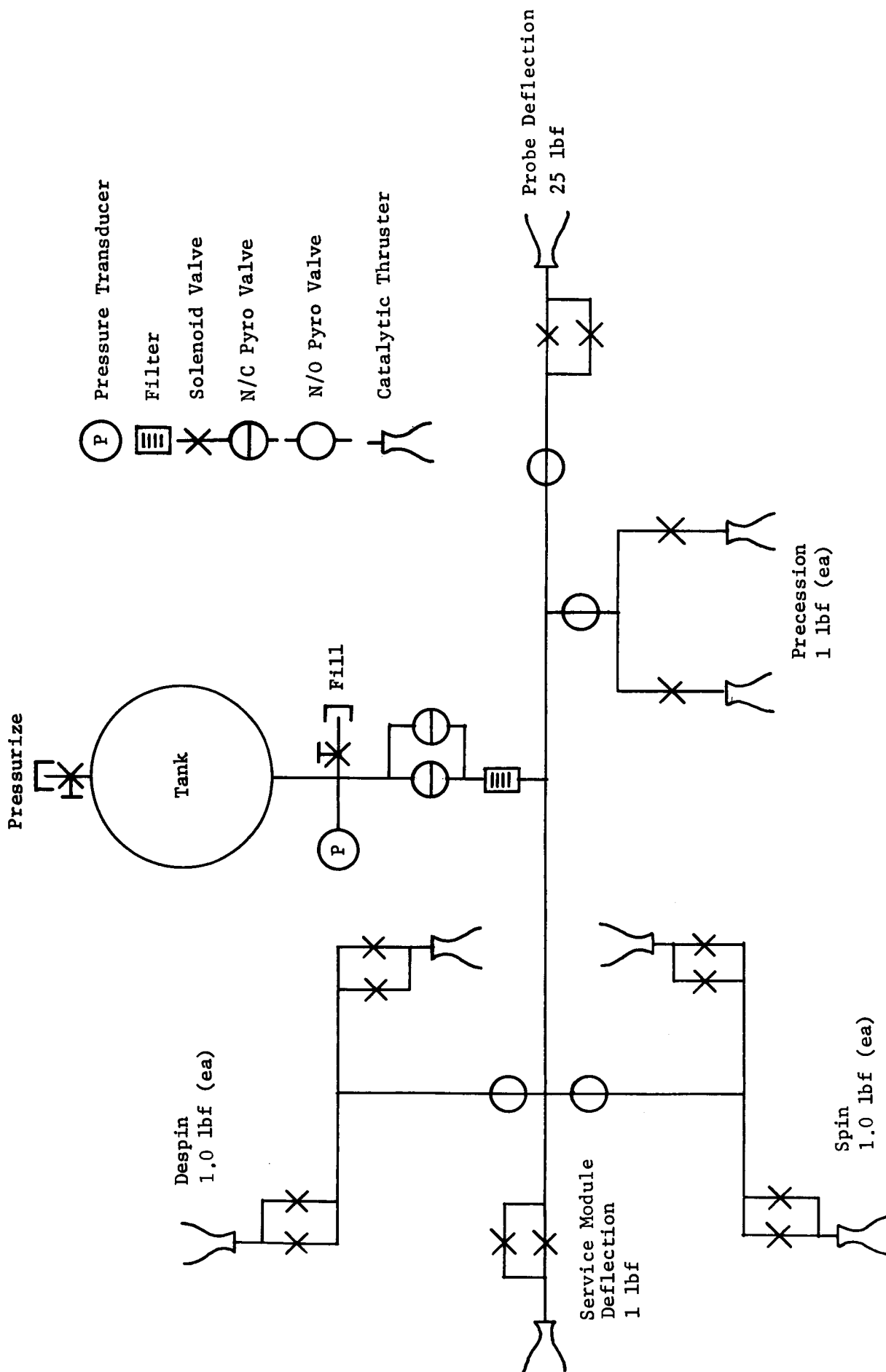


Figure M-8 Reliability Analysis System Schematic Monopropellant Hydrazine System

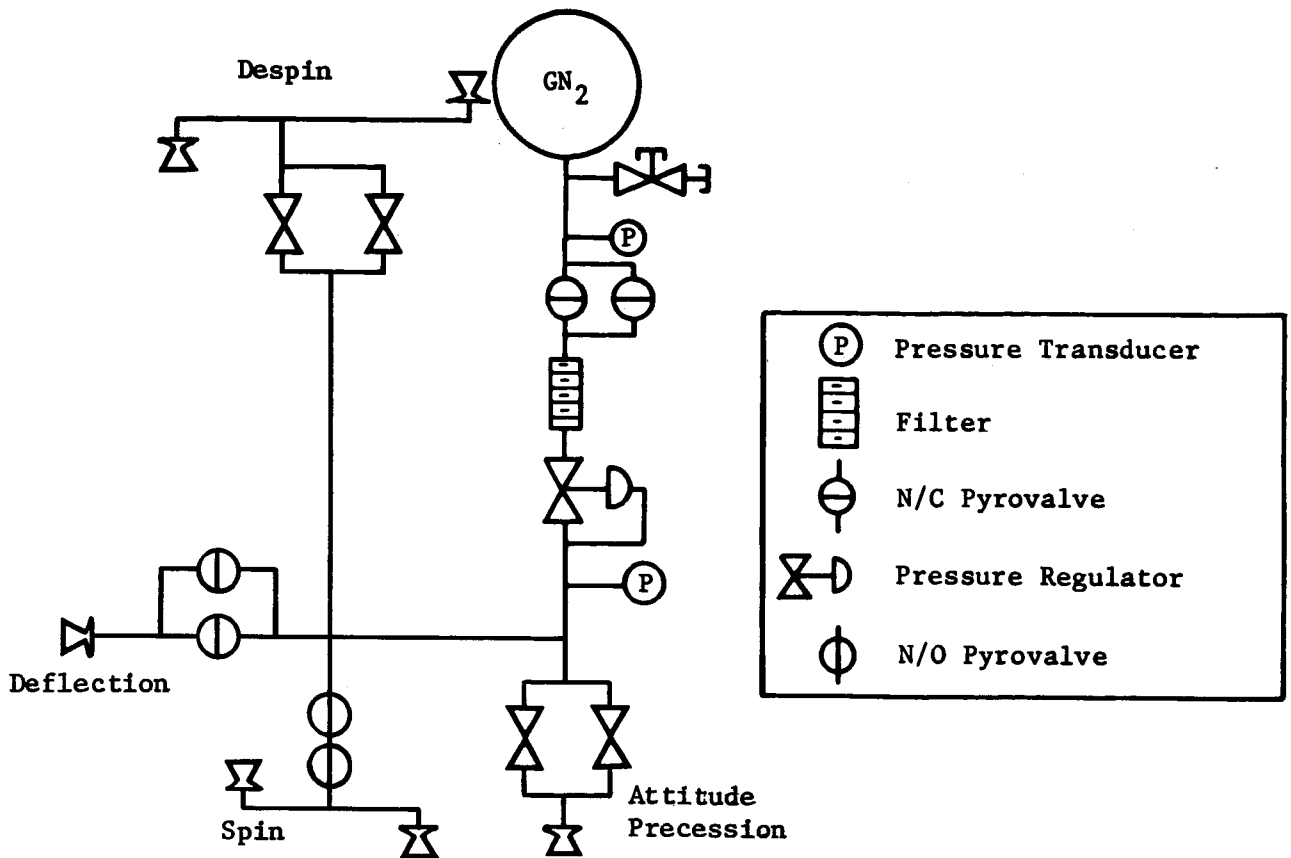


Figure M-9 Reliability Analysis System Schematic Cold Gas Attitude Control System

For a combined system of a solid motor (to provide the ΔV requirement) and the cold gas system (to provide the auxiliary propulsion requirements), the predicted reliability is only slightly greater than 0.994, compared to a predicted reliability for the integrated hydrazine system of nearly 0.996. It is evident that the hydrazine system appears to have a slight advantage with regard to reliability, but the difference is not particularly significant. The principal reason for this difference is the need for a pressure regulator in the cold gas system, whereas the hydrazine system operates in a blowdown mode.

2. GN₂ Subsystem Reliability Analysis

JPL DATA:

Single Valve and Thruster Reliability for 1000 cycles is 0.9622

Q per cycle for valve and thruster - $0.378 (10)^{-4}$

Average Q per valve - $1 (10)^{-6}/\text{cycle}$

Q per thruster - $36 (10)^{-6}/\text{cycle}$

ATTITUDE PROPULSION:

One thruster, two valves in parallel, 1000 cycles of operation

$$\begin{aligned} R &= [1 - (1000(10)^{-6})^2] [1 - 1000(36)(10)^{-6}] \\ &= (0.999999) (0.999964) = 0.99996 \end{aligned}$$

SPIN:

Two thrusters, two NO squib valves in series, one cycle of operation

Q for squibs - 0.0003/operation

$$\begin{aligned} R &= [1 - 36(10)^{-6}]^2 [1 - 0.0003^2] \\ &= (0.99993) (0.99999^+) = 0.9999 \end{aligned}$$

DESPIN:

Two thrusters, two valves in parallel, one cycle of operation

$$R = [1 - 36(10)^{-6}]^2 [1 - (10^{-6})^2]$$

DEFLECTION:

One thruster, redundant pyro valves, one operation, Rx 1.0

SUPPLY SUBSYSTEM:

2 squib valves N/C in parallel

Q/valve - 0.003

$$R = 1 - 0.003^2 = 1 - 9 (10)^{-8} \approx 1.0$$

FILTER:

$$R \approx 1.0$$

REGULATOR:

Q = 2.5 (10)⁻⁶/cycle

1000 cycles estimated

$$\begin{aligned} R &= 1 - 10^3 (2.5) (10)^{-6} \\ &= 0.9975 \end{aligned}$$

R_{TOTAL} SUBSYSTEM

$$= (0.9999) (0.9999) (0.9975)$$

$$= 0.99736$$

3. Monopropellant Hydrazine System Reliability Analysis

Valve (single) and thruster reliability = 0.9479/1000 cycles

$$Q \text{ per cycle} = \frac{(1-0.9479)}{1000} = 52(10)^{-6} \text{ for valve and thruster}$$

$$Q \text{ for valves: Marquardt, } Q = 0.1(10)^{-6}/\text{cycle}$$

$$RADC, \quad Q = 1.6(10)^{-6}/\text{cycle}$$

$$TRW, \quad Q = 0.3(10)^{-6}/\text{cycle}$$

Use $Q = 1(10)^{-6}$ as conservative estimate

$$Q \text{ for thrusters} = 51(10)^{-6}/\text{cycle}$$

ΔV THRUSTER:

One thruster with parallel valves and a N/O squib shut off
Operation: <5 cycles

Valves are redundant to "fail to open" (parallel) and redundant to "fail to close" (N/O squib valve).

$$R = [1 - 5(51)(10)^{-6}] [1 - 5(10)^{-6}]^2$$

$$= 0.99975 \text{ for open and operate mode}$$

Use of N/O squib valve results in $R \approx 1.0$ for fail to close mode

PRECESSION:

Two thrusters, each with single valves and a N/O squib valve.
Operation 1000 cycles. Thrusters are redundant in that either can perform the function

$$\begin{aligned} R \text{ (per leg)} &= [1 - (1000)(10)^{-6}] [1 - 1000(51)(10)^{-6}] \\ &= (0.999)(0.949) = 0.948 \quad Q = 0.052 \end{aligned}$$

For redundant thruster operation:

$$R_{\text{Total}} = (1 - 0.052^2) = 0.9973$$

SPIN:

Two thrusters, each with parallel valves and a N/O squib valve

Operation: 1 cycle

$$\begin{aligned} R &= [(1 - (10)^{-12}) (1 - 51 (10)^{-6})]^2 \\ &= (0.99995)^2 = 0.9999 \end{aligned}$$

DESPIN:

Same configuration as spin, but 5 cycles

$$\begin{aligned} R &= [1 - 255 (10)^{-6}]^2 \\ &= 0.9995 \end{aligned}$$

DEFLECTION:

One thruster, parallel valves. Valves must open once.

$$\begin{aligned} R &= (1 - 10^{-12}) (1 - 52 (10)^{-6}) \\ &= 0.9995 \end{aligned}$$

SUPPLY SYSTEM:

Parallel N/C squib valves

Q/valve - 0.0003

$$R_{\text{Total}} = 1 - 0.0003^2 = 1 - 9 (10)^{-8} \approx 1.0$$

Filter: $R \approx 1.0$

TOTAL SUBSYSTEM:

$$\begin{aligned} R &= (0.99975) (0.9973) (0.9999) (0.9995) (0.9995) \\ &= 0.9959 \end{aligned}$$

D. PLUME CONTAMINATION

Although a rigorous analysis of the solid motor plume is beyond the scope of this study, a cursory analysis was performed to identify the magnitude of the problem, and provide confidence that the selected solution (canted nozzles) is valid. To minimize the effects of the exhaust plume on the mother spacecraft, it is planned that the probe will have separated at least 315 m (1000 ft) from the mother spacecraft before the probe solid motor is fired, but even at this distance, the impingement problem can not be ignored. If the exhaust products were entirely gaseous, they probably could be tolerated, but unfortunately, they contain a large solid content. The 16% Al contained in the propellant oxidizes to form Al_2O_3 solid particles that comprise ~34% of the exhaust products by weight. These particles are of sufficient size and are traveling at sufficiently high velocities that they constitute, in effect, a small belt of low velocity micrometeoroids. Their impact on science instruments (lenses, in particular), thermal control coatings, and thin insulation blankets can produce very detrimental effects that must be avoided if at all possible. Since the aluminum is essential in the propellant for attainment of high performance (specific impulse), it can not easily be eliminated, but impact on the spacecraft can be prevented to a degree by proper aiming of the exhaust flow. The approach to evaluating the problem follows.

- 1) To estimate the magnitude of the plume impingement problem for solid propellant motors containing significant percentages of aluminum, it is necessary to know the approximate sizes of the solid particles in the exhaust, as well as the flow direction and velocity.
 - a) Regarding particle size, Reference 1 states "no theories capable of providing a particle size distribution have appeared." However, direct measurements reported in Reference 2 indicate that the solid (predominantly Al_2O_3) particles are essentially spherical in shape, and have "a mass average diameter between 2 and 3 μ ." Further, it was observed that "the particle size seems to be insensitive to engine size, configuration, propellant ingredients, input aluminum particle size, and chamber pressure."

- b) A comprehensive analytical study of solid particle flow paths reported in Reference 3 concludes that "only the smallest particles follow the gas and that the largest particles are concentrated near the axis, filling only about a third of the nozzle area at the exit plane."
 "Thus the particle flow field in any nozzle exit cone is essentially conical and the particles' drag on the gas will force the gas flow field to be essentially conical also." Figure M-10 shows quantitative results of the analyses for a nozzle with a divergent 15° half angle. The streamlines shown represent the outer boundaries for particles of the size indicated. Thus it will be seen that the heavy (5 to 10 μ diameter) particles appear to continue indefinitely on straight streamlines within the boundary of the extended nozzle exit cone. The lighter particles, however, follow slightly curved paths that extend outside the cone. The number of particles traveling outside the 15° half-angle cone is relatively small, but it definitely is not zero.

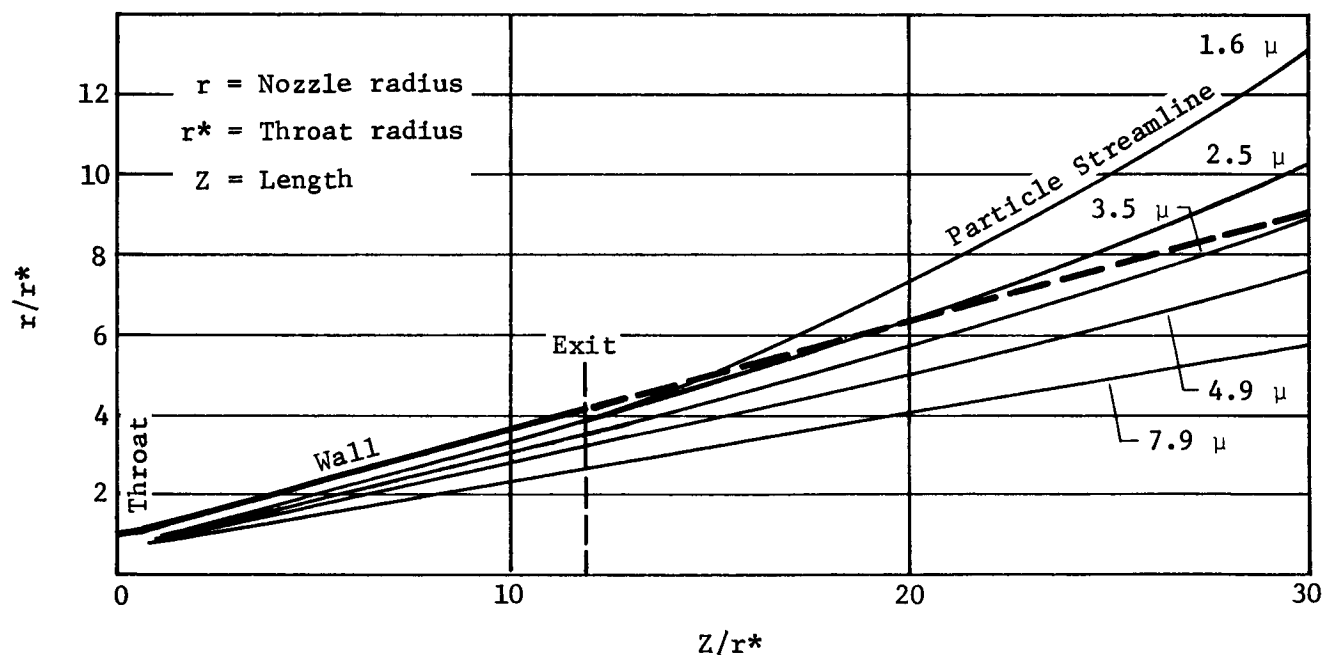


Figure M-10 Solid Particle Streamlines

- c) The velocity of the particles issuing from the nozzle will be of the same order of magnitude as the effective exhaust velocity ($V_e \approx 9000$ fps for a high performance solid propellant motor). Reference 1 notes that "particles of less than 2μ diameter will follow the gas velocity and temperature quite closely, whereas larger particles exhibit sizeable lags."
- 2) Using the above data, a rough order of magnitude estimate of the impingement effects on a mother spacecraft may be as follows:
- a) Assuming an average particle size of 2μ diameter, and a spherical shape, the mass of the average particle is

$$m = \frac{\pi}{6} \frac{0.002^3}{25.4} \frac{248}{1728} = 3.7(10)^{-14} \text{ lbm/particle}$$

- b) Assuming the solid propellant motor contains 27 lbm propellant to be consumed in ~ 15 sec, the rate of generation of exhaust products is

$$\frac{27}{15} = 1.8 \text{ lbm/sec}$$

- c) Using the following theoretical exhaust composition for the TP-H-3062 propellant (Reference 4).

<u>Constituent</u>	<u>mol/100 gm</u>	<u>M</u>	<u>% by wt</u>
HCl	0.5674	36	20.40
N ₂	0.2944	28	8.25
H ₂ O	0.2435	18	4.38
H ₂	1.4583	2	2.92
CO	1.0023	28	28.04
CO ₂	0.0351	44	1.54
Al ₂ O ₃	0.3334	102	34.00
Other			.47
			<u>100.00</u>

it is evident that the Al_2O_3 particles will be generated at a rate of

$$0.34(1.8) = 0.61 \text{ lbm/sec, or}$$

$$\frac{0.61}{3.7(10)^{-14}} = 1.65(16)^{13} \text{ particles/sec}$$

- d) Assuming a nozzle divergence half angle of 15° and a separation distance of 1000 ft between the nozzle (probe) and target (spacecraft), the cross-sectional area of the extended cone is found to be

$$A = \frac{\pi}{4} [2(1000) \tan 15^\circ]^2 = 225,000 \text{ ft}^2$$

- e) Assuming the flow to be uniform across the cross section of the cone (This is only a very rough approximation.), the rate of impact on the spacecraft is found to be

$$\begin{aligned} \frac{1.65(10)^{13}}{225,000} &= 7.4(10)^7 \text{ particles/ft}^2/\text{sec} \\ &= 5.1(10)^5 \text{ particles/in.}^2/\text{sec} \end{aligned}$$

The rate of impact will decrease markedly during the 15-sec burn time of the motor, but the total number of impacts probably would still be $>(10)^6$ particles/in.²

The particles probably do not have sufficient momentum to penetrate multilayer insulation blankets, but they undoubtedly would degrade the performance of an insulation blanket, in addition to contaminating instrument lenses and thermal control coatings.

- 3) The use of canted nozzles obviously will alleviate the problem, but not eliminate it entirely. With canted nozzles it would be expected that none of the heavier ($>5 \mu$ diameter) particles would impact the spacecraft. Likewise, the vast majority of the lighter particles would be directed away from the spacecraft, but a few of the smaller particles would travel on a collision course. The question remains whether the number of impacts of these particles is sufficient to be of any real concern. It has been tentatively concluded that the impacts do not present a significant problem, but this is worthy of further investigation.

E. REFERENCES

- 1) R. F. Hoglund: "Recent Advances in Gas-Particle Nozzle Flow." *ARS Journal*, May 1962.
- 2) B. Brown and R. P. McArty: "Particle Size of Condensed Oxide from Combustion of Metallized Solid Propellants." Proceedings of 8th International Combustion Symposium, Williams & Wilkins Co., Baltimore, Maryland, 1962.
- 3) James R. Rliegel: "Gas Particle Nozzle Flows." Proceedings of the 9th International Symposium on Combustion, Academic Press, Inc., New York, N.Y., 1963.
- 4) Thiokol Correspondence
- 5) Aerojet Letter, re: Reliability
 - a) Development of an Adhesively Bonded Beryllium Propulsion Structure for the Mariner Mars 1971 Spacecraft, JPL, TM 33-517, January 1972.
 - b) Chester A. Vaughan: "Apollo Reaction Control Systems." AIAA Paper No. 68-566. Presented at AIAA 4th Propulsion Joint Specialist Conference, Cleveland, Ohio, June, 1968.
 - c) Surveyor Project Final Report, Part I, Volume II, JPL TR 32-1265, July 1969.
 - d) Mariner Mars 1969 Final Project Report, Development, Design, and Test. JPL TR 32-1460, November 1970.
 - e) Planetary Explorer Liquid Propulsion Study, Final Report, Report No. RRC-71-R-249, Rocket Research Corporation, Redmond, Washington, 1971.

APPENDIX N

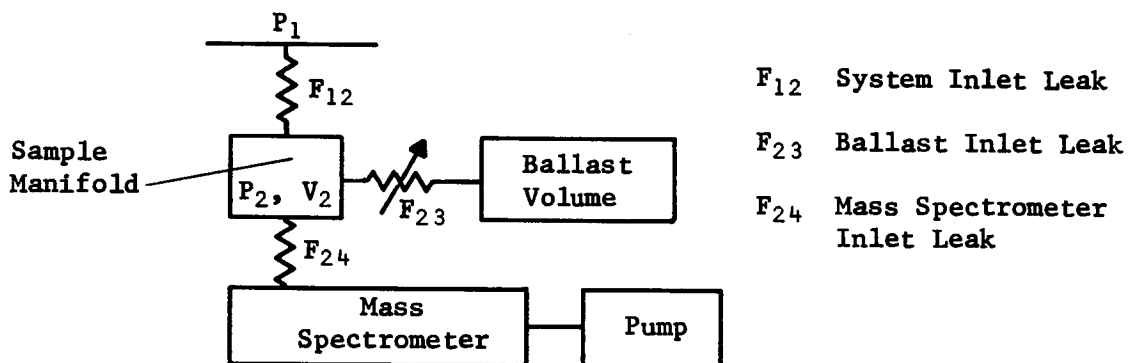
RESPONSE TIME FOR A BALLAST VOLUME TYPE
MASS SPECTROMETER INLET SYSTEM

W. Fraser

March 7, 1972

TO: S. L. Russak, K. Ledbetter, L. Bergquist
 FROM: W. Fraser
 DATE: 07 March 1972
 SUBJECT: Response Time For A Ballast Volume Type Mass Spectrometer Inlet System

A previous memorandum* has discussed an inlet system for a mass spectrometer which descends slowly through the atmosphere of a planet, such as Venus or Jupiter, which has a dense atmosphere. The system is shown schematically in the figure below:



Mass Spectrometer Inlet System

The system functions by maintaining a constant pressure in the manifold. This is accomplished with a variable, servo controlled, inlet leak to the ballast volume. With inlet system volumes of the order of a liter and descent times of a few thousand seconds, such a system can be operated so as to present a constant pressure of a few torr to the mass spectrometer inlet leak.

A concern with an inlet system for a mass spectrometer on a planetary descent probe is its response time. This response time is determined by the leak conductances and system volumes and, for some gases, by reactions between the sample and the inlet system surfaces. The subject of this memorandum is the calculation of the system response time for gas, inlet surface combinations for which surface reactions contribute negligibly. This then represents, for a given set of system parameters, a calculation of a lower bound on the response time.

*P71-44487-281, L. Bergquist and W. Fraser: *Venus Mass Spectrometer Inlet System, Preliminary Analysis and Proposed Laboratory Investigation.*

The configuration analyzed here is subject to the following assumptions:

1. The system has been open long enough that the servo controlled ballast inlet is maintaining the manifold pressure at a constant level.
2. The pressure in the ballast volume is much lower than the manifold pressure. This occurs at high altitude where the response time is longest.
3. Gas flow through the mass spectrometer can be neglected relative to that into the ballast volume.
4. An incremental partial pressure step occurs for one atmospheric constituent.

The partial pressures $P^{(2)}$ and $P^{(1)}$ of the incremented gas and the rest of the gas in the manifold can be described in terms of the flow conductances and volumes of the above figure by the following equations:

$$V_2 \frac{dP^{(2)}}{dt} = (P_1^{(2)} - P^{(2)}) F_{12} - P^{(2)} F_{23}$$

$$V_2 \frac{dP^{(1)}}{dt} = (P_1^{(1)} - P^{(1)}) F_{12} - P^{(1)} F_{23}$$

$$P^{(1)} + P^{(2)} = P_0 \text{ (A Constant)}$$

Here, $P_1^{(1)}$ and $P_1^{(2)}$ are the partial pressures in the external atmosphere.

We now wish to add an increment, ϵ , to the external partial pressure, $P_1^{(2)}$, and calculate the resulting manifold pressure, $P^{(2)}$, as a function of time thereafter.

$$P_1^{(2)} = \begin{cases} P_{10}^{(2)}, & t < 0 \\ P_{10}^{(2)} + \epsilon, & t \geq 0 \end{cases}$$

$$P_1^{(1)} = P_{10}^{(1)}$$

$P_{10}^{(1)}$ and $P_{10}^{(2)}$ are the partial pressures in the atmosphere prior to adding the increment.

The resulting variations, $\delta P^{(1)}$ and $\delta P^{(2)}$, from initial partial pressures, $P^{(1)}$ and $P^{(2)}$, in the manifold as described by:

$$V_2 \frac{d(\delta P^{(2)})}{dt} = F_{12} \frac{P_0^{(1)}}{P_0} \epsilon - (F_{12} + F_{230}) \delta P^{(2)}$$

$$\delta P^{(2)} + \delta P^{(1)} = 0$$

where $P_0^{(1)}$ is the initial partial pressure in the manifold of gas other than the incremented gas

and F_{230} is the initial value of the flow conductance into the ballast volume.

The differential equation for $\delta P^{(2)}$ has the following solution:

$$\delta P^{(2)} = \epsilon (1 - f_0^{(2)}) \frac{P_0}{P_1} (1 - e^{-t/T})$$

where ϵ is the increment in the atmospheric partial pressure of the test gas

$f_0^{(2)}$ is the fractional abundance of the test gas prior to the step increase

P_0 is the manifold pressure

P_1 is the atmospheric pressure

and T is the response time constant given by: $T = \frac{P_0 V_2}{P_1 F_{12}}$

Thus a step, ϵ , in the atmospheric partial pressure results in a step, $\epsilon (1 - f_0^{(2)}) P_0 / P_1$, in the manifold, or sample, pressure with a rise time of $P_0 V_2 / P_1 F_{12}$.

APPENDIX O

AEROSHELL STRUCTURE PARAMETRIC WEIGHT STUDY

T. B. Sharp

June 16, 1972

AEROSHELL STRUCTURE PARAMETRIC WEIGHT STUDY

I. INTRODUCTION

A parametric structural weight study was performed to evaluate the weight of the aeroshell structure as a function of pressure, base diameter, structural material, and shell construction. Four aeroshell diameters, two methods of construction, and two materials were considered in this study. The range of aeroshell diameters and design pressures was selected to encompass the various mission constraints for a Jupiter probe as well as probes to Saturn, Uranus, and Neptune.

II. METHOD OF AEROSHELL ANALYSIS

Conical Shell - Two types of construction (sandwich and frame stabilized monocoque) were considered for the shell structure of the aeroshell. Both types of construction were analyzed assuming a uniform external pressure on a conical shell which is simply supported at the boundaries. The basic equation for general instability allowable is:

$$P_{cr} = \frac{0.736 E}{\frac{L}{R} \left(\frac{R}{t} \right)^{5/2}} \quad [0-1]$$

where:

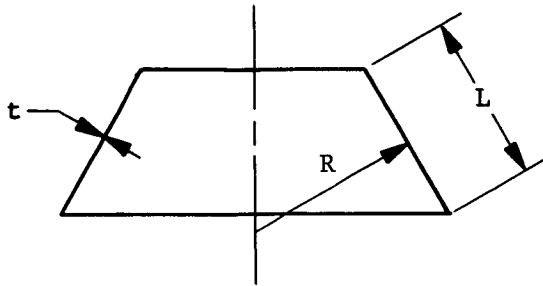
P_{cr} = allowable pressure

E = Young's modulus

L = slant height of the cone

R = average slant radius of the cone

t = cone shell thickness



The two types of construction for the conical shells are idealized to monocoque structures using the assumption that under the discussed loading condition, shell structures having equal radii of gyration in the circumferential direction will work to the same stress level before failing in general instability. Required applicable to the two types of construction considered. These modifications are discussed below.

Sandwich Construction

By equating radii of gyration for monocoque to radii of gyration for sandwich over some finite width, b ,

$$\left[\frac{bt_m^3}{12bt_m} \right]^{1/2} = \left[\frac{2bt_f \left(\frac{d}{2} \right)^2}{2bt_f} \right]^{1/2} \quad [0-2]$$

where:

t_f = thickness of sandwich face sheet

d = centroidal distance between face sheets

t_m = thickness of monocoque skin

solving for t_m

$$t_m = 1.73 d \quad [0-3]$$

using the assumption of equal stress

$$\frac{PR}{t_m} = \frac{P_s R}{2t_f} \quad P_s = \frac{2Pt_f}{t_m} \quad [0-4]$$

where

P_s = critical collapse pressure for sandwich cone and substituting Equations [0-3] and [0-4] into Equation [0-1], the general instability equation for conical sandwich shells is

$$P_s = \frac{3.35Et_f d^{3/2}}{LR^{3/2}} \quad [0-5]$$

In addition to the general instability discussed above, the face sheet material is checked against yielding. It is also assumed that the sandwich core is of sufficient density and cell size as to preclude face wrinkling and intercellular buckling of the face sheets.

Frame Stabilized Monocoque Construction

The frame stabilized monocoque construction consists of a constant thickness skin stabilized by circumferential frames with zee (or channel) cross sections. The general instability equation for this type of construction is developed in the same manner as for the sandwich construction.

By equating radii of gyration over the same finite width, b ,

$$\left[\frac{bt^3}{12bt} \right]^{1/2} = \left[\frac{I}{b_s \bar{t}} \right]^{1/2} \quad [0-6]$$

where

b_s = frame spacing

t = smear thickness of frame and skin

I = moment of inertia of one frame and b_s width of skin about an axis parallel to generator of conical shell.

solving for t

$$t = \left[\frac{12I}{b_s \bar{t}} \right]^{\frac{1}{2}} \quad [0-7]$$

using the assumption of equal stress

$$\frac{P_R}{t_m} = \frac{P_F R}{\bar{t}} \quad P_F = \frac{\bar{t} P}{t_m} \quad [0-8]$$

where

P_F = critical collapse pressure for frame/skin cone, and substituting Equations [0-7] and [0-8] into Equation [0-1], the general instability equation for frame stabilized monocoque conical shells is

$$P_F = \frac{0.736 E \bar{t}}{LR^{3/2}} \left[\frac{12I}{b_s \bar{t}} \right]^{3/4} \quad [0-9]$$

In addition to the general instability discussed above, various local instability checks must be made for the frame stabilized monocoque structure. As suggested in Reference 4, the various elements of this structure are assumed to be flat plates.

The local instability check for the frame elements, is expressed in general equation form as:

$$P = \frac{K \pi^2 E}{12(1 - \nu^2)} \left(\frac{t_r}{b_r} \right)^2 \left(\frac{\bar{t}}{R} \right) \quad [0-10]$$

where

K = depends on boundary condition of frame elements

t_r = frame element thickness

b_r = frame element width

ν = poissons ratio

Local instability of the cone skin, between frames, is checked by the use of two equations. Equation [0-11] assumes the skin to be a flat plate and best accounts for the edge restraint for very close frame spacing. Equation [0-12] assumes the skin to be a truncated cone and best accounts for the benefit of hoop continuity for wide frame spacing; therefore, the higher allowable from these two equations is used.

$$P = \frac{K\pi^2 E}{12(1-\nu^2)} \left(\frac{t_s}{b_s} \right)^2 \left(\frac{\bar{t}}{R} \right) \quad [0-11]$$

$$P = \frac{0.736 E \bar{t}}{b_s} \left(\frac{t_s}{R} \right)^{3/2} \quad [0-12]$$

where

t_s = skin thickness

b_s = frame spacing

Analysis consists of selecting appropriate element sizes so that all the stability requirements will be satisfied, the structure will not yield and a minimum weight structure will be achieved.

End Ring

Analysis of the shell structure of the aeroshell assumes the ends of the cone to be simply supported. An end or edge ring is required to provide this support and to prevent general instability of the cone in the $N = 2$ mode of buckling. Analysis of the end ring was performed to establish a ring of minimum mass which is sufficiently stiff to prevent the inextensional form of buckling of the cone shell. Prevention of the inextensional form of buckling allows the design of the cone shell wall and end ring to be uncoupled. The equation which evaluates the end ring stiffness properties is

$$\frac{I_r}{A^B} = \frac{\psi}{C \left(E_r^{1-B} \right)} \quad (\text{Ref 3}) \quad [0-13]$$

where

I_r = moment of inertia of end ring about its centroidal axis
parallel to generator of conical shell

A = cross-sectional area of end ring

B = generalized stiffness parameter

C = depends on shell properties and ring-eccentricity parameter,
(ψ)

E_r = Young's modulus of end ring

ψ = ring eccentricity parameter

Once the cross-sectional shape of the end ring is determined, the end ring moment of inertia and area can be expressed as a function of a characteristic depth and thickness of the specified shape. The characteristic depth and thickness may then be varied, within design constraints, to obtain a minimum mass end ring.

Nose Cap

General stability of the spherical nose cap is checked using an empirical equation from Reference 2. The equation which predicts the nose cap buckling pressure is

$$P = 0.278 E \left(\frac{t}{R} \right)^2 \quad [0-14]$$

where

R = radius of curvature

Application

The aeroshell is analyzed as two conical shells with the payload frame located between. The forward cone is subjected to an external uniform collapsing pressure producing compressive hoop and longitudinal stresses. The aft cone is subjected to an external uniform collapsing pressure producing compressive hoop and longitudinal tensile stresses.

The general instability equation used in this analysis is for structure subjected to an external uniform pressure loading. This is not the case for the aft cone. The stabilizing effect of the longitudinal tensile stresses in the aft cone results in a slightly conservative design, but the general instability equations will be used for both cones.

Analysis of the sandwich structure consists of determining the proper face thickness and core height, for a given cone geometry and design pressure that will achieve a minimum weight structure and satisfy the stability equations and yield requirements.

The general instability allowable of a conical shell is based on the mid-cone geometry of the shell. The general instability allowable of a frame stabilized shell is based on the mid-cone frame spacing and frame geometry. Each element of the mid-cone geometry is checked for local instability. The selected skin thickness and frame geometry at mid-cone is held constant for the entire cone, but the frame spacing is varied forward and aft of the midcone geometry to achieve a minimum weight structure.

III. APPROACHES CONSIDERED FOR PARAMETRIC STUDY

Four basic components (Fig. 0-1) of the aeroshell were considered for the weight study. In the analysis of these components, certain dimensional parameters were restricted in an attempt to ensure a practical design and a fair comparison of structural weights. A detailed list of the parametric controls is discussed later in this section.

The four aeroshell geometries considered varied only in the base diameter dimension. The four base diameters studied were 2.5, 3.0, 3.5, and 4.0 ft. In all cases, the cone half angle was 60° . The nose cap was assumed to be spherical with a 9.0-in. radius of curvature and a 4.5-in. base radius. The diameter of the payload ring was assumed to be one-half of the cone base diameter. Previous studies have shown that the location of the payload ring has a negligible effect on the cone shell weight. No weight allowance was made in this parametric study for the payload ring.

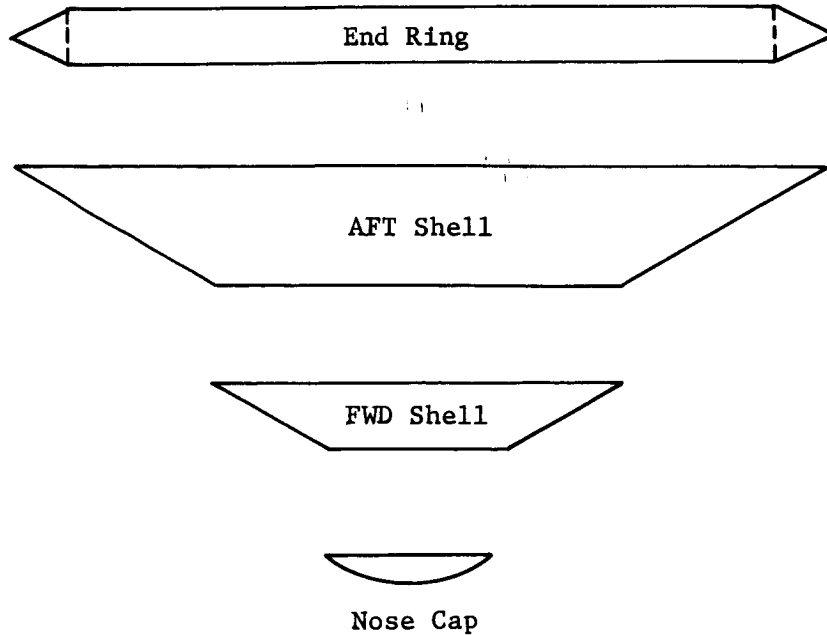


Figure O-1 Aeroshell Components

In the analysis of the aeroshell, only the entry aerodynamic pressures were considered, i.e., a vented aeroshell. The aeroshell weights presented in this study include the cone shell, nose cap, and end ring weights. The aeroshell weights are considered optimum and no allowance was made for difficulty encountered in obtaining the selected dimensions (tolerances) and weight growth caused by fabrication (fasteners, splices, etc.). Sandwich construction includes weights for face sheets, core material, adhesive, and edge members. The weight allowance for edge members was based on each cone being fabricated in quarter sections and each section bounded by an edge member.

The cone shell weights for frame stabilized skin consists of skin and frame weights. The skin is assumed constant thickness for each cone and the frame cross-section geometry is constant for each cone.

The two type of materials considered for this study were 7075-T6 aluminum and 6Al-4V titanium, Cond III. The material properties used were assumed at 200°F and are shown in Table O-1.

Table O-1

<u>7075 -T6 Aluminum</u>	<u>6Al-4V Titanium III</u>
$F_{TU} = 71,000 \text{ psi}$	$F_{TU} = 143,000 \text{ psi}$
$F_{CY} = 63,000 \text{ psi}$	$F_{CY} = 135,000 \text{ psi}$
$E_C = 10 \times 10^6 \text{ psi}$	$E_C = 15.7 \times 10^6 \text{ psi}$
$\rho = 0.101 \text{ lb/in.}^3$	$\rho = 0.16 \text{ lb/in.}^3$

For the sandwich construction, only the face sheet material was varied. The material for the other sandwich components remained constant over the entire range of the parametric study for both face sheet materials. Table O-II lists the sandwich component materials and weights. The end ring material was the same as the selected face sheet material.

Table O-2

Face Sheets	7075-T6 Aluminum or 6Al-4V Titanium
Core, Aluminum	$\rho = 0.00470 \text{ lb/in.}^3$
Adhesive	$\rho = 0.00167 \text{ lb/in}^2$ (two surfaces)
Edge Members, Aluminum	$\rho = 0.101 \text{ lb/in.}^3$

For the frame-stabilized skin construction, the skin and frames and end ring were of the same material.

The range of design pressures considered was from 50 to 600 psi.

Parametric Controls

In this parametric study, certain dimensional parameters were restricted in an attempt to ensure a practical design configuration. Figure O-2 shows the two types of construction considered and designates the dimensional parameters which were controlled. Table O-III lists the minimum values of these controlled dimensions.

Table O-3

MINIMUM GAGES AND DIMENSIONS					
TYPE OF CONSTRUCTION	t_s	t_c	t_r	b_r	b
Sandwich	0.005	0.10	-	-	-
Frame Stabilized Skin	0.020	-	0.015	0.50	0.25

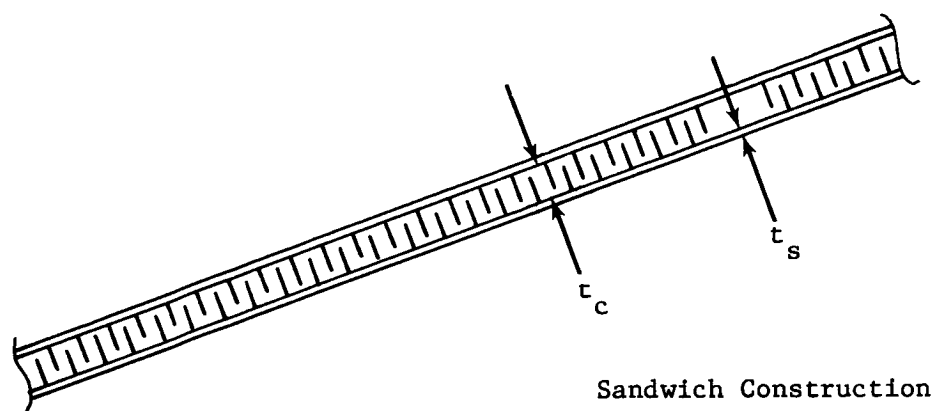
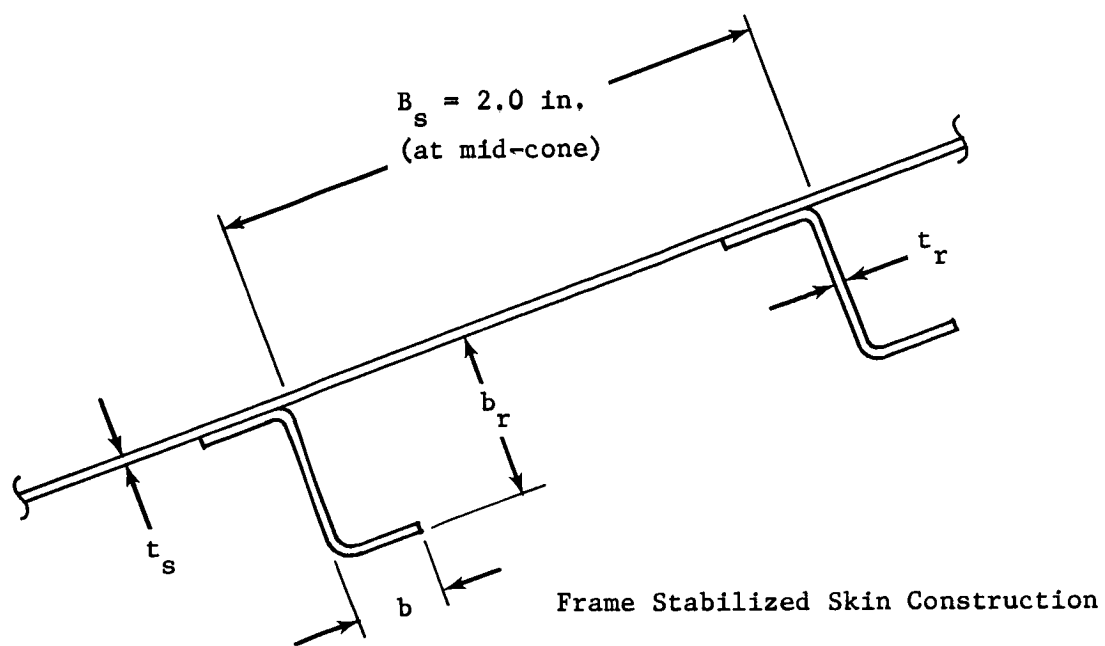


Figure 0-2 Structural Details

Figure 0-3 shows the cross-sectional shape of the end ring and the range of the controlled dimensions which were used for the weighing of the end ring.

IV. RESULTS OF PARAMETRIC STUDY

A detailed weight breakdown for the four basic aeroshell components is shown in Tables 0-4 thru 0-7. The total aeroshell weights are depicted graphically in Figures 0-4 thru 0-7 as a function of design pressures and base diameters. Figures 0-8 thru 0-11 show a comparison of aeroshell weights versus design pressures for the two types of construction and materials considered.

Figures 0-8 thru 0-11 indicate that for the lower range of pressures considered, the aluminum frame-stabilized skin construction produces the lightest weight aeroshell. The titanium frame-stabilized skin construction is relatively inefficient at the lower pressures but becomes more efficient at the higher pressures. The aluminum structure reach a working stress equal to its compressive yield strength at much lower pressures than do the titanium structures; thus aluminum is the more efficient material for either type of construction at the lower pressure range. As the pressure increases and the titanium reaches a working stress equal to its compressive yield strength, then titanium becomes the more efficient of the two materials for both types of construction. The pressures at which the aluminum and titanium curves cross each other is dependent on the base diameter of the aeroshell. (Fig. 0-8 thru 0-11). This cross over point occurs at lower pressures for the larger diameter aeroshell because these shells are more efficient, i.e., for a given design pressure, a larger percentage of the shell structure material is working to its compressive yield strength.

In general, the weight of the sandwich construction was not very competitive with frame-stabilized skin construction at the higher design pressures. When the design stresses of the frame/skin construction are equal to the sandwich face skin stresses, the sandwich construction carries a weight penalty because of the additional components that are not really necessary to carry membrane loads, i.e., adhesive, core, and edge members. At the lower design pressures, when the frame/skin elements are in the instability range, the sandwich face sheets are capable of working to the

compressive yield strength of the material; consequently the sandwich construction weight becomes much more competitive with that of the frame-stabilized skin construction. At very low design pressures (below the 50 psi considered in this study) sandwich construction would prove to be the lighter weight method of construction. This can be seen by extrapolating the curves of Figures)-8 thru 0-11 to design pressures of less than 50 psi.

It is recognized that the total weight of sandwich shell construction is dependent on more variables than that of frame stabilized skin construction. It then follows that the aeroshell weights shown in this study are perhaps more optimum for frame/skin construction than for the sandwich construction. But, in general, for the design pressures, the methods of construction, and types of materials considered in this study, the following summary statements are applicable. Frame-stabilized skin construction results in a more practical method of fabrication and lighter weight aeroshell than sandwich construction. For the lower range of design pressures, an aluminum structure is lighter than titanium but for the higher range of design pressures, a titanium structure will result in the lighter aeroshell structure.

V. DISCUSSION OF USAGE OF CURVES

The curves presented in this appendix provide the basic structural weights for 60° (half angle) conical aeroshells using two methods of construction, two types of materials and a wide range of design pressures. The curves also cover a range of base diameters from 2.5 to 4.0 ft and may be interpolated for base diameters not shown. The aeroshell weights shown represent a nearly optimum weight for the cone shell, nose cap, and end ring. In order to arrive at a complete aeroshell weight, the weights of the payload ring, heat shield, and any other applicable structure should be added to the curve weights shown herein. It should also be noted that the weights shown are considered optimum, it is suggested that a non-optimum factor be applied to these weights to account for material tolerances, splices, fasteners, etc.

It should be emphasized that aeroshell weight curves reflect certain assumptions and constraints which have been previously listed in detail in this section. The curves should be used only as a preliminary guide towards estimating an aeroshell weight. Obviously an accurate aeroshell weight may only be determined after a specific aeroshell design has been established.

VI. REFERENCES

1. V. I. Weingarten, E. J. Morgan, P. Seide: *Final Report on Development of Design Criteria for Elastic Stability of Thin Shell Structures*. Report No. STL/TR-60-0000-19425, Space Technology Laboratories, December 1960.
2. R. Roark: *Formulas for Stress and Strain*, Fourth Edition
3. S. C. Dixon, J. B. Carline: *Preliminary Design Procedure for End-Rings of Isotropic Conical Shells Loaded by External Pressure*. NASA Technical Note, NASA TN D-5950.
4. E. H. Wickell, R. F. Crawford: *Optimum Ring Stiffened Cylinders Subjected to a Uniform Hydrostatic Pressure*. Paper No. 578F, Society of Automotive Engineers, October 1962.
5. Monsham Barúch, Josef Singer, Ovaclic Harari: *General Justability of Conical Shells with Non-Uniformly Spaced Stiffeners Under Hydrostatic Pressure*. Israel TAE Report No. 37, Israel Institute of Technology-Department of Aeronautical Engineers, Haifa
6. NASA Structural Analysis Manual

Table 0-4 Aeroshell Weights, lb

FRAME STABILIZED SKIN - BASE DIAMETER = 4.0 ft										
PRESSURE	ALUMINUM					TITANIUM				
	AFT CONE	FWD CONE	NOSE CAP	END RING	TOTAL	AFT CONE	FWD CONE	NOSE CAP	END RING	TOTAL
50	10.6	2.8	0.3	3.0	16.7	14.4	3.9	0.3	5.0	23.6
100	13.5	3.6	0.4	3.7	21.2	18.2	4.9	0.5	5.3	28.8
200	20.3	4.5	0.5	4.9	30.2	23.4	6.1	0.6	6.4	36.5
300	29.2	5.2	0.6	8.3	43.3	27.2	7.0	0.8	7.2	42.2
400	38.3	6.0	0.7	16.5	61.5	33.0	7.7	0.9	8.3	49.9
500	47.3	6.9	0.8	27.6	82.6	40.4	8.3	1.0	11.7	61.4
600	56.3	7.7	0.9	42.0	106.9	47.7	9.1	1.1	18.1	76.0

SANDWICH - BASE DIAMETER = 4.0 ft										
PRESSURE	ALUMINUM					TITANIUM				
	AFT CONE	FWD CONE	NOSE CAP	END RING	TOTAL	AFT CONE	FWD CONE	NOSE CAP	END RING	TOTAL
50	15.7	2.6	0.3	3.0	21.6	11.9	2.6	0.3	5.0	19.8
100	24.5	3.7	0.4	3.7	32.3	16.7	3.1	0.5	5.3	25.6
200	42.2	6.2	0.5	4.9	53.8	27.2	4.6	0.6	6.4	38.8
300	59.8	8.7	0.6	8.3	77.4	37.7	6.3	0.8	7.2	52.0
400	77.1	11.2	0.7	16.5	105.5	48.2	7.9	0.9	8.3	65.3
500	94.4	13.6	0.8	27.6	136.4	58.6	9.6	1.0	11.7	80.9
600						69.0	11.2	1.1	18.1	99.4

Table 0-5 Aeroshell Weights, 1b

FRAME STABILIZED SKIN - BASE DIAMETER = 3.5 ft									
PRESSURE	ALUMINUM					TITANIUM			
	AFT CONE	FWD CONE	NOSE CAP	END RING	TOTAL	AFT CONE	FWD CONE	NOSE CAP	TOTAL
50	7.7	2.0	0.3	2.8	12.8	10.5	2.7	0.3	17.9
100	9.8	2.5	0.4	2.9	15.6	13.3	3.4	0.5	21.6
200	13.5	3.2	0.5	4.0	21.2	16.9	4.3	0.6	26.9
300	19.7	3.6	0.6	4.7	28.6	19.5	4.9	0.8	30.8
400	25.6	4.1	0.7	8.0	38.4	22.2	5.5	0.9	34.8
500	31.7	4.6	0.8	13.7	50.8	26.9	5.9	1.0	40.9
600	37.6	5.1	0.9	20.7	64.3				

SANDWICH - BASE DIAMETER = 3.5 ft									
PRESSURE	ALUMINUM					TITANIUM			
	AFT CONE	FWD CONE	NOSE CAP	END RING	TOTAL	AFT CONE	FWD CONE	NOSE CAP	TOTAL
50	9.2	1.8	0.3	2.8	14.1	8.4	1.9	0.3	15.0
100	14.4	2.5	0.4	2.9	20.2	11.5	2.2	0.5	18.6
200	24.9	4.2	0.5	4.0	33.6	18.7	3.1	0.6	27.5
300	35.3	5.9	0.6	4.7	46.5	25.9	4.2	0.8	36.5
400	45.6	7.5	0.7	8.0	61.8	33.0	5.3	0.9	45.4
500	55.7	9.2	0.8	13.7	79.4	40.2	6.4	1.0	54.7
600	65.8	10.9	0.9	20.7	98.3	47.3	7.4	1.1	64.0

Table O-6 Aeroshell Weights, lb

FRAME STABILIZED SKIN - BASE DIAMETER = 3.0 ft									
PRESSURE	ALUMINUM					TITANIUM			
	AFT CONE	FWD CONE	NOSE CAP	END RING	TOTAL	AFT CONE	FWD CONE	NOSE CAP	TOTAL
50	5.4	1.3	0.3	2.3	9.3	7.4	1.7	0.3	13.1
100	6.8	1.6	0.4	2.3	11.1	9.3	2.2	0.5	15.7
200	9.0	2.1	0.5	2.6	14.2	11.7	2.8	0.6	18.8
300	12.3	2.4	0.6	3.1	18.4	13.4	3.2	0.8	21.6
400	16.1	2.6	0.7	3.8	23.2	14.9	3.5	0.9	23.8
500	19.8	2.9	0.8	5.7	29.2	17.0	3.8	1.0	26.6
600	23.6	3.2	0.9	8.8	36.5	20.1	4.1	1.1	30.8

SANDWICH - BASE DIAMETER = 3.0 ft									
PRESSURE	ALUMINUM					TITANIUM			
	AFT CONE	FWD CONE	NOSE CAP	END RING	TOTAL	AFT CONE	FWD CONE	NOSE CAP	TOTAL
50	6.1	1.2	0.3	2.3	9.9	5.7	1.3	0.3	11.0
100	9.5	1.6	0.4	2.3	13.8	7.6	1.4	0.5	13.2
200	16.4	2.6	0.5	2.6	22.1	12.2	1.9	0.6	18.4
300	23.1	3.7	0.6	3.1	30.5	16.6	2.6	0.8	24.2
400	29.8	4.8	0.7	3.8	39.1	21.5	3.2	0.9	30.1
500	36.5	5.8	0.8	5.7	48.8	26.0	3.9	1.0	35.7
600	43.1	6.9	0.9	8.8	59.7	30.6	4.6	1.1	41.8

Table 0-7 Aeroshell Heights, 1b

FRAME STABILIZED SKIN - BASE DIAMETER = 2.5 ft									
PRESSURE	ALUMINUM					TITANIUM			
	AFT CONE	FWD CONE	NOSE CAP	END RING	TOTAL	AFT CONE	FWD CONE	NOSE CAP	TOTAL
50	3.5	0.7	0.3	1.9	6.4	4.8	1.0	0.3	9.2
100	4.4	0.9	0.4	1.9	7.6	6.1	1.2	0.5	10.9
200	5.7	1.2	0.5	1.9	9.3	7.6	1.6	0.6	12.9
300	7.2	1.3	0.6	2.1	11.2	8.7	1.8	0.8	14.4
400	9.4	1.5	0.7	2.5	14.1	9.6	2.0	0.9	15.6
500	11.5	1.6	0.8	2.9	16.8	10.5	2.2	1.0	17.1
600	13.8	1.7	0.9	3.5	19.9	12.0	2.3	1.1	19.1

SANDWICH - BASE DIAMETER = 2.5 ft									
PRESSURE	ALUMINUM					TITANIUM			
	AFT CONE	FWD CONE	NOSE CAPQ	END RING	TOTAL	AFT CONE	FWD CONE	NOSE CAP	TOTAL
50	3.9	0.8	0.3	1.9	6.9	3.7	0.8	0.3	7.9
100	5.9	0.9	0.4	1.9	9.1	4.8	0.9	0.5	9.3
200	10.0	1.5	0.5	1.9	13.9	7.4	1.1	0.6	12.2
300	14.1	2.1	0.6	2.1	18.9	10.2	1.4	0.8	15.5
400	18.2	2.7	0.7	2.5	24.1	12.9	1.8	0.9	18.7
500	22.2	3.3	0.8	2.9	29.2	15.7	2.1	1.0	22.2
600	26.3	4.0	0.9	3.5	34.7	18.4	2.5	1.1	25.7

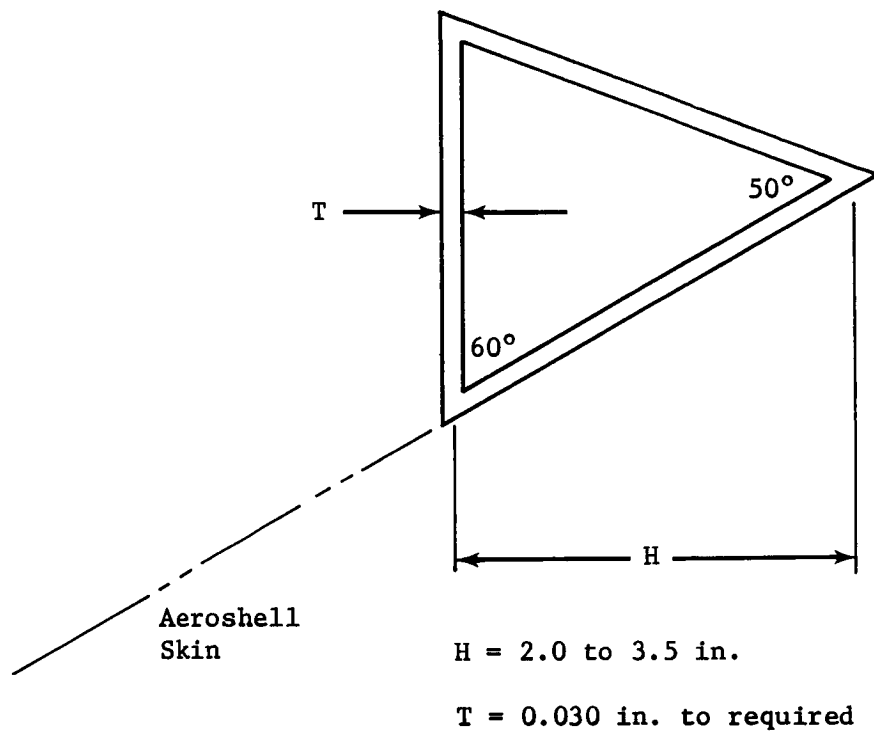


Figure 0-3 End Ring Cross Section

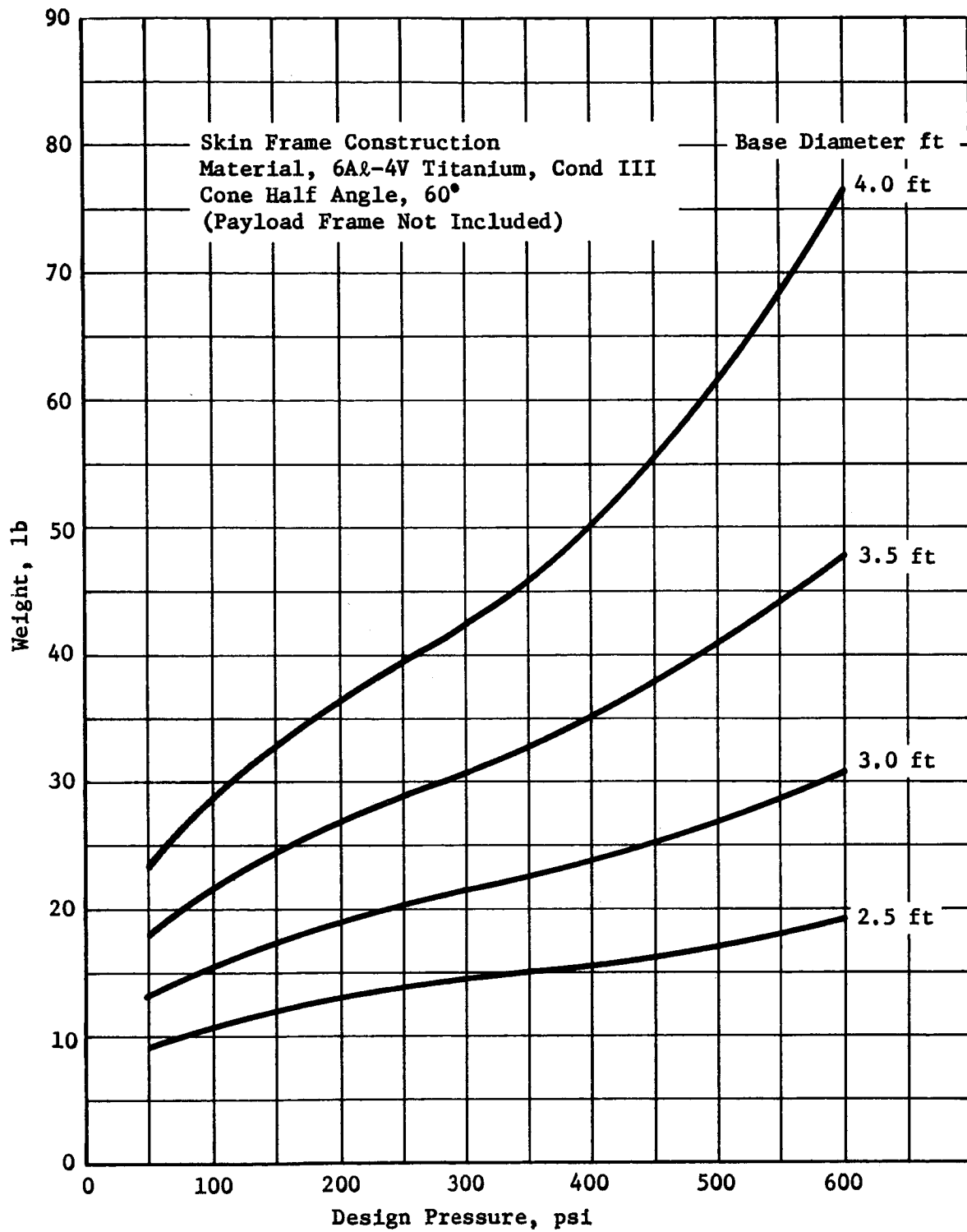


Figure O-4 Aeroshell Weights

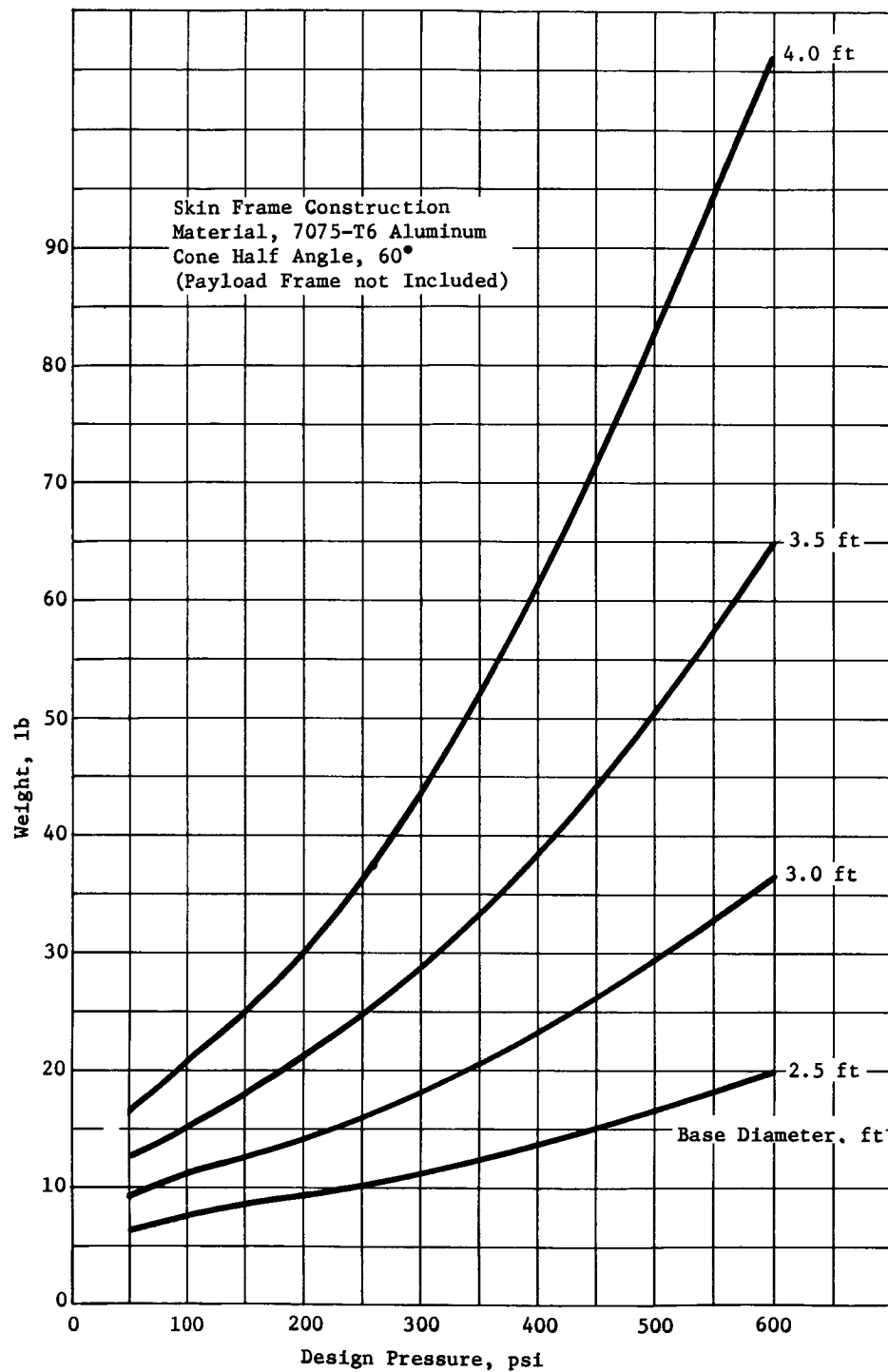


Figure O-5 Aeroshell Weights

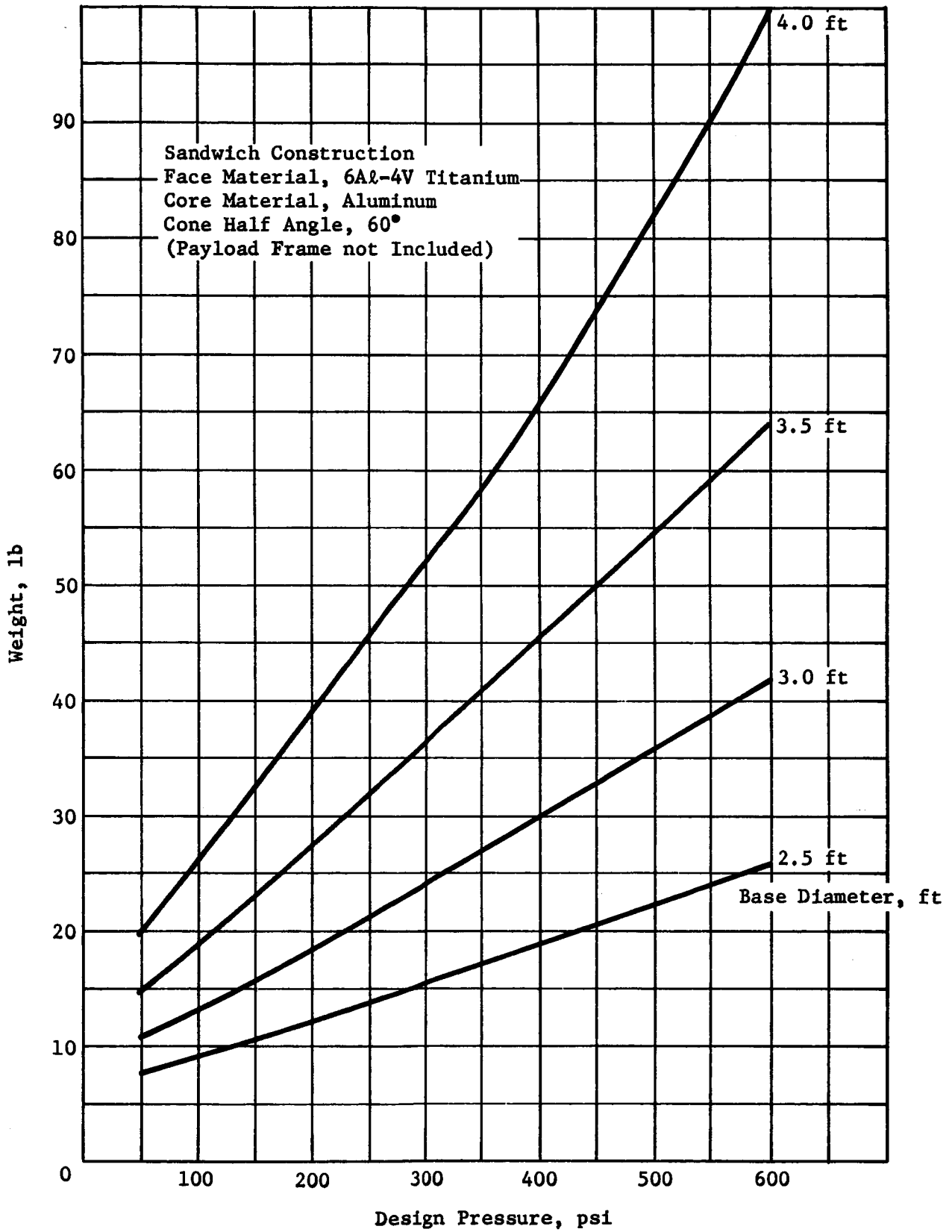


Figure O-6 Aeroshell Weight

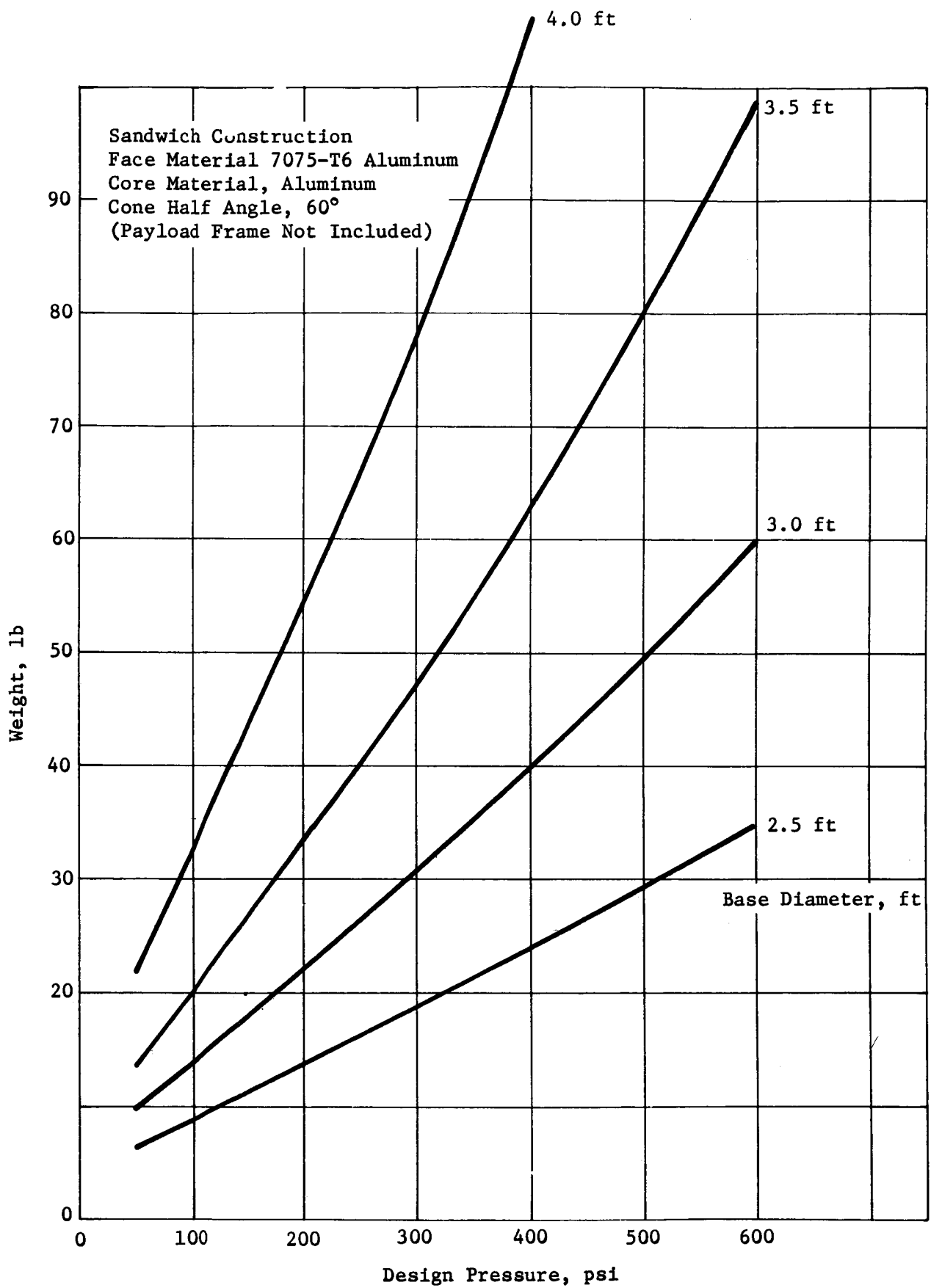


Figure O-7 Aeroshell Weight

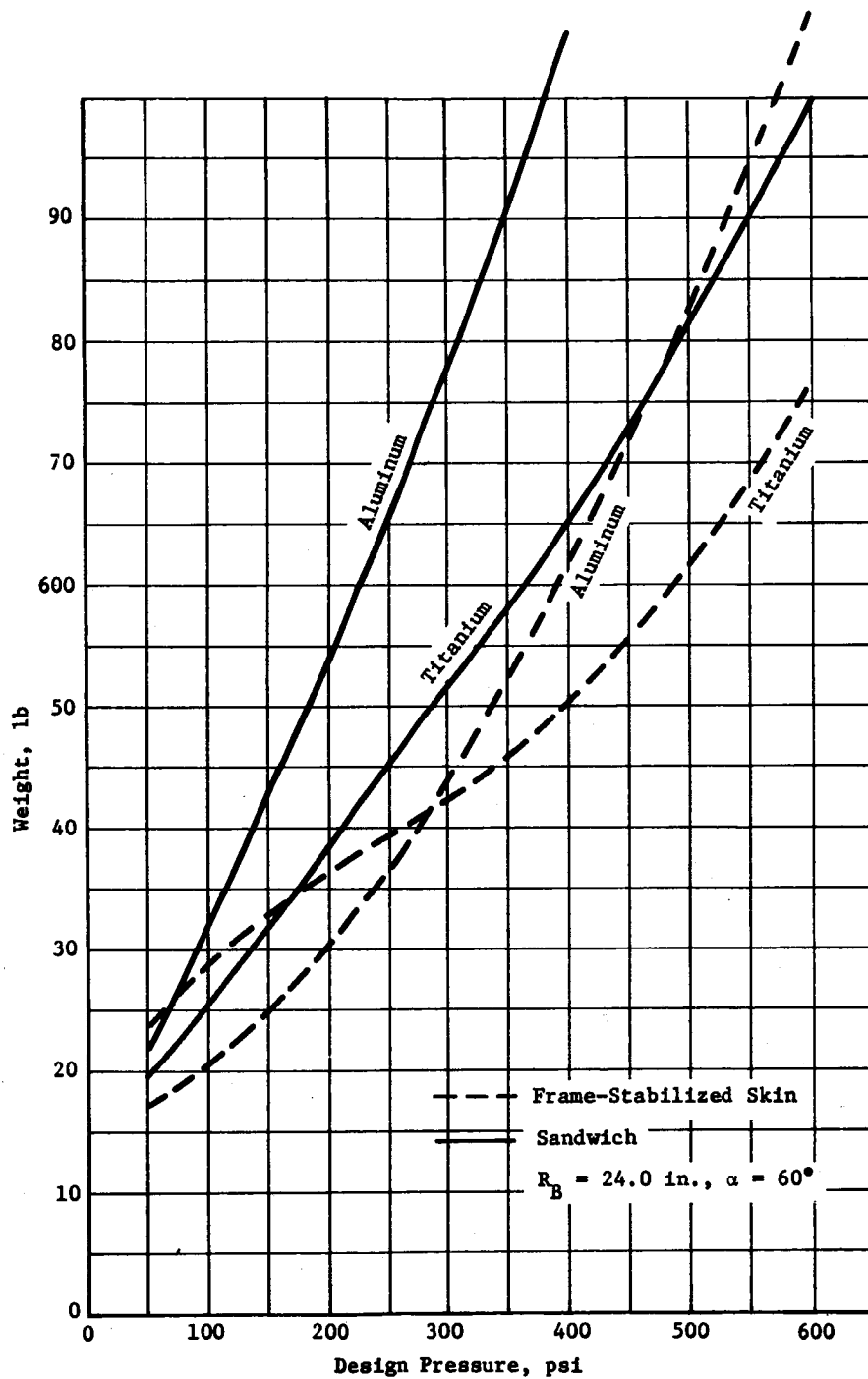


Figure O-8 Aeroshell Weights

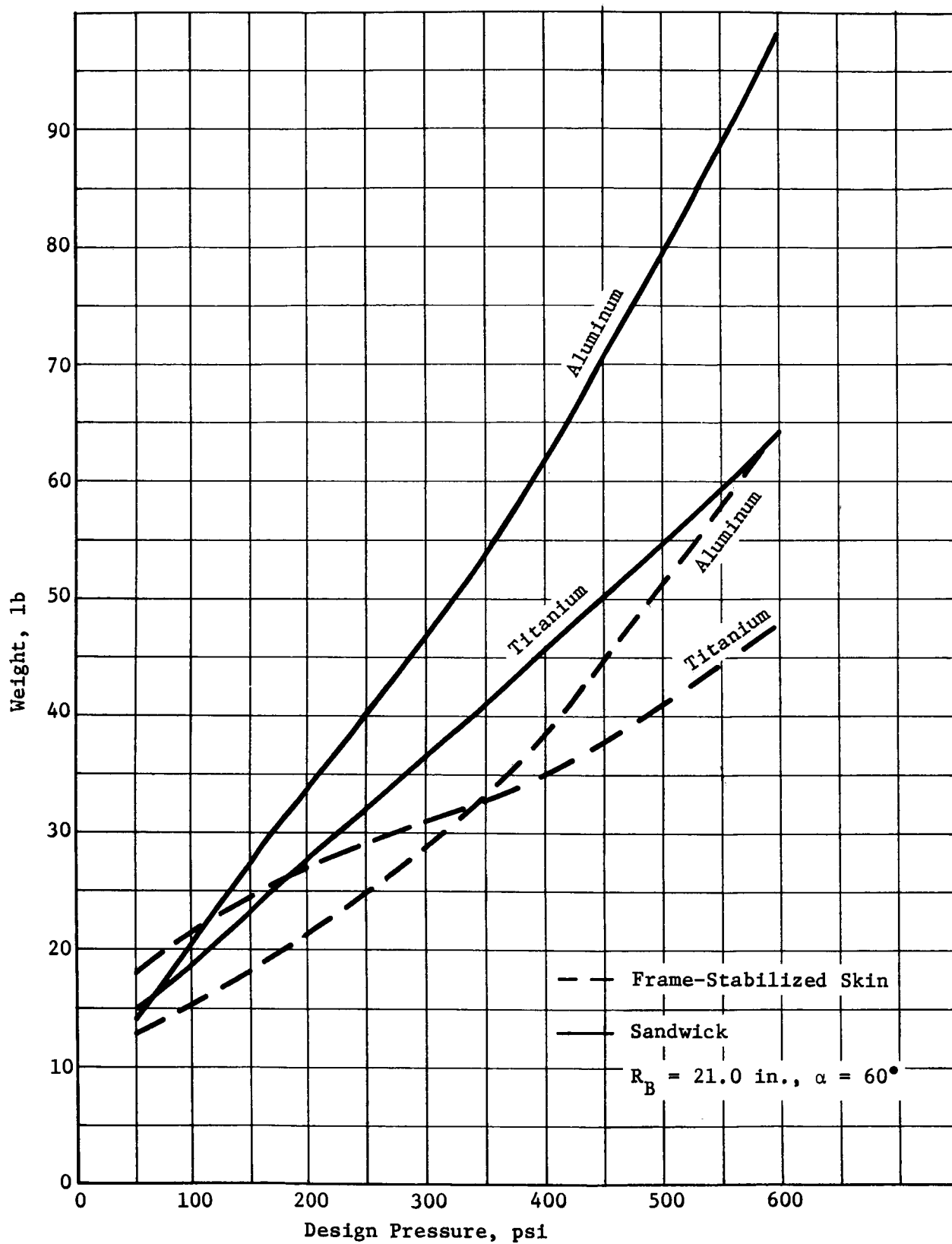


Figure 0-9 Aeroshell Weights

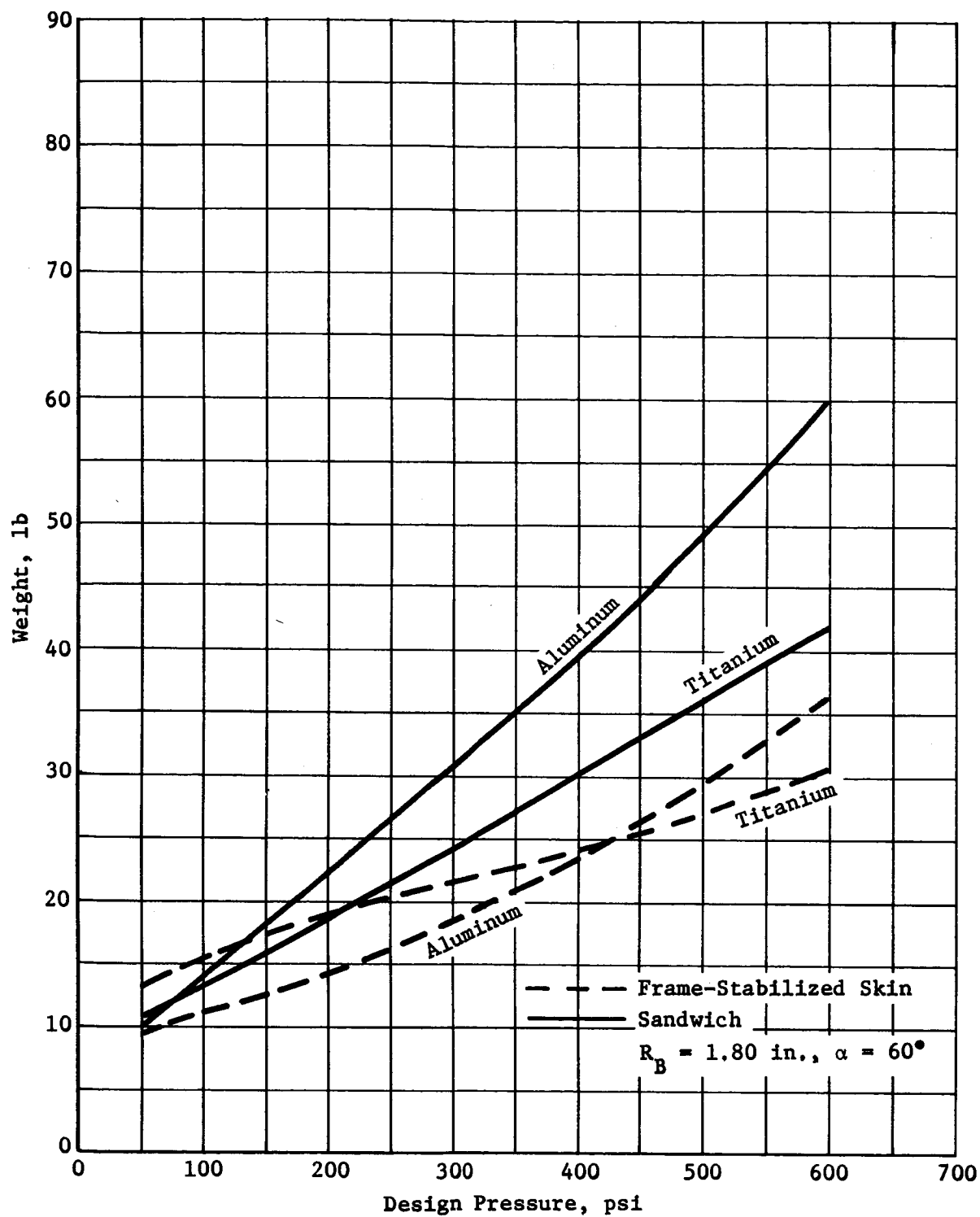
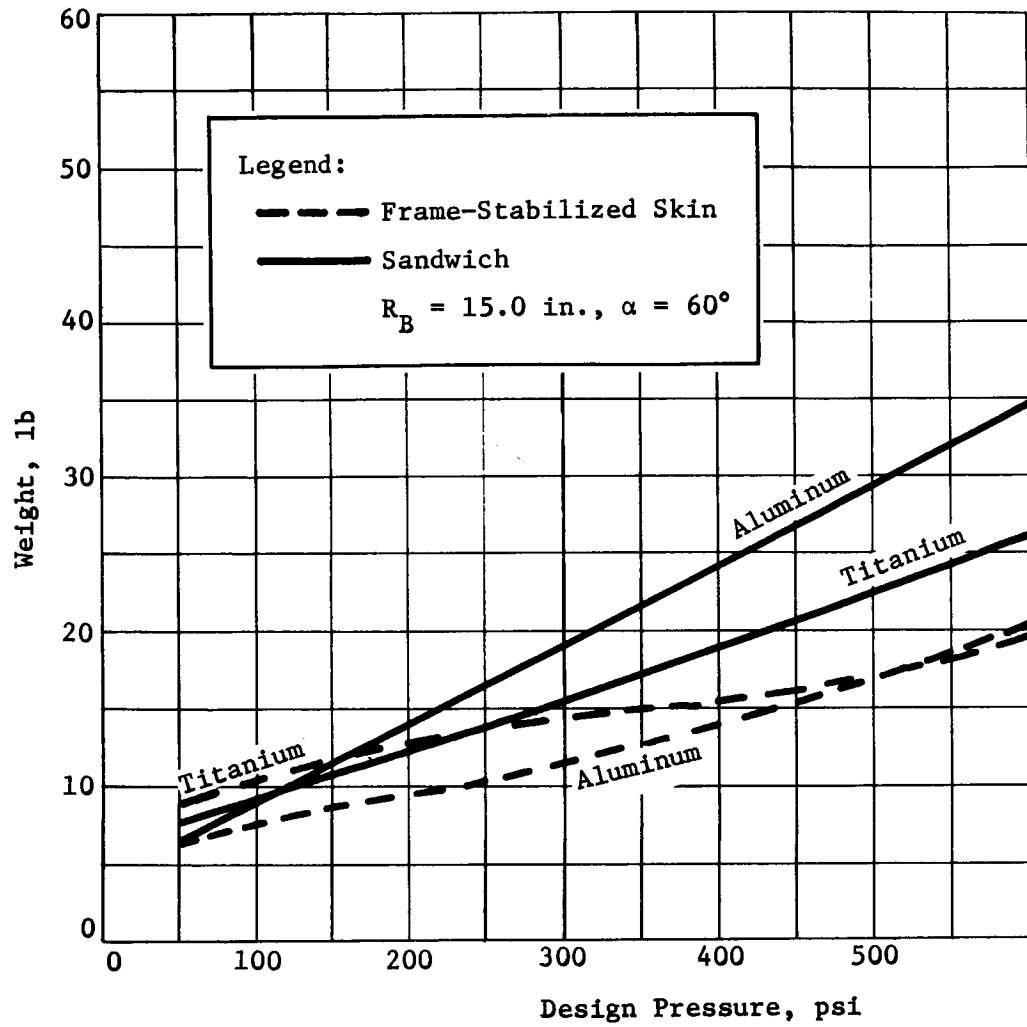


Figure O-10 Aeroshell Weights



600

Figure O-11 Aeroshell Weights

APPENDIX P

LIGHTWEIGHT JUPITER PROBE DEFINITION

J. Hungate

June 16, 1972

LIGHTWEIGHT JUPITER PROBE DEFINITION

During the study, the definition of the nominal Jupiter probe had been completed and work on the parametric analyses, identified in Figure V-1, Vol II of this report, was just beginning when a meeting between personnel of JPL and Martin Marietta, indicated that the weight of the nominal Jupiter probe exceeded its expected weight. Therefore, it was agreed that the constraints for the nominal Jupiter probe would be held constant except for those in Table P-1. The effort resulted in the probe configuration shown in Figure P-1 with the corresponding weight breakdown shown in Table P-2. Estimated MMC-MOPS modification is presented in Table P-3. Using a 1350-lb spacecraft weight results in a spacecraft-probe-system weight of approximately 1750 lb.

The probe was defined without knowledge of the entry uncertainty and with only a cursory link analysis which estimated the RF power to be 23 watts at 1 GHz when using a 5-ft diameter spacecraft antenna.

Table P-1 Constraints for Light Weight Probe

MOPS at 1350 lb

T-111 (5-Seg)/Centaur/Burner II

Probe Weight + S/C Modification Weight \leq 400 lb (Goal)

$R_P = 6 R_J$

Probe Deflection Mode

Deflection Radius = 30×10^6 km ($\Delta V = 210$ m/s)

Entry Angle = 10° (Deceleration Force Reduced From 1500 g to 764 g)

Deceleration to $< M = 1$ at 100 mb (Entry Ballistic Coefficient
= 0.65 slug/ft²)

Depth of Penetration = 10 bars

Atmosphere - Cool/Dense (Descent Ballistic Coefficient = 0.12
slug/ft²)

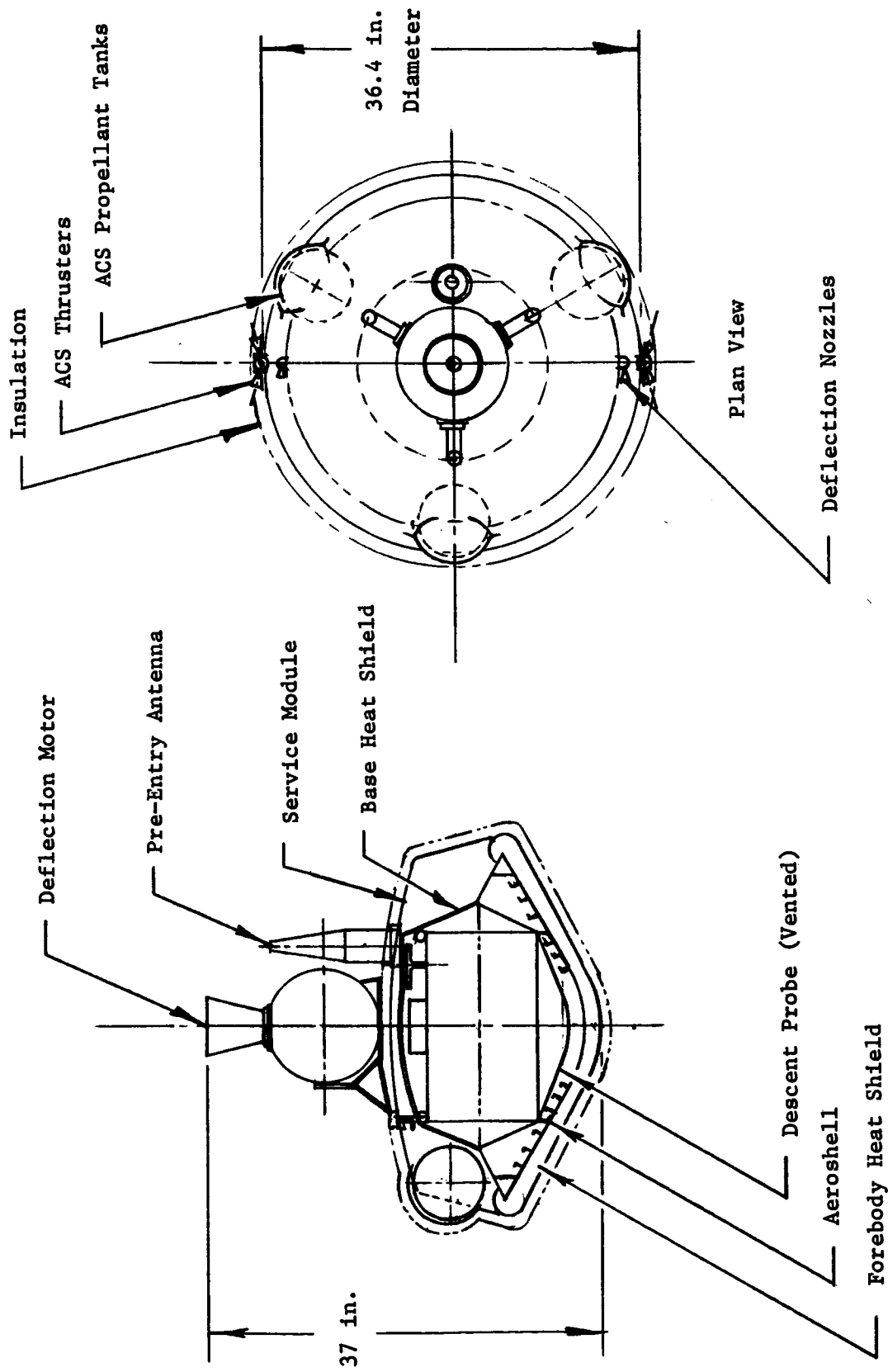


Figure P-1 Light Weight Jupiter Probe Configuration

Table P-2 Weight Breakdown for Lightweight Jupiter Probe

<u>Probe Weight Statement</u>	<u>lb</u>	<u>kg</u>
Science	17.50	7.9
Power and Power Conditioning	10.6	4.8
Cabling	12.50	5.7
Data Handling	5.20	2.4
Attitude Control Subsystem	18.98	8.6
Communications	4.5	2.0
Pyrotechnic Subsystems	11.96	5.4
Structures	59.45	27.0
Forward Heat Shield	62.0	28.2
Mechanisms	12.20	5.5
Thermal	13.70	6.2
Propulsion (Dry)	7.5	3.4
Propellant	27.6	12.5
Engineering Instrumentation	0	0
Margin - (15% of above)	39.50	17.9
Weight Ejected (Total)	303.28	137.5
<u>Weight Ejected</u>	303.28	137.5
Deflection Propellant		
Deflection Propulsion Module & Support (-43.2 lb)		
Nitrogen Gas		
<u>Weight Despun</u>	260.08	118.0
Probe Service Module (-53.41 lb)		
<u>Weight at Entry</u>	206.67	93.7
Ablator Lost During Entry (-45.0 lb)		
<u>Post-Entry Weight</u>	161.67	73.3
Base Cover Quadrants (-22.66 lb)		
<u>Weight on Parachute Initially</u>	139.01	63.0
Entry Probe Body Assembly (-57.5 lb)		
<u>Weight on Parachute Final</u>	81.5	36.9
Main Parachute (-2.80 lb)		
<u>Final Descent Weight</u>	78.5	35.6

Table P-3 MOPS Modification for the 6 R_J Probe

	<u>Lb</u>
Probe Structural Adapter	9.00
Spin Table	20.00
Environmental Cover & Separation	27.20
Receiver Antenna (5-ft diameter)	14.80
Antenna Pointing Drive	5.00
Receiver	2.40
Cabling	2.00
Thermal Control	2.30
Data Handling	0.00
15% Contingency	12.40
	<hr/>
	95.10

APPENDIX Q

SEPARATION SPRING ANALYSIS

R. Moses

June 20, 1972

SEPARATION SPRING SYSTEM

It has been shown by analyses and test that a helical compression-spring system is capable of separating spacecraft in orbit satisfactorily, with low tip off rates at separation. This was evaluated for the Air Force Vela satellite and other satellites.* To evaluate the separation of a typical probe from a carrier satellite, the following analysis was performed, using a reference probe weight of 147 kg (325 lbm) and spacecraft weight of 499 kg (1100 lbm). It is shown that the weight of such a system is very nominal.

The total energy imparted to two separating bodies = $E_1 + E_2$ and

$$E_1 = 1/2 M_1 V_1^2 \text{ and } E_2 = 1/2 M_2 V_2^2$$

where

M_1 = probe mass

M_2 = spacecraft mass

V_1 = probe imparted velocity

V_2 = spacecraft imparted velocity

Total energy then is

$$E_T = 1/2 M_1 V_1^2 + 1/2 M_2 V_2^2 = 1/2 M_1 V_1^2 + 1/2 M_1 \times \frac{M_2}{M_1} \left(V_1 \times \frac{M_1}{M_2} \right)^2$$

$$E_T = 1/2 M_1 V_1^2 + 1/2 M_1 V_1^2 \times \frac{M_2}{M_1} \times \frac{M_1^2}{M_2^2} = 1/2 M_1 V_1^2 + \frac{M_1}{M_2} 1/2 M_1 V_1^2$$

$$E_T = \left(1/2 + \frac{M_1}{2M_2} \right) M_1 V_1^2 \quad \text{or} \quad V_1 \sqrt{\frac{2E}{M_1 \left(1 + \frac{M_1}{M_2} \right)}}$$

* G. D. Palmer and D. H. Mitchell: "Analysis and Simulation of a High Accuracy Spacecraft Separation System." *Journal of Spacecraft and Rockets*, Vol. 3, No. 4, April 1966.

however,

$$V_2 = V_1 \frac{M_1}{M_2}$$

Therefore,

$$\Delta V = V_1 + V_2 = 1 + \frac{M_1}{M_2} \sqrt{\frac{2E}{M_1 \left(1 + \frac{M_1}{M_2}\right)}}$$

This can also be written:

$$E_T = \frac{\Delta V^2 M_1}{2 \left(1 + \frac{M_1}{M_2}\right)}$$

For a separation velocity of 0.91 m/sec (3 ft/sec), the spring energy to separate a 147 kg (325 lbm) probe from a 499 kg (1100 lbm) spacecraft is:

$$E_T = \frac{3^2 \times 325/32.2}{2 \left(1 + \frac{325/32.2}{1100/32.2}\right)} = 35.06 \text{ ft lbf of energy.}$$

For a 3-spring separation system, the energy/spring - 11.7 ft lbf.

It can be shown from spring design tables that spring weight will be in the vicinity of 0.57 kg/Nm (0.017 lbm per ft lbf of energy) for springs having a mean-coil-diameter/wire-diameter ratio of 8 (normal usage). Thus, the springs would each weight 0.09 kg (0.199 lbm). This is an insignificant weight for the separation energy.